Genomic and transcriptomic predictors of post-treatment HIV remission during primary HIV infection

Panagiota Zacharopoulou

Harris Manchester College

University of Oxford

A thesis submitted for the degree of

Doctor of Philosophy

Trinity 2024

Acknowledgements

First and foremost, I would like to express my deep gratitude to my main supervisor Professor John Frater, for giving me the opportunity to join an incredible team and contribute to such a meaningful and impactful project. John, thank you for showing me how exciting science is, for guiding me through this journey, for teaching me how to stand on my own feet, and even to run—sometimes wildly! I am also immensely grateful to Dr. Azim Ansari, my co-supervisor, for his invaluable teaching, brilliant ideas, and unwavering support, which meant so much to me. Additionally, I would like to thank my co-supervisor, Professor Philip Goulder, for the fascinating discussions on interferons and his insightful feedback. I could not have wished for better supervisors.

I am grateful to all participants of SPARTAC, HEATHER, BONDY and RIO, who very generously committed their time and efforts to research-none of this would be possible without them. Thank you to Professor Sarah Fidler and the RIO steering commitee, as well as the clinical staff, for their assistance and their patience with RIO screening.

I have been extremely lucky to work with the best people, whose support and friendship was invaluable. Nic Robinson and Helen Brown, without whom we would be completely lost; Lucia Parolini, Devinder Srai, Ming Lee, Dan Coneyworth, Chanice Knight, Tim Tipoe, Kahlio Mader, Mohammed Altaf, Carla Nel, Julia Edgar, Nina Hardy, the extended family; Emily Adland, Danny Hambidge, Nick Herbert, Hattie Parker, Thiruni Adikari, Matt Edmans, and to those who abandonded us; Matt Jones, Matt Pace, Jeremy Ratcliff, Ane Ogbe, and David Malone; Thank you all for the heated lunchtime debates, the art club, the cakes, going through single cells clustering conondrums, crafting songs while processing COVID samples and ah, yes, your scientific input. Special mention to the Escape the Country gang- Cecilia Jay, Ollie Sampson and Nick Lim; the journey wouldn't have been the same without you guys!

I love Oxford for the people who made it feel like home. Shout out to my HMC Friends; Lea Ballenberger, Josef Lolacher, Monty Ochocki, Jonas Schuff, Leoni Boyle, Madeline Tatum, Melody Li, Maxime Kayser, Leonie Hoff, Jan Langemeyer, Marie Smidstrup, David Brugger - I am just grateful for having you in my life. Here

is to more bike rides, motivation vibes in the Mediterranean, girls nights, ceilidhs, boat trips, utter judgeent, the gym, house parties, fine dining and 4-year-plans!

Thank you to Telenia Louri and Lena Pantavou, my best friends, for constantly trying to get me back home and thus reminding me of how much I mean to them. There is no greater honor than being a part of your families and in the lives of Antonis and Aliki. Also to my family; my aunts, uncles, cousins, and my new brother-in-law, who make our family feel like a real-life version of *My Big Fat Greek Wedding* and the most comforting nest.

Unquantifiable thanks to my parents, Katerina and Kostas, for always supporting my wildest ideas and helping me face absolutely anything. Mostly to my sister, Fi, who is my greatest strength and inspiration; without you I would have crushed a million times in the past few years.

Above all, a huge ta to my favorite baby, Yiannis; if you were born four years earlier there is absolutely no way this DPhil would have been finished.

Penny Zacharopoulou
Peter Medawar Building, Oxford University
Trinity 2024

Contributions to this thesis

All the work presented herein was predominantly conducted by me and supervised by Professor John Frater, Dr Azim Ansari and Prof Philip Goulder.

I would like to thank all the participants who made this research possible, as well as those involved in organising and carrying out RIO, HEATHER, SPARTAC and BONDY clinical trials.

Blood processing and PBMC handling for HEATHER and BONDY samples was performed by the members of the Frater Group at the Medawar Building. Blood processing and PBMC handling for RIO samples was performed by the members of the laboratory at St Mary's Clinical Trials Centre, Imperial College London as well as by members of the Frater Group at the Medawar Building. Helen Brown and Nicola Robinson assisted with DNA extraction, sequencing and library preparation. Amanda Williams assisted with in-house sequencing. The protocol for SGA was adapted by Dr Lilian Nogueira (Nussenzweig Group, Laboratory of Molecular Immunology, Rockefeller University). The code for the Rockefeller bnAb sensitivity prediction model was provided by Dr Thiago Oliveira (Nussenzweig Group, Laboratory of Molecular Immunology, Rockefeller University).

Chapter 2: Prevalence of resistance-associated viral variants to bnAbs in key populations of people with HIV

A subset of Env sequences (obtained from RIO samples using the Q4PCR assay) were provided by the Nussenzweig Group, Laboratory of Molecular Immunology, Rockefeller University.

Content from this chapter is included in two manuscripts published in Frontiers in Immunology and Current Opinion in HIV and AIDS :

- Zacharopoulou P, Lee M, Oliveira T, Thornhill J, Robinson N, Brown H, Kinloch S, Goulder P, Fox J, Fidler S, Ansari MA, Frater J. Prevalence of resistance-associated viral variants to the HIV-specific broadly neutralising antibody 10-1074 in a UK bNAb-naïve population. Front Immunol. 2024 Mar 18;15:1352123. doi: 10.3389/fimmu.2024.1352123. PMID: 38562938; PMCID: PMC10982389.

- Zacharopoulou P, Ansari MA, Frater J. A calculated risk: Evaluating HIV resistance to the broadly neutralising antibodies10-1074 and 3BNC117. Curr Opin HIV AIDS. 2022 Nov 1;17(6):352-358. doi: 10.1097/COH.0000000000000764. PMID: 36178770; PMCID: PMC9594129.

Chapter 5: Predicting bnAb sensitivity in the RIO trial

Clinical and demographic data were provided by Dr Ming Lee and the Imperial Clinical Trials Unit. The pharmacokinetic models were developed by Dr Ming Lee, who also provided the bnAb concentration predictions used in this chapter. The ELISPOT assay data used in this chapter was provided by Dr Timothy Tipoe. A subset of Env sequences (obtained from RIO samples using the Q4PCR assay) were provided by the Nussenzweig Group, Laboratory of Molecular Immunology, Rockefeller University.

Chapter 6: Expression of type I interferon-associated genes at antiretroviral therapy interruption predicts HIV virological rebound

This study was based on a research proposal submitted by Dr Mathew Jones to BHIVA. Sample processing and RNA extraction was performed by Nicola Robinson. Dr Emmanuele Marchi assisted with the analysis of the data.

Content from this chapter is included in a manuscript published in Scientific Reports:

- Zacharopoulou P, Marchi E, Ogbe A, Robinson N, Brown H, Jones M, Parolini L, Pace M, Grayson N, Kaleebu P, Rees H, Fidler S, Goulder P, Klenerman P, Frater J. Expression of type I interferon-associated genes at antiretroviral therapy interruption predicts HIV virological rebound. Sci Rep. 2022 Jan 10;12(1):462. doi: 10.1038/s41598-021-04212-9. PMID: 35013427; PMCID: PMC8748440.

Chapter 7: An exploratory study of the impact of bnAbs on the host immune response

Sample processing was performed with the assistance of Nicola Robinson. TCR sequencing analysis was performed by Devinder Srai. Clinical and demographic data were provided by Dr Ming Lee and the Imperial Clinical Trials Unit.

Abstract

HIV control remains poorly understood, with only a small subset of individuals successfully suppressing the virus following treatment during primary HIV infection. One of the most promising strategies for HIV cure is broadly neutralising antibodies (bnAbs), which have shown to substantially prolong time to viral rebound in absence of antiretroviral medications. Understanding the mechanisms underlying this control is essential for improving clinical care. This thesis investigates the interplay between HIV and the host to uncover key determinants of HIV control, following antiretroviral treatment and treatment with two broadly neutralizing antibodies (bnAbs), 10-1074 and 3BNC117.

To assess the feasibility of bnAb-based interventions, this thesis first analyzes the prevalence of bnAb resistance-associated mutations at a population level throughout the pandemic, as well as in viral reservoirs of key populations with primary HIV infection. The goal is to determine whether screening for resistance prior to bnAb administration could improve treatment efficacy. Additionally, the origins of bnAb resistance-associated mutations are examined to identify factors associated with an increased risk of resistance emergence. The relationship between proviral and circulating viruses is also investigated to assess whether proviral sequencing can serve as a reliable proxy for resistance screening. Finally, the accuracy of bnAb sensitivity predictions is evaluated in individuals who received bnAbs as part of the RIO trial, correlating baseline sensitivity predictions with clinical outcomes post-treatment while accounting for other viral and host factors.

This work then shifts focus to the host immune response, exploring how transcriptomic changes may provide insights into mechanisms of post-treatment viral control, whether following antiretroviral or bnAb therapy. Bulk RNA sequencing of CD4+ T cells from post-treatment controllers and from early progressors is used to identify gene expression signatures that may predict time to viral rebound after treatment interruption. In a final chapter, single-cell transcriptomic profiling of PBMCs from RIO trial participants who experienced long-term viral control post-bnAb treatment is conducted. This analysis aims to elucidate bnAb-induced changes in immune cell gene expression and to investigate the potential vaccinal effects of bnAbs at a transcriptomic level.

Overall, this work highlights key challenges associated with bnAb treatment and contributes to the broader understanding of post-treatment HIV control. The findings may help inform the design of more effective treatment strategies incorporating bnAbs.

Contents

List of Figures

List of Tables

List of Abbreviations

DNA . . . . . deoxyribonucleic acid

cDNA . . . . . complementary DNA

RNA . . . . . ribonucleic acid

CXCR4 . . . . HIV entry receptor

CCR5 . . . . . HIV entry co-receptor

CD4 . . . . . a co-receptor of MHC class II

CD8 . . . . . a co-receptor for MHC class I

TCR . . . . . T-cell receptor

ELISPOT . . . enzyme linked immunospot

ELISA . . . . . enzyme linked immunosorbent assay

CRF . . . . . circulating recombinant form

bnAb . . . . . broadly neutralising antibodies

ART . . . . . antiretroviral treatment

PHI . . . . . primary HIV infection

HIV . . . . . human immunodeficiency virus

AIDS . . . . . acquired immuno-deficiency syndrome

PWH . . . . . people living with HIV

SIV . . . . . simian immunodeficiency virus

ATI/TI . . . . (analytical) treatment interruption

QVOA . . . . . quantitative viral outgrowth assay

Q2VOA . . . . quantitative and qualitative viral outgrowth assay

PCR . . . . . polymerase chain reaction

qPCR . . . . . quantitatve PCR

PBMC . . . . peripheral blood mononuclear cells

IPDA . . . . . intact proviral DNA assay

Q4PCR . . . . quadruplex quantitative PCR assay

ddPCR . . . . digital droplet PCR

psi . . . . . packaging site

FLIPS . . . . . full-length individual proviral sequencing assay

TILDA . . . . tat/rev induced limiting dilution assay

RT . . . . . reverse transcription

TF . . . . . transmitting founder

MSM . . . . . men who have sex with men

SGA . . . . . single genome amplification

TLR . . . . . toll-like receptor

CTL . . . . . cytotoxic lymphocytes

Th . . . . . T helper cells

Tfh . . . . . T follicular helper cells

MHC . . . . . major histocompatibility complex

nAb . . . . . neutralising antibody

CDR . . . . . complementarity-determining region

SHM . . . . . somatic hypermutation

HBV and HPC hepatitis B and C

NRTI . . . . . nucleoside reverse transcriptase inhibitors

NNRTI . . . . non-nucleoside reverse transcriptase inhibitors

PI . . . . . protease inhibitors

INSTI . . . . . integrase strand transfer inhibitors

DRM . . . . . drug resistance mutation

NGS . . . . . next-generation sequencing

EC . . . . . elite controller

LTNP . . . . . long-term non-progressors

HLA . . . . . human leukocyte antigen

PTC . . . . . post-treatment controller

LRA . . . . . latency-reversal agent

LPA . . . . . latency promoting agent

HDACi . . . . histone deacetylase inhibitors

Fab . . . . . antigen-binding fragment

Fc . . . . . crystallizable fragment

NK cell . . . . natural killer cell

ADCC . . . . . antibody-dependent cellular cytotoxicity

ADCP . . . . . antibody-dependent cellular phagocytosis

CDC . . . . . complement dependent cytotoxicity

HR . . . . . hazard ratio

NJ tree . . . . neighbour-joining tree

ML tree . . . . maximum likelihood tree

FDR . . . . . false discovery rate

CL3 . . . . . containment level III

PCA . . . . . principle component analysis

PNG . . . . . potential N-glycosylation site

ER . . . . . early rebounder

GSEA . . . . . gene-set enrichment analysis

sc RNA-seq . single cell RNA sequencing

EM cell . . . . effector memory cell

MAIT cell . . mucosal-associated invariant T cell

Treg cell . . . T regulatory cell

DGE . . . . . differential gene expression

NKT . . . . . NK T cells

DC . . . . . dendritic cells

pDC . . . . . plasmatoid DC

CM cell . . . . central memory cell

VL . . . . . viral load

IFN-I . . . . . interferon type I

TTR . . . . . time to rebound

AUC . . . . . area under the curve

GSEA . . . . . gene set enrichment analysis

WGCNA . . . weighted gene co-expression network analysis

PPI . . . . . protein-protein interaction

padj . . . . . adjusted p-value

MSA . . . . . multi-sequence alignment

HXB2 . . . . . Clade B HIV reference genome

IC50, IC80 . . half-maximal and 80% inhibitory concentrations, respectively

1

Human Immunodeficiency Virus (HIV)

Contents

1.1 An overview of the global HIV pandemic

Human Immunodeficiency Virus Type 1 (HIV) was identified as the cause of Acquired Immuno-Deficiency Syndrome (AIDS) in 1984 (Blattner et al., 1988), and it has since emerged as a global pandemic. While Sub-Saharan African countries are still impacted the most by the pandemic, with 25.6 million people out of a global total of 39 million living with HIV in this region by the end of 2022, the response has led to widespread antiretroviral treatment and a steep decrease in new infections. However, there has been a concerning increase of new infections in Eastern Europe and central Asia as well as the Middle East and North Africa (49% and 61% increase since 2010) highlighting the ongoing urgency of the pandemic. In contrast to the improved outcomes for the Sub-Saharan African countries, over half of people living with HIV (PWH) in the aforementioned regions (51%) did not have access to treatment, representing the lowest treatment uptake rates worldwide. These lags stem from inadequate prevention and treatment programs in these countries, as well as the social stigma and marginalisation in certain high-risk populations, such as men who have sex with men, sex workers and people who inject drugs (UNAIDS, 2023).

1.1.1 The origin of HIV

The two main types of HIV are HIV-1 and HIV-2, two closely related viruses but with significantly different genetic and clinical/ epidemiological patterns. Both HIV-1 and HIV-2 descended from simian immunodeficiency viruses (SIVs), which were discovered in several African primate species (Hahn et al., 2000; Sharp & Hahn, 2011). Due to genetic relatedness with viruses infecting *Pan troglodytes troglodytes* and *Cercocebus atys atys*, these primates have been identified as the sources of zoonotic transmissions of HIV-1 and HIV-2 to man, respectively (Gao et al., 1999; Sharp & Hahn, 2011). Most likely, the transmission to humans occurred through contact with chimpanzee and gorilla blood, while hunting for and consuming bush meat (Sharp & Hahn, 2011). Phylogenetic analyses using

molecular clocks infer that the most recent common ancestor (tMRCA) to HIV-1 date to the 1920s while the tMRCA to HIV-2 date to the beginning of 1940s (Kirchner, 2023; Rambaut et al., 2004).

1.1.2 HIV-1 Subtypes and geographic distribution

Multiple separate cross-species SIV transmission events have resulted in four different HIV-1 lineages: groups M (major), O (outlier), N (non-M, non-O) and P (Ndjoyi-Mbiguino et al., 2020). Of these, group M is the most prevalent and accounts for the vast majority of HIV infections around the world. Group M can be further stratified into subtypes or clades (A-D, F-H, J, K, and L), sub-subtypes and their circulating recombinant forms (CRFs), which differ by approximately 20% in their genome sequences and their distributions vary by geographic region (Kijak & McCutchan, 2005; Kirchner, 2023; Robertson et al., 2000). CRFs can further recombine with recombinants or pure subtypes and hence increase the number of recorded CRFs, which is currently estimated to >120 (Tee et al., 2022).

Globally, C is the dominant HIV-1 clade, followed by clade A and CRF01-AE (Bbosa et al., 2019; Hemelaar et al., 2019; A. Williams et al., 2023). Although different clade proportions have been reported over the years, all studies concur on the increase in the number and prevalence of CRFs in the course of the pandemic (Hemelaar et al., 2019; A. Williams et al., 2023). At a regional level, clade C predominates in southern Africa and India, where it accounts for more than half of HIV-1 infections, while A is more common in East Africa, Russia and Eastern Europe. CRF01-AE is found in southeast Asia and CRF02-AG in West Africa. Although clade B is responsible for fewer infections globally compared to other clades, it is responsible for most infections in western and central Europe, North America, parts of South America and Oceania, which make it the most widespread clade worldwide (Hemelaar et al., 2019).

This thesis is focused on studying HIV-1 infection and the responses of HIV-1 hosts in treatment and cure approaches.

1.2 HIV structure and genome

HIV is a lentivirus, a genus of retroviruses. An HIV virion is spherical and measures approximately 100-130 nm in diameter and contains its genome in a conical capsid, surrounded by a host-derived membrane studded by viral proteins. The HIV genome is diploid, consisting of two copies of a 9.2 kb long positive sense, single-stranded RNA. Normally the two copies are identical but hybrid genomes may occur during infection with more than one clade. The HIV genome contains 9 genes which encode fifteen viral proteins (Apetrei C, Hahn B, Rambaut A, Wolinsky S, Brister JR, Keele B, 2021; Freed, 2015; Kirchhoff, 2021) (Figure 1.1);

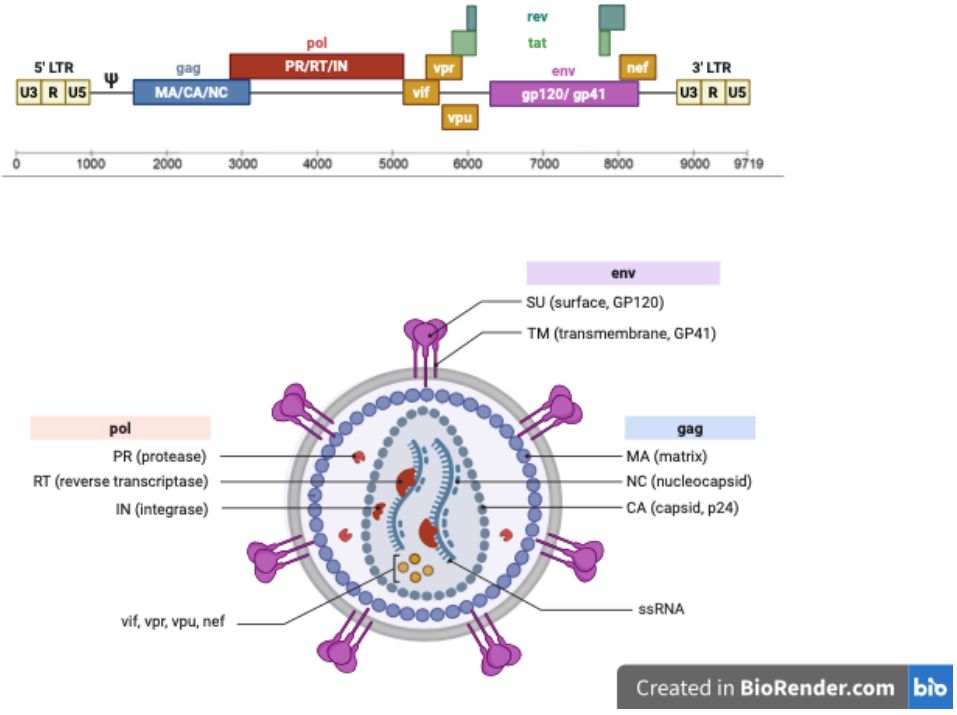

Figure 1.1: The HIV genome and the structure of an HIV virion

- ***gag***; group specific antigen. *gag* encodes the most highly conserved, and therefore most immunogenic proteins. The processed protein products of Gag are responsible for the physical structure of the viral capsid (p24), the matrix (MA) that stabilises the structure of the outer membrane and the nucleocapsid (NC) that helps with the RNA genome structure inside the

capsid. CD8+ T-cell response to Gag has been associated with better viral control and low viral load (Kiepiela et al., 2007).

- ***pol***; provides the enzymes required for viral reproduction. *pol* codes for reverse transcriptase (RT), RNAse H, integrase (IN) and Protease (PR). PR cleaves the Pol and Gag precursor into functional proteins, RT with RNAse H transcribes viral RNA to double stranded DNA (dsDNA) and IN is required for the integration of the dsDNA into the host cell genome.

- ***env***; envelope; the primary protein coded by *env* is gp160, which is then cleaved into gp120, an N-terminal external glycoprotein and gp41, which spans the membrane. Three of these gp120:gp41 heterodimers form the envelope glycoproteins (7-14 per virion) that are anchored on the surface of the lipid membrane, enclosing the virion (T. Zhou et al., 2010). Viral entrance to host cell is facilitated by the envelope proteins binding to the cluster of differentiation 4 (CD4) receptors. Env is covered by host-derived N-linked glycans attached on >30 potential N-glycosylation sites (PNG), and cover the majority of its surface (Zhu et al., 2000). This "glycan shield" is able to shift and conceal the protein so that it is not recognised by the immune system and support the stability of the trimer (Daniels & Saunders, 2019; Mouquet et al., 2012; Wagh et al., 2020). One of the most well-known examples of glycan shifting is the N332 glycan, which has been shown to shift between positions 332 and 334, after the appearance of antibodies that target it. The number of PNGs has been shown to change at different stages of infection with transmission founder (TF) viruses having fewer PNGs than isolates sampled during chronic infection (Derdeyn et al., 2004). Moreover, the conformation of Env changes transiently, allowing the exposure of certain epitopes only under specific circumstances, such as post-receptor binding. Env consists of variable regions (V1V2-V5), which form loops, interspersed with conserved regions (C1-C5) in a linear amino-acid sequence (Wyatt et al., 1998). While

the conserved regions are well-protected by the N-glycans the highly variable regions take up the more accessible regions on Env.

- ***tat (HIV trans-activator)*** and ***rev(regulator of expression of virion proteins)***; essential regulatory proteins for HIV replication. Tat enhances viral transcription efficiency by binding and regulating the phosphorylation of cellular factors, which results in an augmented transcription of all HIV genes. Tat is also released by infected cells in the cytoplasm, where it induces the apoptosis of infected bystander T-cells. Rev promotes the export of spliced or partially spliced RNA from the nucleus to cytoplasm, where it can be translated.

- ***nef* (negative factor)**, ***vif***, ***vpr* (lentivirus protein R)**, ***vpu* (virus protein U)**; accessory regulatory proteins for viral infectivity. Nef can protect infected cells from host immune surveillance and targeting by cytotoxic T-cells, by downregulating the major histocompatibility complex type-1 (MHC-1 or Human Leukocyte Antigen in humans- HLA) on the cell surface, mainly HLA-A and HLA-B (Collins et al., 1998). Nef and Vpu are used to downregulate CD4 on the cell surface and thereby decreasing Env-CD4 interaction and limiting the exposure of Env on the cell surface (Yucha et al., 2023). Vif is important for *in vivo* replication of virions in specific cell-types through the inhibition of cytoplasmic defenses.

1.2.1 HIV life cycle

HIV persistence is established through iterative cycles of cellular infection and viral replication. These cycles can be broadly categorised into four distinct stages; binding and entry, uncoating, reverse transcription and proviral integration. The initial attachment occurs via the gp120 on the virion, which interacts with the CD4 receptor expressed on the surface of approximately 60% of circulating T-lymphocytes in blood and thymus, macrophages, dentritic cells. While this is the primary target of the virus, a subsequent conformational change exposes a

domain that binds to either CCR5 (M-tropic viruses) or CXCR4 (T-tropic viruses) chemokine co-receptors. The dual interaction with CD4 and at least one of the two co-receptor allows for a more stable and prolonged attachment, critical for the HIV-host membrane fusion. This process is mediated by gp41 allowing the capsid to enter the cell into the cytoplasm, where the reverse transcription commences immediately. Notably, the high error rate of HIV reverse transcriptase is responsible for viral diversity within the individual and generates a significant number of dysfunctional viruses, incapable of completing their replication cycle and/or produce replication competent viruses (Kuniholm et al., 2022). The viral capsid protects the newly synthesised cDNA from host immune sensing and degradation. The pre-integration complex, comprised of viral cDNA and proteins, is transferred to the nucleus. There, the integrase facilitates the integration of the viral cDNA to the host genome establishing the provirus. The localisation of viral integration has been shown to correlate with viral transcription levels and subsequently to control or disease progression (Jiang et al., 2020). After transcription and provided that the cell is activated, host cell enzymes transcribe the provirus into viral RNA, alongside the host's transcripts. After the cleavage of precursor core and envelope polypeptides into functional viral components, the viral genome is packed into a newly formed virion. The virion is directed towards the plasma membrane, where it acquires its lipid membrane and other host-derived proteins before budding from the cell surface to infect neighboring cells (Yeh et al., 2021).

1.2.2 The viral reservoir

As mentioned in the HIV life cycle section, HIV preferentially infects CD4+ T-cells, the fate of which varies from persistence to cell death (Margolis et al., 2020; Siliciano & Siliciano, 2022). Reports from as early as mid-1990s indicated that some of these cells may persist in the blood and other anatomical compartments indefinitely (such as the gut-associated lymphoid tissues and lymph nodes), harbouring transcriptionally silent viruses in their genome, and serving as the HIV reservoir (Chun et al., 1995, 1997; Finzi et al., 1997). Infection of CD4+ T-cells

that are already in a resting memory state or of actively replicating CD4+ T-cells that subsequently revert to a resting state ensures latency of the reservoir (Chen et al., 2022; Siliciano & Siliciano, 2022). Mild stimulation of certain chemokines and cytokines, such as Chemokine (C-C motif) ligands 19 and 21 (CCL19 and CCL21) and interleukins 4 and 7 (IL4 and IL7), has been found to promote the infection of resting memory T-cells without inducing cell activation (Saleh et al., 2007). Post-infection, several host factors can promote or hinder the establishment of the reservoir; programmed cell death protein-1 (PD-1), Lymphocyte activation gene 3 (LAG-3), T cell immunoreceptor with Ig and ITIM domains (TIGIT), CD30 and the binding of IP-10 to C-X-C motif chemokine ligand 3 (CXCR3) have all been suggested to inhibit the transcription or expression of HIV genes, thereby promoting latency (Chen et al., 2022; Fromentin et al., 2016; Hogan et al., 2018). A recent study that utilised single-cell transcriptomics to profile HIV infected cells in a small Hispanic cohort, showed that the co-expression of IKZF3, interleukin 21(IL-21), BIRC5 and marker of proliferation Ki-67 (MK167) contributed to the proliferation of infected cells that were transcriptionally active (Y. Wei et al., 2023).

However, no marker can identify latent reservoir cells specifically. It has been reported that the reservoir forms immediately after infection (Bekker et al., 2023; Henrich et al., 2017; Krebs & Ananworanich, 2016) but recent research shows that most of the replication-competent reservoir is integrated very close to the initiation of treatment (Abrahams et al., 2019). Less than 5% of the reservoir cells harbour intact, replication-competent proviruses which means that they can contribute to viral rebound upon treatment cessation (Bruner et al., 2016; Ho et al., 2013; Z. Wang et al., 2018). The remaining cells harbour proviruses with hypermutations or large deletions that render the virus non-functional (Z. Wang et al., 2018). That said, defective proviruses are still able to produce immunogenic viral proteins that may contribute to inflammation (Kuniholm et al., 2022; Siliciano & Siliciano, 2022). While it is clear that the virus will establish a latent reservoir in all PWH (Chun et al., 1998), starting antiretroviral treatment early can result in smaller reservoir size and a quicker clearance of infected cells before they enter

the reservoir. This can also lead to more effective HIV-specific immunity against the early, less diverse strains (Buzon MJ, 2014; Leyre et al., 2020; Shelton et al., 2020). Following its formation, the latent reservoir remains dormant, producing only minimal levels of viral proteins that go undetected by the immune system of the host (Chen et al., 2022). Due to their long half-life of 44 months, these cells pose the main barrier to HIV cure, despite the success of antiretroviral treatment in controlling viral replication (Bekker et al., 2023; Cohn et al., 2020). The persistence of the reservoir is mainly attributed to cell-to-cell interactions between infected and uninfected cells (Chen et al., 2022) and to clonal expansion of infected cells in the course of infection (Chomont et al., 2009) but other mechanisms, such as the high expression of B-cell lymphoma 2 (BCL-2) protein in infected cells, may protect the reservoir from CTL responses (Chandrasekar et al., 2022). The expansion is facilitated by viral integration near cell-growth associated genes (Wagner et al., 2014), antigen-stimulated proliferation (Mendoza et al., 2020) or homeostasis (Chomont et al., 2009). Upon reactivation, cells harbouring intact proviruses may start producing and releasing virions. Reactivation happens sporadically when cells encounter antigens or during an inflammatory process. This can result in viral rebound which happens in the majority of cases of complete absence or poor adherence to antiretroviral treatment and selection of resistant clones that leads to drug resistance. Viral rebound usually happens within a few weeks post-treatment interruption (TI or ATI) or failure (J. Z. Li et al., 2016; Siliciano & Siliciano, 2022).

The quantification of the replication-competent reservoir is important when designing and employing cure strategies, in terms of evaluating the treatment efficiency and predicting virndefinedal rebound. Methods such as measuring total HIV DNA, albeit practical and widely used, may overestimate the size of the reservoir, as it does not distinguish between replication-competent and defective proviruses. Measuring cells containing intact HIV proviis emerging as a promis-ingged as a biomarker for predicting the effectiveness of novel HIV cure or remission strategies. Recent studies have demonstrated variations in the intact proviral reservoir following the administration of novel immunotherapeutics, such as broadly

neutralising antibodies (Gaebler et al., 2022; Mendoza et al., 2018). Accurate measurement of the HIV reservoir requires two essential conditions; suppressed viral replication for at least 6-12 months after antiretroviral therapy initiation and exclusion of defective proviruses (Siliciano & Siliciano, 2022). A range of assays have been proposed to measure the size of the replication-competent reservoir and they can be divided into viral outgrowth detection assays and polymerase chain reaction (PCR)-based assays.

Traditional methods, such as the quantitative viral outgrowth assay (QVOA) (Finzi et al., 1997) and its modified versions (Laird et al., 2013; Lorenzi et al., 2016), measure replication-competent virus through *ex vivo* stimulation and cell expansion. In this approach, latently infected CD4+ T cells are serially diluted *in vitro* and stimulated in order to induce viral reactivation. The infected cells are then co-cultured with healthy CD4+ T cells (or a cell line) and p24 ELISA or quantitative PCR (qPCR) are used to detect viral replication in the supernatant. Q^2VOA builds upon QVOA by incorporating genetic analysis of the outgrowth viruses and thus provides information on the viral diversity, drug sensitivity and phylogenetic relationship between the strains (Lorenzi et al., 2016). However, these assays often underestimate the actual reservoir because not all latent proviruses can be activated with a single round of stimulation or replicate under the specific *in vitro* conditions necessary for detection (Ho et al., 2013; Roux & Chomont, 2023). In addition, they are costly, labor-intensive and require a large number of PBMCs and cannot be performed on tissue biopsies.

The simplest method of quantifying the integrated HIV DNA is the HIV total PCR, which combines the use of HIV-specific primers with primers specific for Alu regions, which are found in all human cells. Nevertheless, this assay may overestimate the frequency of cells harbouring intact provirus as it only amplifies a very small fragment of the viral genome. This limitation was addressed with the development of assays such as the intact proviral DNA assay (IPDA) (Bruner et al., 2019) and the quadruplex quantitative PCR assay (Q4PCR) (Gaebler et al., 2019), which were designed to distinguish intact from defective proviruses.

These assays offer greater sensitivity and are more cost- and labor-efficient compared to those measuring replication- competent virus. The IPDA employs digital droplet PCR (ddPCR) to target two highly conserved regions in the HIV proviral genome (packaging site- *psi* and *env*), thereby excluding hypermutated sequences or sequences with deletions. This allows for high-throughput quantification of the intact HIV reservoir, without requiring stimulation or expansion. However, sequence polymorphisms may lead to assay failure and underestimation of reservoir size (Kinloch et al., 2021). Expanding the number of target regions may enhance accuracy (Delporte et al., 2025; Levy et al., 2021; Snippenberg et al., 2022), though it does not address the lack of downstream full-length sequencing analysis.

For this purpose, assays that amplify long fragments or full-length virus, such as the Q4PCR (Gaebler et al., 2019) or Full-Length Individual Proviral Sequencing (FLIPS) (Hiener et al., 2017) were developed. The Q4PCR assay uses a limiting dilution approach to amplify targets from individual templates and a four-probe digital droplet qPCR system targeting conserved HIV regions (*psi, gag*, *pol*, *env*). Positive samples for two or more probes are further verified by sequencing, which enables downstream analyses, such as phylogeny or detection of mutations associated with drug resistance. In a direct comparison, the IPDA estimated a 19-fold higher intact proviral reservoir than Q4PCR, suggesting potential overestimation due to biases favoring amplification of smaller fragments and probe misidentification in IPDA, or differences in cell normalisation methods (Gaebler et al., 2021).

Notably, none of the PCR-based assays provide information on the inducibility of the strains identified as intact, raising questions about their clinical relevance Siliciano & Siliciano (2021). The Tat/Rev Induced Limiting Dilution Assay (TILDA) employs reverse-transcription PCR to quantify the frequency of cells capable of generating multispliced HIV RNA following stimulation, thereby evaluating their transcriptional activity. While TILDA identifies cells that can produce fully elongated, multiply spliced transcripts, it does not confirm their ability to generate infectious virions (Einkauf et al., 2019).

In all, each of these assays offers unique advantages and limitations, making the optimal choice dependent on the specific research or clinical application. If the goal is to precisely quantify intact proviruses while minimising overestimation, assays like Q4PCR or the Rainbow assay provide greater specificity than IPDA by targeting multiple HIV regions, although they still require sequencing confirmation. For high-throughput and cost-effective reservoir quantification, IPDA remains widely used despite its tendency to overestimate intact proviruses. Meanwhile, TILDA provides insight into transcriptional activity but does not confirm replication competency, highlighting the need for complementary approaches. Ultimately, no single assay fully captures the complexity and the diversity of the HIV reservoir and a combination of PCR-based and viral outgrowth assays may be necessary to achieve the most comprehensive assessment.

1.2.3 Viral Diversity

One of the hallmarks of HIV is its extensive diversity within and among hosts, due to the highly error-prone HIV RT, the frequency of replication cycles per day, and the influence of host immune responses (Rambaut et al., 2004). Previous studies have shown that HIV evolves faster within host compared to the general population (Lythgoe & Fraser, 2012). The amount of diversity is remarkable, with untreated HIV generating 10 billion viral particles daily in an individual (Kijak & McCutchan, 2005; Rambaut et al., 2004). However, in some transmissions, such as heterosexual or mother-to-child transmissions, HIV infection stems from a single TF, as evidenced by analyses of env sequence complexity in the bloodstream (Derdeyn et al., 2004; Keele et al., 2008). In these cases, a bottleneck effect may occur, where viruses with higher fitness are selected. This bottleneck phenomenon can occur during various stages of transmission, either within the donor or the recipients, highlighting how selection shapes early viral populations (Joseph et al., 2015). In other transmissions, like men who have sex with men (MSM) or in intravenous drug users, it's not uncommon to transmit multiple viruses due

to higher exposure risk and a comparatively less rigorous selection process (G. van Zyl et al., 2018).

Shortly after the transmission of a single TF, the viral population within the recipient is homogeneous but rapidly diversifies as it adapts in the new host environment, aiming to evade immune responses or revert to wild-type. The rate of diversification varies across viral genes, with structural genes experiencing higher rates of mutation compared to viral enzymes(Salazar-Gonzalez et al., 2008). The env protein, the sole viral protein present on the virion surface, is the target of anti-HIV antibodies, which exert significant pressure on the genome. In response to this pressure, *env* accumulates mutations that account for 35% of diversity observed between clades and 20% within a single subtype (Lynch et al., 2009). Even within the same gene, different regions have a different rate of variation. Li et al. reported the non-synonymous substitution rate in the hypervariable regions of *env* at 14 x 10^{-13} substitutions/ year while the average rate for the whole genome was estimated at 10 x 10^{-3} (W.-H. Li et al., 1988). Interestingly, viruses in one compartment can differ significantly from viruses in another compartment within the same person (Simmonds et al., 1991). HIV can mutate extensively while maintaining its fitness and infectivity, meaning that an individual can harbour a diverse range of viruses that are genetically related but not identical. These viruses will continue to mutate in order to adapt to the ever-changing host environment and even revert to wildtype, provided that the selection pressure is lifted and that by doing so there is a gain in viral fitness. Most importantly, previous variants "archived" in the latent reservoir contribute to the diversity and can source drug-resistant clones that may lead to treatment failure.

Viral heterogeneity can be influenced by a number of factors. For instance, in scenarios involving multiple TFs, viral populations diversify not only through mutating but also through recombination events (Lemey et al., 2006; G. van Zyl et al., 2018). Following initiation of treatment viral diversity tends to decrease as the population of infected cells declines, illustrating the impact of therapeutic interventions on viral dynamics and diversity within hosts (Kearney et al., 2014).

Additionally, due to different selection pressures in each stage of infection, the virus diversifies at slower or faster rates. It has been suggested that during the earlier stages of infection and due to the less sufficient adaptive immune responses, the viral evolution is slower and progressively becomes faster at the later stages of chronic infection. Therefore, the earliest the treatment initiation the less diverse the reservoir is expected to be (Shankarappa et al., 1999). Furthermore, stochastic nucleotide mutations, even if they do not impact the actual protein (synonymous mutations), also contribute to viral heterogeneity (Frost et al., 2018).

The development of molecular and computational biology techniques such as sequencing, has helped measuring, analysing and understanding HIV diversity. One approach to study the heterogeneity of intra-host viral populations is to define their evolutionary relationships by phylogenetics. The construction of phylogenetic trees facilitates the visualisation of genetic pairwise distances among HIV sequences and estimates the difference between sequences (G. van Zyl et al., 2018). As shown previously, these distances exhibit a correlation with time, thereby enabling the inference of evolutionary dynamics within HIV populations and confirm that HIV conforms to a molecular clock (Leitner & Albert, 1999; Zanini et al., 2015). In order to increase the resolution and the accuracy of those trees when looking at individual hosts, single HIV sequences are amplified with single-genome amplification (SGA)(Palmer et al., 2005). As previous studies have demonstrated, contrary to using conventional PCR, SGA allows the detection of minority clones and reduces the artifacts that may occur due to recombination of multiple templates (Jordan et al., 2010; Salazar-Gonzalez et al., 2008). However this is a laborious and costly method with limitations, such as the limited information on the full length virus and the limited number of obtained amplicons even after several rounds of amplification.

1.3 Stages of Infection

HIV infection may occur after sexual contact with an individual with detectable viral load, mother-to-infant transmission or percutaneous inoculation. The risk of

a productive infection is different for each route, taking into account other factors, such as viral load and stage of infection of the transmitting partner, genital inflammation, etc. As mentioned in section 1.2.3, depending on the route of transmission (Shaw & Hunter, 2012), the majority of infections are established by a single fit TF. A stringent population bottleneck allows only variants with specific features, such decreased sensitive to interferon and less glycosylated envelope proteins (Fenton-May et al., 2013; Gnanakaran et al., 2011) to be transmitted. However, it is not unusual for more than one viruses to be simultaneously transmitted, especially in those cases where the virus does not need to encounter the mucosal barrier (Macharia et al., 2020).

The progress of untreated HIV infection is defined by CD4+ T-cell counts and clinical symptoms and it is divided into the early infection, including primary infection (PHI), which span up to 1 and 6 months post HIV acquisition respectively, chronic infection (>6 months) and AIDS (Naif, 2013) (Figure 1.2).

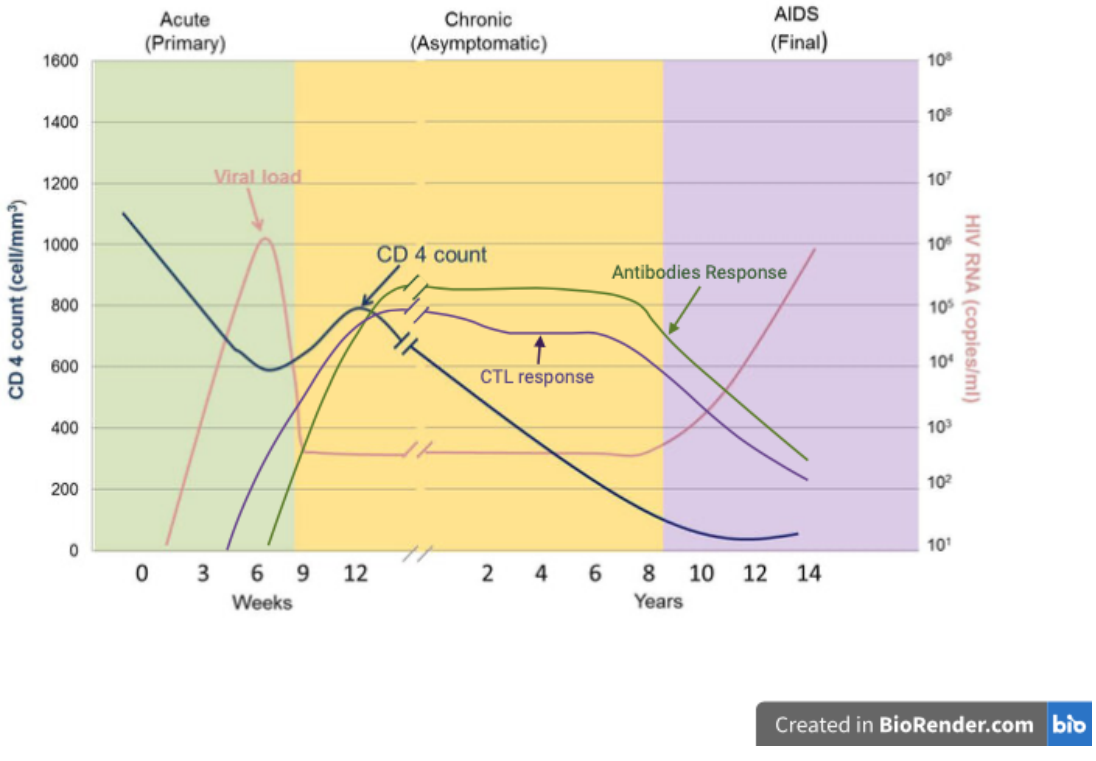

Figure 1.2: The stages of untreated HIV infection. Adapted from [@Manoto2018]

1. Human Immunodeficiency Virus (HIV)

During PHI, plasma viremia reaches high levels before it is partially controlled by the host immune response, which leads to an improvement in symptoms and limited immunological recovery for most individuals (Fidler & Fox, 2016). This period can be further categorized using the Fiebig staging system, which classifies early HIV infection into distinct stages (I–VI) based on the sequential appearance of virological and serological markers (Fiebig et al., 2003). The correct diagnosis of early HIV infection is important not only for managing the symptoms but also for limiting transmissions in the community. Since standard HIV antibody tests may not detect the virus early in infection, more sensitive tests are required. The key diagnostic approaches include (Fidler & Fox, 2016):

- HIV RNA test; detects viral RNA in the blood within days to weeks after exposure. Most sensitive test for the diagnosis of early infection.
- HIV p24 antigen test; detects the p24 protein before antibodies emerge within 2-4 weeks of exposure
- HIV antigen-antibody (Fourth generation) test; detects both p24 and antibodies, within 2-4 weeks of exposure
- HIV antibody (Third generation) test; detects antibodies against HIV within weeks to months after exposure, at the stage of the seroconversion. Unreliable for the diagnosis of PHI.
- Recent Infection Testing Algorithm (RITA) is a method to distinguish recent HIV infections from longer ones. RITA combines multiple biomarkers such as antibody detection, viral load, CD4 count and patient history. It is used to confirm a PHI diagnosis rather than diagnose, especially in surveillance settings (Aghaizu et al., 2014).

1.4 Innate and adaptive immune response against HIV

The innate immune response is initiated by the host cells using their pathogen recognition receptors (PRR) to recognise pathogen-associated molecular patterns (PAMP) within the virions. PRRs include RIG-1- like receptors and Toll-like Receptors (TLR), for instance TLR7 and TLR8. These trigger the production of pro-inflammatory cytokines that regulate the migration of immune cells on the site of the infection. The sharp increase of the viral load in the acute phase can be attributed to the high number of CD4+ T-cells that are recruited, first at the infection site and later in the draining lymph nodes and gut tissue, and become targets for further infection. At this stage, the relationship between viral titres in the blood and CD4+ T-cell count is inverse, due to the high rate of CD4+ T-cell infection and death. Within days of infection, PRRs activate the Nuclear Factor κB (NFκB) transcription factors, which subsequently activate host restriction factors, for example APOBEC3 and TRIM5, that restrict viral replication by hypermutation and inducing premature virion uncoating, respectively (Ganser-Pornillos & Pornillos, 2019). The rise of viral load, until it reaches its peak at 21-28 days post transmission, enhances the production of inflammatory cytokines, led by Interferon Type I (IFN-I) and Interleukin (IL) 15 which are produced by dendritic cells (DC). Notably, infected cells, compared to virions, are better recognised by DCs and induce a stronger IFN-I response (Lepelley et al., 2011). This cytokine storm induces the differentiation of naive CD4+ T-cells into T helper (Th), which produce Tumor Necrotic Factor (TNF) and IFN-γ, in response to viral proteins, and T follicular helper cells (Tfh), which are involved in priming the CD8+ T-cell (also known as cytotoxic T-cells or CTL) response (Kazer et al., 2020; McMichael et al., 2010; Porichis & Kaufmann, 2018).

The CTL response is key in the host defense against HIV. Viral proteins that get fragmented inside infected cells are presented on the cell surface after binding to major histocompatibility complex (MHC) proteins. CTLs can recognise 8-10

amino acid long peptides bound on MHC Class I and subsequently kill the infected cell (Rock & Goldberg, 1999), whereas CD4+ T-cells can recognise 13-17 amino acid long peptides on MHC Class II and cause a production of cytokines and the activation of CTLs (Rudensky et al., 1991). The maximum of CTL response is reached after the viral load reaches its set point where it remains steady, 12-20 weeks after the peak.

The rapid decline of plasma viremia post its peak is attributed to the activity of CD8+ T-cells, which can recognise and target cells that harbour viral peptides, mainly Gag. This exerts selection pressure to the virus, which may affect fitness and thereby viral replication rate (Chang & Altfeld, 2010; B. Walker & McMichael, 2012). In case the pressure is lifted, such as after transmission in a new host, some viruses may revert back to wild type (Ranasinghe & Walker, 2018).

While T-cells are undergoing activation, Natural Killer (NK) cells are modulated by antigen presenting cells on the site of infection and their activity is enhanced by type I interferons. Different subsets of NK cells can produce IFN-γ, which modulates adaptive immunity or directly lyse infected cells by secreting cytolytic granules, perforin and granzyme A (Nuvor, 2018).

Although antibodies targeting Env are detectable in the plasma within the very first weeks of infection, these have shown to be ineffective in controlling the virus (Bertagnolli et al., 2020). The reason why the initial antibody response to HIV is 'non-neutralising' is the production of dysfunctional Env; this 'viral debris' displays epitopes that are not found on the functional protein and effectively draws the host immune response away (Parren et al., 1997). In an acute HIV infection cohort, Keele et al (Keele et al., 2008) showed that the only mutations observed during viral evolution pre-peak viremia were on the CTL epitopes, therefore early antibodies are not likely to exert any selection pressure on the virus at this stage. The first neutralising antibodies (nAb), which are strain-specific, as they are limited in neutralising autologous virus, emerge approximately 12 weeks post transmission. Contrary to non-neutralising antibodies, nAbs block viral entry directly or by hindering the conformational changes necessary for entering the cell. Primarily,

nAb epitopes map to V1V2 and V3 variable env loops, which are protected by the dense env glycan shield (X. Wei et al., 2003). The virus, however, manages to always stay one step ahead of nAbs through selection of resistant variants, by substituting specific amino acids and acquiring insertions or shifting glycans to remove access to epitopes (Daniels & Saunders, 2019; Moore et al., 2009; X. Wei et al., 2003). Moreover, nAbs may shift their neutralisation activity towards viral debris or defective virus, which in return will move the selection pressure away from replicating viruses (Parren et al., 1997). During natural infection, nAbs undergo affinity maturation and as a result they evolve to recognise viral particles more efficiently. While almost all PWH develop antibodies with some level of cross neutralisation 2-3 years post-transmission, only a small proportion (10-25% of PWH) are able to produce antibodies capable of neutralising a wider range of viruses and only 1% develop highly potent broadly neutralising antibodies (bnAb), later in the course of infection (Caskey & Kuritzkes, 2022; McCoy & McKnight, 2017; Rusert et al., 2016). However, at that stage bnAbs are not able to effectively control the virus, most likely due to the exhaustion of the other immune response components (Anne et al., 2009). Development of breadth has been associated with high viremia, low CD4+ T-cell count at set point, viral diversity and duration of infection (Gray et al., 2011; Landais & Moore, 2018). More than 300 bnAbs have been identified and characterised since their discovery in the 1990s (Griffith & McCoy, 2021). Many bnAbs exhibit features including long heavy chain complementarity-determining region 3 (CDRH3), high rate of somatic hypermutation (SHM), ability to interact with multiple antigens and insertion/deletions. bNAbs are discussed further in section 1.6.

In summary, both the innate and adaptive immune response are unable to control HIV progression, as they are not fast or potent enough at the early stage of infection.

1.5 Research for cure

Despite the availability of effective antiretroviral treatment (which are presented in this section), that effectively suppresses HIV replication and allows PWH to lead long and healthy lives, a cure for HIV remains an unmet goal. ART does not eliminate the virus; instead, it requires lifelong adherence, and any interruption can lead to viral rebound due to the persistence of the reservoir. Additionally, access to ART remains a challenge in some regions and drug resistance can compromise treatment efficacy. Lastly, lifelong ART has an increased risk of ART-associated side effects and contributes to social stigma, as it is a visible marker of HIV status (Buell et al., 2016).

Research into HIV cure strategies, ranging from latency reversal and immune-based therapies to bnAb treatment and gene editing, has impacted medicine beyond the management of HIV itself. Understanding how the immune system interacts with persistent viral infections has provided insights on other HIV-associated co-morbidities, such as cancers and cardiovascular diseases and other viral infections, such as Ebola, Zika and influenza (Schwetz & Fauci, 2019). Moreover, insights from HIV cure research, including targeting viral reservoirs, boosting immune responses, and overcoming immune exhaustion, could shape treatments for other persistent or latent infections, such as hepatitis B (HBV), which forms viral reservoirs and a cure still remains to be found (Nassal, 2015). Thus, while ART has transformed HIV into a manageable condition, continued research into curative and alternative treatment strategies remains crucial not only for achieving an HIV cure but also for advancing the broader field of infectious disease therapeutics.

1.5.1 Current antiretroviral treatments

The current approach for treating HIV involves antiretroviral treatment (ART), which aims to achieve viral suppression (<50 copies/mL of blood) and hence reduce the mortality and morbidity associated with HIV, as well as to reduce transmission. ART utilises various medications that target different stages of the viral life cycle.

These are classified by their mechanism of action; nucleoside reverse transcriptase inhibitors (NRTI),non-nucleoside reverse transcriptase inhibitors (NNRTI), protease inhibitors (PI), integrase strand transfer inhibitors (INSTI), entry inhibitors, including CCR5 agonists and fusion inhibitors, and pharmacokinetic enhancers.

In order to maximise effectiveness and reduce the risk of developing resistance, treatment usually involves a combination of at least three drugs from two or more classes. Most ART regiments, if taken as prescribed, are able to successfully suppress viremia long-term and prevent the emergence of *de novo* drug resistant mutations (DRM). However, pre-existing DRMs which can be transmitted from donors, may compromise treatment success (Derache et al., 2019). The effect of DRMs on HIV is also diverse; depending on the mutation, some may decrease the viral fitness and/or infectivity of the virus compared to wild-type, where no selection pressure is present (Brenner et al., 2002) and some may only have a minor impact (Kühnert et al., 2018). It is not uncommon for viruses with DRMs to revert to wild-type alleles, as mentioned in section 1.2.3. In their review Frost et al. (Frost et al., 2018) argue for a stochastic process of evolution, based on data showing variation at timing and development of DRMs among different PWH.

To prevent treatment failure in individuals and the spread of DRMs in the community, clinicians often use HIV drug resistance testing to predict the response to ART regiments (Clutter et al., 2016). Genotypic testing through next-generation sequencing (NGS) is the test of choice, as an accurate, fast and cost-effective method (Günthard et al., 2019; Metzner, 2022). Genotypic assays can determine the presence of mutations associated with drug resistance in *pro* and *RT* genes and the viral tropism in the V3 region of *env*. The interpretation of these outcomes is based on pre-existing knowledge and more recently in machine learning algorithms which have been trained to assess the impact of certain mutations, based on experimental data (Blassel et al., 2021; Günthard et al., 2019). Phenotypic assays on the other hand are more expensive, time consuming and less accurate under certain circumstances, such as in individuals with low viral load and may select for more fit viruses that replicate better compared to less fit viruses with DRMs

(Nijhuis et al., 2001). It is common for drug resistance to be assessed using cell-free virus in plasma, where this is possible. Replicating HIV is short-lived and may derive from anatomical compartments and as such, it can provide a snapshot of drug resistance status that dominates at that time. Nevertheless, the archived variants in the reservoir, although very likely defective, could also harbour DRMs and may re-emerge and source viral rebound (G. U. van Zyl et al., 2022).

The timing of treatment initiation has been shown to be of paramount importance. Specifically, there is evidence that commencing treatment during PHI may limit viral diversity and the size of the reservoir, preserve the functionality of T- and B-cells and facilitate the restoration of immune responses (Buzon MJ, 2014; V. Jain et al., 2013; Sáez-Cirión et al., 2013).

1.5.2 Types of HIV control

Since the early days of the pandemic, there have been reports of PWH who showed delayed or no evidence of progression and have managed to maintain virological and immunological control for extended periods of time (Cao et al., 1995; Deeks & Walker, 2007). This long term control of HIV without continuous treatment is referred to as "functional cure", after an intervention has been implemented. Unlike a sterilising cure where all replication-competent virus is eradicated, as in the case of the Berlin patient, replication-competent proviruses continue to persist in the body but do not cause any symptoms or disease progression (Xu et al., 2017). These individuals were until recently described as long-term non-progressors (LTNP) and only after the development of viral load testing, this group was divided into subgroups, based on their clinical features. LTNPs comprise a 5-15% of all PWH, they maintain a high count of CD4+ T-cells (>500 cells/mmˆ3) and can be clinically stable for years, despite their low to moderate amounts of viremia.

Elite controllers (EC) are an even rarer subset of PWH (0.2 0.5%), who spontaneously control their viral load to undetectable levels (<50 copies/mL) and similar to LTNPs maintain a high count of CD4+ T-cells (Okulicz & Lambotte, 2011; B. D. Walker & Yu, 2013). Notably, the EC phenotype is usually associated

with certain HLA alleles like B*57 and B*27 and with strong immune responses (Goulder & Watkins, 2008). These may include enhanced CD8+ T cell responses that target and eliminate HIV-infected cells, as well as broader and more potent neutralising antibody responses. Furthermore, clones of intact proviruses in the reservoir were reported in higher frequency in EC compared to non-controllers and notably, these were integrated in satellite DNA and genes in the zinc finger family (Jiang et al., 2020).

The third subgroup of HIV controllers consists of individuals capable of maintaining viral suppression following TI (Hocqueloux et al., 2010; Sáez-Cirión et al., 2013). Two comprehensive studies, the Viro-Immunological Sustained CONtrol after Treatment Interruption (VISCONTI) and the Control of HIV after Antiretroviral Medication Pause (CHAMP) study, have provided detailed descriptions of these cohorts. Both studies have reported that the PTC phenotype was more frequent among individuals who initiated ART during PHI (Namazi et al., 2018; Sáez-Cirión et al., 2013). The prevalence of PTC ranges between 0-15%, depending on the studied cohort size, the exact definition of PTC, and the length of ART prior to TI (Martin & Frater, 2018). Studies have indicated that the reservoir in PTCs is smaller compared than non-controllers, especially in specific T-cell populations, although the proportion of intact viruses does not significantly differ (Sáez-Cirión et al., 2013; Sharaf et al., 2018). A recent study comparing 22 PTCs vs non-controllers, found that PTCs exhibit less CD4+ and CD8+ T-cell activation and exhaustion, as well as a stronger Gag-specific CD4+ T-cell and NK cell response (Etemad et al., 2023). In corroboration with this, PTCs and non-controllers were found to show no difference in HIV transcription initiation on a transcriptomic level, but non-controllers did have a higher level of complete transcripts compared to PTCs (Wedrychowski et al., 2023). In comparison to EC, PTCs tend to exhibit lower CD4+ counts prior to ART initiation, higher viral loads, lower levels of T-cell activation and lack the protective HLA alleles (Sáez-Cirión et al., 2013).Transcriptional pathways associated with inflammation, interferon response and TNF were consistently enriched in normal controllers compared to PTC.

The activation of these pathways can stimulate HIV replication and potentially harm other uninfected cells. On the contrary, interferon and p53 pathways were upregulated only temporarily, very soon after ATI (Wedrychowski et al., 2023).

1.5.3 The clinical significance of Analytical Treatment Interruption

The main barrier to achieving a cure, as noted in section 1.2.2, is the latent viral reservoir and the rapid rebound of the virus once the latent cells are reactivated, in absence of ART. Time to viral rebound is typically the primary endpoint in most studies seeking to evaluate new approaches to HIV treatment. Currently, there are no biomarkers or assays capable of accurately predicting viral rebound time. Therefore, the most reliable method for evaluating the effectiveness of a new therapeutic intervention in controlling HIV is ATI. Studies have demonstrated that short-term ATI is generally safe for PWH and does not significantly impact the size or diversity of the latent reservoir (Salantes et al., 2018). Between 2000 and 2017, 150 interventional clinical trials have incorporated ATI (Lau et al., 2019). However it is important to acknowledge that ATI carry certain risks. Concerns about potential health risks for individuals undergoing long-term ATI have led to the inclusion of frequent viral load monitoring, prompt treatment resumption, and transmission prevention criteria in trial designs (El-Sadr et al., 2006; Julg et al., 2019).

It is worth noting that repeated ATIs in individuals treated during PHI with high CD4+ counts, have been proposed to boost the immune response against HIV and inducing viral control, a concept known as the "auto-vaccination hypothesis" (Rosenberg et al., 2000). According to this hypothesis, brief viral bursts during ATI could strengthen the HIV-specific immune response and ultimately lead to viral control or a lower viral set point. Although ATI-induced auto-vaccination has not been confirmed by more recent studies (Fagard et al., 2003; Oxenius et al., 2002), Jain et al. showed that multiple ATIs, when structured alongside another therapeutic intervention, may contribute to generating an immune response that will contribute to viral control (A. Jain et al., 2024).

1.5.4 Non-ART approaches for cure

The limited known cases of HIV control off treatment have fueled hopes for a potential cure or long-term control but they come with risks and scalability issues as a treatment for the general population (Gupta et al., 2020; Hütter et al., 2009; Jensen et al., 2023). However, ART alone is not sufficient for achieving a cure, as as it does not eliminate or reduce the size of the reservoir. Therefore there is a pressing need to explore new cure strategies. Research efforts have been directed towards non-ART approaches to achieve post-treatment HIV remission. These efforts can be broadly categorised into two main strategies:

Targeting the reservoir

- *Shock (or Kick) and Kill*: using compounds called latency-reversal agents (LRAs) to induce the reactivation of HIV transcription in the reservoir in individuals on ART. This process exposes the infected cells to the host surveillance system and response, while ART prevents new infections (Deeks, 2012; Lee et al., 2022). The most extensively studied LRAs are histone deacetylase inhibitors (HDACi) and TLRs. However, the clinical application of this strategy has not yet yielded compelling results, particularly in terms of reducing the reservoir size (Darcis et al., 2017; Deeks et al., 2021; Martinsen et al., 2020).

- *Block and Lock*: aiming to prevent reactivation of the dormant reservoir through latency promoting agents (LPAs) that inhibit viral transcription. This is achieved by targeting viral proteins, such as Tat and In, cell signalling pathways or epigenetic proteins. LPAs can be small molecules like nucleic acids such as short hairpin (sh) or small interfering (si) RNA, or recombinant proteins. The main challenge of this approach *in vivo* is to ensure that it does not adversely affect other cellular functions (Deeks et al., 2021; Vargas & Sluis-Cremer, 2022).

- *Rinse and Replace*: another theoretical approach suggested by (Grossman et al., 2020) involved triggering polyclonal T-cell differentiation by inducing T cell activation with LRAs in order to replace the latent reservoir with healthy cells. This is based on the fact that clonal HIV populations "wax and wane" while on treatment. In this process, infected cells are eliminated due to the continuous activation, differentiation and cell death.

Immune-based Therapies

- *Gene and cell therapy*: modifying immune cell genes to render them resistant to HIV. The identification of CCR5 Delta 32, a mutation that prevents CCR5 from appearing on the cell surface and essentially renders the cells immune to HIV infection (Hütter et al., 2009), has inspired interest in therapies using genetically modified cells (Gero et al., 2024). Researchers have been prompted to harness the gene editing systems to knock CCR5 out of T-cells but these attempts, contrary to stem cell transplantation have not yet been successful in eradicating intact virus (Deeks et al., 2021). Another strategy is cell based therapies, such as chimeric antigen receptor (CAR) to create effector T-cells that recognise to target infected cells (Deeks et al., 2021). Clinical trials are currently testing the efficacy of the treatment in humans (NCT04648046). Finally, there have been attempts to use CRISPR-Cas to cut out the proviral genome from infected cells but the potential off-target effects and delivery issues dictate that this strategy needs more optimisation before it is safe and efficient to use in practice (Hussein et al., 2023).

- *Therapeutic vaccines*: aiming to stimulate the immune system against HIV. Several approaches are being explored in therapeutic HIV vaccine development to induce immune responses; viral vector vaccines, utilising adenoviruses to deliver HIV antigens into immune cells (Harris, 2022), DNA vaccines, using plasmid DNA encoding HIV that is injected straight into host cells and results in the production of viral proteins and dendritic cell vaccines (Barouch, 2008), where dendritic cells can be pulsed by HIV *ex vivo* and are

injected back into the host (García et al., 2013). The first vaccines to undergo clinical evaluation used gp120 to elicit nAbs whereas recently research has been focusing on vaccines that elicit CTL responses (Haynes et al., 2023). While T-cell vaccines alone have not achieved a functional cure, a recent clinical trial demonstrate improved viral control in participants who receive an HIVCAT T-cell immunogen (HTI)-based vaccine (Bailón et al., 2022). In the post-Coronavirus disease 19 (COVID-19) pandemic era, vaccines utilising the messenger RNA (mRNA) technology to encode viral antigens in the host cells, hold promise for the HIV cure field (Mu et al., 2021).

- *Broadly neutralising antibodies*: to neutralise a range of cell-free virus strains and to assist the immune system in targeting HIV. bNabs are discussed in section 1.6, in detail.

1.6 Broadly Neutralising Antibodies

One of the up-and-coming therapeutic approaches under current clinical development is the passive administration of bnAbs, which have been isolated from long-term non-progressors in the early 2000s. The dual functionality of antibodies is the reason why they are considered promising treatment agents; neutralisation of free viruses using their antigen-binding fragment (Fab) regions as well as inducing host immune responses through their crystallisable fragment or Fc regions Caskey et al. (2019). The mechanism of action of bnAbs is discussed in detail in section 1.6.1. Typically, most bnAbs are IgG class and they share some common features that account for their breadth and potency. The most well-know bnAb feature is SHM, which happens within the germinal centers as part of the B-cell affinity maturation process and the mutations are mainly targeted to the complementarity-determining regions (CDRs), which are in contact with the antigen (Victora & Nussenzweig, 2012). Contrary to other antibodies, mutations in the framework regions (FWR) benefit bnAbs as they can make them more flexible and allow for better contact with the antigen and thus ensure better and broader neutralisation (F. Klein et

al., 2013). Equally important is the length of CDRH3, which contains the most sequence diversity and potential to reach usually inaccessible epitopes (Griffith & McCoy, 2021; Haynes, 2015). However, the level of SHM and the length of CDRH3 may differ among antibodies that are classified into groups based on the Env epitope they target. Although antibodies cloned from specific memory B-cells are usually polyreactive, most of the new generation bnAbs are not highly poly- or self-reactive, which suggests that the risk for off-target binding and decreased specificity is small (F. Klein et al., 2013).

The structural characterisation of HIV-1 Env and its complexes with bnAbs has been instrumental in identifying key epitopes and critical binding residues. Advances in imaging techniques, along with the development of native-like Env trimers such as SOSIP (Sanders et al., 2013), have provided information on bnAb-Env interactions and enabled a more precise mapping of the critical binding residues on Env. Currently, seven different env regions are known to serve as bnAb epitopes (residue position numbering is based on the HxB2 reference sequence)

- ***V3 site;*** Interactions between variable 3 (V3) loop and CCR5 or CXCR4, are critical for viral entry. The most conserved regions of V3, its base and crown, are protected from nAbs under variable 1 and 2 (V1V2) loops (Rusert et al., 2011). Only upon binding to CD4, changes in the conformation of Env set of the displacement of V1V2 and expose V3 to allow its interaction with the co-receptors. As mentioned in section 1.3, humoral responses against the V3 region are the first to emerge during early infection, even though its neutralisation activity is practically non-existing (Friedrich et al., 2021). bnAbs targeting the V3 site are the most common in HIV infection and they have been shown to have good potency but limited breadth (51-68% neutralisation breadth) (Bricault et al., 2019; Haynes et al., 2023). The bnAbs in this group, such as 10-1074, PGT121 and PGT128, are able to use their long CDRH3 to interact with glycans (mainly the one attached at PNG N332), penetrate the glycan shield and contact with ^{324}GDIR^{326} linear

sequence at the V3 base (Bricault et al., 2019; Sok et al., 2016). A long CDRH3 means that V3 bnAb precursors are very rare, as B-cells with long CDRH3 BCRs are deleted by immune tolerance mechanisms (Haynes et al., 2023). Different bnAbs in this category may bind on Env from different angles and engage with a range of glycans, such as N301 (PGT128, PGT121), N127 and N156 (PGT121), and N386 and N392 (PGT135) (Barnes et al., 2018).

- ***CD4 binding site (CD4bs);*** The CD4 binding site is one of the most functionally conserved Env regions (Kwong & Mascola, 2012), as it mediates the viral binding to the CD4 receptors of the host cells. Despite its less accessible location within a pocket at the interface of the outer and inner domains, CD4bs can be contacted by antibodies depending on the approach angle (Griffith & McCoy, 2021). Primarily, CD4bs bnAbs rely on their CDRH2 regions to mimic the CD4 contact with Env (such as the VRC01- and 8ANC131/CH235- class bnAbs) but others, such as b12, VRC16 and VRC13, utilise their CDRH3 contacts (Freund et al., 2015; Haynes et al., 2023). VRC01-class bnAbs are the most potent and broad bnAbs and their precursors are more common than others (T. Zhou et al., 2013). Contrary to V3 bnAbs, CD4-mimic bnAbs have been shown to neutralise 80-100% of heterologous viruses (Haynes et al., 2023; Kwong & Mascola, 2012). 3BNC117 and N6 are reported to be the most potent CD4bs bnAbs (Ding et al., 2021). The residues recognised by these bnAbs lie within the inner domain, the Loop D, the CD4 binding loop, and the β_23/loop V5/β_24 region (Lynch et al., 2015; P. Zhou et al., 2019). Although glycans are not incorporated into CD4bs bnAb epitopes, as the CD4bs is not extensively concealed by the glycan shield, glycans surrounding the binding site may be recognised by the bnAbs.

- ***V1/V2 loop;*** Humoral response against the hypervariable V1V2 loops can block the structural conformation of the env trimer and prevent the exposure

of the co-receptor binding site, which is critical for viral entry (Griffith & McCoy, 2021). Those bnAbs targeting V1V2 (namely PG9, PG16, PGDM1400, CAP256.25, PCT64, and CH01) are generally the most potent and are able to neutralise ~70% of the global strains (Sok & Burton, 2018; L. M. Walker et al., 2009). Furthermore, V1V2 bnAb responses are the earliest to emerge, following V3 targeting bnAbs (Landais & Moore, 2018). The key epitopes of the known bnAbs in this class include the glycan attached to N160 and a protein motif on gp120 (Sok & Burton, 2018). Similar to V3 bnAbs, most of V1V2 bnAbs possess characteristically long CDRH3 (Landais & Moore, 2018).

- ***Membrane proximal external region (MPER);*** MPER is one of the most conserved env regions and therefore bnAbs targeting the MPER, such as 2F5 and 4E10, are very broadly neutralising but some may show low to moderate potency (Sok & Burton, 2018). In order to neutralise HIV, MPER bNAbs need to anchor to the viral lipid bilayer, which is the outer layer of the viral membrane and be kept in position to bind to the exposed MPER epitope as soon as it becomes accessible after the co-receptor binding (Haynes et al., 2023; Pinto et al., 2019). MPER bnAbs have been described to exhibit various levels of polyreativity, due to their conserved epitope and the similarities it shares with host-derived phospholipids and lipoproteins (Caillat et al., 2020).

- ***gp120/gp41 interface;*** the interface of gp120 and gp41 is the region where these subunits interact and undergo rearrangements to facilitate viral fusion and entry into the host cell. bNAbs targeting the interface, such as 8ANC195, PGT151 and 35O22, aim to disrupt this interaction by destabilising the timer or by inducing conformational changes (McCoy, 2018). The average breadth of these bNAbs is medium, at 64% (Griffith & McCoy, 2021). The epitopes of interface bnAbs might include glycans, such as N88, N234, N276, N611 or N637 (Wibmer et al., 2017).

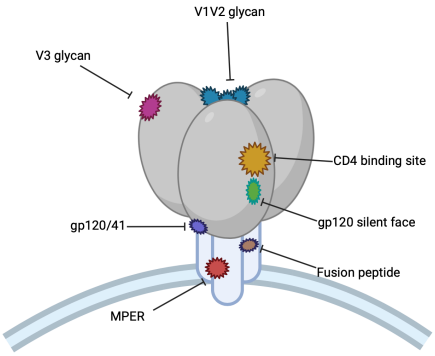

Figure 1.3: bnAb epitopes on HIV Env. Designed on Biorender.com

- ***silent face (SF) of gp120;*** The highly glycosylated silent face of Env is the most recently identified epitope and only two bnAbs targeting this region have been isolated so far, VRC-PG05 and SF12 (Schoofs et al., 2019). Although conserved glycans are incorporated in the epitopes of these bnAbs, their neutralisation breadth has been characterised as medium (Griffith & McCoy, 2021).

- ***fusion peptide (FP);*** the FP is located at the N-terminal region of gp41 and after the gp120 conformation reaches into the target host cell membrane and facilitates viral fusion (Shaik et al., 2019). bnAbs targeting the FP (ACS202 and VRC34.01) bind to the protein as well as recognise glycans (Banach et al., 2023; Yuan et al., 2019).

Similar to drug resistance, resistance to bnAbs may be either transmitted or acquired. Acquired or *de novo* resistance develops when wild-type HIV variants are initially suppressed by bnAbs, but selective pressure during viral replication when bnAb concentration falls below a therapeutic level allows bnAb-resistant mutations to emerge, ultimately leading to viral rebound. In contrast, transmitted resistance occurs when individuals who have never received bnAbs aquire pre-existing resistant variants, potentially compromising treatment effectiveness from the outset. In order to minimise the risk of developing resistance, two or more bnAbs, often targeting different Env epitopes are given in combination. This thesis is focused on therapy with a combination of 10-1074 and 3BNC117.

1.6.1 Mechanism of action and the "vaccinal effect"

bnAbs have three functional components; two antigen binding fragment (Fab) regions and a crystallisable fragment (Fc) region, linked together by a hinge region. Viral neutralisation occurs when the Fab region binds to Env on the viral surface, forming an immune complex that blocks the attachment or fusion of the virus to the target cell (Burton & Hangartner, 2016; Karuna & Corey, 2020). For instance, VRC01, prevents viral attachment to the target cell by binding on the CD4 binding site, preventing the interaction between the viral glycoprotein and the CD4 receptor on the target cell. Moreover, PGT121 and bnAbs in its family engage in allosteric modulation of the CD4 binding site and disrupt viral attachment, through interactions near the V3 loop (Haynes et al., 2015). In addition to free virus neutralisation, bnAbs are able to disrupt cell-associated HIV and cell-to-cell transmission, but unfortunately less efficiently (Karuna & Corey, 2020).

Beyond neutralisation, bnAbs facilitates viral clearance using their Fc-mediated effector functions. Upon binding to the viral antigens, bnAbs can bind on the Fc gamma receptors (FcγRs) expressed on the host immune cells, leading to antiviral actions. There exist several FcγRs, including one inhibitory receptor FcγRIIb and five activating, FcγRI (which is a high affinity receptor), FcγRIia, FcγRRIIc, FcγRIIIa and FcγRIIIb. The binding avidity of Fc-FcγR is enhanced when more than one Fab regions are bound to Env on a virion or an infected cell (Karuna & Corey, 2020). Notably, the expression of different FcγRs varies with the stage of disease; FcγRI is higher in PHI whereas FcγRIIa and FcγRIII are reduced at the stage of chronic infection, reflecting the HIV impact on the immune response (Duchemin et al., 2020). One prominent Fc-effector mechanism is antibody-dependent cellular cytotoxicity (ADCC). It occurs upon Fc-FcγRIIIa binding between the bnAb and an immune cell, most commonly an NK cell, and leads to release of perforin and granzyme B and the subsequent elimination of the target (Phelps & Balazs, 2021; Su et al., 2019). Additionally, immune complex binding to FcγRIa and FcγRIIa on macrophages can trigger antibody-dependent cellular phagocytosis (ADCP),

resulting in the internalisation and destruction of the viral antigen (Phelps & Balazs, 2021). Furthermore, the Fc region of bnAbs can interact with complement proteins in the blood, initiating complement dependent cytotoxicity (CDC). This leads to the destruction of viral antigens through the formation of pores on the membrane by the membrane attack complex (MAC) (Phelps & Balazs, 2021).

In addition to these effector functions, it has been suggested that immune complexes may have immunomodulatory effects and induce strong immune responses, which is known as "vaccinal effect" (Pelegrin et al., 2022; Tipoe et al., 2022), which was initially demonstrated in a murine leukemia virus infection model (Pelegrin et al., 2022). One of the key components is DCs, that following the Fc-FcγR enhance CTL response (Caskey et al., 2019). Neutrophils alone and in cooperation with monocytes also play an important role in inducing a post-antibody treatment immune response, by enhancing Th1-type cytokine and chemokine secretion (Naranjo-Gomez & Pelegrin, 2019; Pelegrin et al., 2022). Finally, NK cells serve two roles; firstly, they eliminate infected cells and control viral replication and as a result they prevent immune exhaustion as well as the establishment of immunosuppressive pathways. Furthermore, NK cells produce IFN-γ, which enhances B-cell helper properties of neutrophils and by extension enhances B-cell responses (Naranjo-Gomez et al., 2021). The impact of Fc-mediated antiviral response has been demonstrated in previous studies on protection of macaques against Simian HIV (SHIV), where they were given a b12 variant with reduced Fcs and had an increased likelihood of infection (Hessell et al., 2007). One of the most impressive cases of sustained virus-specific CTL response attributed to bnAb treatment of SHIV was reported in a study on macaques; one animal maintained very low viral loads and normal CD4+ T-cell counts for more than two years (Nishimura et al., 2017). Interestingly, viral suppression in the controller animals was maintained after bnAb concentration fell below therapeutic levels and it was mediated by CD8+ T-cells, as the virus rebounded after they received anti-CD8 antibodies. Evidence of boosted immune response after bnAb treatment has been been shown in humans as well. An increase in the neutralisation of heterologous

viruses was shown by Schoof et al. when they tested the plasma of PWH who had received treatment with 3BNC117 with controls (Schoofs et al., 2016). More recently, Niessl et al. documented an increase of gag T-cell responses in PWH who received a combination of 3BNC117 and 10-1074 during ATI (Niessl et al., 2020). Enhanced HIV-specific (Gag and Pol)T-cell immunity was also observed in viremic individuals who received 3BNC117 at ART initiation, in the eCLEAR study (Rosás-Umbert et al., 2022). Understanding the mechanisms underlying the vaccinal effect and obtaining compulsive evidence of its occurrence are important is of major interest in HIV cure, as it holds the key for improving bnAb treatment and achieving long-term HIV control.

1.6.2 Therapeutic potential of bnAbs

The isolation of bnAbs from individuals who developed them during natural infection has had a significant impact on the HIV cure field. This breakthrough has enabled the acquisition and utilisation of bnAbs in HIV treatment (F. Klein et al., 2013). Several bNAbs targeting different Env regions, as single agents or in combination with other bnAbs or other therapeutic interventions, have entered human clinical trials since 1992, yielding varying results in terms of their effectiveness in controlling HIV infection (Caskey et al., 2019). Among these, 10-1074 and 3BNC117 have emerged as the most extensively studied anti-HIV bnAbs currently in clinical development (Frattari et al., 2023). Passive administration of 10-1074 (Caskey et al., 2017) and 3BNC117 (Caskey et al., 2015) as monotherapy to viremic PWH was able to reduce viral load; however it was not sufficient to control the virus long term. When given to aviremic individuals, different dosages of 3BNC117 delayed viral rebound by 6.7 (2 doses) and 9.9 weeks (4 doses), on average (Scheid et al., 2016). The combination of 10-1074 and 3BNC117 in suppressed PWH demonstrated viral suppression for much longer than monotherapy - a median of 21 weeks (Mendoza et al., 2018), which was confirmed by other studies later (Gaebler et al., 2022; Sneller et al., 2022). Of note, when administered to viremic participants, the combination of 3BNC117 and 10-1074 was not as effective; although a reduction in

viremia was observed, full viral suppression was only seen in one participant with a low baseline viral load (Bar-On et al., 2018). This suggests that for bnAbs to be fully effective, viral suppression may first need to be achieved with ART. Only participants with chronic infection were recruited in the clinical trials mentioned above, and it is therefore it is suggested that treatment in primary infection may be more effective due to smaller HIV reservoirs and lower viral diversity.

In addition to neutralisation potency, the long-term efficacy of bnAbs in viral suppression depends on their sustained stability in circulation. The longer bnAb concentration is above therapeutic levels, the greater the resulting period of viraemic control. Figure 1.4 presents summary data from currently published clinical trials and shows that increasing numbers of doses of 3BNC117 alone or combined with 10-1074, result in longer periods of control in participants who interrupted ART immediately after receiving bnAbs. A Cox regression analysis using combined data from studies that report both baseline sensitivity and time to viral rebound, showed a 46% decrease in viral rebound per increase in number of bnAb doses (hazard ratio, HR: 0.54, 95% confidence interval, CI: 0.42-0.70, p-value = 0.00004) (Zacharopoulou et al., 2022).

An alternative approach to maintain the concentration of bnAbs in circulation for longer is by extending their half-life through modifications on the Fc region. Two mutations, M428L and N434S, have been identified to produce a long acting version of bnAbs, known as 'LS' (Zalevsky et al., 2010). Clinical trials to assess the efficacy of the LS variants of 10-1074 and 3BNC117 are currently underway (Lee et al., 2021) with the expectation that the LS modification will permit longer dosing intervals (~3-6 months) for effective treatment (Caskey & Kuritzkes, 2022).

1.6.3 The effect of bnAbs on the reservoir

bnAbs can bind to the Env on both virions and on infected cells (Naranjo-Gomez & Pelegrin, 2019). According to Michaud et al., immune complexes with infected cells, rather than with virions, trigger a CTL response via the Fc-FcγR binding to DC (Michaud et al., 2010). This is likely due to the presence of Gag epitopes on infected

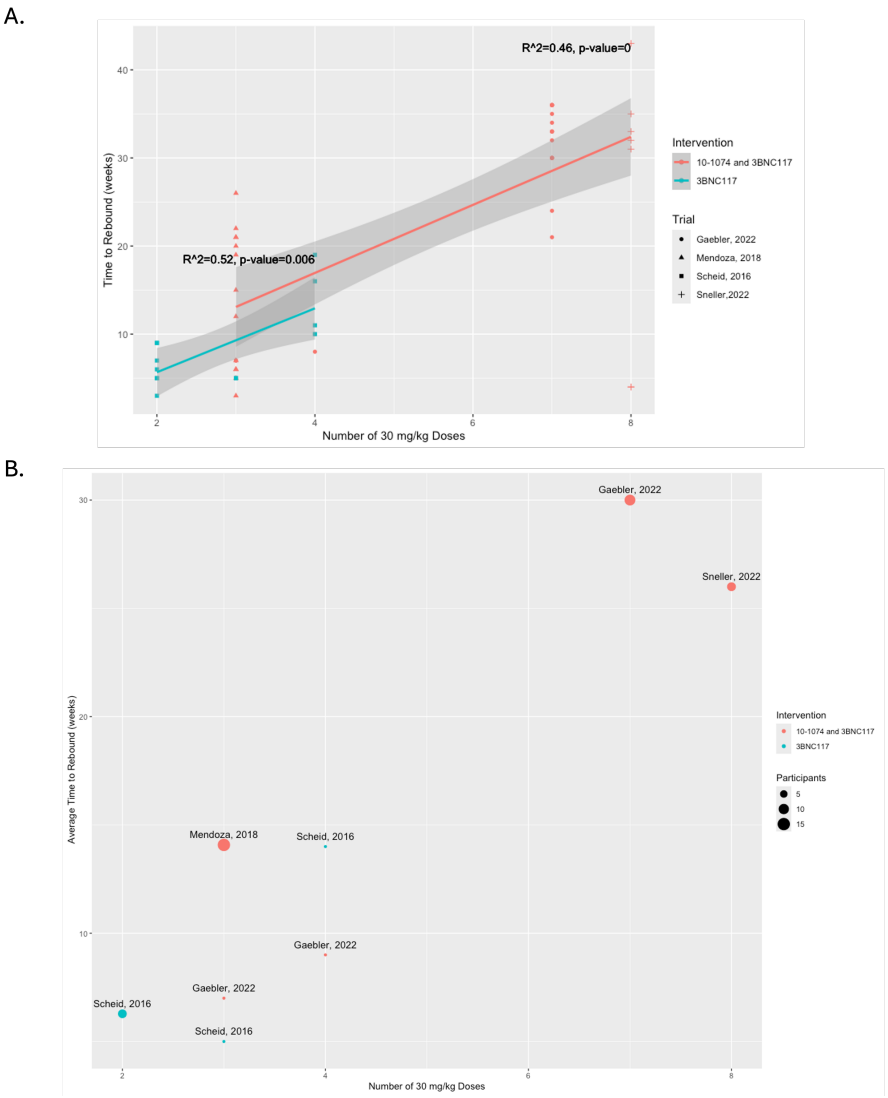

Figure 1.4: Average time to viral rebound after treatment with 10-1074 and 3BNC117 combination or 3BNC117 alone, in participants post ART interruption. The participants in these studies received different number of bNAb doses of 30 mg/kg. Time to viral rebound in weeks is shown on y-axis and number of bNAb doses is shown on x-axis. a. Individual study participants' time to viral rebound data points are shown and each study cohort is represented by a different shape. A fitted line per group (combination of 10-1074 and 3BNC117, and 3BNC117 monotherapy shows the association of number of doses with time to viral rebound. b. Each data point represents a study and their size reflects the number of participants in each arm.

cells, which are recognized by CTLs, while Gag incorporation into virions might be variable or incomplete. Considering that the expression of Env on cell surface is high during active replication and much lower on latent reservoir cells, it is expected that bnAbs would form immune complexes with productively infected cells more frequently than with latently infected cells (Schriek et al., 2024; Van Lint et al., 2013). This could potentially explain the high CD8+ T-cell responses observed in PWH with detectable virus, as shown in the eCLEAR study (Rosás-Umbert et al., 2022). The use of an LRA with 3BNC117 aiming to reactivate the latent cells and to subsequently clear the reservoir did not show any reservoir size reduction (Gruell et al., 2022). On the contrary, Gaebler et al. demonstrated a modest decline of the intact proviral reservoir after 10-1074 and 3BNC117 combination treatment, measured by the Q4PCR assay (Gaebler et al., 2022). This difference in findings could be attributed not only to host factors, such as immune exhaustion, or to the choice of bnAb but also to the assessment of the reservoir size. In all, more studies are needed in order to determine the effect of bnAbs on the reservoir size.

1.6.4 bnAb escape signals and screening for sensitivity

As mentioned in section 1.6, bnAb monotherapy is less likely maintain viral suppression long term due to development of bnAb resistance. Caskey et al observed that resistant clones were selected in all individuals who received 10-1074 (Caskey et al., 2017) and the majority of those who received 3BNC117 (Caskey et al., 2015) at rebound. Furthermore, a 2018 study showed that when 3BNC117 was administered in PWH who underwent ATI, pre-existing 3BNC117 resistance was a strong predictor of shorter time to rebound (Cohen et al., 2018). Pre-existing bnAb resistance detection is crucial in strategies employing combined bnAbs; Mendoza et al showed the difference in the length of viral suppression post treatment with 10-1074 and 3BNC117 between individuals with sensitive (median of 21 weeks) and resistant (median 5 weeks) proviruses at baseline (Mendoza et al., 2018).

Structural data, such as cryo-electron microscopy (cryo-EM) data of bnAb-Env complexes, can provide detailed information about the interaction between bnAbs

and Env and reveal the exact binding sites (section 1.6). However, the definition of these binding sites does not always explain the functional significance of these interactions. In some cases, the mutation of those identified Env residues may not show any impact on neutralisation when tested *in vitro* (Schommers et al., 2020), suggesting that these epitopes may not be as important in a biological framework. Mutations at sites away from the direct bnAb epitope may also induce changes in the conformation of Env thereby affecting bnAb accessibility (Parthasarathy et al., 2024).

Currently, the gold standard for assessing bnAb resistance in viral strains is neutralisation assays, such as the TZM-bl and the Phenosense assays (Patel & Dubé, 2023; Scheid et al., 2016). These phenotypic resistance assays involve infecting HeLa-derived TZM-bl cells—engineered to express CD4, HIV co-receptors, and tat-driven luciferase reporter genes—with a pseudotyped virus carrying the Env of interest. Neutralisation activity is then measured by comparing infection rates in the presence and absence of bnAbs. For this assay to be clinically relevant, it is crucial to isolate and characterise intact proviruses that accurately represent the entire viral reservoir. However, this process is resource-intensive, time-consuming, and may be challenging to interpret in a clinical setting (Hsu et al., 2021; Pahus et al., 2024). Additionally, factors such as differences between *in vivo* and *in vitro* viral reactivation, viral recombination within the host, and reservoir compartmentalisation may compromise assay accuracy (Mendoza et al., 2018). Epitope mapping studies have identified mutations that confer bnAb resistance, facilitating genotypic approaches that provide a binary prediction of bnAb sensitivity—similar to genotypic assays used for antiretroviral drug resistance (Bricault et al., 2019; Dingens et al., 2019; Lynch et al., 2015; Mouquet et al., 2012). However, as demonstrated by Gaebler et al., genotypic predictions performed poorly compared to neutralisation assays in identifying resistant clones in pre-bnAb samples from people with HIV (PWH) who later rebounded with 10-1074-resistant viruses (Gaebler et al., 2022). Notably, *post hoc* neutralisation assays from individuals with PHI enrolled in a 10-1074 and 3BNC117 trial revealed a correlation between baseline bnAb sensitivity

and improved treatment response. Advances in next-generation sequencing and bioinformatics over recent years have led to the development of various *in silico* bnAb sensitivity prediction methods, which may enhance the accuracy of genotypic resistance assays (Salazar-Gonzalez et al., 2008; Travers et al., 2010).

Several computational tools have been developed to predict HIV-1 sensitivity to bnAbs using viral genetic sequences. These tools use various machine learning techniques ranging from rule-based methods to advanced deep learning models, to improve bnAb sensitivity prediction. Some of the earliest approaches, such as those developed by West et al. (West Jr et al., 2013) and Hepler et al. (Hepler et al., 2014) employed decision trees and flexible machine learning algorithms to identify critical residues associated with neutralisation, which could then be used for screening of bnAb resistance in a manner similar to HIV drug resistance genotyping. As machine learning techniques evolved, bnAb sensitivity prediction transitioned from simple feature selection methods to more sophisticated algorithms capable of predicting neutralisation values or probabilities. Notable approaches include random forests (Bricault et al., 2019), Support Vector Machines (SVM) (Hake & Pfeifer, 2017), Gradient Boosting Machine (GBM) (Rawi et al., 2019) and ensemble methods (Williamson et al., 2021). To train, these models use paired neutralisation and env sequences.

A key resource for training bnAb sensitivity prediction models is CATNAP (Compile, Analyze and Tally NAb Panels), a large collection of Env sequences with paired neutralisation data, including IC50 and IC80 values (half-maximal and 80% inhibitory concentrations, respectively) (Yoon et al., 2015). Nevertheless, data for bnAb-resistance sequences for some broad bnAbs, such as 3BNC117 is limited. This may explain the low prediction performance of models when compared to the *in vivo* response to bnAb treatment (Hake & Pfeifer, 2017; Rawi et al., 2019; Yu et al., 2019). In addition, most tools are primarily built upon genomic data of bnAb epitopes and only a few approaches incorporate additional features that influence bnAb binding, such as PNGs (Yu et al., 2019) or even regions outside the predefined epitope sites (Rawi et al., 2019). Interestingly, Meijers et al. employed

a bnAb resistance evolution model that factors in the fitness cost of resistance-associated mutations (Meijers et al., 2021). The model was trained on a small dataset but it suggested that viral escape from bnAbs can be predicted based on intra-host parameters (such as antibody levels and degree of viremia) rather than solely on resistance-conferring mutations.

There is no universal gold standard for bnAb sensitivity prediction, and the choice of tool depends on the specific application. bnAb-ReP by Rawi et al. (Rawi et al., 2019) has been applied in studies examining the prevalence of bnAb resistance (Moraka et al., 2023). While bnAb-ReP provides a more biologically realistic, probabilistic output that reflects the spectrum-like nature of neutralisation sensitivity, setting a threshold is challenging when it comes to clinical practice, where a clear decision point is required. Meanwhile, adaptations of the West et al. algorithm (West Jr et al., 2013)] have been used in high-profile clinical trials to screen for 10-1074 sensitivity (Caskey et al., 2017; Gaebler et al., 2022; Lee et al., 2021; Mendoza et al., 2018) due to its interpretability and the biological relevance of its, otherwise oversimplistic, predictions.

Prediction accuracy notwithstanding, obtaining an adequate number of single HIV sequences that represent the full diversity of circulating viruses or latent proviral sequences is yet another challenge. SGA and sequencing, as discussed in section 1.2.3, is not sufficiently high-throughput; incorporating elements such as capturing single, intact viruses prior to amplification (Gaebler et al., 2021; Levy et al., 2021) in the assay would increase both time and cost efficiency of the process. The combination of improved techniques to achieve high numbers of single genomes, greater sequencing read-length technologies, improved bioinformatic and machine learning approaches, and larger, robust training datasets with integrated functional and clinical data are all key to developing a reproducible and accurate resistance-prediction methodology.

1.7 Summary and Research Questions

While ART effectively controls HIV replication, the latent HIV reservoir persists, posing a barrier to cure. bnAbs, such as 10-1074 and 3BNC117, represent promising novel interventions with the potential to target not only circulating virus but also eliminate infected cells and induce the host immune response to provide long term viral control. Some people who receive ART or bnAbs are able to maintain viral control for months or even years, possibly due to protecting strong immune responses and in the case of bnAb treatment, the "vaccinal effect". Identifying biomarkers that correlate with time to rebound or controller phenotypes may elucidate these mechanisms. Viral resistance to bnAbs is an emerging concern as it limits their efficacy but pre-screening for resistance is a topic of ongoing debate. Currently resistance is identified by costly and laborious *in vitro* neutralisation assays but but there is a need for more efficient methods in routine clinical practice. Genotyping assays paired with *in silico* prediction models have recently become available and used in clinical trials to screen for bnAb sensitivity.

My thesis explores the interplay between host and virus by investigating two key aspects of HIV persistence and control. It is therefore divided into two parts; a virology component and an immunology component. To achieve this, I am using molecular biology assays and sequencing technologies to study HIV *env*, to examine how it evolves during different stages of infection and how these changes may influence the response to bnAbs. Additionally, I employ transcriptomic analyses to identify genetic signatures associated with post-ART control, to assess the impact of bnAbs on the host immune response, including the vaccinal effect, and if, possible, to compare the findings in order to determine the similarities and differences of the control mechanisms in those cases.

The objectives of this thesis are to;

1. Estimate the prevalence of bnAb resistance in key populations of PWH living in the UK.

2. Assess the impact of bnAb resistance mutations in viral control in pre- and post-treatment samples of PWH who received 10-1074 and 3BNC117 treatment.

3. Employ bulk RNA sequencing to study the gene expression of CD4+ T-cells in PTC versus normal progressors, aiming to identify biomarkers of control through bulk RNA-seq.

4. Use single cell RNA sequencing to explore the differences in gene expression of PWH who received bnAbs and maintained viral control for different lengths of time, with the goal of identifying biomarkers associated with the vaccinal effect.

2

Materials and Methods

Contents

2.1 Ethics Statement

All research was performed following relevant guidelines and regulations, and all participants in RIO, SPARTAC, BONDY and HEATHER gave written informed consent to participate. Recruitment to the HEATHER cohort was approved by the West Midlands-South Birmingham Research Ethics Committee (reference 14/WM/1104). Recruitment to BONDY was approved by the London-Stanmore REC (reference 18/LO/1474). SPARTAC was approved by ethics committees in all countries that recruitment was opened. Recruitment to the RIO trial was approved by the London -Westminster Ethics Committee (reference: 19/LO/1669).

2.2 Cohorts

2.2.1 SPARTAC

SPARTAC (Short-Course Antiretroviral Therapy in Primary HIV infection) was an multicentered, open-label randomised, controlled aiming to determine whether short-term ART during PHI can delay loss of CD4+ T-cells up to 350 cells/mm^3 or long term ART would be necessary (The SPARTAC Trial Investigators, 2013). In total 366 participants were enrolled from 8 countries across Europe, Australia, Africa and South America. A 60% of participants were male and 58% had B clade HIV. Only female participants were recruited in SPARTAC in Uganda and South Africa, as recruitment was linked to a vaginal microbicide study. Participants were randomised to either 48 weeks (123 participants) or 12 week of ART (120 participants) and then undergo ATI, or no treatment at all (123 participants), which was at the time the standard of care. Study visits were scheduled at 0, 4, 12, 16, 24, 36, 48, 52 and 60 weeks and then every 12 weeks until the end of the follow-up period, which was completed in 2010, and blood was collected at every study visit. CD4+ and CD8+ T cell counts and viral load (VL) were measured at every study visit. Peripheral blood mononuclear cells (PBMCs) and plasma were isolated and cryopreserved. Time to viral rebound was estimated as time from

ATI to the first two consecutive VL measurements above 400 copies/mL. For those who did not rebound during the follow-up, the date of their last VL report was noted. The clinical data provided for this thesis were collected and analysed by the Medical Research Council clinical Trials Unit (MRC CTU).

Samples from the SPARTAC trial used in this thesis were selected based on their clinical features, such as time to rebound post ATI and/or the availability of longitudinal samples.

2.2.2 HEATHER

HEATHER (HIV Reservoir Targeting with Early Antiretroviral Therapy) was a prospective observational cohort study investigating the impact of early ART initiation on the HIV reservoir of PWH (Martin et al., 2018). The study recruited 442 participants during PHI, either prior to ART initiation (HEATHER A arm) or after they has started ART but fulfilled the set criteria for PHI retrospectively (HEATHER B arm). Most participants were male (424 participants, 96%) and had mainly B clade HIV (41%). The recruitment was conducted in London, at Chelsea and Westminster Hospital, Guy's and St Thomas' and at Imperial NHS Trusts. Study visits where scheduled at 0, 1 (HEATHER A only), 3 (HEATHER A only) and 6 months after enrollment and then every 6 month until the end of the follow-up period. Blood samples were collected at every study visit and PBMCs and plasma were isolated and cryopreserved at every study visit. CD4+ and CD8+ T cell counts and VL were measured at every visit.

Samples from HEATHER used in this study were from those participants who expressed interest in enrolling to RIO and were pre-screened for bnAb sensitivity.

2.2.3 BONDY

The BONDY study (Bone Density in Youth Living with Perinatally-Acquired HIV) is a longitudinal, observational study which aimed to evaluate bone health in 130 young (>15 years old) PWH, who attended the Imperial College Healthcare NHS Trust "900 clinic". The BONDY participants were of a median age of 21 years

and were perinatally infected, were mainly female (57%) and of black ethnicity (82%) (Henderson M.S.C., Fidler S., Cheung M., 2023). Clade information was not available for all participants. Participants in this study were adolescents and young adults aged 15 years or older under lifelong follow up with more than 75% on suppressive ART. Two study visits were scheduled, one at baseline (for all participants) and one 12 months after (only for those participants > 25 years old), at which blood and urine samples were collected. BONDY participants represent a group of PWH who may benefit from a less intensive form of HIV treatment, such as bnAbs. Given their potential suitability and the availability of relevant samples collected during the BONDY study, a subset of these participants was included in a bnAb sensitivity sub-study.

Table 2.1: Summary table of SPARTAC, HEATHER and BONDY demographics

Feature		SPARTAC	HEATHER	BONDY
Intervention		RCT; ATI post 48 or 12 weeks of ART, or standard of care	Observational	Observational
Stage of HIV at enrollment		PHI	PHI	Perinatally acquired HIV
Participants enrolled		366	442	130
Sex	Male	219	424	56
	Female	147	16	74
Age		32 (19-63)	34 (14-66)	21 (18-24)
Clade	B	208	181	NA
	C	120	7	NA
	Other/NA	36	254	NA
Ethnicity	White	NA	358	2
	Black	NA	21	107
	Other	NA	63	21
Country of enrolment	Europe/ Australia/US	212	442	85
	Africa	137	0	0
	Other	17	0	0

2.2.4 RIO

RIO is an ongoing randomised, placebo-controlled, double-blinded prospective phase II study of the efficacy of two bnAbs, 10-1074-LS and 3BNC117-LS (Lee et al., 2021). The recruitment target of this study is 72 participants with PHI, to be randomised in two arms via a two-stage design. In stage A, arm A (36 participants) is given a dose of the long acting version (-LS) of each bnAb (10 mg/kg for 10-1074 and 30 mg/kg for 3BNC117), while arm B (36 participants) receives placebo. Following this, participants in both arms are asked to stop ART. In case of viral

rebound, participant and researchers are unblinded and restart ART. If in arm A, participants complete the study and if in arm B, participants are invited to proceed to stage 2, where they will receive open-label bnAbs followed by a second ATI after 24 weeks. A subset of participants received a second dose of bnAbs 20 weeks after the first, provided that they have had not experienced rebound. Participants in Arm B received the second dose while on ART and remained on ART for another 24 weeks. The first endpoint for RIO is time to viral rebound within the first 20 weeks of TI. The participant demographics of this trial are presented in detail in Chapter 7.

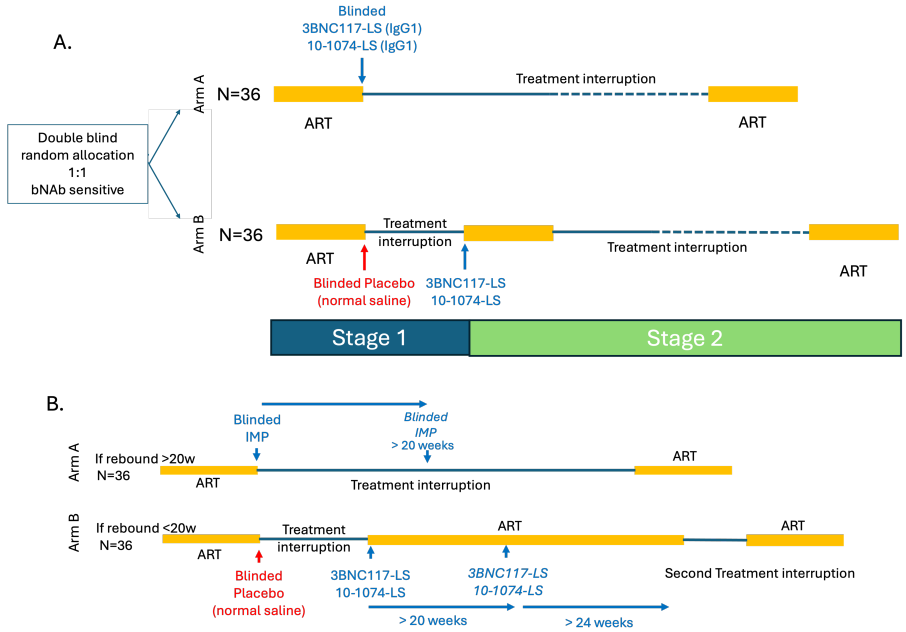

Figure 2.1: The RIO trial study design. (A) Original study design. (B) Phase 2 design

The primary endpoint for RIO was the time of viral rebound was defined as the first timepoint that viral load was measured above 1000 copies/mL and led to viral rebound. Eligible participants should have no documented resistance to bnAbs. For this reason, candidate samples (DNA from peripheral blood) are screened for bnAb resistance prior to recruitment using the method described in section 2.3.

2.2.5 Publicly available datasets

The "curated alignments" section in the los Alamos database (www.hiv.lanl.gov) host a large number of aligned HIV sequences, grouped by project. An alignment of the year 2020 Env sequences, which were deposited in GeneBank, was downloaded from the Web Alignments, where only one sequence per participant is included and problematic sequences are removed. The alignment was processed so that out of 6516 sequences, only 2425 sequences classified as clade B, with a documented year of publication and defined amino acids in the 10-1074 and 3BNC117 residues were retained.

An alignment of HIV DNA sequences from 11 male participants with clade B enrolled in the Multicenter AIDS Cohort Study (MACS) study (Shankarappa et al., 1999), as well as the clinical metadata, was also downloaded from the "special interest alignments" section of the Los Alamos database. This was a prospective study collecting samples from men with HIV living in the United States of America between 1985 and 2019 (Kaslow et al., 1987). The sequences span regions C2-V5 in env and were amplified with limiting dilution PCR for single-genome resolution (Shankarappa et al., 1999).

2.3 bnAb sensitivity screening

2.3.1 PBMC isolation, and DNA and viral RNA extraction

PBMC and plasma for RIO and SPARTAC were isolated at Imperial College London and the samples (PBMCs, plasma and DNA) were shipped to Oxford for storage and downstream assays. Blood samples taken from HEATHER participants were shipped and processed in Oxford. Briefly, blood samples in acid-citrate-dextrose (ACD)-anticoagulated collection tubes were transfered in pre-centrifuged Leukocep tubes containing Lymphoprep (Stemcell Technologies) and centrifuged. Plasma was collected and placed in a -80 C freezer for long term storage. The PBMC layer was transfered into flasks with R0 and centrifuged. PBMCs were transfered to new tubes and washed twice with R10. PBMCs were counted using

a Muse Cell Analyser (Merck Millipore) and they were resuspended at 1 x10^7 cells/mL in freezing mix and aliquoted in CryoTube vials (ThermoFisher). The vials were kept in a Mr Frosty (Nalgene) at -80 overnight and transfered to liquid nitrogen tanks the day after for long term storage.

Genomic DNA was extracted from screening samples either after isolation of PBMCs or directly from blood, if taken in PAXgene tubes (Qiagen). DNA from PBMCs was extracted using the QIAmp Blood Mini kit (Qiagen) as per manufacturer's instructions, including the RNAse-H step. DNA was eluted in RNAse/DNAse free water and stored short term at 4. DNA from whole blood in PAXgene tubes was extracted using the PAXgene Blood DNA Kit (Qiagen).

Viral RNA was extracting using the Qiagen Viral RNA Extraction kit from cryopreserved plasma, as per manufacturer's instructions. A double elution in 2 x 40 ul AVE buffer was performed and RNA was aliquoted into volumes suitable for single use in order to avoid freeze/thaw cycles and stored long term at -80 C.

2.3.2 Single Genome Amplification

SGA is a limited dilution nested PCR used to amplify the DNA of a single cell. HIV *env* was amplified with single genome amplification in 96-well plates. To achieve a Poisson distribution, where a maximum of 30% wells yields a product, the appropriate dilution factor was calculated for each sample. Nested PCR with Platinum Taq (Invitrogen) was used to amplify *env*, with 2 sets of *env* primers:

envB5out	5'-TAGAGCCCTGGAAGCATCCAGGAAG-3'
envB3out	5'-TTGCTACTTGTGATTGCTCCATGT-3'

in the first round and

envB5in	5'-CACCTTAGGCATCTCCTATGGCAGGAAGAAG-3'
envB3in	5'-GTCTCGAGATACTGCTCCCACCC-3'

in the second round. The first round PCR was run at:

Temperature (degrees Celsius)	Time (minutes)
94	02:00
94	00:15
58.5	00:30
68	03:00
	repeat steps 2-4 for a total of 35 cycles
68	15:00
4	for ever

For the second round, 1 ul of the first-round product was used as a template and the mix was run at

Temperature (degrees Celsius)	Time (minutes)
94	02:00
94	00:15
61	00:30
68	03:00
	repeat steps 2-4 for a total of 45 cycles
68	15:00
4	for ever

If no product was amplified, an alternative set of outer primers (half-genome amplification protocol)

R3B6R	5'- TGAAGCACTCAAGGCAAGCTTTATTGAGGC-3'
B3F3	5'-TGGAAAGGTGAAGGGGCAGTAGTAATAC-3'

was used in the first round and envB5in and envB3in were used in the second round. The first round thermocycler protocol is the following:

Temperature (degrees Celsius)	Time (minutes)
94	02:00
94	00:15
55	00:30
68	05:00
	repeat steps 2-4 for a total of 44 cycles
68	15:00
4	for ever

and the second round protocol is the same as for envB5in and envB3in.

If there was no amplification, an alternative set of inner primers could be used with R3B6R and B3F3:

envB5in	5'-CACCTTAGGCATCTCCTATGGCAGGAAGAAG-3'
B3807	5'-GTCTCGAGACGCTGGTCCTACTC-3'

The thermocycler protocols are the same as for R3B6R and B3F3 (first round) and for the envB5in and envB3in (second round). The end products were run on 1% 96-well E-gels (Invitrogen) in a 1:5 dilution with ultra pure water.

2.3.3 cDNA synthesis

env cDNA synthesis from viral RNA was performed using plasma samples, taken during viremia. cDNA was amplified from viral RNA using the SuperScript V First Strand Synthesis System (ThermoFisher), as per manufacturers instruction. In order to achieve maximum efficacy I used the same antisense *env* primer used to amplify *env* DNA of the same participant sample at screening, if successful. If not, I used the Oligo d(T) primer provided with the kit. I have also increased incubation time to 50 minutes to optimise reverse transcription.

2.3.4 Next Generation Sequencing

env amplicons were multiplexed and sequenced in pooled libraries using a custom library preparation protocol. In short, for each library 96 PCR products are diluted 1:5 in a 96-well plate. TDE1 fragmentation enzyme (Illumina) is added in each well to fragment the amplicons and to create sticky ends. A unique combination of barcodes (Illumina) and KAPA HiFi HS Ready Mix polymerase (Roche) is added in each well and the plate is thermocycled using the following protocol:

Temperature (degrees Celsius)	Time (minutes)
72	03:00
98	02:45
98	00:15
62	00:30
72	01:30

Temperature (degrees Celsius)	Time (minutes)
4	repeat steps 2-4 for a total of 8 cycles for ever

After barcoding samples from 8 wells are combined in 12 tubes.

For the clean-up step AmpureXP beads (Beckman Coulter) were added in each tube and after a 5 minute incubation they were put on a magnet until clear. After two washes with 80% ethanol the beads are left to dry for 2 minutes at room temperature. EB elution buffer is then added and the tubes are put back on the magnet until the eluate is clear. The supernatant from all tubes is then transferred to a new tube. The pooled library is sequenced in MiSeq NanoCatridge V3 (150x PE) (Illumina) and sequenced in a MiSeq (Illumina). The output is delivered in demultiplexed fastq files.

2.3.5 Sensitivity prediction with in silico models

The fastq files were processed using a custom computational pipeline, written in python and R and wrapped in bash by the Nussenzweig group, at the Rockefeller University (Gaebler et al., 2022). Both models are trained using paired neutralisation and sequencing data from the CATNAP database (Yoon et al., 2015). The pipeline starts with discarding non-HIV sequences and aligning the remaining ones to the most appropriate HIV reference to build a consensus sequence for each sample. This consensus is used as a reference to re-align all the reads from the sample to. The algorithm then inspects the reads for nucelotide variance per position and discards all reads with less than 70% nucleotide consensus in more than one position within *env.* A final consensus sequence is built per sample and translated to protein.

Sensitivity is predicted using the Rockefeller model, which is based on a model by West et al. (West Jr et al., 2013) (Figure 2.2) and built by the Nussensweig group (Gaebler et al., 2022) A second model, bnAb-ReP (Rawi et al., 2019), was

used for parts of this thesis. bnAb-ReP is a machine learning algorithm trained using a tree-based technique, gradient boosting machine.

The Rockefeller model assesses sensitivity to bnAbs by inspecting the sequence for the presence of specific amino-acid residues:

10-1074	325D/N, 330H/Y, 332N, 333notP, 334S/T
3BNC117	279D/N, 456R, 457D, 458G,459G

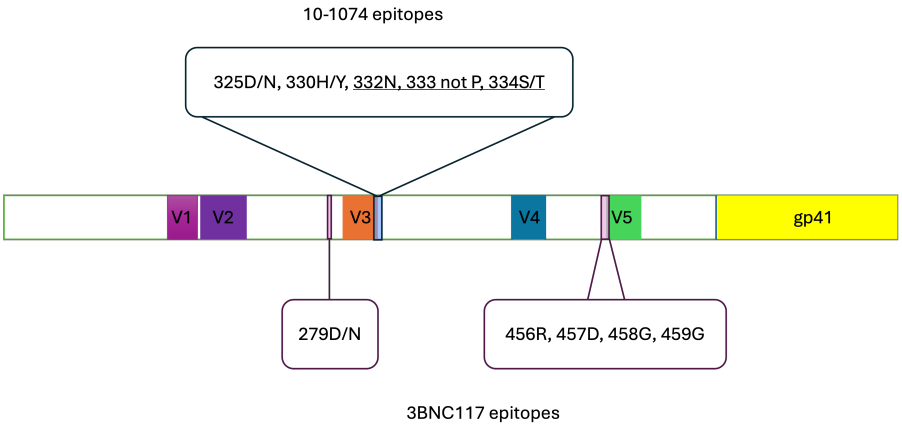

Figure 2.2: The 10-1074 and 3BNC117 epitopes on HIV env. The relative positions of the bnAbs epitopes are shown on HIV Env, along with the positions of the variable regions. The 332 PNG, which is a 10-1074 epitope, is underlined.

bnAb-ReP also uses Env sequences to predict bnAb resistance. In brief, during its training, the model assigns importance scores to sequence features that are found to contribute to its bnAb -specific neutralisation predictions. The output is a neutralisation score, where 0 = 0% neutralisation probability and 1 = 100% neutralisation probability.

2.3.6 Phylogenetic analysis

Neighbour-joining (NJ) phylogenetic trees of protein sequences were constructed using the R package ape to check for inter-sample contamination (Paradis & Schliep, 2019). Maximum likelihood nucleotide trees were built for each individual, using Fastree on NGphylogeny.fr. The trees were rooted on an outgroup sequence (HXB2), which was then pruned while maintaining the tree structure and the

position of the root. Ancestral state reconstruction was performed to estimate bnAb sensitivity of the internal nodes and root. Ancestral state reconstruction was done using R packages ape and trees were visualised using ggplot2 (Wickam, 2016).

2.4 Gene expression analysis from bulk

2.4.1 mRNA extraction and sequencing

CD4+ T-cells were isolated using negative selection (Stem Cell Technologies CD4 enrichment kit) according to the manufacturer's recommendations. Total RNA was extracted using the Qiagen RNA Kit with Qiashredder columns. Material was quantified using RiboGreen (Invitrogen) on the FLUOstar OPTIMA plate reader (BMG Labtech) and the size and integrity analysed on the 2200 TapeStation (Agilent, RNA ScreenTape). Input material was normalised to 100 ng prior to library preparation. Polyadenylated transcript enrichment and strand specific library preparation was completed using NEBNext Ultra II mRNA kit (NEB) following manufacturer's instructions. Libraries were amplified on a Tetrad (Bio-Rad) using in-house unique dual indexing primers. Individual libraries were normalised using Qubit, and the size profile analysed on the 2200 TapeStation. Sequencing was performed using an Illumina Novaseq6000 platform at 150 paired end mode (Illumina).

2.4.2 Gene expression analysis

Alignment was performed with performed with STAR, using Hg19 as the reference and downstream analysis was performed in R.

DESeq2 (Love et al., 2014) was used to compute differential gene expression (DGE) between phenotypes using a featurecounts table. The dataset was filtered for low count reads (>10 reads in 60% of samples). Only genes with a DGE of adjusted p-value of <0.05, after adjusting for multiple testing using Benjamini-Hochberg, and $\log_2$ fold change >1 were considered statistically significant. Gene Set Enrichment Analysis (GSEA) (Mootha et al., 2003; Subramanian et al., 2005)

was used to detect differences in biologically relevant pathways in the dataset. The datasets were pre-ranked by the DESeq2 Wald statistic value. Gene set permutation was set at 1000. Gene sets in the peer-reviewed Reactome pathway database (Jassal et al., 2020) were used as reference. Results satisfying a False Discovery Rate (FDR) cut-off of <25% were considered statistically significant.

Weighted gene Co-expression Network Analysis (WGCNA) is an R package used for gene expression profiling (Langfelder & Horvath, 2008; B. Zhang & Horvath, 2005) and was applied to the identification of genes associated with time to rebound. After pre-processing for low variance, filtering and outlier removal, an appropriate soft-threshold power was selected to promote and penalise the strong and weak gene connections, respectively. Following this, a signed network was created using the one-step approach, according to the package vignette. Genes were organised in modules, based on a common expression pattern and a colour-label was attributed to each to assist identification. The expression of the genes in each module was summarised in an eigenvalue, which was then correlated with the trait of interest to identify the most biologically relevant modules. The modules that were selected for downstream analysis were the ones that has a significant correlation with the trait. The most connected genes (hub genes), which are of functional significance, were defines by their Module Membership (MM>0.8) and their Gene-Trait Significance (GS>0.2) measured with Pearson correlation. The module genes were also uploaded on STRING, an online tool for pathway enrichment, gene ontology annotation and protein-protein interaction visualisation (Szklarczyk et al., 2019) in order to cross-validate the hub genes. Only genes that satisfied the connectivity as well as GS and MM score criteria were considered true hub genes.

Survival analysis was performed using an R package(Terry, 2020).

2.5 Gene expression analysis with Single Cell Sequencing

2.5.1 RNA encapsulation in droplets and cDNA amplification

For this experiment, the Chromium Single Cell 5' Next GEM v2 protocol and reagent kits from 10x Genomics were used, following the manufacturer's guidelines. Samples from 8 RIO participants were processed in two batches on different days. All samples from the UT timepoint were processed first, followed by samples from the UJ timepoint, using the same protocol. Briefly, PBMCs were thawed, washed to remove debris, and counted for viability using an automated cell counter. The cell recovery target was 10000 cells per sample. Therefore, a cell mix consisting of the appropriate volume of 1200 cells/mL and water was loaded into each K well of the Chromium chip. Barcoded GEM beads and partitioning oil were also added to the corresponding wells in the same chip. Encapsulation was performed in the Chromium X in a CL3 environment.

After encapsulation, droplets were collected, and barcoded cDNA was transcribed. The cDNA was then cleaned up and amplified. Each sample was quality-controlled for size and concentration using a Bioanalyzer. Based on the Bioanalyzer traces, 1 ţL of cDNA from each sample was used for TCR amplification, while up to 20 ţL of cDNA was taken forward for Gene Expression (GEX) library construction.

GEX library preparation involved fragmentation of the cDNA, followed by end repair to improve adaptor ligation efficiency. Size selection using SPRI beads was then performed to remove fragments outside of the desired size range. Adapters were ligated to the selected fragments, and samples were indexed to allow for pooling into a single library. A final size selection step and Bioanalyzer QC were conducted to ensure library quality.

2.5.2 Sequencing and analysis

The libraries were sequenced using Illumina NovaSeq X Plus 150 PE, with a depth of 20000 rads per cell per sample in the library. The data were demultiplexed and aligned on the human transcriptome using CellRanger v8 on cloud.10xgenomics.com. Individual seurat (Hao et al., 2023) objects were created using the aligned reads from each sample and the corresponding metadata. Mitochondrial and ribosomal genes (>10%) were regressed out and the most informative genes are identified based on their variance across cells. Principal component analysis (PCA) is performed to reduce dimensionality of data and identify the most significant source of variation. The appropriate number of principal components (PC) then the nearest neighbors are found for each cell based on the PC selected. Next, clustering is performed to group cells with similar expression profiles together. All individual seurat objects are then integrated in a single object in order to combine data and identify shared cell types. To do this, corresponding cells (anchors) between the different datasets are identified based on the expression of selected features. The integrated seurat object was normalised and scaled, variable features were identified, and clustering was performed based on a number of PC selected to contain the most variable genes. Cluster annotation, differential gene expression and pathway analysis was performed downstream, using seurat functions (Hao et al., 2023).

3

Prevalence of resistance-associated viral variants to bnAbs in key populations of people with HIV

Contents

3.1 Context

Treatment with bnAbs, especially with 10-1074 and 3BNC117, shows great promise as a therapeutic intervention for HIV and has been under investigation in clinical trials (Bar-On et al., 2018; Gaebler et al., 2022; Lee et al., 2021; Mendoza et al.,

2018; Sneller et al., 2022). These bnAb demonstrate potent neutralising activity against a wide range of strains; when tested in a panel of 118 strains, 10-1074 was very potent, although with a reported breadth of 63%. 3BNC117, on the contrary, displayed less potency but a much broader neutralisation activity of 89% when tested in the same panel (Griffith & McCoy, 2021). However, the presence of bnAb-resistant proviruses integrated into latently infected cells prior to bnAb exposure, could compromise bnAb efficacy (Cohen et al., 2018; Gunst et al., 2022; Mendoza et al., 2018). This raises concerns about bnAb treatment failure not only for PWH receiving the treatment but more widely, due to the potential for transmission of bnAb-resistant strains, as documented for ART drug resistance (Clavel & Hance, 2004). Successful roll-out of 10-1074 and 3BNC117 as a widely-used therapeutic intervention will be dependent on understanding the degree of bnAb resistance that exists in the general population, especially as responses are likely to be HIV subtype-specific.

In this chapter, the prevalence of mutations in HIV Env that have been associated with resistance to 10-1074 and 3BNC117 in PWH is reported. In the first part of this chapter, I report the prevalence of bnAb resistance associated mutations throughout the HIV pandemic, using publicly available env sequences. In the second part, I present findings on 10-1074 resistance- associated variants in a cohort of individuals with PHI, followed by data on 3BNC117 resistance in the same cohort. This study was conducted in the context of bnAb resistance screening for RIO (Chapter Materials and Methods, Section 2.2.4), where only 10-1074 sensitivity prediction was included in the eligibility criteria, due to lack of confidence in the *in silico* predictions for 3BNC117 sensitivity. For this reason, 10-1074 resistance associated mutations are more extensively studied in this thesis. In the third section, I explore bnAb resistance in the BONDY cohort of young individuals who acquired HIV perinatally and have faced issues with adherence to ART.

3. ***Prevalence of resistance-associated viral variants to bnAbs in key populations of people with HIV***

3.2 Aims

1. To investigate the trend of bnAb resistance throughout the pandemic
2. To quantify the prevalence of 10-1074 and 3BNC117 resistance mutations in key populations living in the UK, who are clinically eligible to receive these bnAbs as treatment.
3. To investigate the correlation of resistance-conferring variants with clinical and viral features

3.3 Results

3.3.1 Prevalence of 10-1074 and 3BNC117 variants resistance in the course of the HIV pandemic worldwide

To explore the broader prevalence of resistance to 10-1074 and 3BNC117, 2425 B clade HIV Env protein sequences sampled between 1983 and 2019 were downloaded from the Los Alamos sequence database and tested for mutations associated with resistance to 10-1074 and 3BNC117 (detailed in Materials and Methods, Section 2.2.5). The resulting analysis revealed a trend of increasing 10-1074 (Figure 3.1A) and 3BNC117 (Figure 3.1B) resistance over the course of the HIV pandemic. The key determinants of HIV sensitivity to 10-1074 are the presence of a sequon at aminoacid positions 332-334 of the HIV Envelope protein (a sequence of N-x-T/S, where x can be anything but P), which allows glycan attachment on the asparagine, and an intact motif on the protein,^{324}G(D/N)IR^{327}, which allows CDRH3 binding. Only 325D/N has been reported to be a 10-1074 sensitivity signature in the ^{324}G(D/N)IR^{327} contact motif, as the rest do not significantly vary (Bricault et al., 2019) (Chapter Materials and Methods, Figure 2.2). The Rockefeller bnAb prediction model determined that 330H/Y was also of importance when predicting sensitivity to 10-1074 (Chapter Materials and Methods, Section 2.3.5). Further analysis in the subset of sequences with 10-1074 resistance-associated mutations, reveals that mutations impacting the 332PNG (in positions 332 and/or 334) are

becoming more frequent with time (Figure 3.1C), potentially driving the 10-1074 resistance pattern identified.

3.3.2 Prevalence of bnAb resistance variants in a UK population with PHI

HEATHER cohort demographics

Samples from 157 HEATHER participants were used to study the prevalence of resistance to 10-1074 based on sequence analysis of HIV *env* (Chapter Materials and Methods, Section 2.2.2). The definition of resistance-conferring variants was based on the features selected by the prediction model built by the Rockefeller group (Chapter Materials and Methods, Section 2.3.5). All participants were on ART at the time of sampling for an average of 5 years (range: 0-18 years). The majority of participants (64.4%) seroconverted between 2013 and 2016 (range: 2001-2020). The median age of the participants at the time of ART initiation was 35 years (range: 18-64 years). All but two participants in this cohort were male (98.7%), and 91 of 92 recorded transmission events were men having sex with men (MSM). The mean average pairwise distance measured in participants who had more than 3 Env sequences available was 0.009 nucleotide substitutions per site (range: 0-0.09). No participants have been exposed to bnAb treatment at the time of sampling.

An average of 16 single, proviral Env sequences per participant (range: 1-72 sequences) was assessed for sensitivity to bnAbs. In total, 2593 Env sequences were analysed for this study. Most participants had B clade HIV (69.4%), followed by F (5.7%), C (4.4%), CRF02-AG (4.4%), CRF01-AE (3.1%), A1 and D/A1 (2.5% each), with other clades representing less than 2% of the cohort (Figure 3.2).

3. ***Prevalence of resistance-associated viral variants to bnAbs in key populations of people with HIV***

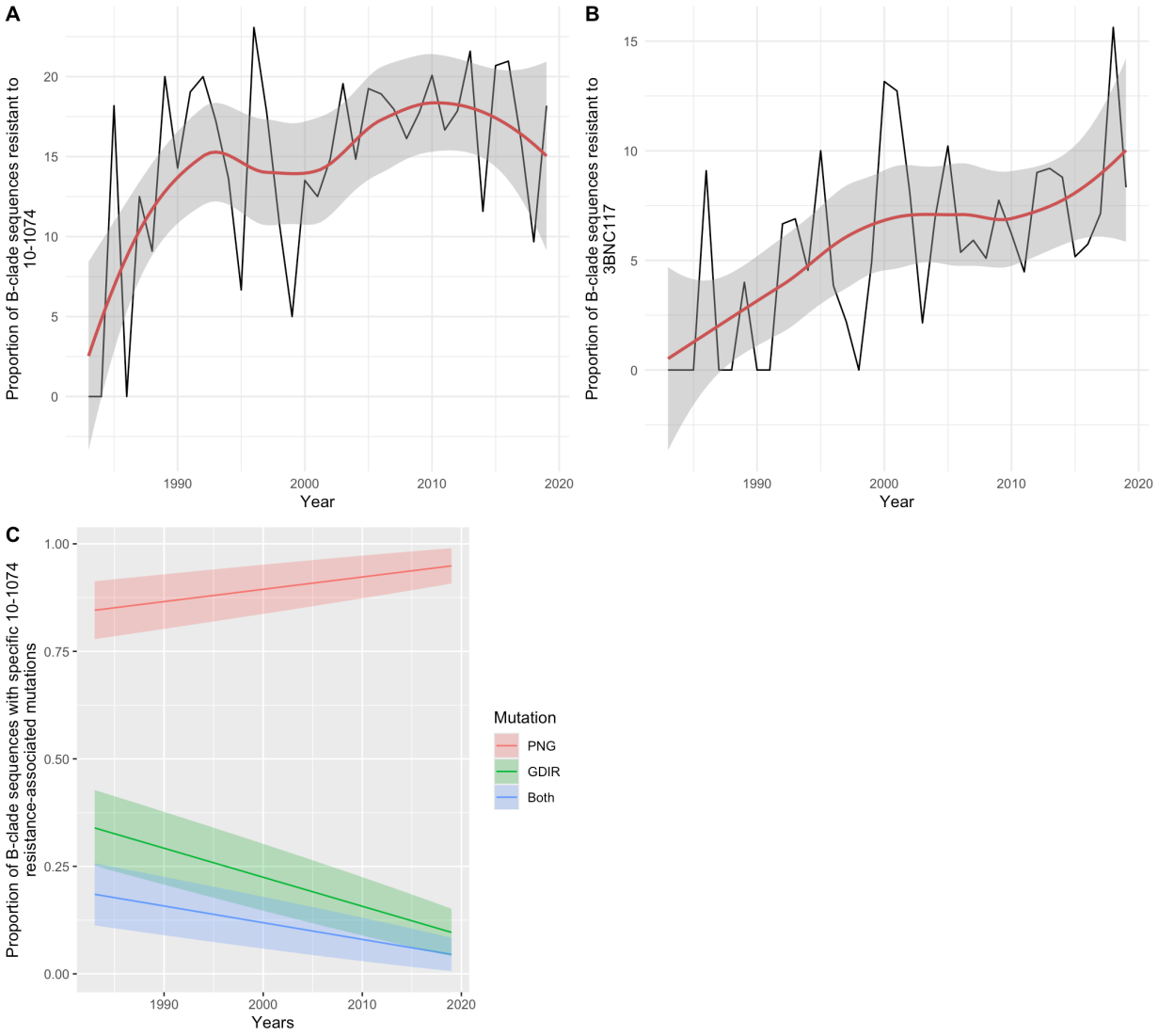

Figure 3.1: Longitudinal bnAb sensitivity analysis of Los Alamos Database B clade env sequences. A-B. Time series analysis showing the proportion of sequences with 10-1074 (A) and 3BNC117 (B) resistance-associated mutations in the total number of sequences available per year. The trend line is shown in red, and the confidence intervals are shaded grey. Years for which less than 5 sequences where available were excluded from the analysis. C. Frequency of individual mutation patterns associated with 10-1074 resistance among all sequences predicted as resistant, sampled throughout the pandemic. The type of mutation is encoded as PNG, for mutations affecting the 332-glycan binding (332-334 sites), GDIR for mutations impacting the binding site on the protein (sites 325 and 330) and Both for mutations occurring in both regions in the same sequence. Each mutation pattern is marked with a different colour. The year of sampling is on the x-axis and the proportion of resistant B-clade sequences per year is on the axis. The coloured bands represent the confidence interval for each fitted line.

3. ***Prevalence of resistance-associated viral variants to bnAbs in key populations of people with HIV***

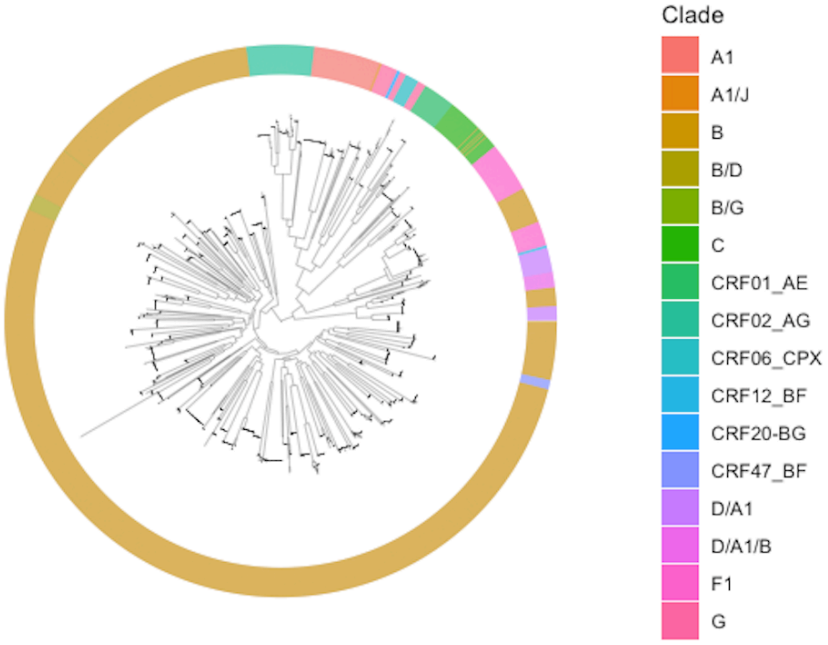

Figure 3.2: ML phylogenetic tree showing all sequences from 157 participants in the HEATHER cohort. The ring layer shows the sequence clades.

Predicted 10-1074 sensitivity in the HEATHER cohort

28.6% of the HEATHER cohort participants had at least one sequence with mutations associated with 10-1074 resistance and 22.9% had 100% sequences predicted as 10-1074 resistant. No participants had previously been exposed to 10-1074 or had received treatment with bnAbs. Co-existence of sensitive and resistant sequences to 10-1074 in the same person was detected in 5.7% of participants in the HEATHER cohort. For this group with mixed sequences, the proportion of resistant sequences varied between 12.5 and 85.7%. Subtype was an important determinant of resistance - most participants with clade B HIV in this cohort were predicted to be sensitive to 10-1074 (81/109; 74.3%). The highest rate of predicted 10-1074 resistance in the cohort was detected in CRF01-AE, although this was only five participants (5/5; 100%) (Figure 3.3).

3. ***Prevalence of resistance-associated viral variants to bnAbs in key populations of people with HIV***

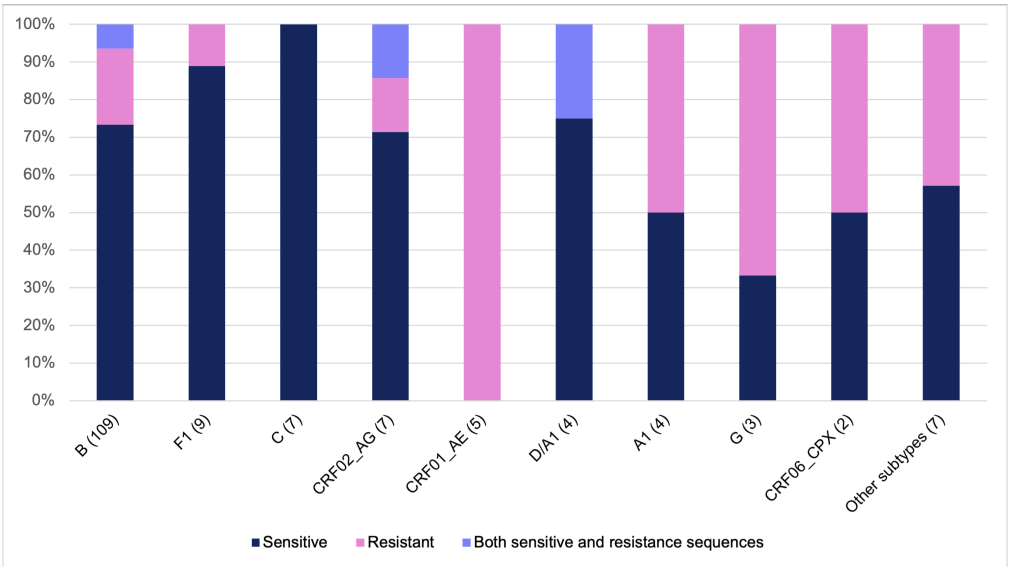

Figure 3.3: Distribution of predicted 10-1074 resistance in different HIV clades in the HEATHER cohort. Barplot showing the distribution of samples with 10-1074 resistance-conferring mutations per clade. The number in brackets is the number of samples. The percentage of samples in each clade is on the y-axis.

Mutations that interfere with the glycan attachment on the PNG at HIV Envelope position 334 were the most common among sequences predicted to be resistant (35 of the 45 sequences with resistance-associated mutations, 77.7%) in the HEATHER cohort. More than half of the potentially resistant sequences (25 of the 45 sequences with resistance-associated mutations, 55.5%) carried mutations at both positions 332 and 334 and furthermore, 64.4% of likely resistant samples in the cohort had a PNG site shift from position 332 to position 334 (Figure 3.4). Notably, 89.2% of those with a PNG at 334 in this dataset also carried a 336T (^{334}N-x-T^{336}), which has a 100% likelihood of glycan occupancy. However, ^{332}N-x-T^{334} was very rare in the sequences with an intact 332PNG. Furthermore, mutations at 330, which has been described as a critical 10-1074 binding site on *env*, most often occur with mutations that affect the glycan binding at position 332 (50% of 4 sequences with 330 mutations in the HEATHER cohort) (Figure 3.4).

3. ***Prevalence of resistance-associated viral variants to bnAbs in key populations of people with HIV***

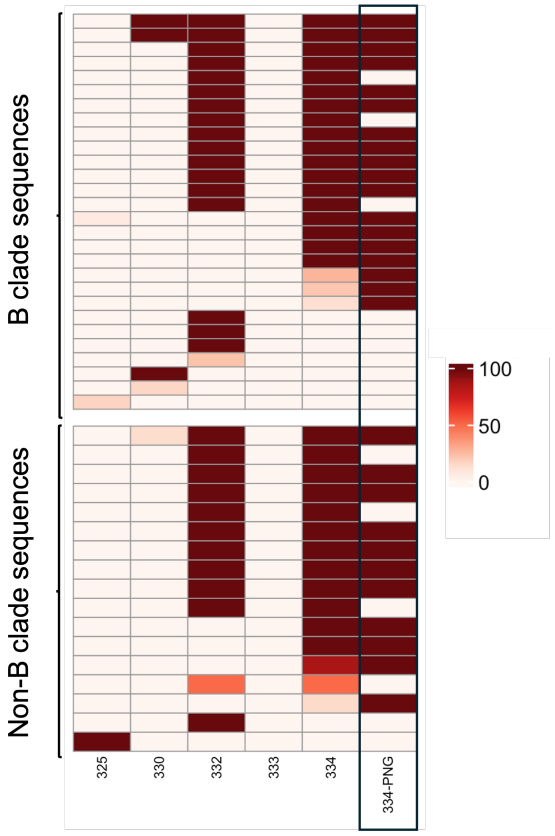

Figure 3.4: Heatmap presenting the frequency of mutated sites in the HEATHER cohort samples. This heatmap illustrates the frequency of mutations in the protein sequence in individual samples at HXB2 Env positions associated with 10-1074 susceptibility. Each row in the heatmap represents a distinct sample, and the first five columns correspond to precise amino acid positions. The last column illustrates the presence of a PNG at position 334. All samples harbouring >1 sequence with predicted resistance to 10-1074 B clade samples are shown in the upper panel and non-B are shown in the lower. The colour scale shows the percentage of sequences with 10-1074-associated mutations, per sample.

The variable loops in HIV Env evolve to evade the host immune response by incorporating insertions and deletions which have been associated with bnAb sensitivity. Alignment-independent methods were used on the HEATHER cohort sequences to measure the lengths of the variable regions (V1, V2, V4 and V5) as well as the number of PNGs within these regions (Table 3.1), using the Variable Region Characteristics tool on the HIV Los Alamos database.

3. ***Prevalence of resistance-associated viral variants to bnAbs in key populations of people with HIV***

Table 3.1: Median and range of length of variable and hypervariable Env loops and number of PNG within the same regions.

Variable Loop	Median	Range
V1 + V2	71	59-93
V3	37	33-38
V4	31	20-49
V5	13	10-25
Hypervariable V1+ V2	30	19-52
Hypervariable V4	15	4-33
Hypervariable V5	7	4-19
V1 + V2 PNG	6	4-9
V3 PNG	2	0-2
V4 PNG	4	2-7
V5 PNG	2	0-3
Hypervariable V1 + V2 PNG	2	2-7
Hypervariable V4 PNG	13	0-5
Hypervariable V5 PNG	30	0-5

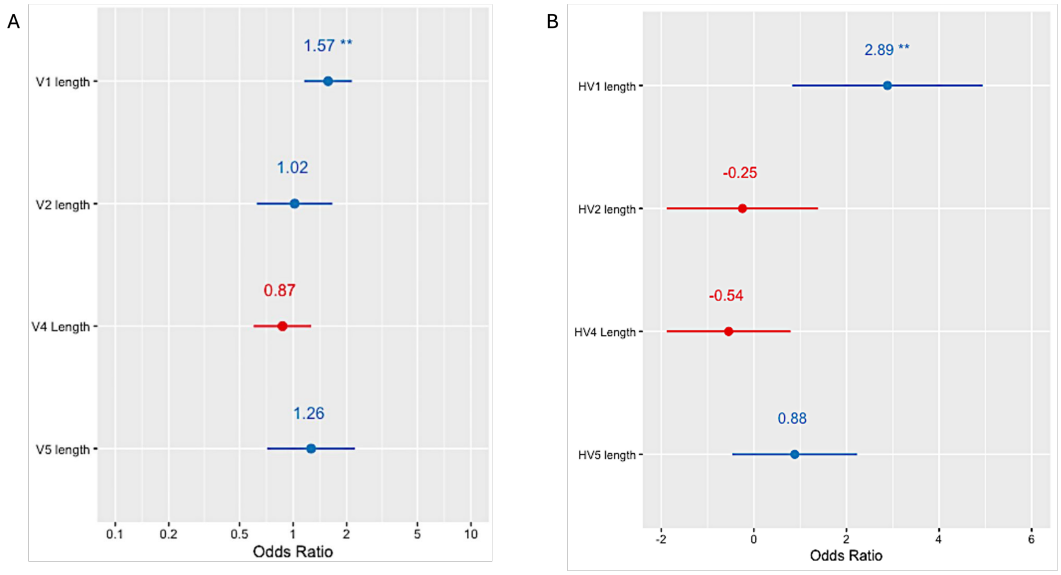

Figure 3.5: Forest plots showing the odds ratio of 10-1074 resistance in relation to each of (A) the HIV Env variable loop lengths and (B) the Hypervariable loop lengths in the HEATHER cohort. ** indicates a p-value<0.001.

A multivariable logistic regression with mixed effects, accounting for intra-patient variability and clade, showed that only the length of variable V1 loop (Figure 3.5A) as well as the length of the hypervariable V1 loop (Figure 3.5B) were significantly associated with the presence of resistance-conferring mutations (OR=1.57, p-value<0.01 and OR=2.89, p-value<0.01, respectively). No statisti-

cally significant relationship between 10-1074 resistance-conferring mutation and the number of PNGs within the variable regions was observed.

Predicted 3BNC117 sensitivity in the HEATHER cohort

Due to the high neutralisation breadth of 3BNC117, the currently available resistant sequences might be insufficient to train a robust and generalisable prediction model for 3BNC117 resistance prediction. Predictions for 3BNC117 sensitivity and, by extension, features associated with resistance, are therefore considered largely unreliable (Zacharopoulou et al., 2022). The contact residues of 3BNC117 have been located in Loop D (HXB2 positions 274-283, the CD4 binding site (364-374) and the β_23 V5 loop (455-471) (Cohen et al., 2018; Schoofs et al., 2016). However, for this thesis, 3BNC117 resistance prevalence was assessed using the criteria of the Rockefeller 3BNC117 sensitivity prediction model. Resistance to 3BNC117 was observed in fewer HEATHER participants than 10-1074 resistance; 15.2% of participants had at least one sequence predicted as 3BNC117 resistant but co-existence of sequences that were predicted as sensitive and sequences predicted as 3BNC117 resistant were observed in 8.2% of participants. The proportion of resistant sequences in this subgroup of participants ranged between 1.3 and 35.4%, with a mean of 10%. Similar to 10-1074, most of our HEATHER participants with clade B HIV were predicted to be sensitive to 3BNC117 (92/109; 84.4%) and the largest rates of resistance were found among F1 clade participants, with 3/9 (33%) participants having 100% resistant sequences (Figure 3.6).

3. ***Prevalence of resistance-associated viral variants to bnAbs in key populations of people with HIV***

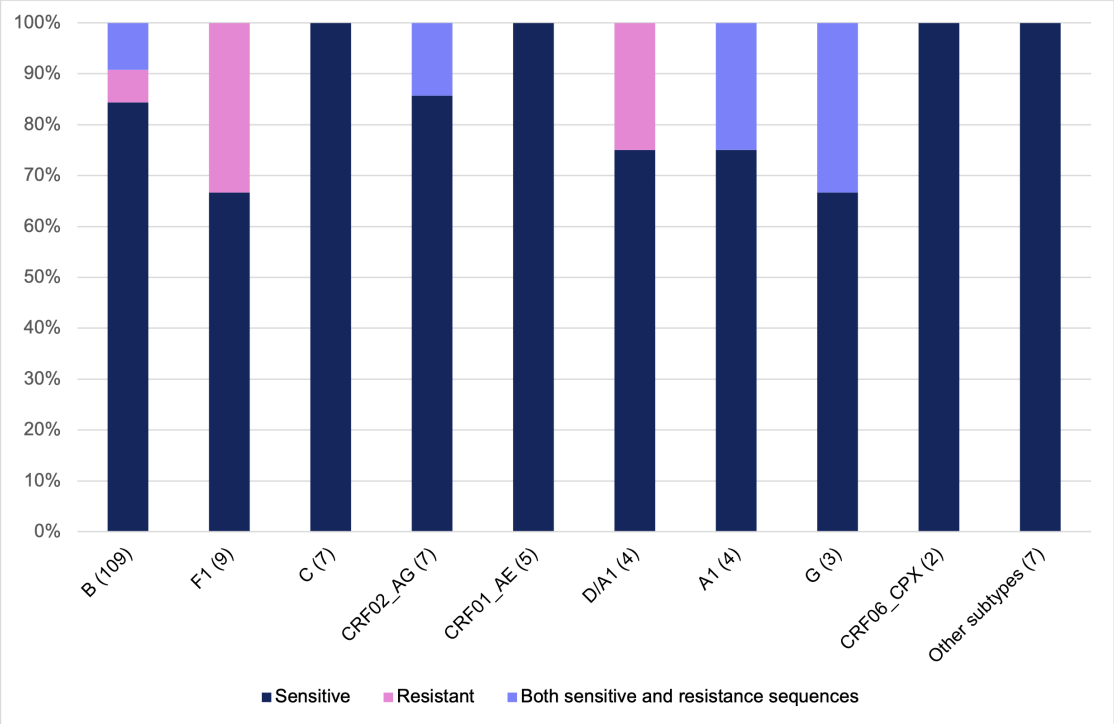

Figure 3.6: Barplot showing the distribution of samples with 3BNC117 resistance-conferring mutations per clade. The number in brackets is the number of samples. The percentage of samples in each clade is on the y-axis.

Notably, only 2 of all 157 participants had 100% resistant sequences to both 10-1074 and 3BNC117 and they both had clade B HIV. Another B clade participant had both resistant and sensitive sequences to both bnAb and one participant with G clade had all sequences predicted as 10-1074 resistant and some of them also had mutations associated with 3BNC117 resistance.

Sensitivity analysis of the HEATHER cohort identified site 459 as the most affected with regards to variations predicted to confer 3BNC117 resistance, followed by site 456 (12 and 10 participants out of 24 participants with resistant sequences, respectively). Contrary to 10-1074, no patterns of linked mutations were observed for 3BNC117 (Figure 3.7). No variable or hypervariable loop showed any correlation with 3BNC117 resistance conferring mutations.

3. ***Prevalence of resistance-associated viral variants to bnAbs in key populations of people with HIV***

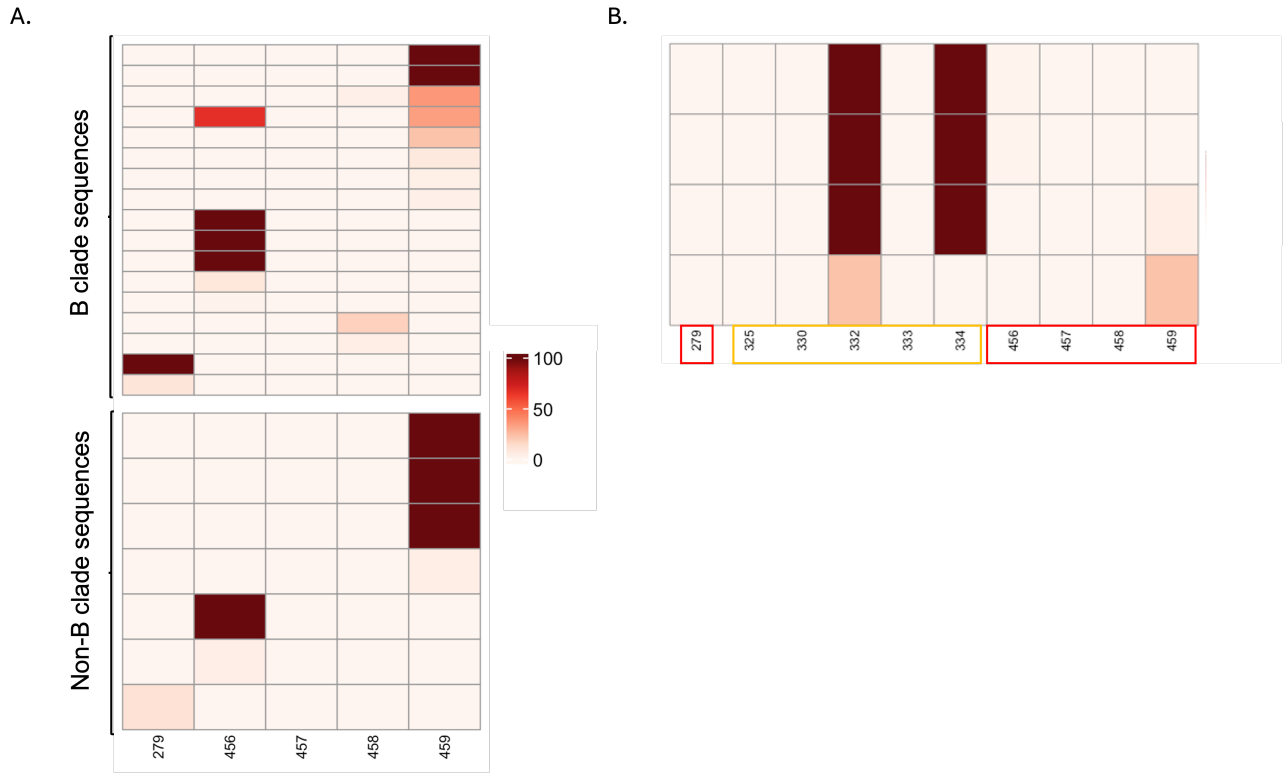

Figure 3.7: Heatmaps presenting the frequency of 3BNC117 resistance associated mutation sites in the HEATHER cohort samples. Each row in the heatmaps represents a distinct sample, and the columns correspond to precise amino acid positions. Panel A heatmap illustrates the frequency of mutations in the protein sequence in individual samples at HXB2 Env positions associated with 3BNC117 susceptibility. B. This heatmap shows the frequency of resistance-associated mutations for participants who had sequences resistant to both bnAb or a mix of 10-1074-resistant and 3BNC117-resistant sequences. Sites associated with 10-1074 sensitivity are in a yellow box and sites associated with 3BNC117 are in red boxes. The colour scale shows the percentage of sequences with 10-1074-associated mutations, per sample.

3.3.3 Prevalence of 10-1074 and 3BNC117 resistance variants in the BONDY cohort of PWH

BONDY cohort demographics

Samples from a total of 31 individuals who acquired HIV perinatally and were enrolled in the BONDY cohort were included in this study. At the time of sample collection, seven of these participants had a detectable plasma viral load. The median viral load of those individuals was 148 copies/ml (range: 82-748000 copies/ml). The median time from seroconversion to sampling was 22 years (range 18-32 years). Proviral Env was amplified for 21 (67.7%) of all participants but due

to mutations that rendered Env dysfunctional, assessible sequences were available only for 16 (51.6%) (Figure 3.8A). An average of 3 sequences was obtained per participant (range: 1-13 sequences). For participants whose sequences could not be successfully amplified or for whom only dysfunctional *env* sequences were obtained, clade information was extrapolated where possible from available clinical data or from the dysfunctional sequences. These extrapolations were based on sequence classification, even when large deletions or premature stop codons were present. In terms of viral subtype distribution, the majority of participants in this cohort had clade C HIV (9/31, 29%), followed by A1 (7/31, 22.5%) , B (3/31, 9%) and others in a frequency $>$ 6.5% (Figure 3.8B). Interestingly, participants whose samples yielded only dysfunctional *env* sequences had with clade CRF49-cpx (1/1, 100%), A1 (2/5, 28.5%) and C (2/9, 22.2%) (Figure 3.8C).

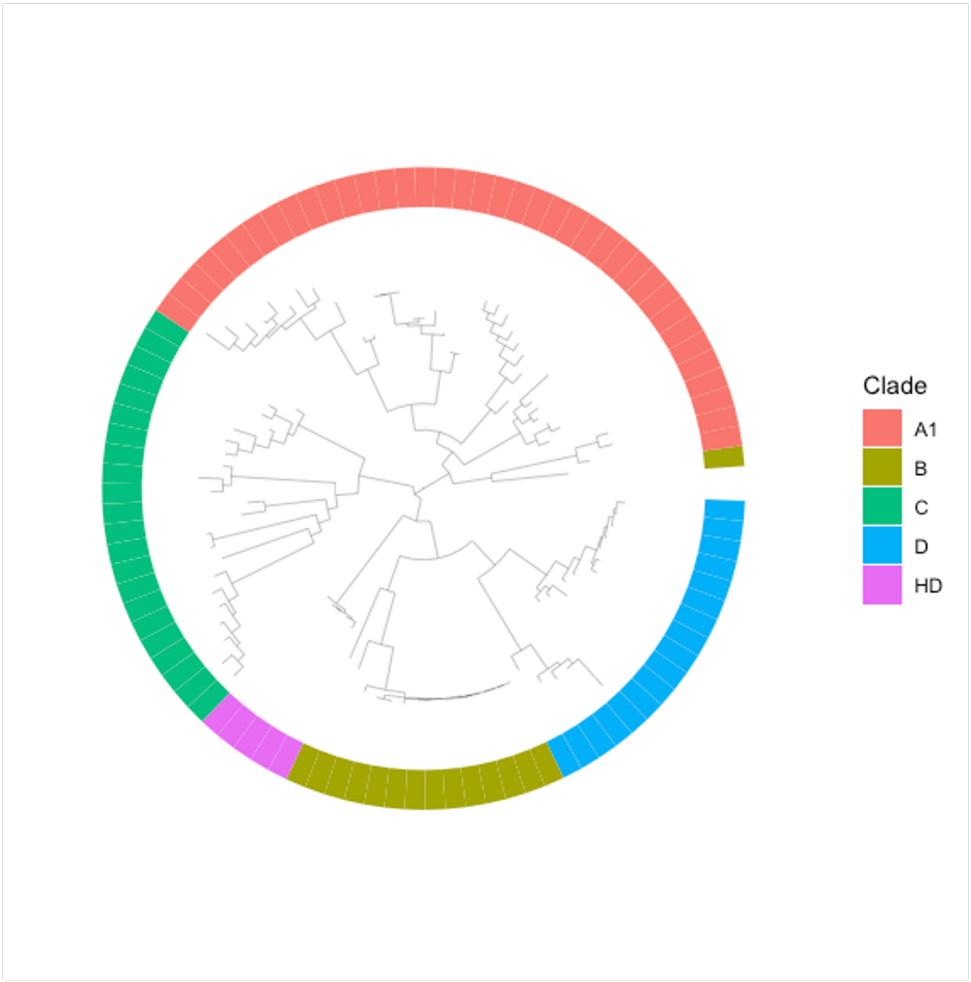

3. ***Prevalence of resistance-associated viral variants to bnAbs in key populations of people with HIV***

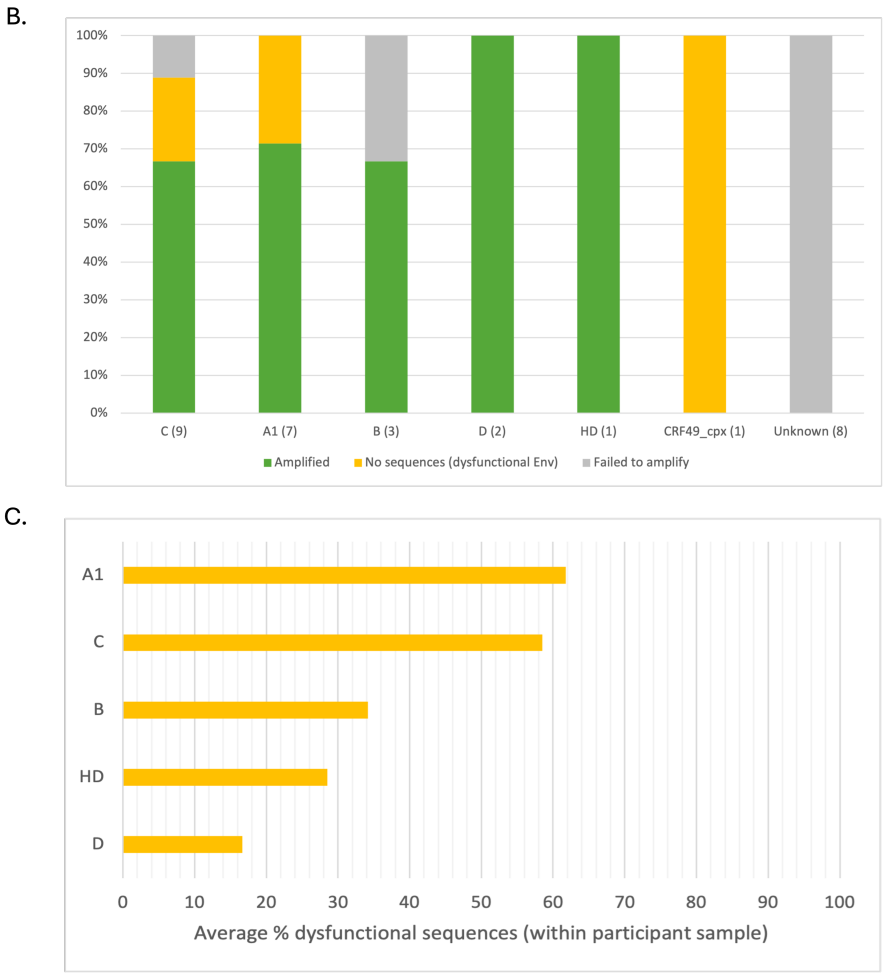

Figure 3.8: BONDY cohort clade distrbution and sequence quality.(A)ML phylogenetic tree showing all availble sequences from 16 participants in the BONDY cohort. The ring layer shows the sequence clades.(B) Barplot showing the BONDY participant sample clades and the output of amplification and sequencing; samples with functional sequences, samples with no sequences due to mutations that render Env dysfunctional and samples that failed to amplify (C) Barplot showing the average proportion of within-sample dysfunctional sequences per clade

The average proportion of dysfunctional sequences within-sample was 53.2% (range: 12.5-100%) and the samples with the highest proportion of dysfunctional sequences (>60%) were A1 clade samples. Among participants for whom more than three *env* sequences were available for analysis, the mean average pairwise distance was calculated to be 0.05 nucleotide substitutions per site, ranging from 0.01 to 0.09 substitutions per site.

3. ***Prevalence of resistance-associated viral variants to bnAbs in key populations of people with HIV***

Distribution of bnAb resistance-conferring variants

Resistance to bnAb was assessed using the Rockefeller model. The analysis of the BODY sample sequences revealed high rates of resistance to both bnAb. Evidence of some degree of 10-1074 resistance was detected in 62.2% of participant samples (10 of 16 participants with amplified and sequenced Envs). 10-1074 resistance-associated mutations were found in A1 clade (85.7% of all A1 clade samples) and in clade C (66.6% of C clade samples) (Figure 3.9A). Only 1.8% of participants had at least one resistant sequence to 3BNC117 and only 1 of them had 100% 3BNC117 resistant sequences (Clade HD, Figure 3.9B). One participant was found to harbour 100% 10-1074 resistant sequences, of which 50% also had 3BNC117 resistance mutations and one other had all sequence predicted as 3BNC117 resistant, of which 20% were 10-1074 resistant, as well.

Similarly to the HEATHER cohort findings, the most frequent mutations associated with 10-1074 resistance were found to impact the 332PNG site, with coinciding mutations at 332 and 334 (72.7% of samples with at least one 10-1074 resistant sequence with functional Env sequences). The site that was mostly affected in 3BNC117 resistant samples was 456 (2/3 samples with functional Env sequences, which had at least one sequence predicted as 3BNC117 resistant) (Figure 3.10).

3. ***Prevalence of resistance-associated viral variants to bnAbs in key populations of people with HIV***

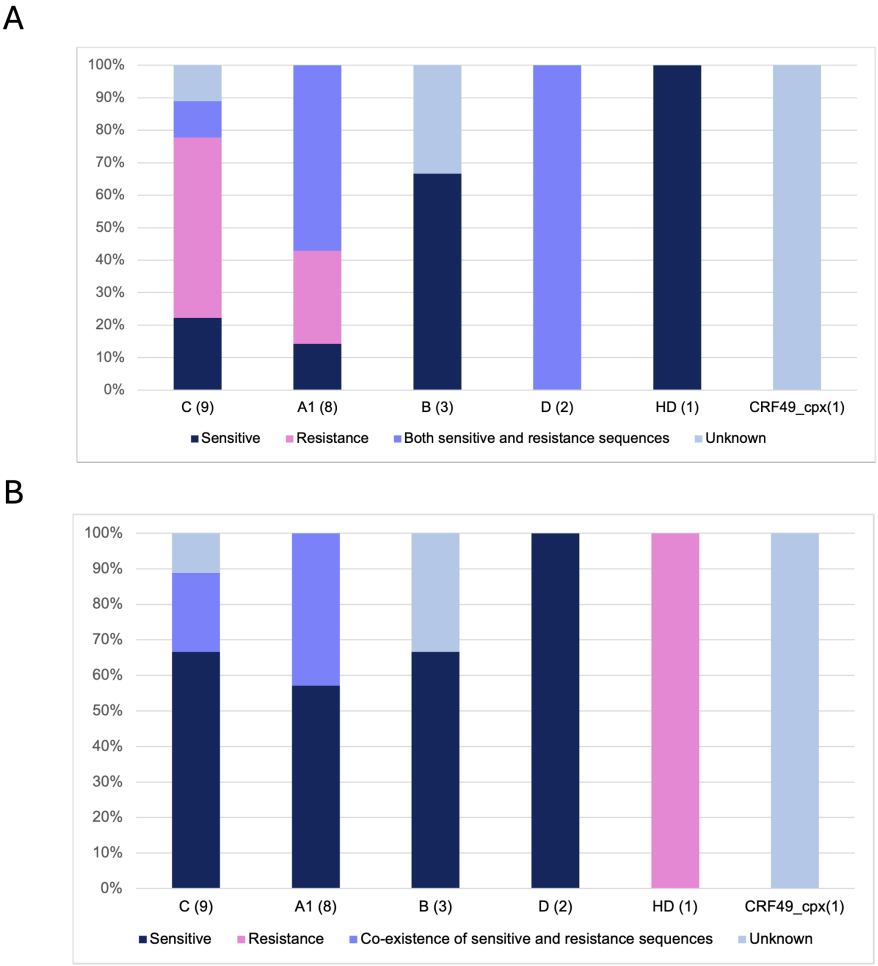

Figure 3.9: Predicted resistance to bnAb in the BONDY cohort. Barplots showing predicted resistance to (A) 10-1074 and (B) to 3BNC117, per clade

3. ***Prevalence of resistance-associated viral variants to bnAbs in key populations of people with HIV***

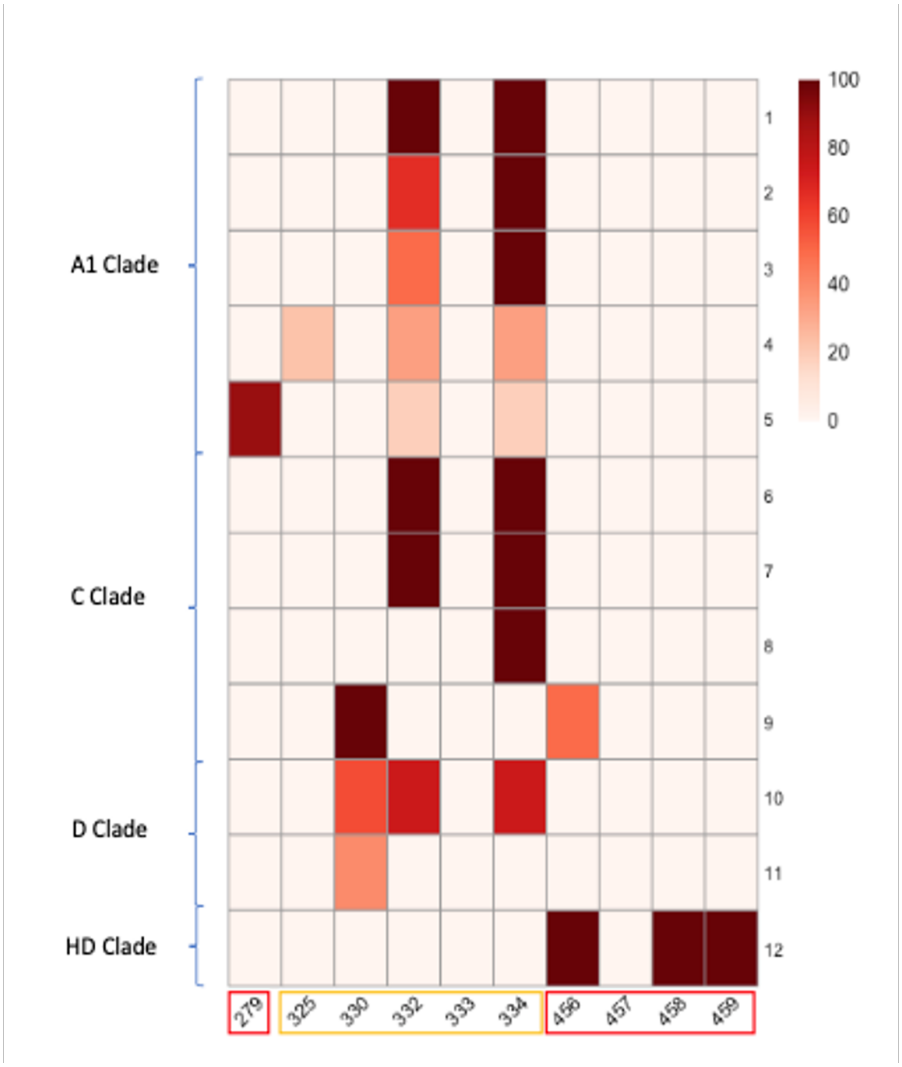

Figure 3.10: Heatmap showing the presence of mutations predicted to confer resistance to 10-1074 and 3BNC117. The residue positions at the bottom of the heatmap are numbered after HXB2 and are related to 10-1074 sensitivity (yellow box) and 3BNC117 sensitivity (red box). Each row represents one of the samples in the cohort with at least one resistant sequence to either 10-1074 or 3BNC117 and they are sorted based on clade, as it is shown on the left of the heatmap. The intensity bar represents the proportion of sequences per sample that carry resistance-conferring mutations.

3.4 Discussion

This study was the first to evaluate the prevalence of 10-1074 associated mutations in a bnAb treatment-naive population with PHI in the UK using viral sequencing from the HIV reservoir. In the absence of a gold standard for predicting bnAb resistance, we used specific *env* residues to define 10-1074 resistance, from samples

of DNA, whilst the virus was suppressed on ART, which were selected by an algorithm based on West et al. (West Jr et al., 2013), which has been previously used to assess sensitivity to 10-1074 (Gaebler et al., 2022; Mendoza et al., 2018) and 3BNC117 (Gunst et al., 2022).

The first step was to assess the current prevalence of 10-1074 and 3BNC117 resistance-associated mutations and examine how their frequency has evolved throughout the HIV pandemic by analysing B clade Env sequences from the Los Alamos database. This analysis is particularly relevant as it provides insight into the necessity of screening for these mutations prior to treatment or prevention strategies and contributes to the optimisation of vaccine design. The analysis revealed an increase in the prevalence of 10-1074 resistance-associated mutations and a more moderate increase in 3BNC117 resistance-associated mutations between 1983 and 2019. This is in line with previous studies demonstrating a shift toward greater resistance to neutralizing antibodies (Bouvin-Pley et al., 2013; Bouvin-Pley et al., 2014; Bunnik et al., 2010; Wieczorek et al., 2023). The observed increase in resistance to nAbs over time has been attributed to viral adaptation to the humoral immune response at the population level (Bunnik et al., 2010). These changes in Env may also impact bnAb contact sites, which we have defined as critical sensitivity residues in this study, thereby contributing to the observed increased prevalence of bnAb resistance-associated mutations. The main limitation of this analysis is that only one sequence was obtained per individual in this study, hence no single-genome resolution of the quasispecies per host is obtained. In addition, no clinical data were provided for these sequences and so the stage of infection and the treatment status was unknown. Lastly, uneven distribution of available samples across different timepoints may have introduced bias in the time-series analysis. Although statistical bootstrapping was employed to mitigate the effects of this imbalance and to enhance the reliability of the analyses, it should be noted that such corrective measures may not fully compensate for the lack of uniform sampling.

Previous studies have demonstrated that the recognition of the 332 glycan is necessary for 10-1074 binding, so any disruption of the glycan site would confer

resistance to this bnAb, whereas variations on the 10-1074 GDIR binding region on the protein are better tolerated (Bricault et al., 2019). We demonstrated that 10-1074 genotypic sensitivity varies among different HIV subtypes, suggesting that treatment with 10-1074 may be less effective in people who live with non-B clades of HIV, for example, subtype CRF01-AE HIV. In particular, we found that 25.7% of participants with B clade in HEATHER had at least one sequence with 10-1074 resistance-associated mutations as opposed to participants with CRF01-AE who were predicted as 10-1074 resistant in 100%. These findings are comparable to previous study results, showing that 88.5% of the B-clade viruses were neutralised *in vitro* by 10-1074 at an average of 80% inhibitory concentrations (Caskey et al., 2017) or, that CRF01-AE viruses are extremely resistant to 10-1074 (Bricault et al., 2019). C clade viruses, which are most abundant in the regions where HIV is an ongoing public health issue, were found to carry no 10-1074 resistance associated mutation in individuals with PHI in HEATHER but only 33.4% of BONDY participants with clade C were predicted as sensitive. This may indicate that intermittent viremia for long periods due to poor ART adherence may lead to emergence of resistant variants, unless the bnAb resistance-associated mutations were transmitted.

The analysis of the HEATHER cohort sequences identified that the most frequently appearing substitutions in resistant sequences impact the binding to the 332-supersite glycan. Instead, the PNG site was shifted from position 332 to position 334 in most of these sequences. A glycan at this position could, however, serves as a target for other neutralising antibodies and bnAbs, as well as a marker of lower viral infectivity (Anthony et al., 2017; Cai et al., 2018). In addition, Caskey et al. (Caskey et al., 2017) observed some reversion of 10-1074 escape mutations (such as D/K332 and I/A334) to wild type in PWH, when 10-1074 levels started dropping in the blood conferring less selection pressure, indicating that the escape mutations may have a fitness cost. Changes in the combined length of variable region V1 have been reported to play a role in evading humoral immune responses (Bricault et al., 2019; J. et al., 2011; Sutar et al., 2021). We found that, in the HEATHER cohort,

a longer V1 loop was strongly associated with the presence of 10-1074 resistance-conferring mutations. According to previous studies, a longer V1V2 region protects against neutralising antibodies by shielding the V3 epitopes (Rusert et al., 2011). The fact that a longer V1 length is associated with 10-1074 mutations may indicate that 10-1074 resistance is developed in the mutated sequences in the process of escaping from V3-targeting host nAbs. Further analysis in larger sample sizes may result in more precise estimates and in elucidating the relationship between variable loop lengths and 10-1074 resistance-conferring variants.

Consistent with the literature, mutations associated with 3BNC117 resistance were infrequent in the samples obtained from participants in HEATHER and BONDY, which can be explained by the high neutralisation breadth of 3BNC117. The most frequently observed mutation was found on position 459 in the V5 loop, which has been mentioned in previous studies of 3BNC117 (Caskey et al., 2015; Scheid et al., 2016). Notably, 3BNC117 may be a better treatment option for people with non-B clade viruses, who are more likely to be resistant to 10-1074.

The lack of information on the intactness of the viruses corresponding to the Env sequences analysed in this chapter is a limitation of our findings. It is possible that sequences carrying bnAb resistance-associated mutations have defects in genomic regions outside of Env, rendering them incapable of producing replication-competent viruses. If these resistant variants are not intact, they may not pose a significant threat to the effectiveness of bnAb treatment. The analysis of Env sequences from intact viruses produced using methods such as the Q4PCR may be needed to confirm our findings.

The interpretation of genotypic assays and prediction algorithms has proven to be problematic, especially for predicting bnAb sensitivity where structural interactions between aminoacids are more complex than they are for drug resistance (Mayer et al., 2001; Metzner, 2022). I have therefore been cautious here to interpret the results as likely predicting resistance, rather than being an absolute finding, although the algorithms for 10-1074 are better than for some other bnAbs, such as 3BNC117 (Hake & Pfeifer, 2017; Rawi et al., 2019; Yu et al., 2019). To

accurately predict bnAb resistance, more clinical outcome data is needed matching sequence variation to viral suppression after bnAb therapy. Nevertheless, it is likely that should bnAb become a mainstream therapy or prophylactic treatment, a genotypic approach to screening combined with consideration of viral subtype will be most pragmatic.

A key observation in this study was the difference in the prevalence of bnAb resistance-associated mutations between the two cohorts; HEATHER, comprising individuals with PHI, and BONDY, consisting of young adults who acquired HIV perinatally. One potential contributing factor to this discrepancy is the observed variation in average pairwise distance in the two studies. A higher average pairwise distance reflects increased intrahost viral diversity, which may cause the emergence of escape mutations under selective pressure of nAbs. In the BONDY cohort, which exhibited a higher average pairwise distance, a greater prevalence of dysfunctional *env* sequences was also observed. This may reflect a more complex and viral reservoir, in which defective proviral genomes have accumulated over time, maybe due to efforts to escape the immune response. Importantly, the difference in viral diversity and bnAb resistance-associated mutation profiles between the two cohorts may also be attributed to the distinct viral clades present in each cohort. Participants in HEATHER had predominantly clade B virus, whereas the BONDY cohort was composed primarily of individuals infected with non-clade B viruses, including clades A1, C, and CRFs. In addition, the sex for the BONDY participants in this study was unknown; however, the majority of BONDY participants were female whereas all HEATHER participants were male. It is therefore possible that factors associated with clade or sex had an impact on the mutation prevalence and the functionality differences observed between the two studies.

In summary, the presence of pre-existing bnAb resistance-associated mutations poses a challenge to the effectiveness of bnAb treatment in PWH, potentially diminishing its long-term utility as a treatment option. This may however be minimised with proactive screening and combination therapy approaches, especially in people with increased viral diversity, chronic infection or specific viral clades.

3. ***Prevalence of resistance-associated viral variants to bnAbs in key populations of people with HIV***

Should resistance be equally prevalent for other bnAbs with therapeutic potential, this has implications for screening programmes for the wide population to ensure maximum efficacy.

4

Evolution of bnAb sensitivity

Contents

4.1 Context

Despite the promises of bnAb treatment for HIV, the emergence of resistance to bnAbs remains a critical challenge to the effort of controlling HIV, as it may compromise treatment efficacy, escalate the risk for acquisition and spread of resistant variants, and increase the need for new treatment strategies. In a study by Mendoza et al., individuals receiving 10-1074 and 3BNC117 on ATI with pre-existing reservoir resistance to either or both bnAbs, experienced similar time

to rebound as individuals who underwent ATI without bnAbs (Mendoza et al., 2018). Similar findings have previously been reported by Caskey et al for 10-1074 monotherapy (Caskey et al., 2017), by Cohen et al. for 3BNC117 monotherapy (Cohen et al., 2018) and by Gunst et al. in a study of 3BNC117 with Romidepsin (Gunst et al., 2022).

Pre-existing bnAb resistance in individuals who have never received bnAbs may arise through different mechanisms, including transmission or *de novo* emergence of resistant variants during untreated infection in response to host immune response. Understanding the origins of bnAb resistance in bnAb-naive individuals is critical for optimising clinical decision making, improving clinical outcomes and informing public health strategies.

Screening for pre-existing bnAb resistance in plasma or in the reservoir has been a debate topic in the scientific community. One of the arguments against screening PLW on ART for bnAb resistance is that reservoir sequences from blood might be a poor proxy for rebound virus (Patel & Dubé, 2023). Indeed, the reservoir viruses are by majority replication incompetent and thus it may be difficult to obtain a representative sample that accurately reflects the entire resistance profile of the rebound virus. Furthermore, it is possible that provirus screening could identify variants that are not clinically relevant and would not influence the efficacy of bnAb treatment. In addition, the screening assays that are currently available may not be sensitive enough to capture low-frequency resistance mutations withing the reservoir compared to circulating virus, leading to incomplete or misleading resistance profile. Screening the plasma virus is currently the gold standard for assessing ART resistance because it reflects the actively replicating virus responsible for current viremia. Plasma virus resistance testing is directly relevant to treatment efficacy and helps guide adjustments to the ART regimen to suppress viral replication. Although screening proviral reservoir sequences for ART resistance is acceptable when individuals are aviremic, whether bnAb sensitivity in the reservoir is reflected in the plasma or not is not yet clear.

4.2 Aims

In this chapter, I aim to study the origin of bnAb resistance-associated mutations and determine whether it is more likely for resistance to be transmitted or evolve within host who never received bnAbs. In particular, I endeavor to

1. Investigate the evolution of bnAb resistance during untreated HIV infection
2. Explore the relationship of pre-ART Env RNA and DNA sequences during PHI to proviral Env sequences sampled during ART, in terms of bnAb resistance phenotypes
3. Compare bnAb sensitivity based on Env sequences sampled from participants on ART (proviral Env sequences from PBMCs in the blood) and at the time of rebound (circulating viral Env sequences from plasma), post ATI.

4.3 Results

4.3.1 Cohorts

SPARTAC

12 SPARTAC (Chapter Materials and Methods, Section 2.2.1) participants who were randomised to receive no ART (which reflected the standard of care at the time), and for whom longitudinal PBMC and/or plasma samples were available were selected for this study. Samples were collected at baseline (Week 0), week 12, and Week 24 and/or Week 52. All participants were men in the UK with clade B HIV. No participants received bnAbs at any point.

RIO ARM B

In order to compare bnAb sensitivity of proviral Env in the reservoir and of rebound Env sequences in plasma post-ATI, we used samples from 18 participants who were randomised to RIO Arm B (Chapter Materials and Methods, Section 2.2.4). The samples that were studied for the purpose of this study were screening samples, before participants were recruited in the trial and samples taken at the

time of rebound, after participants stopped ART and received placebo. Participants in this arm were unblinded once they experienced viral rebound meeting pre-defined thresholds under the study protocol and they were then invited to participate in the second stage of the trial where they received open-labelled bnAbs after restarting ART (section 2.2.4). An average of 17.6 sequences were obtained for each participant at screening (range: 3-42) and 14 at rebound (range: 1-44).

4.3.2 bnAb sensitivity evolution in longitudinal samples from bnAb-naive PWH

In order to study the evolution of mutations associated with bnAb resistance, I sequenced longitudinal samples from SPARTAC participants. DNA (and cDNA, if available) was extracted for 12 participants. Sequences for only one timepoint were obtained for 3 samples and therefore these were not included in the study. A total of 176 sequences were obtained from 9 participants with an average of 19 sequences per participant (range: 10-38 sequences). bnAb resistance-conferring mutations were detected in 4 out of 9 participants. Env was amplified from proviral sequences for most participants and only for 1 participant Env sequences were amplified from circulating plasma virus. Mutations associated with 10-1074 resistance were found in samples from 3 participants and mutations associated with 3BNC117 were detected in samples from 2 participants.

Mutations disrupting the 332 PNG at position 334 were found in almost all sequences sampled at both Week 12 (100% of all sequences) and Week 52 (88% of all sequences) for SUC036029. On the contrary, mutations at 332 were detected in 13% of sequences at Week 12 for SUP033003 and the proportion increased to 25% in the sample taken 12 weeks after. The proportion of mutations (site 325) in the baseline sample from SUW036049 was 0.9% and no other resistant sequences were detected in samples from Week 12 or Week 52 (Table 4.1).

However, mutations at the 3BNC117-resistance associated site 459 were found in the samples from Week 12 (10% of all sequences) but not in samples from Weeks 0 or 52. Finally, only one sequence with a mutation at 459 site was detected

Table 4.1: Evolution of 10-1074 resistance in SPARTAC. Proportion of Env sequences with 10-1074 resistance-associated mutations at baseline, week 12 or week 24, and week 52 post diagnosis

Participant ID	Baseline	Week 12	Week 24	Week 52
SUC036029	NA	1.00	NA	0.88
SUP033003	0	0.14	0.25	NA
SUW036049	0.09	0.00	NA	0

in a baseline sample from SUL214001 and not in any samples from Week 12 or 52 (Table 4.2).

Table 4.2: Evolution of 3BNC117 resistance in SPARTAC. Proportion of Env sequences with 3BNC117 resistance-associated mutations at baseline, week 12 or week 24, and week 52 post diagnosis

Participant ID	Baseline	Week 12	Week 24	Week 52
SUL214001	0.11	0.0	NA	0
SUW036049	0.00	0.1	NA	0

Due to the small number of participant samples and to the low number of sequences obtained from them, I used the same resistance prediction methodology on Env sequences from samples taken from participants recruited to the MACS, which are publicly available on the Los Alamos HIV sequence database (detailed in Methods, section (**?**)(publicdatasets)). In this analysis, I tested 8 samples for bnAb sensitivity using using the Rockefeller prediction model. All had clade B Env plasma sequences, collected across longitudinal visits. Evidence of evolving resistance was found in 5 out of 8 participants (2 participants had sequences with resistance mutations at only one timepoint and 1 had no resistant sequences in samples from any timepoint) (Appendix, Table A.1). A total of 744 sequences of the C2-V5 Env region from the five participants P2, P4, P7, P10 and P11 were included in this study. An average of 11 sequences per visit (range: 2-24 sequences) was available across a median of 7 visits per participants (range: 3-23 visits), throughout a median of 44 months post seroconversion (range: 42-80 months).

The most frequent mutation observed in this cohort was a single mutation at HXB2 position 334, which was detected in all 5 participants. Mutations affecting

332 alone or with a mutation at 334 were observed in 2 participants. Mutations affecting other sites (330 and 334, 330, 325 and 332, 456, 279 and 334, and 279, 332 and 334) were seen in single individuals. The largest variety of mutations was detected in P10, who seems to have developed 5 different mutations, including a combination of 279 with 334 or with 332 and 334. Only 3 participants had mutations associated with 3BNC117 resistance.

In this cohort, the first 10-1074 resistance-associated mutations are detected at a median of 44 months post seroconversion (range: 30-70 months) while the first 3BNC117 mutations are seen for the first time after a median of 85 months (range: 42-86 months). In order to investigate which mutations were the most prominent within participants and whether there was their emergence had any impact on the viral load, I plotted the proportion of sequences that carried mutations in different sites and the viral load for samples from different timepoints (Figure 4.1). It is shown that a S/T334G mutation was present only in a sample from a single visit in participant P2 (Figure 4.1A), contrary to a R456S, which increased up to 100% of all sequences until the end of follow up. On the contrary, the proportions of sequences with shift of PNG to 334 (334N-x-336S/T) progressively increase above zero and remain high for months in participants P10, P11 and P7 (Figure 4.1D, E and C), although the number of visits for the latter is small. The frequency of mutations at position 332 is correlated with the viral load trend, as an increase of viral envelopes with mainly N332T and a minority of N332S coincides with a viral load spike, which drops as well as the frequency of mutated viruses. Following the short decline, viruses carrying 332 mutations increase up to 80% of all sequences, this time N332S and N332T in equal proportions and a minority of N332A. Notably, the frequency of resistant viruses in participant P10 (Figure 4.1B and D) dropped to zero, indicating a reversion to wild type.

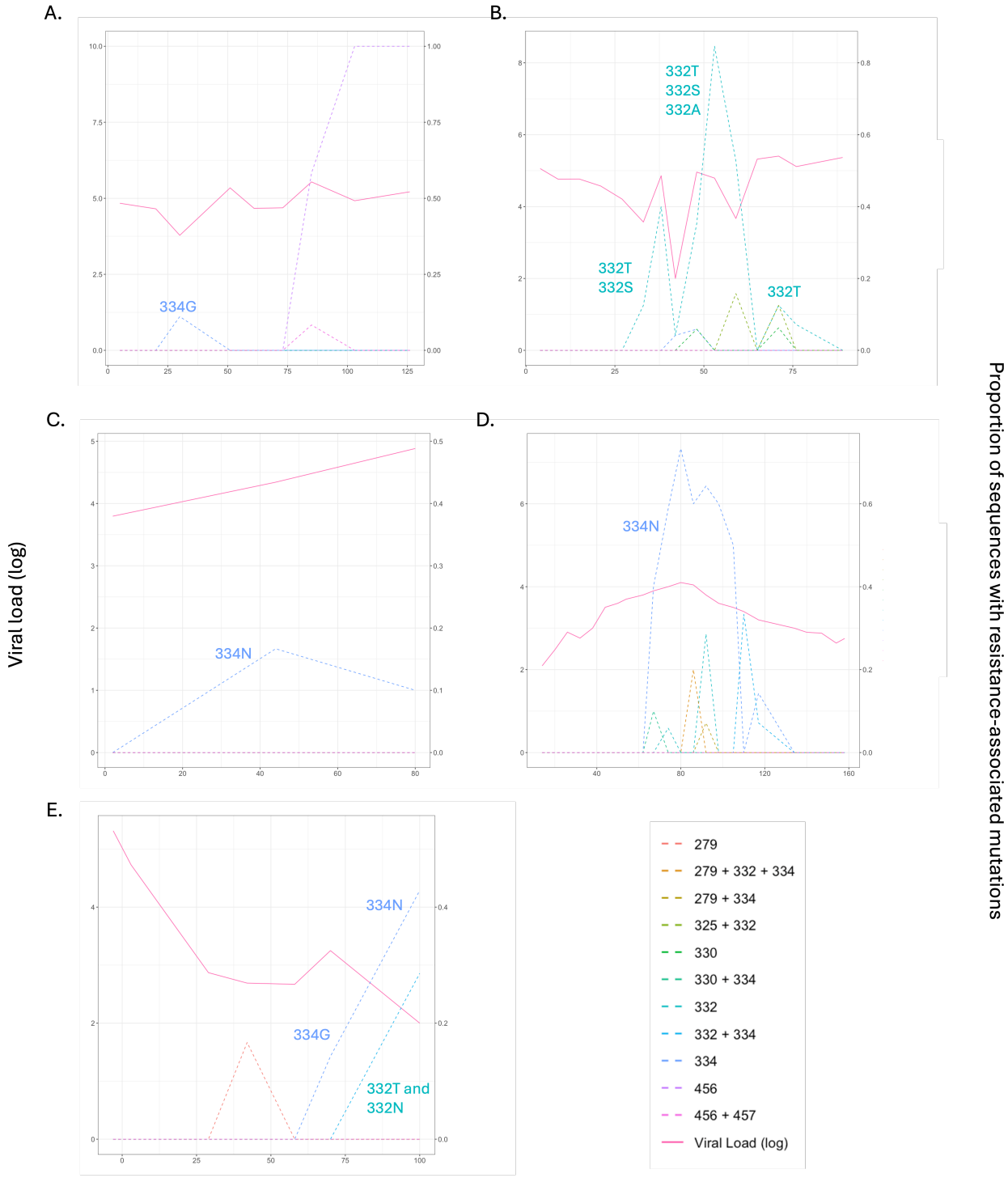

Figure 4.1: Viral load and proportions of bnAb resistance-associated mutations. Each plot (A-E, for participants P2, P4, P7, P10 and P11 respectively) shows the log viral load (y axis on the left) and the proportion of sequences preddicted as resistant to bnAbs (y axis on the right), with each mutation or mutation combination showed in different colour. The x axis shows the time post seroconversion (in months), when plasma samples where taken for every participant.

4.3.3 Pre-ART and reservoir bnAb sensitivity reporting

In order to explore the origin of resistant sequences within the HIV reservoir, I investigated the potential contribution of pre-existing bnAb resistance mutations present in the blood plasma just prior to the initiation of ART to the development of the viral reservoir. This analysis entailed comparing the presence and prevalence of resistance mutations in the circulating virus and PBMCs before treatment. Six HEATHER participants (Section 2.2.2) with paired samples before and during ART were included in this cohort. Their average time from seroconversion to ART initiation was 50 days (range: 33-70 days) and their pre-ART samples were taken on a median of 2 days before ART start (range: 0- 35 days). Five out of six participants in this subset had B clade HIV and one had D/A1 clade (Table 4.3).

Table 4.3: Evolution of bnAb resistance in HEATHER. Proportion of HEATHER participant sequences predicted as resistant to bnAbs, on samples taken pre-ART initiation (RNA and DNA) and during ART (DNA).

	Proportion of mutated sequences								
ID	Pre-ART DNA	Pre-ART RNA	on-ART DNA	Mutations	Resistance to	ART start Date	pre-ART Visit Date	Seroconversion Date	Clade
SM025	0.00	0.10	0.04	458 (pre) and 459 (on-ART)	3BNC117	2014-01-13	2014-01-08	2013-12-14	B
SM044	0.17	0.12	0.03	459	3BNC117	2014-05-15	2014-05-11	2014-03-21	B
ST431	NA	0.00	0.01	456	3BNC117	2015-02-09	2015-02-09	2014-12-02	B
ST377	NA	1.00	1.00	332,334	10-1074	2014-06-08	2014-05-13	2014-04-24	B
ST385	0.00	0.00	0.14	334	10-1074	2014-06-17	2014-06-17	2014-04-08	D/A1
ST413	0.25	0.00	0.27	334	10-1074	2014-10-23	2014-10-23	2014-09-20	B

All participant samples from the on-ART timepoint had at least one resistant sample to either 10-1074 or 3BNC117. Out of six participants, two lacked pre-ART DNA sequences. No evidence of resistance was found in the pre-ART samples from participants ST431 and ST385, although the limited number of sequences obtained pre-ART ST431 should be noted. Despite a lower proportion of resistance in the on-ART sample, comparable proportions of resistant sequences were observed in the pre-ART samples from SM044, considering the differing numbers of total sequences. Consistent with the on-ART sample, all sequences obtained from ST377 were resistant. In contrast, SM025 exhibited resistance sequences only in the pre-ART

plasma component but not in the DNA sample. However, the low number of pre-ART sequences in this case and the distinct mutation sites (458 and 459) in the pre-ART RNA and on-ART DNA samples should be considered. Similarly, ST413 had resistant sequences only in the pre-ART DNA sample but not in the on-ART DNA.

4.3.4 bnAb sensitivity evolution through ancestral state reconstruction

In the absence of longitudinal data and relevant dating, ancestral state reconstruction can be used to infer the sensitivity phenotype of the founding virus. Here, ancestral state reconstruction was performed from the nine HEATHER participants (Chapter 3.3.2), who had sequences with and without 10-1074 resistance-associated mutations using bootstrapped maximum likelihood nucleotide trees. The ancestral state is displayed as a pie chart at the root of each tree and the likelihood of sensitivity and resistance is illustrated by different colours. The analysis revealed that in five of the samples (Figure 4.2A-E), the inferred root was very likely sensitive, indicating that the ancestral strain in these patients was most likely susceptible to 10-1074. The most common mutations observed in these samples were introducing an asparagine at position 334 (N334), with a PNG emerging at 334 rather than at 332. In the remaining four trees (Figure 4.2F-I), a large amount of uncertainty was associated with the status of the most recent common ancestor of the sequences, although these ancestral strains were slightly more likely to be resistant to 10-1074. As viral evolution is not likely to happen during suppressive ART, this suggests that the ancestral strain in these participants may have already possessed genetic mutations associated with 10-1074 resistance, consistent with transmission of bnAb resistant strains, or that evolution of these mutations occurred shortly after transmission before ART was started.

The same process was followed for samples from participants who harboured sequences with and without 3BNC117 resistance-associated mutations. Three participants with more than one sequence predicted as 3BNC117-resistant had tree roots predicted as sensitive to 3BNC117 (Figure 4.3A-D). All three participants

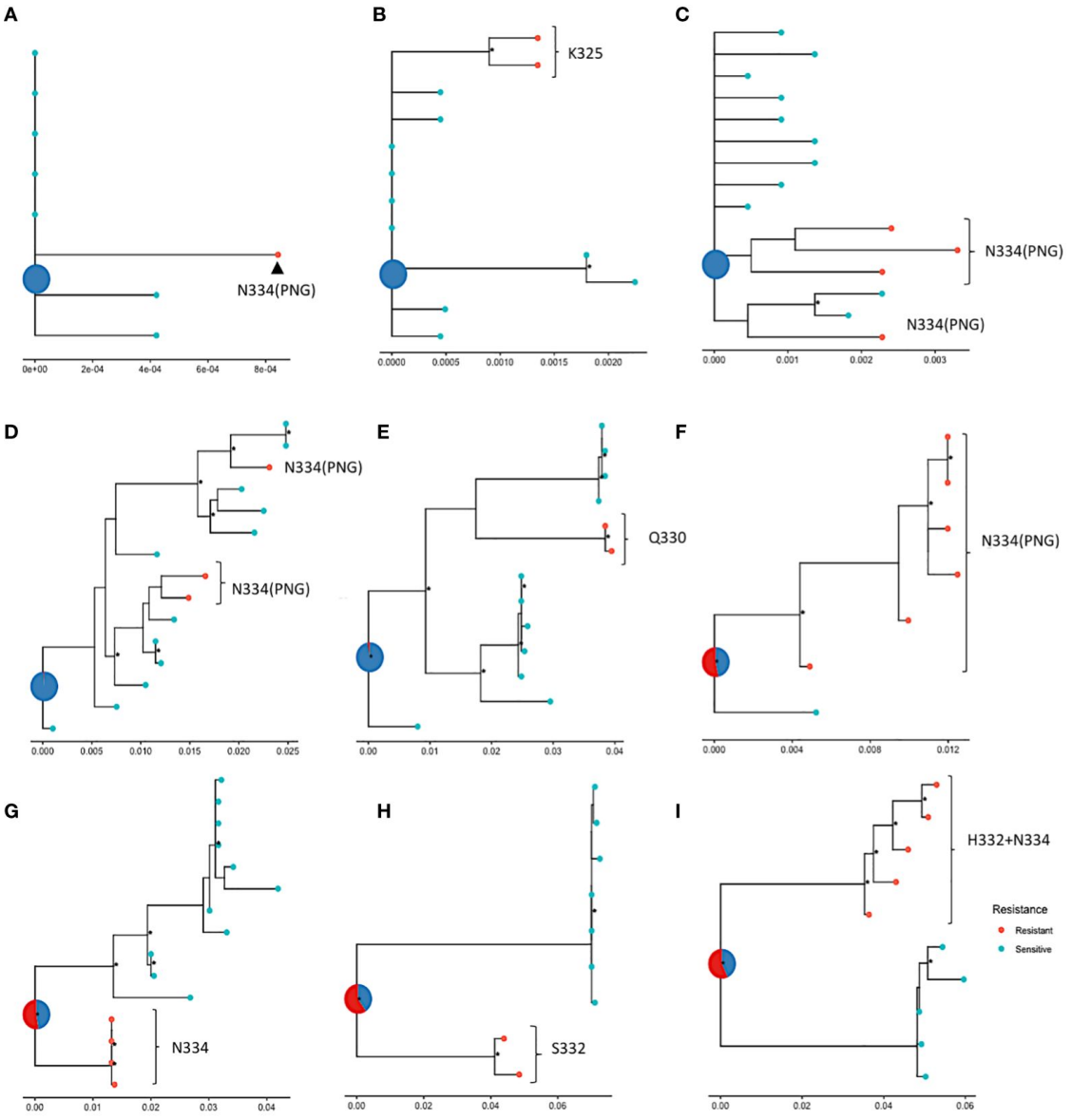

Figure 4.2: ML phylogenetic trees tracing the evolution of nucleotide sequences in nine participants (AI) from the HEATHER cohort, amplified with SGA, with ancestral roots annotated with predicted sensitivity. Red points indicate 10-1074 resistant and blue points indicate sensitive sequences. The status of the most recent ancestor is represented as a pie chart at the root of the tree; (AE) show trees with roots predicted to be sensitive (or most likely sensitive) to 10-1074 and (FI) show trees with roots predicted to be most likely resistant to 10-1074. Data are for proviral nucleotide sequences and maximum likelihood bootstrap support values exceeding 60% are marked with a *. The scale indicating the number of mutations per site based on the length of branches can be found at the bottom of each tree plot.

had different mutations associated with 3BNC117 resistance. For one participant, the sensitivity of the inferred root could not be predicted (Figure 4.3D). That participant had sequences predicted as resistant to 10-1074, and the prediction for the root was likely resistant to 10-1074 (Figure 4.2H).

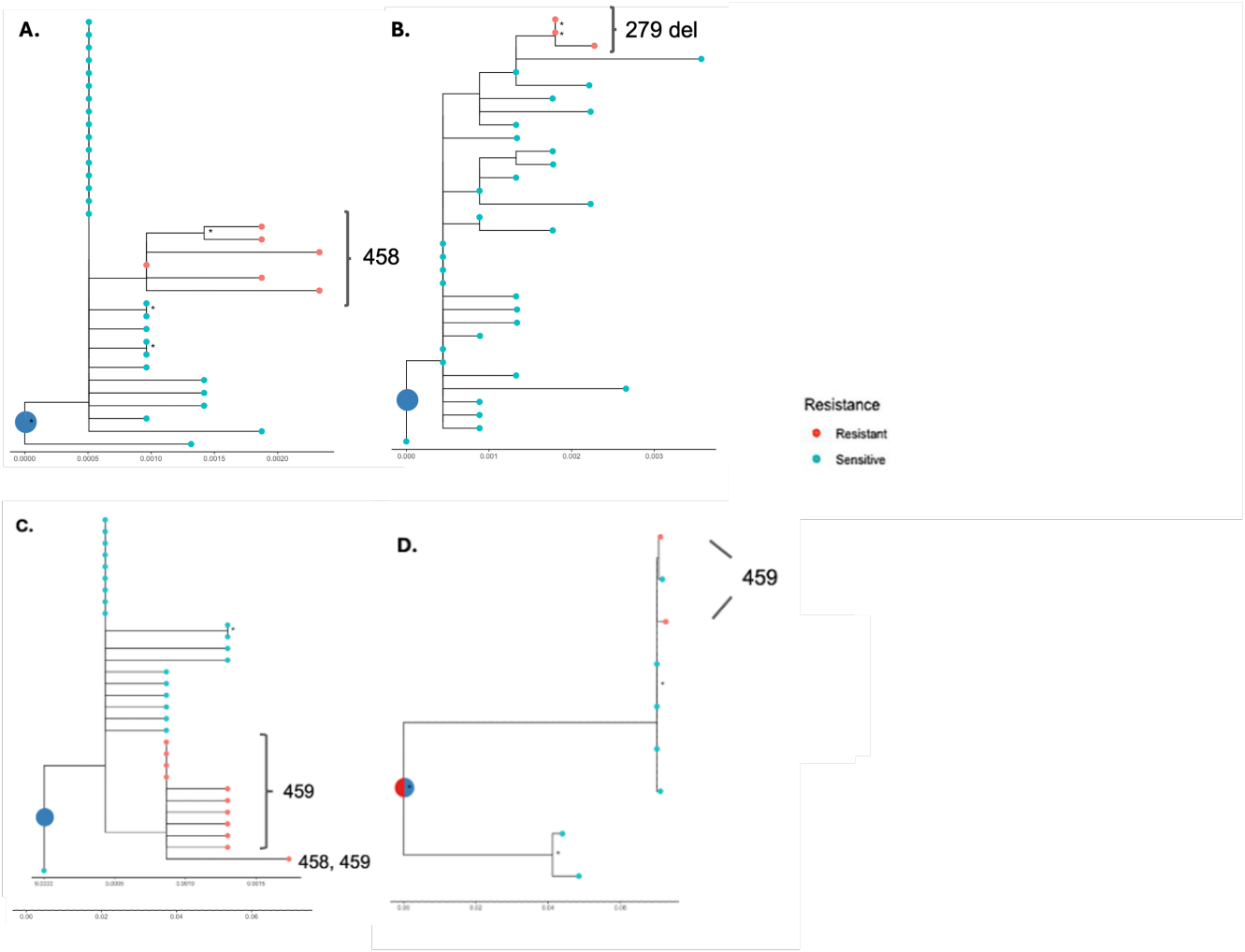

Figure 4.3: ML phylogenetic trees tracing the evolution of nucleotide sequences in four participants (AD) from the HEATHER cohort, amplified with SGA, with ancestral roots annotated with predicted sensitivity. Red points indicate 3BNC117 resistant and blue points indicate sensitive sequences. The status of the most recent ancestor is represented as a pie chart at the root of the tree; (AC) show trees with roots predicted to be sensitive (or most likely sensitive) to 3BNC117 and (D) shows a tree with roots predicted to be equally likely sensitive and resistant to 3BNC117. Data are for proviral nucleotide sequences and maximum likelihood bootstrap support values exceeding 60% are marked with a *. The scale indicating the number of mutations per site based on the length of branches can be found at the bottom of each tree plot.

4.3.5 Comparison between reservoir and rebound virus bnAb sensitivity

The combination of Q4PCR assay with sequencing has been proposed as a reliable assay for sequence-based bnAb sensitivity prediction. This is based on the fact that the reservoir is predominantly composed of non-intact proviral sequences incapable of viral replication, which could confound analyses based solely on Env SGA. While Q4PCR offers a more accurate assessment, its resource-intensive nature poses challenges for implementation in the diagnostic pipeline. The Arm B of the RIO trial provided valuable insights into viral rebound selection. By withholding ART after a placebo dose, participants in this arm were allowed to experience viral rebound, revealing the naturally emerging viral variants from the reservoir. This approach enabled the identification of viruses that would likely source the rebound, offering a more direct assessment of bnAb sensitivity. In this section, I compare baseline proviral sequences obtained through Env SGA and Q4PCR and compared it to the rebound in order to determine whether SGA alone is sufficient for reliable bnAb sensitivity prediction.

Env sequences from proviruses were amplified from samples taken from RIO Arm B participants before TI, while being virally suppressed by long term ART, and from plasma at the time of the first post-TI rebound, in absence of any intervention. A total number of 18 participants had paired baseline sequences (obtained through the Q4PCR assay and/or SGA), as well as Stage 1 rebound sequences (Table 4.4).

Table 4.4: Demographics of the RIO Arm B participants with paired baseline and first rebound Env sequences. The number of baseline sequences obtained through SGA and through the Q4PCR assay is presented

Participant	No Seq Baseline	Baseline Intact (QPCR)	Baseline SGA	No Seq Rebound	Time from Diagnosis to ART (months)	Time from ART to TI (years)
001-002	10	7	3	14	1	7.8
001-003	42	3	39	6	1	5.1
001-009	12	12	0	2	1	5.4
001-013	14	0	14	32	10 days	5.9
001-017	3	0	3	1	1	4.8
001-019	3	0	3	4	1	4.4
001-020	24	0	24	18	1	8.5
002-001	13	0	13	26	1	20.0
002-004	42	28	14	7	1	19.6
003-001	22	9	13	12	18 days	4.5
003-004	6	0	6	12	2	3.6
003-005	20	9	11	30	1	9.4
005-004	12	1	11	3	1	3.0
005-006	14	0	14	19	1 day	4.6
006-010	30	0	16	7	2	10.1
007-007	15	0	15	44	1	5.9
008-010	21	0	21	13	5	8.3
008-014	17	0	17	2	1	4.5

Linear mixed-effect models were used on R to investigate the effect of the compartment on sensitivity prediction for each bnAb in each prediction model, controlling for intra-patient variability. I compared the impact of the compartment on sensitivity prediction using two data sets; one contained only baseline Env sequences obtained through SGA and paired rebound sequences (SGA data set, 17 participants) and the second contained only baseline Env sequences obtained through Q4PCR and paired rebound sequences (intact dataset, 8 participants). The models for both data sets showed no difference in sensitivity predictions between the reservoir and the rebound virus, albeit with a effect size for both bnAbs in the SGA dataset (10-1074= 0.88, 3BNC117: -0.77, p-value>0.1 for both) compared to intact dataset (10-1074: 0.5, 3BNC117: 102, p-value>0.1 for both).

ID	Provirus			Rebound		
	No Seq Screening	10-1074	3BNC117	No Seq Screened	10-1074	3BNC117
001-002	10			14		
001-003	42			6		
001-009	12			2		
001-013	14			32		
001-017	3	1		1		
001-019	3			4		
001-020	24		1	18		
002-001	13			26		1
002-004	39			7		
003-001	22	4		12	4	
003-004	6			12		
003-005	20			30		
005-004	12			3		
005-006	14			19		
006-010	30			7		
007-007	15			44		
008-010	21			13		
008-014	17			2		

Figure 4.4: Sensitivity prediction in baseline provirus and rebound plasma virus.Tables showing 10-1074 and 3BNC117 predicted sensitivity in provirus (baseline) and in plasma (at first rebound), using the Rockefeller model. Fully sensitive indicates that none of the sequences sampled at this timepoint contained mutations associated with bnAb resistance. Likewise, fully resistant signifies that all sequences at this timepoint harbored mutations known to confer bNAb resistance.

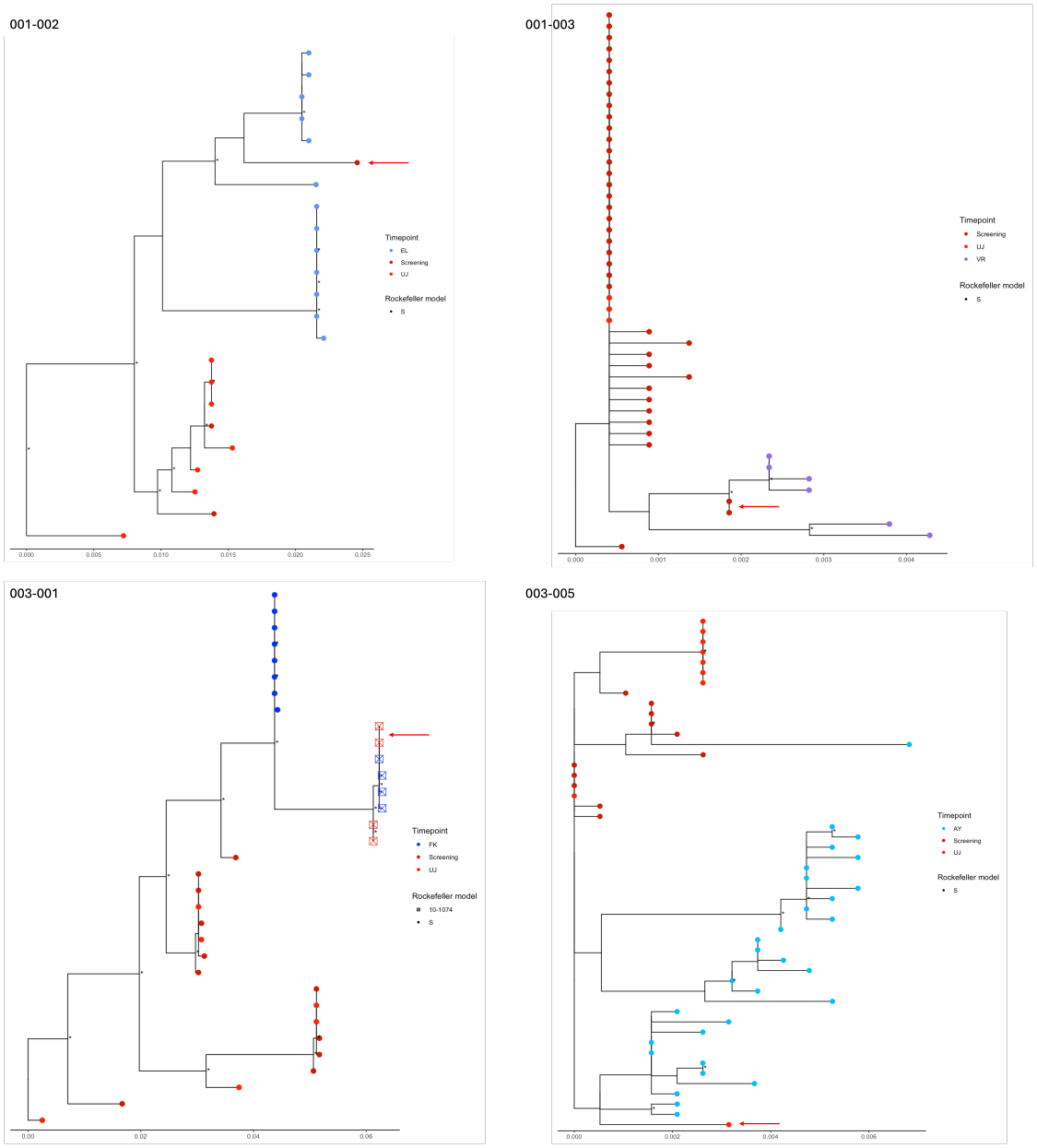

Figure 4.5: ML phylogenetic trees tracing the evolution of nucleotide sequences in four Arm B participants (A-D) from the RIO cohort, amplified with SGA. For each participant sequences sampled from baseline (annotated as Screening and UJ, in dark red and red respectively) and from the Stage 1 post-TI rebound were used. Shape indicated bnAb sesnsitivity beased on the Rockefeller model predictions. Sequences labelled as UJ were aqcuired hrough Q4PCR assay and they were from intact virus. Arrows mark the sequences that cluster closest to the plasma Env sequences from post-TI.

Figure 4.4 shows the sensitivity predictions by the Rockefeller algorithm (Materials and Methods, Section 2.3) before and after Stage 1 rebound for all 18 Arm B participants. Baseline sequences here consist of both normal SGA and Q4PCR

intact baseline sequences. In two participants, resistance mutations were detected at baseline but not at rebound; both of them were SGA samples. In participant 003-001, mutations associated with 10-1074 resistance was detected in a proportion of sequences at baseline and at rebound; notably, the same mutations were found in intact and SGA baseline sequences.

Pairwise distances between SGA and Q4PCR baseline Env sequences and the rebound viral sequences in 4 Arm B participants were also calculated and visualised in phylogenetic trees. The SGA sequences clustered closer to the rebound sequences in two participant samples, participants 001-002 and 001-003) (Figure 4.5). In participant 003-005, an intact sequence obtained through Q4PCR was the one that clustered the closest to the rebound and in 003-001 sequences obtained through both assays were a similar distance away from the rebound virus. In addition, the resistance-associated mutations which were found at baseline SGA proviral sequences were also detected in Q4PCR intact proviral Env sequences 4.5.

4.4 Discussion

In this chapter, I studied the origins of pre-existing resistance to 10-1074 and 3BNC117 by analysing data from SPARTAC, HEATHER and RIO participant samples processed and sequenced in Oxford and from MACS, which are available in an online database. The aim was to identify the source of bnAb resistance in bnAb-naive PWH and whether it is more likely to be transmitted or to emerge during within-individual evolution.

The analysis of the Env sequences sampled longitudinally from participants in the MACS study showed that resistance to bnAbs emerges more than 30 months after seroconversion and this may explain the absence of resistance evolution in our SPARTAC participants, which were sampled the latest 52 weeks post seroconversion. This is in line with the timing of host immune responses, such as nAbs, which can exert selection pressure at epitopes related or similar to the bnAb epitopes in our study (Section 1.4). In most participants in this cohort, viruses with mutations

in more than one position arose in later stages of infection and were usually preceded by single mutations. A PNG shift to position 334 was observed 2 of 5 participant and it was one of the mutations that proliferated throughout time, before reverting back to WT. Of note, while 69% of all participants with 100% resistance to 10-1074 in HEATHER had mutations at both 332 and 334, those participants harboring both sensitive and resistant sequences usually had a single mutation (8 in 9 participants, 88.8%), commonly at 334. This suggests that mutations at 334, especially those which allow the PNG shift, may offer an equilibrium of fitness cost and escape potential as long as the virus is under immune pressure.

The number of sequences and samples obtained from SPARTAC was not adequate for a statistically significant analysis and only description of the findings was achieved. It is noted that one in three SPARTAC participants, SUC036029, had 93% of all sequences amplified from their week 12 and week 52 samples carrying a mutation associated with 10-1074, and specifically S/T334N, which conferred a shift of the PNG from position 332 to 334. One sensitive sequence in a total of 10 found in the week 52 sample could indicate the beginning of reversion to wildtype of a 10-1074 resistant virus which was transmitted to the participant. Indeed, reversion of 334 mutations to wild-type has been reported by Caskey et al., in individuals who received 10-1074, when bnAb concentration fell below therapeutic levels (Caskey et al., 2017). Moreover, a bulk Env sequence from baseline, amplified by a former student in the group, showed that the S/T334N mutation existed at that timepoint, hence reinforcing the hypothesis of resistance transmission. However, sequences from SUE036028, a participant who belonged in the same transmission chain as SUC036029 (the two participants acquired HIV on the same date from the same donor (English et al., 2011)) had no evidence of the S/T334N mutation in their baseline sample. Although the size of this cohort is very small, the presence of at least one baseline pre-existing mutations in two of 12 participants (SUC036029 and SUW036049) is slightly below the prevalence of 10-1074 resistance in the HEATHER cohort, which was presented in Chapter 3, but this may be due to the low number of sequences obtained from the SPARTAC participants. The

prevalence of 3BNC117-associated resistance in this cohort is in line with the prevalence of 3BNC117 resistance in the HEATHER cohort. Last, two of these participants were included in a study of development of plasma neutralisation breadth during untreated HIV infection (Granger et al., 2021). SUV214008, who carried no mutations associated with 10-1074 resistance at baseline or week 52, developed heterologous neutralisation targeting the 332 site, but this happened only after 180 weeks post enrollment. On the contrary, SUP033003, who had minor N332I mutations at week 12 and 24 samples, was found to have CD4-bs targeting Abs before he developed heterologous neutralisation. Notably, those sequences also had Asp at position 279.

The characterization of ancestral state resistance in HEATHER participants with mixed resistance showed that it is possible for founder viruses to be resistant or sensitive, which highlights the heterogeneity of bnAb resistance in the population. Our findings from an ART-treated PHI cohort differs from those in chronic infection, such as MACS, where there is more viral exposure to immune selection pressure. The co-existence of resistant and sensitive viruses within a host may reflect viral escape from early immune response with cross-reactivity to escape from bnAbs (Anthony et al., 2017). It is also possible that mutations that confer 10-1074 resistance come at a fitness cost and a resistant virus may revert to the sensitive wild type when bnAb serum levels drop and the selection pressure reduces (Caskey et al., 2017).

Understanding the origins and dynamics of viral sequences with bnAb-resistance conferring mutations is critical for informing effective therapeutic decisions. Currently only replicating viruses in plasma are used routinely for drug resistance screening and monitoring purposes (Panel on Antiretroviral Guidelines for Adults, 2022). Furthermore, it is advised that in cases where PWH have no detectable or low viral load, drug resistance test results performed on proviruses are interpreted with caution (Chu et al., 2022). A counterargument to the reliance on proviral DNA for resistance testing suggests that it may not accurately reflect the real-time resistance landscape of the virus. Indeed, the proviral reservoir might harbor

a diverse range of viral variants, some of which may not be actively replicating and thus clinically irrelevant. By comparing bnAb sensitivity predictions of paired proviral and plasma sequences from the same RIO Arm B participants at baseline and time of rebound respectively, I sought to establish the reliability of proviral-based bnAb resistance testing as a surrogate for plasma-based assessment. More specifically, mixed effect models for bnAb sensitivity predictions showed no difference in sensitivity in plasma and in provirus, regardless of whether the Env sequence came from an intact or a potentially non-intact provirus. In addition, in three out of four participants for whom Env sequences were amplified from SGA and from intact proviruses at baseline, the SGA sequences clustered closer to the rebound than the Env sequences from intact. This could be attributed to the higher number of SGA sequences obtained but provides evidence that in this PHI cohort there is high likelihood that the SGA sequences represent the replication-competent reservoir. The exact same mutations were observed in critical epitopes in paired sequences from 001-009 and 003-001, while 1 resistance sequence in each of 001-017 (S/T334N) and 001-020 (G458S) found at baseline was not represented in the respective rebound population. This discrepancy may be attributed to the likelihood that the resistant variant belonged to the 95% defective proviral population or to the low number of rebound sequences obtained, especially in the case of 001-017, where a single rebound sequence was amplified. On the contrary, one sequence amplified from the rebound timepoint of 002-001 was predicted as resistant with a D/N325E. This was one of 26 sequences that might have been missed at baseline, as only 13 sequences were screened. The impact of these mismatches should be assessed when the rebound sequences from the post-bnAb rebound timepoint, if any, are studied. These results will clarify whether bnAb pressure in these participants should facilitate the proliferation of the resistant viruses over the sensitive. The results of this analysis demonstrate a very high degree of concordance in bnAb resistance profiles between proviral and plasma HIV sequences, suggesting that testing provirus is as reliable as testing circulating viral sequences. Nevertheless, these findings are limited to a cohort of PHI with less

viral diversity in the reservoir and a lower likelihood of missing resistant variants, when compared to chronic infection.

Overall, these findings suggest that pre-existing bnAb resistance-associated mutations in individuals with PHI are more likely to be transmitted than to arise through within-host evolution. Mutations on epitopes critical for bnAb binding, as defined by existing resistance prediction models, are likely to emerge but primarily at later stages of infection. In light of these findings, it is possible that individuals with chronic HIV infection may have a higher prevalence of pre-existing bnAb resistance-associated mutations and this should be considered when developing therapeutic strategies that include the administration of bnAbs to these individuals. Additionally, the study found that proviral DNA sequencing, regardless of whether it originates from intact or non-intact viruses, can be a reliable surrogate for plasma-based bnAb resistance testing, especially in early-stage infection. Further research in different cohorts of PWH with varying stages of infection and clinical/virological characteristics is necessary to validate these findings and inform more effective HIV treatment strategies.

5

Predicting bnAb sensitivity in the RIO trial

Contents

5.1 Context

Recent trials in humans have revealed that the combination (Bar-On et al., 2018; Gaebler et al., 2022; Mendoza et al., 2018) or individual administration (Caskey et al., 2015, 2017; Scheid et al., 2016) of 10-1074 and 3BNC117, have led to prolonged viral suppression and delayed viral rebound. These findings suggest the potential of these bnAbs as a standalone treatment or with other interventions to maintain long-term viral control. However, in all trials a proportion of participants will experience viral rebound earlier than expected, which has been attributed to viral

resistance to bnAbs.

Several studies have demonstrated a rising trend of bnAb resistance throughout the pandemic (Bouvin-Pley et al., 2013; Bouvin-Pley et al., 2014; Bunnik et al., 2010; Stefic, Bouvin-Pley, Braibant, et al., 2019; Stefic, Bouvin-Pley, Essat, et al., 2019) and Chapter 3, section 3.3.1. It is therefore crucial to establish a reliable bnAb sensitivity screening method before implementing bnAbs as standard treatments in clinical practice. Env sequencing and bnAb sensitivity prediction algorithms have been used to restrict bnAb administration to those PWH who were more likely to benefit from the treatment (Mendoza et al., 2018) or retrospectively, to analyse the correlation between sensitivity and viral rebound (Cohen et al., 2018; Gaebler et al., 2022; Gruell et al., 2022; Gunst et al., 2022).

The RIO trial is the largest study testing the efficacy of the long acting versions (LS) of 10-1074 and 3BNC117, which utilised a novel trial design concept, where participants were randomised into a treatment or a placebo group, who also received treatment at a later stage. Screening for bnAb resistance using a sequence-based predictions was included in the eligibility criteria of RIO. Given the limited accuracy of 3BNC117 resistance predictions, it was decided that these data would be excluded from the eligibility criteria for the RIO trial. Hence, to be eligible to enroll in RIO, no evidence of full 10-1074 resistance should be present in baseline Env sequences from clinically eligible candidates, using the Rockefeller sensitivity prediction criteria. Nevertheless, there is lack of conclusive evidence regarding the value of sequence-based prediction models and more specifically of the Rockefeller model.

In this chapter, I aimed to evaluate the performance of the Rockefeller predictions based on clinically-relevant outcomes. I then ran correlations between baseline predictions and these metrics to identify participants that fell under a different sensitivity class and in particular to the Resistant class. Subsequent analyses focused on characterising these resistant individuals to elucidate potential viral or clinical features contributing to the discrepancy between predicted classification

and classification based on outcomes. I leveraged these insights to refine the baseline prediction criteria.

5.2 Aims

1. Present the preliminary clinical outcomes of RIO and evaluate the efficiency of bnAbs based on molecular analysis
2. Assess the performance of the Rockefeller sensitivity prediction model
3. Examine the impact of baseline sensitivity predictions in clinical outcomes
4. Explore the use of other viral features or clinical information that may refine the sensitivity predictions.

5.3 Results

The findings reported in this section are not the official trial outcomes. These are based on my own analyses obtained from viral load data, and my own interpretation of when viral rebound happened (as a committee will make the final decision at the end of the study). For some participants trial Arm has been inferred using pharmacokinetic data. Although it is expected that the results will be similar to the final report, there may be some differences.

5.3.1 Demographics of the RIO cohort

The RIO trial design is described in detail in Chapter 2, section 2.2.4. At the time of writing this chapter, 66 participants were recruited in RIO and 2 participants were still blinded as to which trial arm they had been randomised to. The Rockefeller model employed a sequence-based approach to predict viral sensitivity by identifying specific amino acid residues as predictive markers. These features were used to classify each Env sequence in samples obtained from each participant as either sensitive or resistant (Chapter 2, Section 2.3.5).

All participants included here were male and mainly white or white British (86%). The median age of participants at the time of enrollment was 39 years old.

Although there is a difference in the median age of participants in arms A and B, this difference is not statistically significant (Wilcoxon test p-value=0.07). All participants had started ART during PHI and they had been on treatment for a median of 5 years prior to enrollment. No participant had detectable viral load at the time of enrollment (VL<20 copies/ml) and the median CD4+ T cell count at baseline was 791 cells/mm^3. The majority had B clade HIV (72%), followed by C (6.3%), F1 (6.3%) and other in a frequency of ~3% or less (Table 5.1). An average of 19.3 single proviral *env* sequences was obtained at screening per participant (range: 1-88) through SGA (Chapter Materials and Methods, 2.3.2). The median pairwise distance of baseline sequences from the RIO participants was very small; median PWD = 0.0019, range: 0.00011- 0.026. This is likely due to the fact that all participants were treated during PHI and the diversity of the reservoir was low, as expected.

Table 5.1: Summary table of RIO participant characteristics

Characteristic	Overall N = 66	A N = 32	B N = 31	Blinded N = 3
Clade				
B	46 (72%)	22 (73%)	22 (71%)	2 (67%)
C	4 (6.3%)	1 (3.3%)	3 (9.7%)	0 (0%)
F1	4 (6.3%)	2 (6.7%)	2 (6.5%)	0 (0%)
A1	2 (3.1%)	1 (3.3%)	1 (3.2%)	0 (0%)
CRF02-AG	2 (3.1%)	1 (3.3%)	1 (3.2%)	0 (0%)
D/A1	2 (3.1%)	1 (3.3%)	1 (3.2%)	0 (0%)
CRF06-CPX	1 (1.6%)	0 (0%)	1 (3.2%)	0 (0%)
CRF31-BC	1 (1.6%)	0 (0%)	0 (0%)	1 (33%)
CRF73-B G	1 (1.6%)	1 (3.3%)	0 (0%)	0 (0%)
G	1 (1.6%)	1 (3.3%)	0 (0%)	0 (0%)
Unknown	2	2	0	0
Race				
White or White British	57 (86%)	28 (88%)	26 (84%)	3 (100%)
Asian - Any Other Asian Background	3 (4.5%)	3 (9.4%)	0 (0%)	0 (0%)
Black or Black British - African	3 (4.5%)	1 (3.1%)	2 (6.5%)	0 (0%)
Other	3 (4.5%)	0 (0%)	3 (9.7%)	0 (0%)
Sex				
M	66 (100%)	32 (100%)	31 (100%)	3 (100%)
Age (Baseline)	39 (32, 46)	36 (31, 42)	44 (32, 52)	41 (36, 52)
Time on ART (Baseline)	5.00 (4.00, 7.00)	5.00 (3.00, 6.00)	5.00 (4.00, 7.00)	9.00 (4.00, 9.00)
CD4 count (Baseline)	722 (602, 930)	676 (602, 921)	791 (629, 1,014)	811 (454, 820)
Time of viral control since last bnAb dose (Weeks)	26 (12, 40)	19 (12, 41)	29 (12, 50)	7 (0, 14)
Sensitivity (Baseline)				
Sensitive	47 (71%)	22 (69%)	23 (74%)	2 (67%)
Minor 10-1074	6 (9.1%)	1 (3.1%)	4 (13%)	1 (33%)
Minor 3BNC117	5 (7.6%)	3 (9.4%)	2 (6.5%)	0 (0%)
3BNC117	3 (4.5%)	2 (6.3%)	1 (3.2%)	0 (0%)
NA	3 (4.5%)	3 (9.4%)	0 (0%)	0 (0%)
10-1074	2 (3.0%)	1 (3.1%)	1 (3.2%)	0 (0%)

[1] n (%); Median (Q1, Q3)

The concentration of bnAb was quantified at multiple timepoints throughout the duration of the study and pharmacokinetic (PK) data were modeled for a subset of the RIO participants. In Arm A, bnAb concentrations reached 50 ug/ml at weeks 21 and 23 and 10 ug/ml at weeks 50 and 49 for 10-1074 and 3BNC117, respectively. Likewise, bnAb concentrations in Arm B dropped to 50 ug/ml on week 25 for both bnAbs and to 10 ug/ml at weeks 52 and 48 for 10-1074 and 3BNC117, respectively (Figure 5.1A).

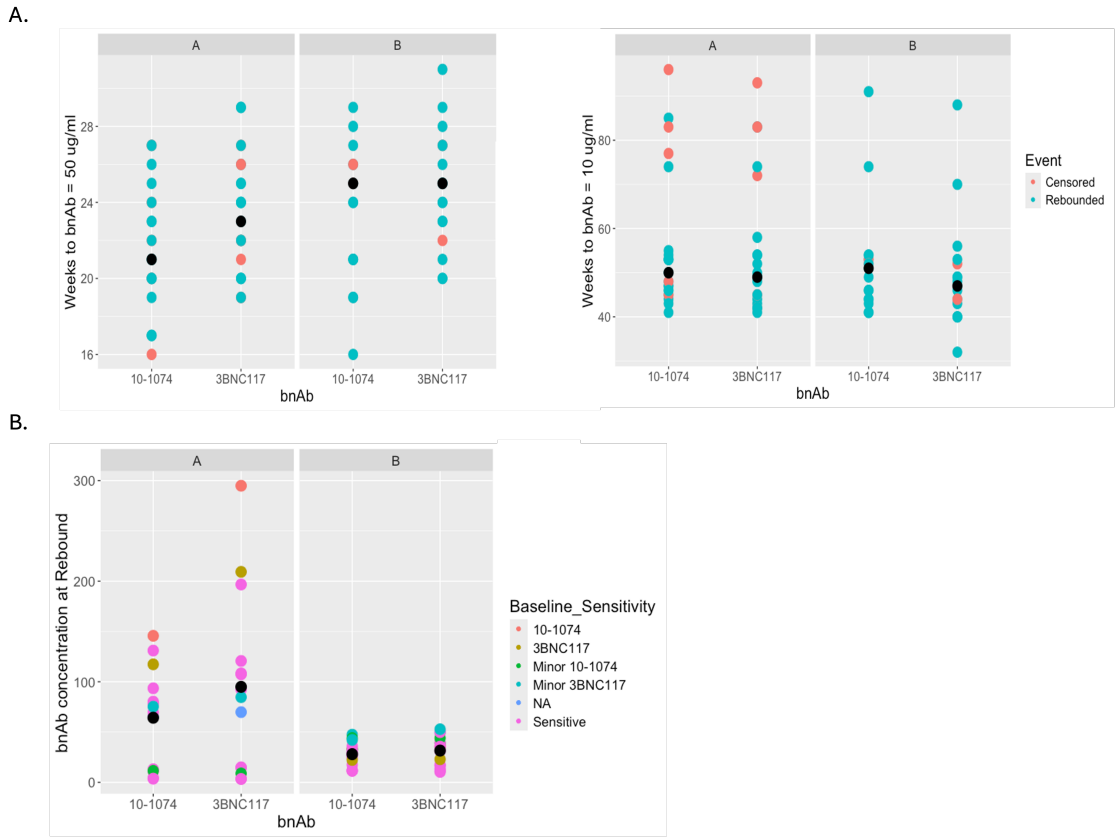

Figure 5.1: bnAb concentration keypoints. Panel A show the Weeks when bnAb concentration reached 50 ug/ml (left panel) and 10 ug/ml (right panel). Each dot represents a participant in Arm A or B and each colour indicates whether participant rebounded or not. Panel B shows bnAb concentrations at rebound for participants in Arm A and B, and bnAb concentration at 2nd TI, for Arm B participants. The black dot in all panels marks the median.

The median bnAb concentration at the time of rebound for Arm A participants who were classified as sensitive at baseline was 36 ug/ml and 30 ug/ml for 10-1074 and 3BNC117, respectively. Sensitive Arm B participants rebounded at a median

10-1074 concentration of 28.93 ug/ml and a median concentration of 3BNC117 of 30.97 ug/ml. As expected, Arm A participants who were predicted as bnAb resistant at baseline rebounded when the estimated concentration of bnAbs was high; 10-1074 concentration was 146 ug/ml and 3BNC117 concentration was 294 ug/ml. The median concentration of bnAbs at rebound was 35.8ug/ml for both bnAbs in Arm A and 35.5 and 35.7 ug/ml for 10-1074 and 3BNC17 respectively in Arm B (Figure 5.1B).

Sensitivity and resistance-associated mutations analysis

To characterise the sensitivity of viruses in the reservoir, single genome amplification of *env* was performed from all potential participants at screening, and sequences were used for bnAb sensitivity predictions. Although the presence of full 10-1074 predicted resistance was an exclusion criterion for RIO, 2 participants with initially non-amplifiable Env sequences who were enrolled (3% of the cohort) were found in a post-hoc analysis to have 10-1074 resistance-associated mutations in 100% of their baseline sequences. Six participants (9.1%) had a minority of sequences with 10-1074 resistance-associated mutations and 3 (4.5%) were not amplified at the time of enrollment. Due to the low confidence in 3BNC117 sensitivity prediction accuracy, these data were not taken into consideration at participant recruitment (Table 5.1). Nevertheless, it is noted that in this cohort a total of 3 participants were predicted as fully resistant to 3BNC117 and 4 had only a minor proportion of sequences predicted as 3BNC117 resistant at baseline.

A total of 12 participants with clade B had at least one resistant sequence to either bnAb; specifically 11% had low-frequency 10-1074 resistance, 8.7% had minor 3BNC117 resistance and 6.5% had 100% of their sequences predicted as resistant to 3BNC117. Two out of 4 samples from participants with F1 clade were predicted as 100% resistant to 10-1074 and both participants with D/A1 clade HIV enrolled in the trial had minor resistance to either 10-1074 or 3BNC117 (Figure 5.2).

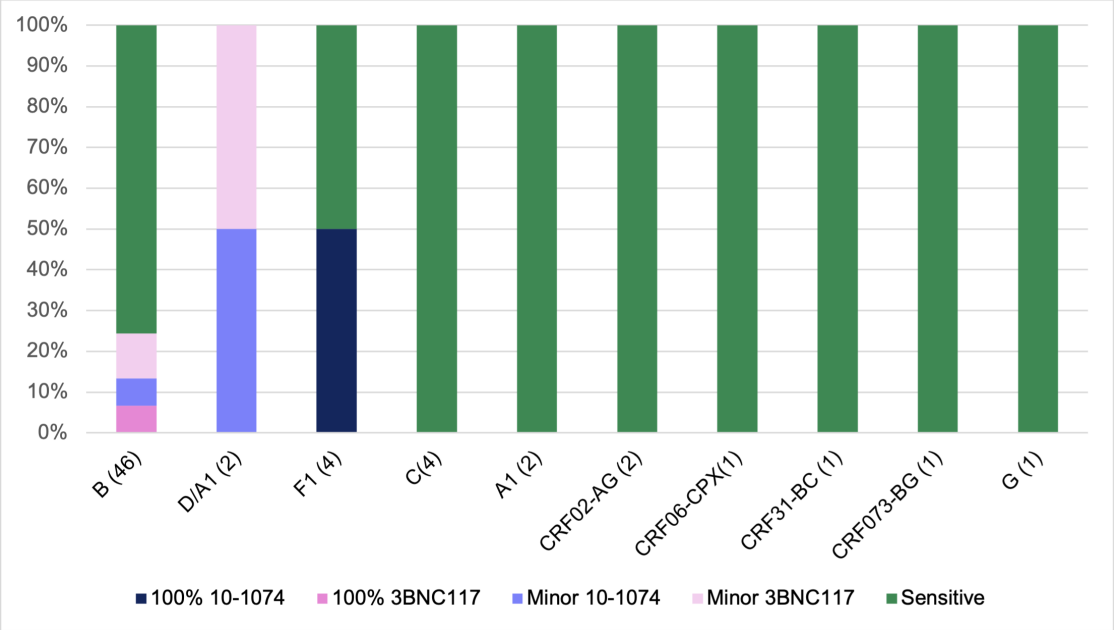

Figure 5.2: Sensitivity per clade in the RIO cohort. The number of individuals per clade is shown in the x axis. The proportion of sequences classified as sensitive or with different proportion of bnAb resistance-associated mutations (indicated by colour) is shown in the y axis.

Pre-existing mutations associated with 10-1074 resistance were detected in various sites with the 10-1074 epitope region. The two participants who were predicted as fully resistant to 10-1074 harbored either N332K (participant 001-008) or N332T and S/T334N, which resulted in a shift of the PNG from position 332 to 334 (participant 001-009). Mutations at 334 were the most commonly found resistance-associated mutation in participants with 10-1074 minor resistance. The change of the 334 residue to asparagine found in one participant with clade D/A1 HIV who had minor 10-1074 resistance lead to shift of 332 PNG to position 334. Other mutations contributing to minor 10-1074 resistance included G/D/T325K and H/Y330Q, identified in two clade B participants (Table 5.2).

The clinical outcomes of RIO

The length of viral control during TI is the most important clinical outcome in trials testing the efficacy of HIV cure strategies. Stage 1 of the RIO Arm B, where participants were taken off ART and rebounded in the absence of any intervention,

Table 5.2: Analysis of mutations at known bnAb epitopes per clade

Clade	WT	Mutation	Resistance
B clade	S/T334	R (2), G (1)	Minor resistance
	G/D325	K (1)	Minor resistance
	H/Y330	Q (1)	Minor resistance
	D/N279	1 (Q)	Full resistance
	G458	D (1)	Minor resistance
	G459	E (2), D (1), R (1), S (1)	Minor resistance
	G459	V (1), D (1)	Full resistance
D/A1	S/T334	N (1)	Minor resistance
	G459	S (1)	Minor resistance
F1	N332	K (1)	Full resistance
	N332 + S/T334	T + N (1)	Full resistance

served as a control group of individuals who normally progress following TI. To visually represent the impact of bnAb treatment on time to rebound, a survival curve was generated and the Kaplan-Meier method was employed to estimate survival probabilities in different treatment arms, with time to rebound serving as the endpoint. As shown in Figure 5.3, the control group experienced a viral rebound a median of 4 weeks (range: 1-8 weeks) post-TI. Participants in Arm A who received bnAbs maintained viral control for longer (median time of viral control = 26 weeks). Notably, participants in Arm B, who received bnAbs plus a median of 23 weeks of ART, rebounded a median of 6 weeks post-TI , which was similar to the control group. A 45.5% of Arm A participants were still undetectable at 20 weeks post TI in contrast to 21% of participants randomised in Arm B and underwent a 2nd TI.

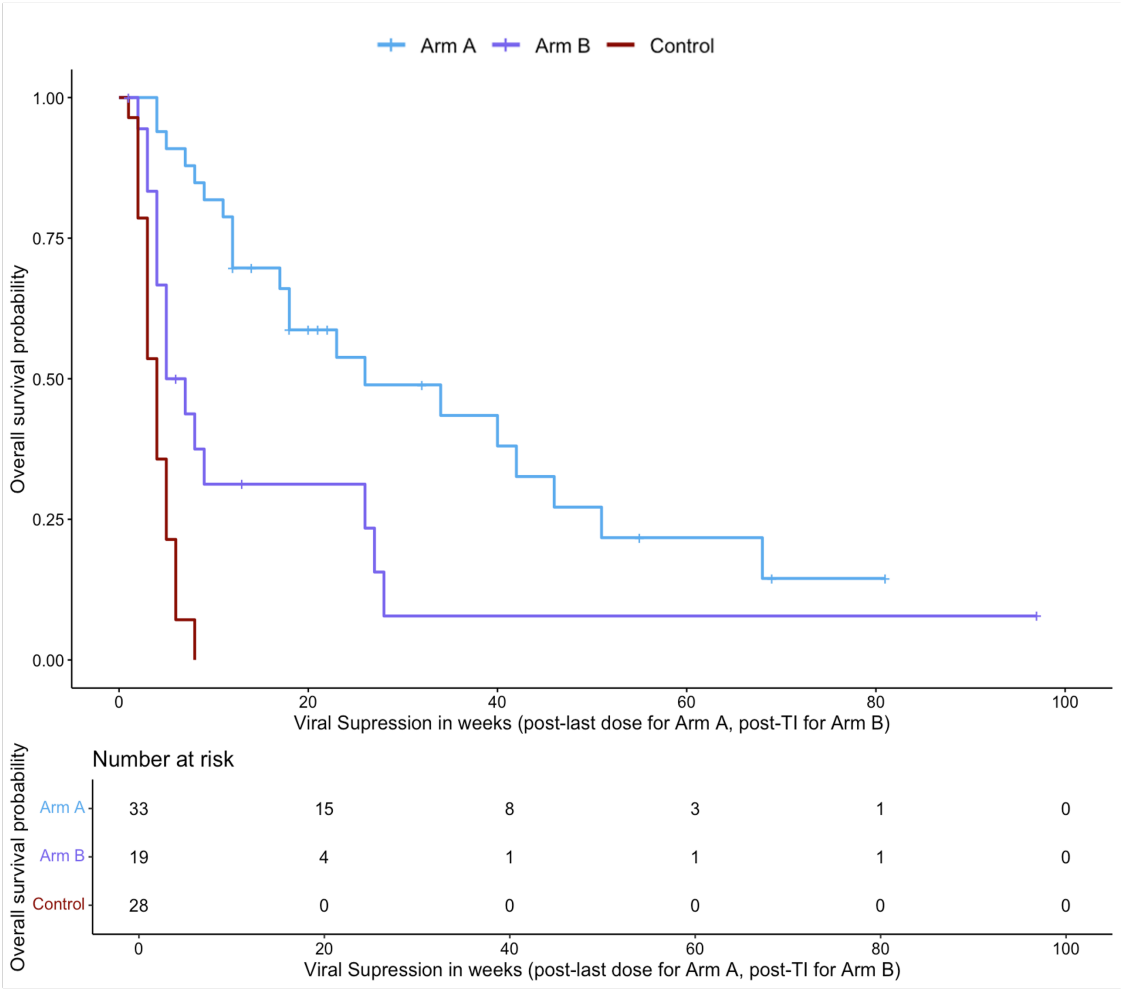

Figure 5.3: Time to Viral Rebound in RIO Arm A, Arm B, and Control Group.Kaplan-Meier survival curves for time to viral rebound in participants from Arm A, Arm B, and a control group. The x-axis represents the time in weeks since last bnAb dose for Arm A and since TI for Arm B and Control group participants, and the y-axis represents the proportion of participants who have remained free of viral rebound.

The Arm B of the RIO trial was designed to test the efficacy of bnAbs at sustaining control after a period of 6 months co-administration with ART, which was built in to allow the bnAbs to be washed out. This design aimed to quantify the time to rebound post-second TI at a time where bnAb concentration was anticipated to be undetectable. Any control should therefore be due to the vaccinal effect and not bnAb suppression. This was combined with the idea that the moderate presence of antigen would induce a vaccinal effect that enhances the host immune response and controls viremia for a longer period. However, due to the logistics of the trial, only 17 participants (of a total of 26 participants

who entered Stage 2) received bnAbs when their VL was >50 copies/ml (65.3%). The median viral load at bnAb dosing in Stage 2 was 126 copies/ml, ranging from 20 (undetectable)- 32800 copies/ml. In addition, due to receiving ART for ~6 months post bnAb dosing, viral evolution was expected to be seized and no selection pressure from bnAbs was expected to be exerted on the virus.

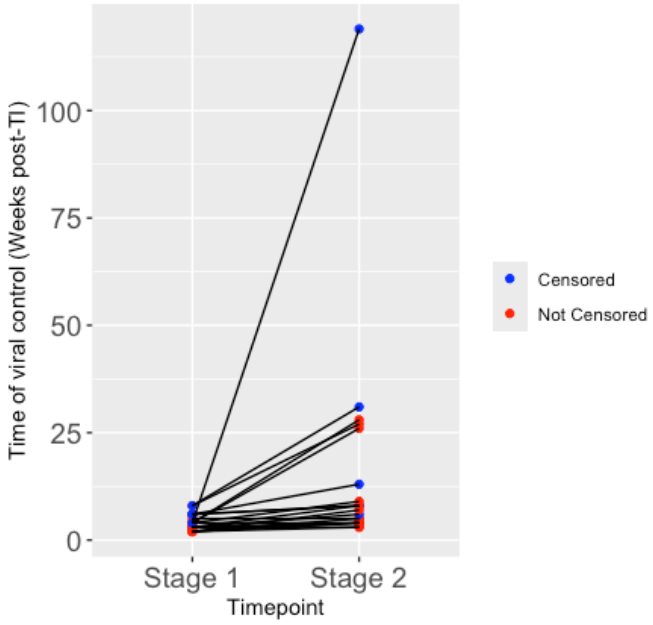

Figure 5.4: Time of viral control at Stage 1 and Stage 2 TI. Y axis shows time of viral control post-TI for Arm B participants who underwent TI at Stage 1 and Stage 2 (x axis). Lines connect paired dots, which represent each participant. Participants who experienced viral rebound post-2nd TI are coloured in red and participants who have not rebounded after 2nd TI are coloured in red.

Interestingly, for 3 of the 20 Arm B participants who experienced rebound after their second treatment interruption (15%) the interval between the Stage 2 TI and viral rebound was exactly the same as the interval between Stage1 TI and viral rebound, where they received no other intervention. Additionally, 6 participants who achieved Stage 2 treatment interruption (30%) maintained viral control for 1-2 weeks longer post-interruption during Stage 2 compared to Stage 1. Lastly, 11 participants (55%) maintained viral control post-bnAb administration for at least twice as long as during Stage 1, with three individuals achieving viral control for a median of 27 weeks (Figure 5.4).

To investigate the factors influencing the time of viral control at stage 2, I used an accelerated failure time (AFT) model. Several variables were considered, including viral load at bnAb dosing, the concentration of the two bnAbs at the time of 2nd TI, sensitivity at baseline, the number of responses to Gag measured by Interferon Gamma ELISPOT assays at the 2nd TI and the time to rebound at the 1st stage TI. Lasso regression retained the viral load at the time of dosing, sensitivity at baseline and the time of rebound at the 1st stage TI to be used in the AFT model. The analysis was performed in 17 participants for whom data of all covariates were available (Table A.2).

The AFT model suggested that time of viral control at Stage 2 is influenced by sensitivity and the viral load at dosing. Higher viral load at the time of dosing and presence of bnAb resistance-associated mutations at baseline are associated with shorter time to the event, which in this case is rebound (value =-0.41 and -1.48, pvalue= 0.02 and 0.003, for viral load at dosing and sensitivity respectively).

Impact of sensitivity predictions on time of viral control

Next, I looked into how the stratification of participants into "Resistant" or "Sensitive" based on the Rockefeller predictions would relate to time to rebound (Figure 5.5). Only participants with 100% resistance-associated mutations to either bnAb or non-amplified sequences at baseline were classified as resistant, for the purpose of this analysis and all else were classified as sensitive. The sensitive group had a median time of post-bnAb viral control of 34 weeks post-last bnAb dose in Arm A whereas participants with full baseline resistance to bnAbs rebounded similarly to the control group (median time of viral suppression 5 weeks post-last dose). Participants classified as sensitive in Arm B rebounded a median of 6 weeks post-TI whereas those predicted as fully resistant rebounded a median of 3 weeks post-TI. One of 22 sensitive participants was still undetectable 80 weeks after last-bnAb dose in Arm A and 3 participants in Arm B maintained control for at least 25 weeks post-TI.

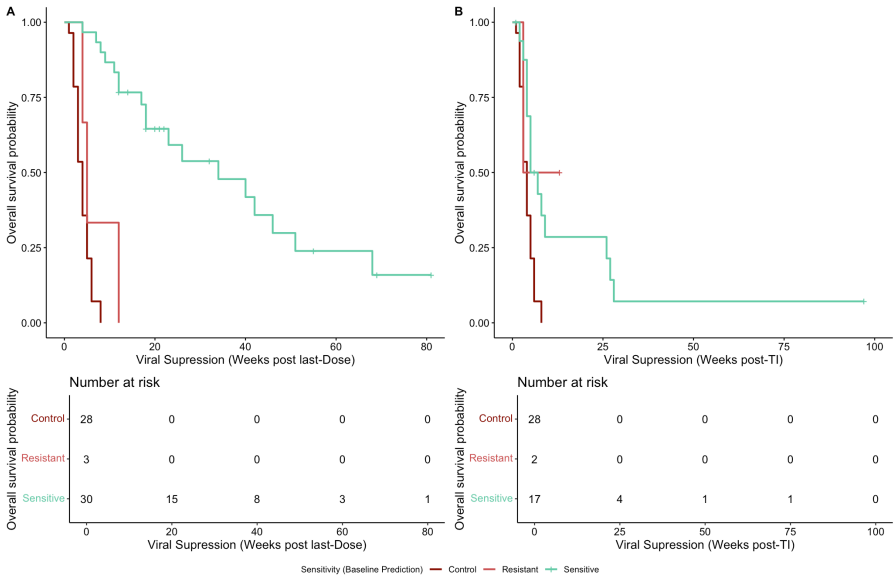

Figure 5.5: Time to Viral Rebound and bnAb sensitivity per RIO arm. Kaplan-Meier curves for participants in RIO Arm A (A) and Arm B (B). The plots compare the duration of viral suppression in different groups of participants based on bNab sensitivity predictions.

Participants predicted as resistant who rebounded rapidly in Arm A had resistance associated mutations in 332+334 (participant 001-008) and 3BNC117 resistance-associated mutations in 279. Mutations at 459 either in 100% or in a minor proportion of of baseline sequences did not seem to impact viral control, as all participant harboring mutations at 459 maintained control for a median of 18.5 weeks (range: 14-30 weeks), when taking into consideration the longest time of viral control achieved with 1 or 2 doses of bnAbs. Similarly, participants with mutations at 334 in a minority of baseline sequences maintained control for a median of 32 weeks.

Arm B participants with mutations at 332 (full resistance) or at 332 (minor resistance) at baseline, rebounded within 3 weeks after their 2nd TI. On the contrary, participant 007-012 with full baseline resistance predicted at baseline due to 459 mutations maintained control for more than 13 weeks. Participant 003-001 harbored mutations at 330 in a small proportion of baseline sequences and experienced viral blips which were spontaneously controlled soon after. At rebound, the same mutations as in baseline were detected in 100% of the sequences.

However, participant 003-001 maintained viral control for longer than 97 weeks post the 2nd TI.

The effect of bnAb treatment on the rebound Env sequences

At the time of writing, a total of 21 RIO participants had experienced a post-bnAb rebound and their rebound virus was sequenced and assessed for bnAb sensitivity (Table 5.3).

Table 5.3: Post-bnAb rebound sensitivity prediction. Participants from Arms A and B who have rebounded post-bnAb treatment, mutations identifies and clinical characteristics.

ID	Sensitivity (Baseline)	Escape residue (Baseline)	Sensitivity (post-bnAbs)	Escape residue (post-bnAbs)	Arm	Number of bnAb doses
001-008	10-1074	332T and 334N	10-1074	332T and 334N	A	1
001-009	10-1074	332K	10-1074	332K	B	2
003-002	3BNC117	279Q	3BNC117	279Q	A	1
001-017	Minor 10-1074	334N	10-1074	334N	B	2
003-001	Minor 10-1074	330Q	10-1074	330Q	B	1
001-020	Minor 3BNC117	458S	Sensitive	NA	B	2
001-010	Sensitive	NA	10-1074	334N	A	1
001-018	Sensitive	NA	10-1074	334R	A	2
006-003	Sensitive	NA	10-1074	332D/S	A	1
007-001	Sensitive	NA	10-1074	332K or 334S	A	1
001-002	Sensitive	NA	10-1074	334G	B	1
001-003	Sensitive	NA	10-1074	334N	B	1
001-021	Sensitive	NA	Minor 3BNC117	458R	A	1
001-004	Sensitive	NA	Sensitive	NA	A	1
001-005	Sensitive	NA	Sensitive	NA	A	1
003-009	Sensitive	NA	Sensitive	NA	A	1
002-001	Sensitive	NA	Sensitive	NA	B	1
003-004	Sensitive	NA	Sensitive	NA	B	2
006-010	Sensitive	NA	Sensitive	NA	B	1
007-003	Sensitive	NA	Sensitive	NA	B	2
007-007	Sensitive	NA	Sensitive	NA	B	2

Of those, 15 participants were predicted as fully sensitive at baseline which means that they harbored no bnAb-associated mutations in their proviral Env sequences, 3 had minor resistance to either bnAb and 3 had all sequences carrying

bnAb resistance-associated mutations. Nearly half of participants (47%) who were predicted as fully sensitive at baseline, were predicted to be bnAb resistant post-bnAb treatment. Interestingly, out of 7 participants with "new" resistance at rebound, 6 had 10-1074 resistance-associated mutations and only one had minor resistance to 3BNC117.

All participants who were predicted as resistant to 10-1074 (fully or with minor resistance) rebounded with the same mutations, post-bnAb treatment (Table 5.3). 003-002, who was the only participant predicted as 3BNC117 resistant at baseline to rebound, had rebound viruses harboring the same mutations as at baseline, D/N279Q. All mutations identified in the rebound sequences from participants who were predicted as fully sensitive or with minor resistance at baseline were on the 332 PNG, and therefore reduce the likelihood of a glycan binding on the site to zero. Specifically, 67% participants with 10-1074 resistance at rebound had mutations at site 334, 25% in 332 and one participant (007-001) had mutations at either 332 or 334 (Figure 5.6).

A.

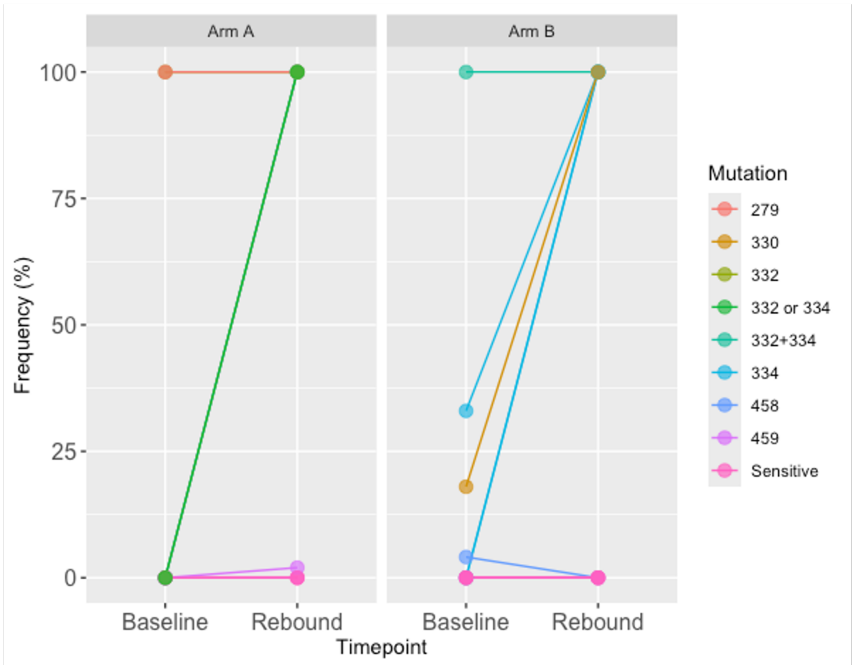

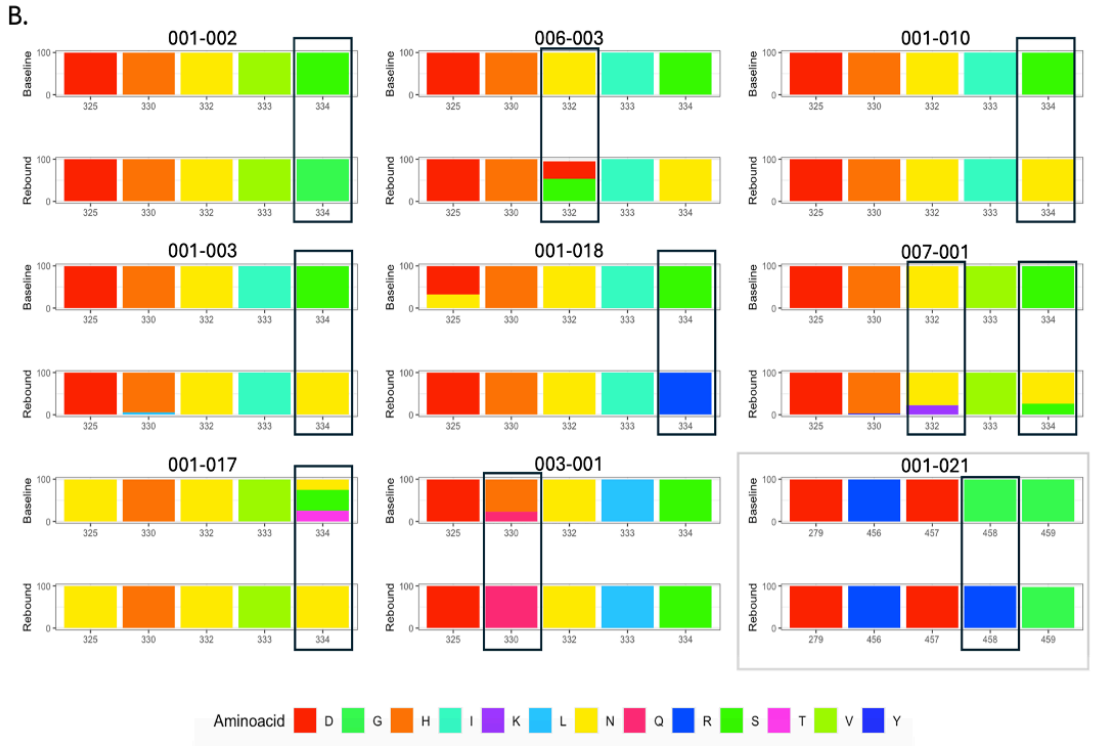

Figure 5.6: bnAb resistance-associated mutations prevalence.A. Frequency of mutated residues before and after bnAb treatment, per Arm. Color indicates the site(s) affected. B.Amino acid variants at 10-1074 and 3BNC117 epitopes before and after treatment with bnAbs. Colour charts showing the variation between baseline and rebound samples inRIO participants who were predicted as sensitive at baseline and rebounded with resistance to 10-10-74 or to 3BNC117 (in a grey box). The frequency of each amino acid is represented by the height of the height of the bar.

5.3.2 Assessing the performance of the sensitivity prediction model

To assess the Rockefeller prediction performance the definition of an outcome metric that accurately reflected the endpoint of interest was required. One outcome metric was defined based on time to rebound within the critical 8-week post-treatment period, as defined by the placebo group maximum rebound time frame (as presented in Figure 5.3). Specifically, participants who rebounded earlier than 8 weeks post-last dose are more likely to have pre-existing resistance which would lead to immediate treatment failure. For the purpose of this analysis these participants were classified as $\text{Resistant}_{\text{TTR}}$. In contrast, participants who maintained control for longer than 8 weeks post-last bnAb dose, were classified as $\text{Sensitive}_{\text{TTR}}$, on the

basis that they were not likely to have strong pre-existing resistance.

A second outcome metric was based on the relationship of bnAb concentration levels and time to rebound. A threshold of 50 ug/ml was defined based on the outcomes of bnAb neutralisation assays, were the inhibitory concentration for 80% of the viruses in the culture (IC80) > 50 ug/ml suggests high resistance to bnAbs. Therefore, if participants rebounded before bnAb concentration levels fell below 50 ug/ml they would be more likely to have highly resistant viruses. These participants are classified as $\text{Resistant}_{\text{PK}}$, for the purpose of this thesis. An association between sequence-based sensitivity predictions and this metric would also suggest an ability to predict clinical response to bnAbs.

In order to reduce the complexity of analysis, only data from the 33 Arm A participants, who received bnAbs without any other intervention, were used. Despite bnAb concentrations being below 50 ţg/mL at the time of rebound, it was challenging to definitively attribute rebound to low bnAb concentrations. This is because the rebounds occurred within the ART wash-out period, making it difficult to distinguish between the effects of waning ART and bnAb insufficiency (Table 5.1).

Predicting pre-existing resistance likelihood using an outcome based on TTR

First, I explored the Rockefeller sensitivity predictions performance against the outcome based on time to rebound. A statistically significant association between sequence-based predictions and the sensitivity classification based on time to rebound was observed using Chi-squared test with Yates' continuity correction (p-value <0.01).

Table 5.4: Assessment of sensitivity predictions in participants who were recruited in RIO. Participants are classified as sensitive or resistant at baseline based on the Rockefeller bnAb sensitivity prediction model and the trial eligibility criteria. Sensitvity classification post-bnAb treatment as sensitive or resistance is based on time to rebound.

Characteristic	Sensitive					Resistant		
	Overall N = 29	**Minor 10-1074** N = 1	**Minor 3BNC117** N = 3	**NA** N = 3	**Sensitive** N = 22	**Overall** N = 3	**10-1074** N = 1	**3BNC117** N = 2
Sensitity Classification (TTR)								
Sensitive	27 (93%)	1 (100%)	3 (100%)	3 (100%)	20 (91%)	1 (33%)	0 (0%)	1 (50%)
Resistant	2 (6.9%)	0 (0%)	0 (0%)	0 (0%)	2 (9.1%)	2 (67%)	1 (100%)	1 (50%)

[1] n (%)

Classification using the Rockefeller model was approximately 91% accurate in classifying individuals as sensitive or resistant, based on this TTR-based metric (p-value=0.03). In addition, out of the 30 individuals who were predicted as sensitive using the sequencing based classifier approximately 93% were found to be sensitive based on their time to rebound (Table 5.4). This suggest that the Rockefeller model predictions perform very well at selecting participants who are more likely to maintain control for longer 8 weeks and therefore are less likely to have pre-existing resistance.

Predicting the likelihood of response to bnAbs using an outcome based on PK levels

Pharmacokinetic data for bnAbs, available for 22 of 33 participants in Arm A, provided a novel approach to classifying individuals with regards to sensitivity to bnAbs. Under the assumption that a bnAb concentration of 50 ug/ml signifies a threshold for viral rebound, participants' sensitivity was characterised based on whether viral rebound occurred before or after this concentration was reached. As presented in Table 5.5, 65% of participants predicted as sensitive at baseline were less likely to be resistant, as they rebounded after bnAbs concentrations fell below 50 ug/ml. Conversely, 5 participants who did not have any baseline bnAb resistance associated mutation at baseline were characterised as $\text{Resistant}_{\text{PK}}$. Notably, both participants who were predicted as resistant at baseline were classified as $\text{Resistant}_{\text{PK}}$.

Table 5.5: Assessment of sensitivity predictions in participants who were recruited in RIO. Participants are classified as sensitive or resistant at baseline based on the Rockefeller bnAb sensitivity prediction model and the trial eligibility criteria. Sensitvity classification post-bnAb treatment as sensitive or resistance is based on PK data.

	Sensitive					Resistant		
Characteristic	**Overall** N = 29	**Minor 10-1074** N = 1	**Minor 3BNC117** N = 3	**NA** N = 3	**Sensitive** N = 22	**Overall** N = 3	**10-1074** N = 1	**3BNC117** N = 2
Sensitivity classification based on PK (50 ug/ml)								
Sensitive	13 (65%)	1 (100%)	0 (0%)	1 (50%)	11 (69%)			
Resistant	7 (35%)	0 (0%)	1 (100%)	1 (50%)	5 (31%)	2 (100%)	1 (100%)	1 (100%)
Unknown	9	0	2	1	6	1	0	1

[1] n (%)

5.3.3 Viral features associated with bnAb resistance

bnAb sensitivity predictions by the Rockefeller model, bnAb-ReP and bnAb neutralisation assays

First, I sought to investigate if alternative methods of predicting bnAb sensitivity at baseline, such as bnAb-ReP or bnAb neutralisation assays, would classify participants in a different category. bnAb-ReP, a frequently used model for predicting antibody sensitivity based on sequence data, provides neutralization probability estimates for individual bnAbs. Analysis of a total of 1671 RIO Env sequences from Arm A and Arm B with paired Rockefeller and bnAb-ReP predictions, revealed a strong linear correlation between predictions from the two models for 10-1074 sensitivity (R^2 =0.73, p<0.01). However, this correlation was not observed for 3BNC117 predictions (R^2=0.04, p-value<0.01).

To investigate the impact of bnAb resistance-associated mutations on IC80, I analyzed 62 RIO sequences for which neutralisation assays were performed. These assays measured the bnAb titers required to neutralise pseudoviruses carrying Env sequences amplified from participants with SGA. Sequences with an inhibitory concentration 80% (IC80) titer greater than or equal to 25 were classified as bnAb resistant, while those with an IC80 titer less than 25 were classified as sensitive. A moderate positive correlation (r = 0.40, p-value < 0.05) was observed between the Rockefeller predictions for 10-1074 and the 10-1074 IC80 titers, suggesting a moderate degree of agreement between the two. I attempted to calculate the correlation between the Rockefeller prediction and IC80 for 3BNC117 in the same dataset but, due to the lack of variation in the Rockefeller prediction, this could not be computed. This suggests that there is insufficient data to establish a meaningful relationship between these two variables for 3BNC117. The analysis revealed that that sequences harboring the H/Y330Q mutation, which was associated with 10-1074 resistance by the Rockefeller model (participant 003-001), had a low IC80 value. Variability was observed within the same participant (001-003), with one sequence displaying a significantly lower IC80 (0.018) compared to others (median

IC80 > 50). High IC80 values for 10-1074 were also reported for a proportion of sequences from participant 001-021 who was predicted as fully sensitive. Of note, high IC80 values were reported for 001-002 and 001-009 sequences which were lacking Rockefeller model-predicted 3BNC117 resistance associated mutations (Table 5.6).

Table 5.6: Frequency of mutated residues in the known bnAb epitopes per clade.

ID	IC80 10-1074	IC80 3BNC117	Mutations
001-002	0.08	0.53	no mutations
	0.00	0.55	no mutations
	0.06	0.99	no mutations
	0.00	43.28	no mutations
	0.00	50.00	no mutations
	0.01	50.00	no mutations
	0.07	50.00	no mutations
	50.00	50.00	S/T334G
	50.00	50.00	S/T334G
	50.00	50.00	S/T334G
001-003	50.00	0.09	S/T334N
	50.00	0.09	S/T334N
	50.00	0.14	S/T334N
	0.02	0.17	no mutations
	15.71	4.54	S/T334N
001-009	29.68	0.77	N332K
	50.00	25.19	N332K
	50.00	50.00	S/T332K
	50.00	50.00	S/T332K
	50.00	50.00	S/T332K
	13.41	0.33	no mutations
	50.00	0.33	no mutations
	50.00	0.45	no mutations
	50.00	0.45	no mutations
	50.00	0.57	no mutations
	2.76	0.60	no mutations
	0.19	0.97	no mutations
	50.00	1.08	no mutations
	50.00	1.16	no mutations
	50.00	1.19	no mutations

001-021			
	50.00	1.26	no mutations
	50.00	1.45	no mutations
	50.00	1.54	no mutations
	50.00	1.62	no mutations
002-004	27.67	0.18	no mutations
	31.02	0.34	no mutations
	39.39	0.36	no mutations
	29.26	0.76	no mutations
	50.00	0.81	no mutations
	9.20	1.00	no mutations
003-001	0.31	0.01	H/Y330Q
	0.78	0.01	H/Y330Q
	0.24	0.02	no mutations
	1.82	0.03	no mutations
	0.36	0.18	no mutations
	0.94	0.25	no mutations
006-003	50.00	0.45	N332D
	50.00	0.51	N332D
	50.00	0.63	N332S
	50.00	0.64	N332S
	0.08	0.69	no mutations
	50.00	0.78	N332D
	50.00	0.79	N332D
	50.00	0.93	N332S
	50.00	0.94	N332S
	50.00	0.96	N332S
	50.00	1.03	N332S
	50.00	1.34	N332D

Participants predicted as sensitive at baseline but resistant based on clinical outcomes or neutralisation assays; what can we learn from these participants?

To make bnAb sensitivity screening more efficient as well as to gain more understanding on bnAb sensitivity features, sequences from participants initially predicted as sensitive but found Resistant using the TTR or the PK outcomes, were

examined to identify common viral features that could potentially confer resistance. Eight Arm A participants who satisfied these criteria were included in this analysis and their clinical features are shown in Table A.3.

Participant 004-003 received a second dose of bnAbs six weeks after he experienced a transient viral rebound (blip) to 5840 copies/ml, which subsequently resolved without further intervention. At the time of second dose, the viral load was reported at 101 copies/ml. However, insufficient sequencing data at baseline and at each of the rebound timepoints did not allow any further genomic analysis. Participants 006-003 and 007-001 had 100% of their rebound sequences harboring 10-1074 resistance-associated mutations, suggesting either pre-existing resistance missed at baseline or *de novo* development during bnAb concentration decline. Of note, these participants rebounded close to the timepoint when bnAb concentrations were falling below the 50 ug/ml threshold and it was not clear if they should be classified as resistant or sensitive. Hence, these samples were not included in this analysis.

Identification of additional sites of escape

To enhance the predictive accuracy of the Rockefeller model, I sought to identify novel epitopes associated with bnAb resistance. To do this, I compared sequences from participants initially predicted as sensitive but classified as resistant based on clinical outcomes (Table A.3) and those who demonstrated high IC80 values in bnAb neutralisation assays despite lacking known resistance-associated mutations (Table 5.6). For this analysis, I looked at sequences from 10 participants. However, certain limitations did not allow the use of all participant sequences in this dataset; bnAb-resistance mutations were detected in the rebound viruses of participants 006-003 and 007-001, suggesting that resistant sequences were not sampled at baseline but became dominant during viral rebound. Furthermore, rebound sequences for participants 001-032, 004-003, 007-014, and 007-016 were unavailable and therefore these participants were excluded from this analysis.

Analysis of the MSA for participant 003-009 revealed no clear evidence of amino acid substitutions in the protein sequences that could be confidently attributed to

selection pressure from broadly neutralising antibodies (bnAbs). Additionally,the phylogenetic tree showed minimal divergence between baseline and rebound sequences, suggesting limited evolutionary changes associated with viral rebound (Figure 5.7). These findings might indicate that resistance to bnAbs was present at baseline, potentially residing in epitopes that have not yet been fully characterised.

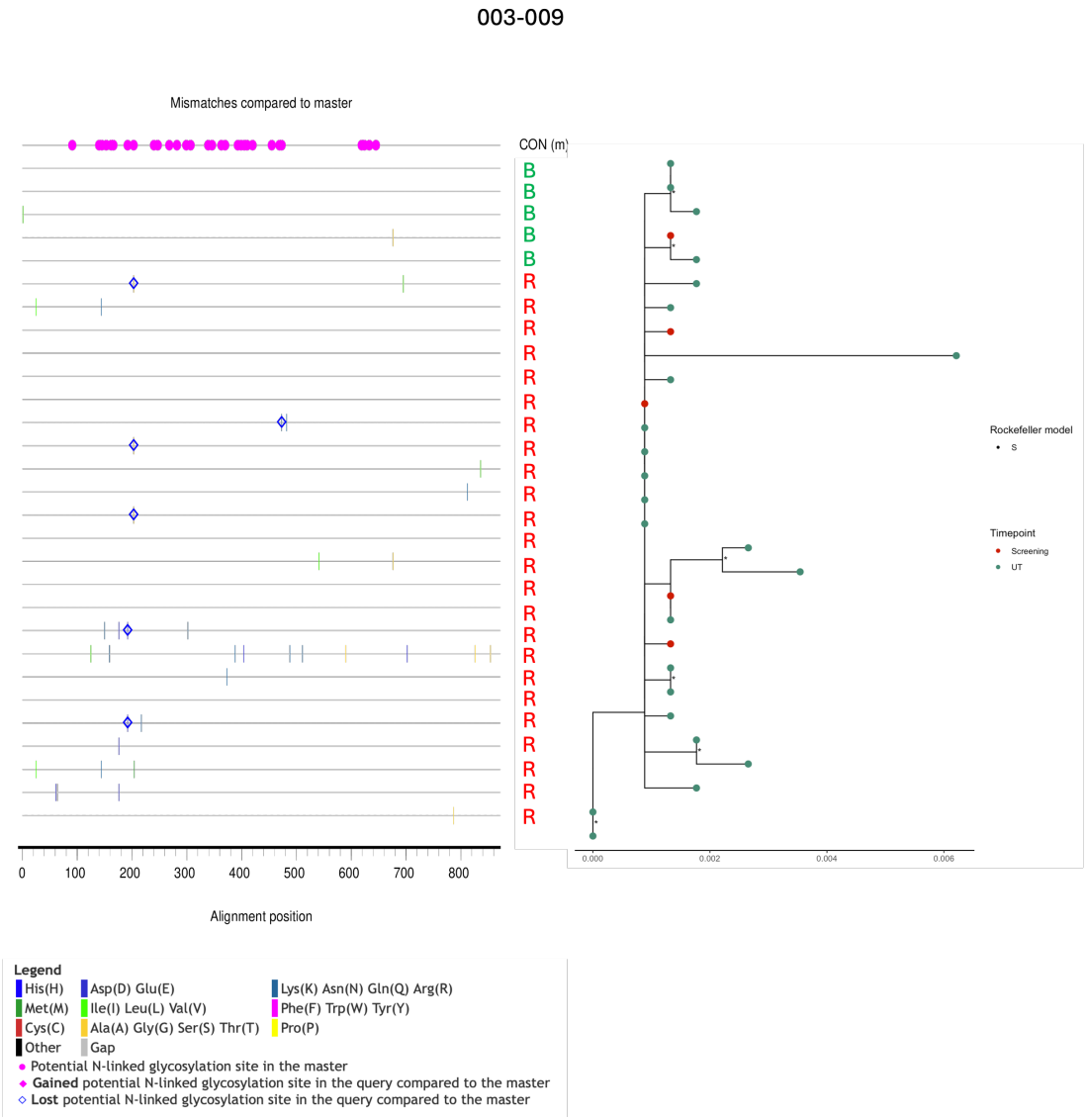

Figure 5.7: MSA plot and ML tree for participant 003-009. MSA plot showing the differences in AA between sequences sampled as baseline, marked with a green B and from rebound marked with a red R. The consensus sequence of all 003-009 sequences was used, as no substancial clustering of sequences per timepoint was observed, as shown in the ML nucleotide phylogenetic tree on the right. Sequences from different timepoints (Screening= baseline and UT = rebound) are marked with different color tip point. A tree scale is shown at the bottom of the tree.

5. Predicting bnAb sensitivity in the RIO trial

An inspection of the multi-alignment (MSA) plot containing sequences from participant 001-021 identified a unique combination of mutations, 325N and 330Y, exclusively present in the rebound samples. This specific combination was not observed in any other participant sequences in the RIO or the HEATHER cohorts. The neutralisation assay data for participant 001-021 revealed high 10-1074 IC80 values (>50 ug/ml) for all rebound as well as one of the baseline sequences tested. However, the one baseline sequence with IC80>50 did not have the 325N + 330Y combination. A series of insertions within HXB2 133-134, caused alteration to the protein sequence and the distribution of PNGs in the region. In particular, all rebound sequences but only a minority of baseline sequences (10/28 baseline sequences) had an extra PNG within this region (Figure 5.8A). Interestingly, all sequences with this extra PNG in the inserted region and at HXB2 135 had an IC80>50 for 10-1074. However, the presence of intact PNGs in the same regions in samples from other participants did not show IC80>50 ug/ml.

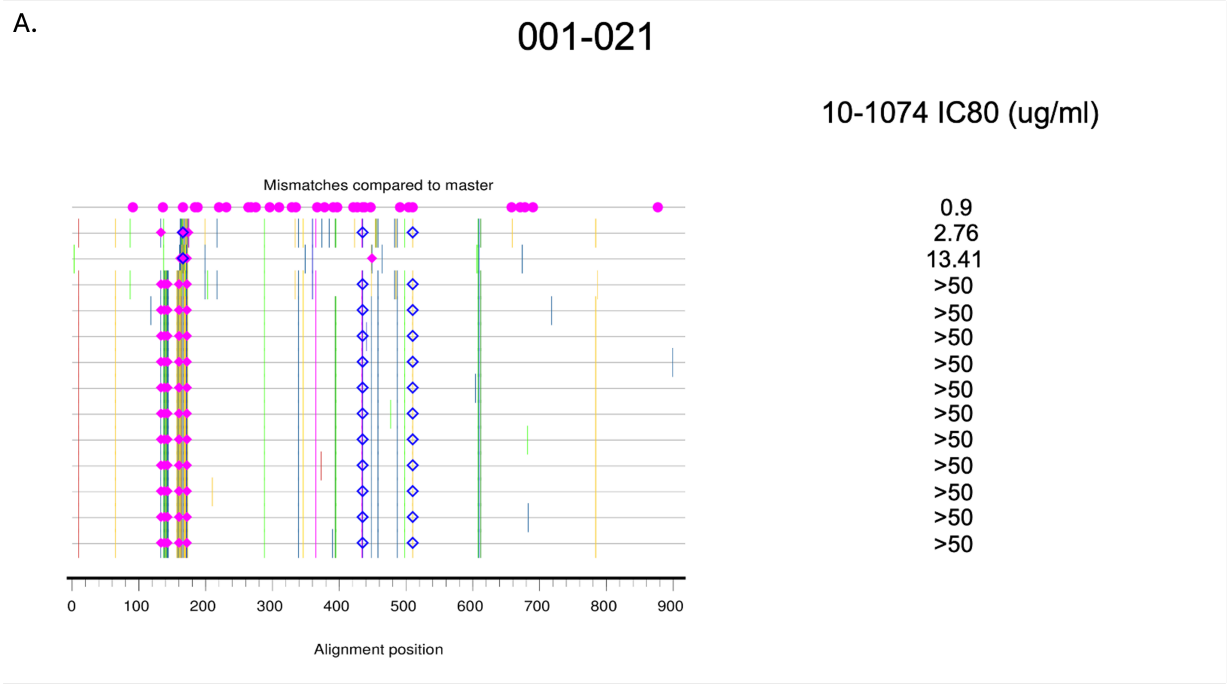

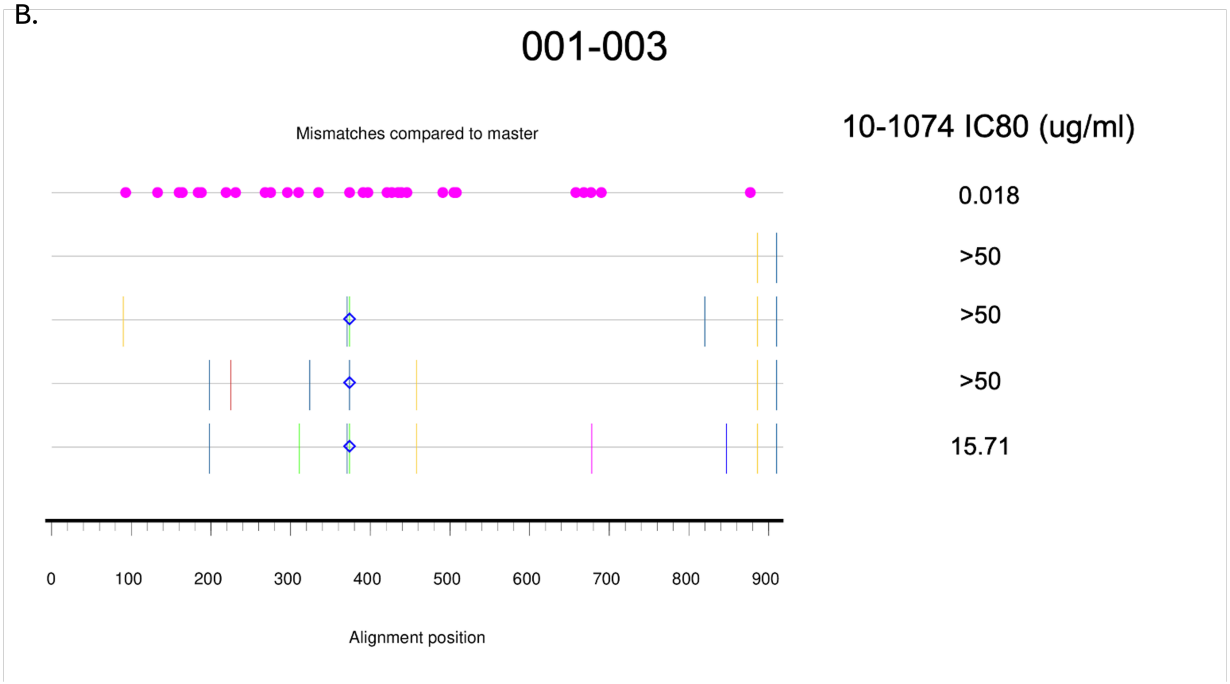
B.
001-003
Mismatches compared to master
10-1074 IC80 (ug/ml)
0.018
>50
>50
>50
15.71
0
100
200
300
400
500
600
700
800
900
Alignment position

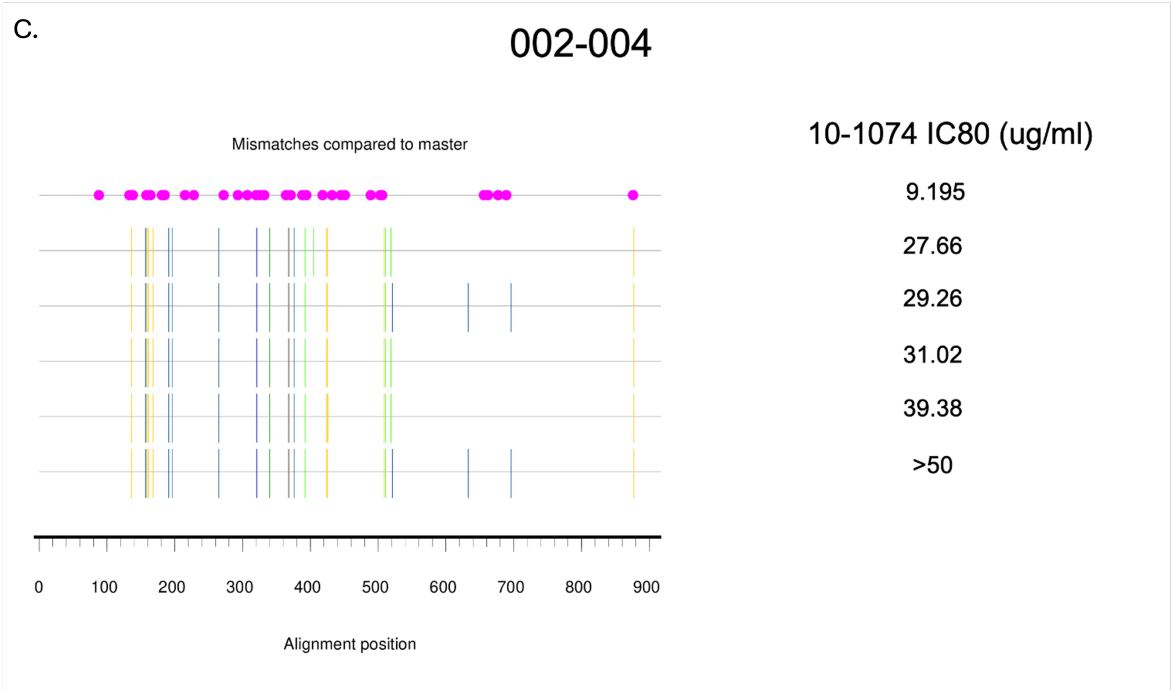
C.
002-004
Mismatches compared to master
10-1074 IC80 (ug/ml)
9.195
27.66
29.26
31.02
39.38
>50
0
100
200
300
400
500
600
700
800
900
Alignment position

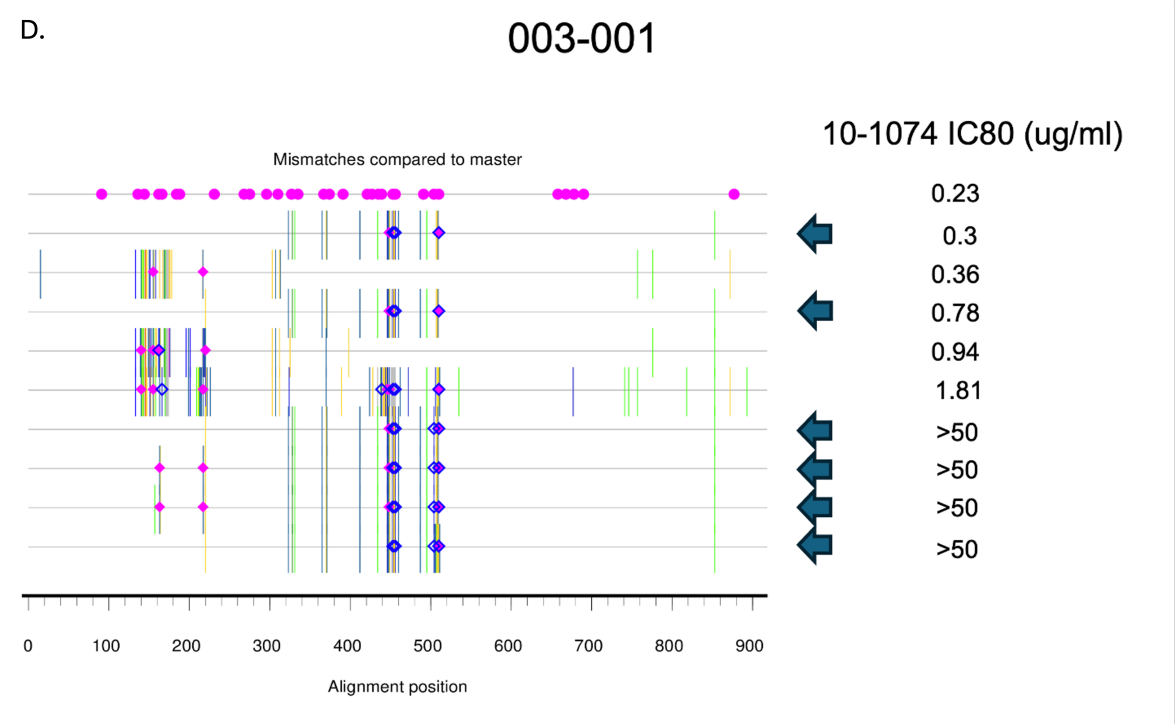

Figure 5.8: MSA plots and paired IC80 values for RIO participants. MSA plots and paired 10-1074 nautralisation assay concentrations are shown for participants 001-021, 001-003, 002-004 and 003-001 (A-D). The sequence with the lowest IC80 value was used as a master for comparison in the MSA plots. Blue arrows mark the 003-001 sequences that harbor the 330Q mutations.The alignment positions in each plot are numbered using a participant-specific reference.

Despite harboring the same S/T334N mutation, sequences from participant 001-003 exhibited varying IC80 values for 10-1074 neutralisation. While two sequences displayed low IC80 values (0.018 and 15.71), others had IC80 values >50. Comparative analysis of the five Env protein sequences revealed no unique residues associated with the resistant phenotype (IC80 $>$ 50) (Figure 5.8B). Conversely, several distinct residues were identified when comparing sequences with higher IC80 values (IC80 $>$ 25) to those with IC80 $<$ 10 (Figure 5.8C). Notably, participant 003-001 possessed sequences with the same Y/H330Q mutation but displayed varying IC80 values, including two sequences with IC80 $<$ 1 (Figure 5.8D). No residues exclusively associated with 10-1074 resistance were identified in the above. As for 3BNC117 neutralisation assays, two participants had sequences with high IC80 (>40) but no 3BNC117 resistance-associated mutations were observed. Sequences

from participant 001-002 that were found to be resistant to 3BNC117 in neutralisation assays shared an E at position 466, instead of a Q, which was prevalent in the sensitive sequences. However, 466E was the most common residue in sequences from different participant across different timepoints in the RIO cohort. Similarly, the one residue that distinguished sequences with a low IC80 from those with a high IC80 for 3BNC117 was 348E instead of 348K, which was present in the resistant sequences but also in most of other sequences across the RIO cohort.

Variable loop length as predictive markers of bnAb sensitivity

Env hypervariable loops (HV), known for their proximity to bnAb epitopes and potential impact on antibody binding were examined to assess their role in sensitivity. Recent studies have reported a statistically significant association of longer HV1 with a higher IC50 for 10-1074 and an association of longer HV5 with a higher IC50 to 3BNC117 (Bai et al., 2024). The relationship between IC80 values and HV lengths was examined in a subset of RIO participants with available IC80 data from neutralisation assays. Separate mixed-effects models were fitted for IC80 values of 3BNC117 and 10-1074, with HV1, HV2, HV4, and HV5 lengths as predictors. Results indicated that longer HV1 and shorter HV4 were associated with an increased 10-1074 IC80 (estimates for H1=-2.45 and for HV4 = -2.53 ; $p < 0.01$ for both), while longer HV2 and shorter HV4 were more likely to be found in viruses with higher 3BNC117 IC80 (estimates for HV2 and HV4 = 3.13, -3.02 respectively; $p < 0.01$ for both). A generalised linear mixed-effects model was employed to assess the association between HV lengths and a categorical outcome of resistance or sensitivity to bnAbs, defined as IC80 values greater or less than 50, respectively. In this case, only the length of HV4 demonstrated statistically significant but negligible association with resistance for both bnAbs. Here, I compared the length of variable and hypervariable loops, as well as the number of PNGs, in sequences from participants predicted as sensitive at baseline but subsequently developing resistance. All six participants included in this analysis

from both treatment arms experienced rebound with 100% prevalence of 10-1074 resistance-associated mutations.

Out of 6 participants examined here, the average length of variable loop 4 (V4) and HV4 were shorter at rebound compared to the average lengths at baseline for 2 participants, 001-003 and 001-010. A decrease was also observed in the average number of PNGs at the same regions in rebound viruses versus at baseline, in the same participants. Although V5 and HV5 lengths remained the same at rebound as at baseline, participants 001-003 and 001-010 was short of one PNG on average one PNG at V5 at rebound, and 001-010 lost a PNG at HV5 as well. Participant 007-001 also showed a decrease in HV4 length at rebound but not in V4. In addition, the rebound virus gained 1 V4 PNG at rebound but lost 2 at HV4, on average. The same pattern was observed for V5 and HV5 PNGs for 007-001; a gain was observed in V5 PNGs and a loss of two PNGs was seen at HV5. An increase in V1 and HV1 (and subsequently in V1V2 and HV1V2) was observed in 001-018 which caused the loss of a PNG site in these regions, on average. A decrease in the same regions was observed in 001-018, without affecting the average number of PNGs in these regions (Table A.4).

How similar are latent reservoir and rebound viruses?

A study by Bar et al. suggested that VRC01 can restrict viral rebound by limiting the reactivation of multiple latent viruses and therefore the rebound virus was more clonal (Bar et al., 2016). Maximum likelihood phylogenetic trees of baseline and rebound sequences from participants in Arm A who rebounded in high concentration of bnAbs (>50 mg/ml) to investigate if 10-1074 and 3BNC117 targeted and suppressed specific viral lineages within the reservoir. In four participants, rebound sequences clustered within the baseline proviral sequences, which suggests pre-existing resistance (Figure **??**A). Indeed, participants 003-002 and 001-008 were predicted as fully resistance to 0-1074 and 3BNC117 respectively at baseline. On the contrary, no mutations associated with bnAb resistance were

found in baseline sequences from either 003-009 or 006-003, although 006-003 rebounded with fully 10-1074-resistant viruses.

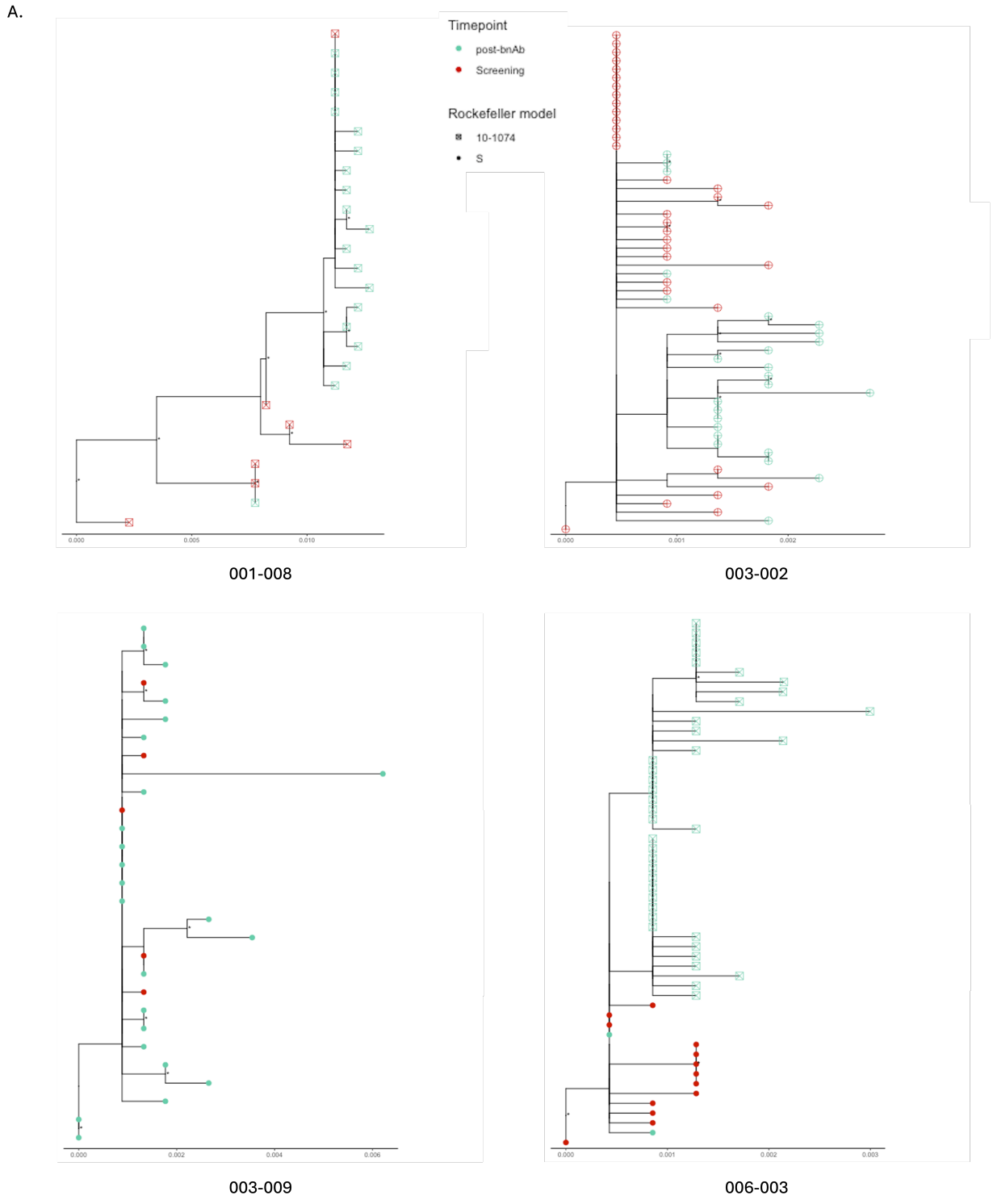

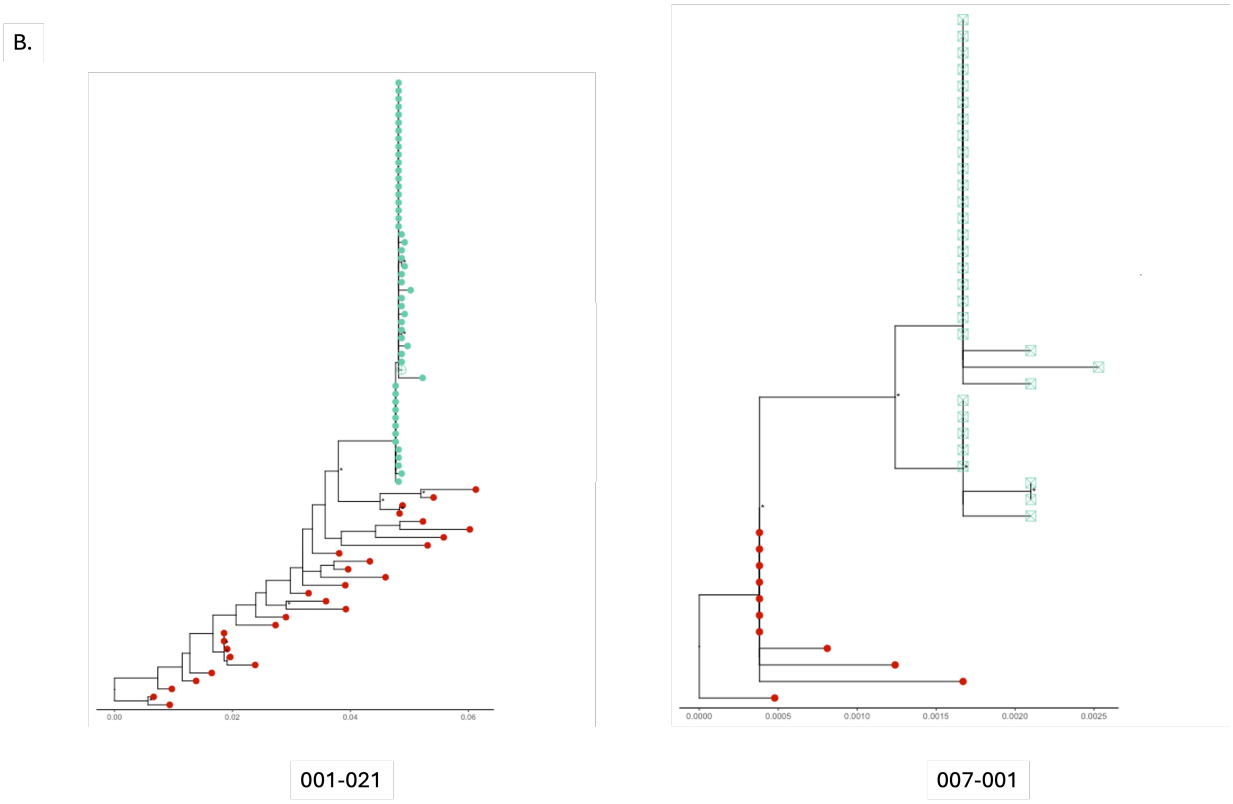

Figure 5.9: ML phylogenetic nucleotide trees of RIO participants. Panel A shows participants with intermingling rebound and reservoir sequences and panel A shows participants whose rebound and reservoir sequences cluster separately. Tips color and shape indicate the timepoint and sensitivity (based on the Rockefeller model). The scale bar indicates genetic distance.

Interestingly, rebound viruses from 001-021 and 007-001 were found to form distinct clusters (Figure **??**B). In particular, participant 001-021 baseline sequences were more diverse whereas the rebound cluster consisted of nearly identical sequences. On the contrary, the baseline reservoir of participant 007-001 was less diverse but the rebound was polyclonal, which may suggest bnAb-induced selection pressure.

5.4 Discussion

In this chapter I studied the impact of treatment with 10-1074-LS and 3BNC117-LS on the virus of individuals with PHI and sensitive reservoir. Participants were randomised into two arms: Arm A received bnAbs, while Arm B received

placebo. All participants, who were initially on ART, had a planned interruption to assess viral rebound after their dose. In Arm B, participants who experienced viral rebound were subsequently offered bnAb therapy. This design allowed us to observe the impact of bnAbs in the absence or not of ART and to identify viruses that emerged from the reservoir and contributed to rebound. Although the findings presented in this chapter are not based on the official RIO trial outcomes I expect no significant differences between these findings and the ones to be presented at the end of the trial.

In line with the findings of clinical trials previously conducted (Caskey et al., 2017; Gaebler et al., 2022; Mendoza et al., 2020; Scheid et al., 2016), 10-1074 and 3BNC117 significantly prolonged the median time of viral control in Arm A participants compared to the control group. Narrowing down to participants who were classified as sensitive to bnAbs at baseline, the median time of viral control was 26 weeks post-TI compared to 4 weeks post-TI for the control group. An increase in time of viral control, albeit smaller, was observed also in Arm B participants who maintained viral control for a median of 6 weeks post their 2nd TI, compared to the 4 weeks of the control group. Of note, after receiving bnAbs, nearly half of Arm B participants (47.3% of the Arm B participants who had a second TI) maintained viral suppression for at least twice as long as they did during the first TI, at Stage 1. Longer time of viral control at Stage 2 compared to Stage 1 TI was positively correlated with higher levels of bnAb at the time of Stage 2 TI (Rho= 0.56 for 10-1074 and Rho= 0.62 for 3BNC117, p-value 0.02 and 0.009 respectively).

Participants in the RIO trial were selected based on bnAb sensitivity predictions generated by the Rockefeller model. While the model was initially intended as a proxy for predicting viral rebound, its accuracy in assessing actual bnAb response was limited. The model demonstrated high accuracy in predicting delayed viral rebound for participants in Arm A compared to the control group, but it struggled with predicting viral control achieved before bnAbs fell to low concentrations (<50 ug/ml). Although the RIO trial was not designed to evaluate bnAb efficacy in individuals with full pre-existing resistance, a small number of participants with

10-1074 resistance were inadvertently enrolled to the trial. Notably, these individuals experienced viral rebound within a time frame comparable to the control group. The assessment of sensitivity predictions was limited by the low number of participants for which rebound sequences amplified and sequenced, the low number of participants for which bnAb concentrations were measured and the lack of resistant participants to use as a comparator. In addition, the design of Arm B did not allow the inclusion of those participants in this analysis as it was not possible to classify the bnAb sensitivity for most of them based on the outcome. Predictions generated for 1671 RIO Env sequences by bnAb-ReP demonstrated strong correlation with those of the Rockefeller model for 10-1074 but exhibited less concordance for 3BNC117. A moderate correlation was observed between the Rockefeller predictions and sensitivity defined based on IC80 titers for 10-1074 but not for 3BNC117.

The bnAb epitope residues that were found most frequently mutated were 334 (within the 10-1074 epitope) and 459 (within the 3BNC117 epitope), which is consistent with the findings from the HEATHER cohort (3.3.2). Other mutated residues in lower frequency were 325, 330 and 332 and 279 and 458 affect the binding of 10-1074 and 3BNC117. Two participants who harbored 332 and 332+334 mutations at baseline rebounded rapidly, within 4 and 5 weeks after dosing. Mutations in other sites, 334 and 459, did not appear to lead to earlier rebound. While the 330Q mutation was initially observed at low frequency in the baseline sample from Arm B participant 003-001, it became dominant in the post-bnAb rebound sample. Despite this, the participant spontaneously controlled following the blip and subsequently maintained prolonged viral suppression. This suggests that while 10-1074 may exert selection pressure on residue 330, either the resulting mutation did not confer resistance to bnAbs or it significantly impacted viral fitness and infectivity in a way that a second rebound to lead to treatment failure was not possible. Other factors, such as a bnAb-induces enhancement of the host immune response and CTL activation could influence the overall outcome of the treatment. The observation that individuals harboring identical Env mutations

exhibited varying duration of viral control post-bnAb treatment suggests the influence of complex factors beyond the predictive capacity of these mutations. Our focus on Env sequences alone, neglecting potential impacts from the full-length viral genome and replication capacity, limits the depth of our analysis. In cases of minor resistance, the possibility of archived, replication-incompetent viral variants cannot be disregarded. Additionally, the influence of mutations in regions outside the Env, as well as the potential role of bnAbs in enhancing immune clearance, warrant further investigation. The restricted sampling to PBMCs and plasma might have overlooked viral reservoirs in other compartments, such as the gut, brain, and CSF.

In addition, despite the presence of bnAb resistance-associated mutations in some individuals, a lack of consistent correlation between these mutations and high IC80 values was observed. In some cases, sequences without detectable mutations exhibited high IC80 values, indicating that other factors might influence bnAb sensitivity beyond the presence of these specific amino acid mutations, such as post-translation modifications. No specific residues associated with bnAb resistance were identified after examining MSA of participants for which discrepancies between observed IC80 values and lack of bnAb resistance-associated mutations were observed. This may be attributed to the low number of participants and sequences for which neutralisation assays were performed to this time. A machine learning approach may be more efficient in identifying such novel residues and better inform sensitivity prediction when more neutralisation assays are performed at the end of the trial. It is worth noting that although genetic analysis is a powerful tool for predicting bnAb sensitivity, it does not always capture the full picture. There are indeed additional factors, such as protein structure and folding as well as the actual presence of glycans in PNGs, which influence bnAb resistance and may not be apparent from analysing the Env sequence. It may therefore be necessary to combine sequence analysis with other approaches, such as structural analysis and 3D modeling of the protein and its interactions, to develop better predictions for bnAb sensitivity.

6

Expression of type I interferon-associated genes at antiretroviral therapy interruption predicts HIV virological rebound

Contents

6. ***Expression of type I interferon-associated genes at antiretroviral therapy interruption predicts HIV virological rebound***

6.1 Context

Most people with HIV who are receiving ART will experience rebound viremia if they stop treatment. However, a small proportion of ART-treated individuals can stop therapy and maintain undetectable viremia for months and, in some cases, years (Etemad et al., 2019; Martin et al., 2017; Sáez-Cirión et al., 2013). Other individuals spontaneously suppress HIV viremia in the absence of therapy and maintain undetectable viral loads for many years. These 'elite controllers' or 'long-term non-progressors' are likely protected by strong T cell responses restricted by protective HLA alleles (Goulder & Watkins, 2008). Identifying biomarkers which predict outcomes following TI would provide enormous value to both understanding mechanisms of PTC and identifying new drug candidates. Multiple clinical factors and molecular biomarkers which correlate with time to rebound have been proposed to elucidate these mechanisms (Conway et al., 2019; Hurst et al., 2015; Krebs & Ananworanich, 2016; Martin et al., 2017; Sharaf et al., 2018; Stöhr et al., 2013; J. P. Williams et al., 2014) however the host factors that affect the responsiveness of T cells have not yet been thoroughly characterised (Hyrcza et al., 2007), especially at a transcriptome level.

RNA sequencing (RNA-seq) offers a powerful tool for unraveling the complex interplay between the host and HIV virus, particularly in understanding the mechanisms underlying the post-treatment controller phenotype. By profiling the transcriptome of immune cells from PWH, RNA-seq can identify deferentially expressed genes or enriched gene pathways associated with a specific phenotype over another, such as PTC versus normal progressors. These gene signatures may reveal critical host factors involved in immune activation and viral control.

6. ***Expression of type I interferon-associated genes at antiretroviral therapy interruption predicts HIV virological rebound***

6.2 Aims

1. Identify genes or gene-sets expressed by CD4+ T cells that might associate with longer periods of post-treatment control.

6.3 Results

6.3.1 Cohort

18 SPARTAC participants who had received 48 weeks of suppressive ART commenced during PHI were initially analysed. The SPARTAC study is described in more detail in Materials and Methods (2.2.1). Participant selection was based on time to viral rebound following treatment interruption (Gossez et al., 2019) and on availability of viable PBMCs. All women in this cohort had C clade HIV and all men had non-C clades (75% had B or B recombinant virus and 25% had D clade HIV (Table A.5). They were then stratified by time to rebound (>400 HIV RNA copies/ml of plasma). Blood samples were taken at Week 0 (Baseline) at the time of starting ART and at the time of TI, 48 weeks later. The demographics of the participants are presented in Table A.5. Following a pre-analysis step, 14 female participants were selected for further analysis, to decrease the impact of confounding variables, specifically the linear relationship between sex and viral clade as well as the lack of paired samples from both timepoints.

6.3.2 Clustering of participants based on clinical response

Clustering analysis of RNA expression of SPARTAC trial participants revealed distinct groups based on gender and viral subtype (Figure 6.1). Therefore, to avoid potential confounding effects, we only included female participants in this analysis. We identified 14 female participants who had received 12 months of ART commenced during PHI followed by TI. All had viable samples of PBMCs taken at the point of TI (Week 48) and for 11 participants samples were also available at pre-therapy Baseline (Week 0). Viral rebound was reported if viral

6. ***Expression of type I interferon-associated genes at antiretroviral therapy interruption predicts HIV virological rebound***

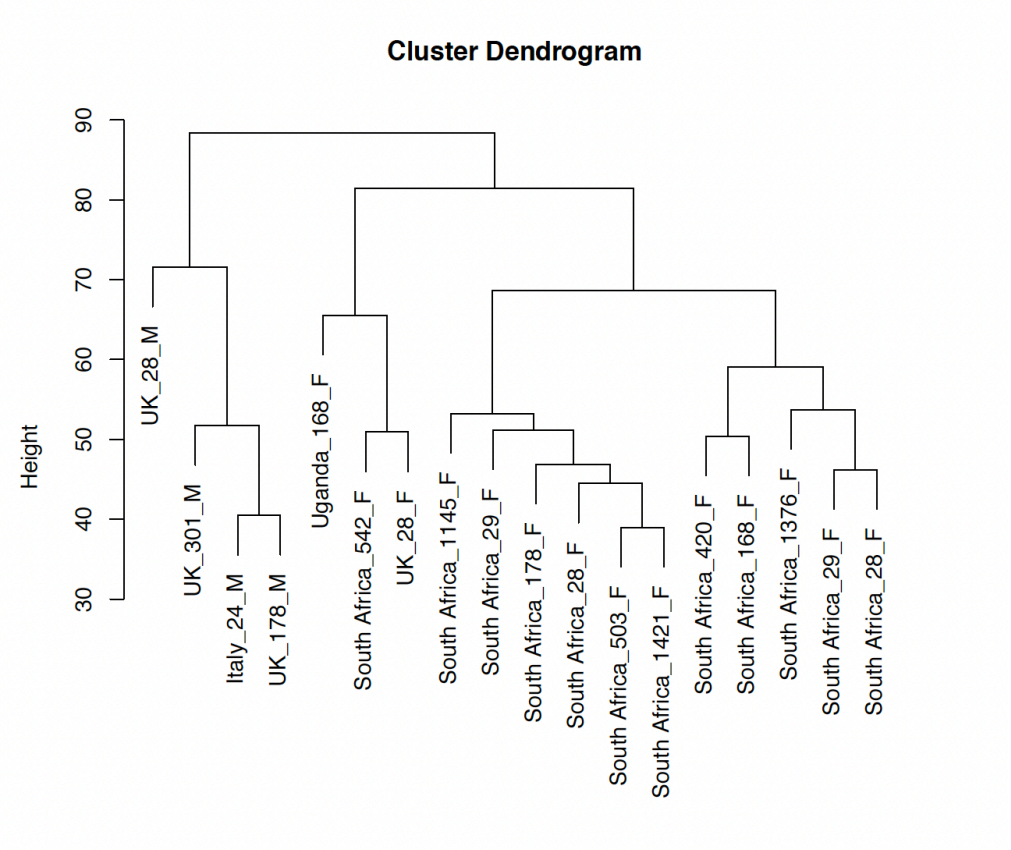

Figure 6.1: Participant clustering based on gene expression

load post-TI was measured > 400 copies/ml in two consecutive visits. 'Days to viral load rebound after TI' was used to define clinical phenotypes and structure the comparative analysis (Table A.5).

Based on observations in SPARTAC and other cohorts (Colby et al., 2018, 2020; Etemad et al., 2019; Stöhr et al., 2013) we defined early rebounders (ER) following TI (rebound<100 days) and post-treatment controllers (PTC) (rebound >100 days post-TI). HLA Class I typing for these participants revealed both protective (eg HLA B81:01, B57:03) and deleterious (eg HLA B58:02) alleles within the cohort, but no relationship with outcome, suggesting—based on this surrogate marker—that the CD8 T cell response was not driving the clinical phenotype. Interestingly, the B35:01 allele was identified in 0/5 ER, but 3/10 PTCs—not a statistically significant difference, but consistent with findings from the VISCONTI cohort (Sáez-Cirión, 2019).

6.3.3 Differential Gene Expression and Gene Set Enrichment Analysis show a strong association of type I interferon pathways with sustained control of viremia

Differential Gene Expression (DGE) analysis was used to identify individual genes that were differentialy expressed in certain clinical groups. From a total of 12,891 genes, those with a reported adjusted p-value (padj) < 0.05 were considered as significantly differentialy expressed. Two genes were found to be significantly differentialy expressed between PTC and ER, namely *POMC* and *IFITM3*. *IFITM3,* an interferon stimulated gene involved in immune response, was upregulated in PTC whereas *POMC,* a gene which encodes a precursor polypeptide for a variety of peptide hormones, was downregulated. This small number of genes identified by DGE is not surprising in view of the sample size and participant heterogeneity.

To get a broader view of genetic predictors of rebound, we identified functionally linked gene sets using Gene Set Enrichment Analysis (GSEA), which was performed on all genes ranked by their corresponding Wald statistics from the DESeq2 analysis output. Only pathways with a False Discovery Rate (FDR)<0.25 were considered significantly enriched. The majority of pathways enriched in PTC vs ER, namely 'Interferon alpha/beta', 'O-glycosylation' and 'response to elevated platelet pathways', are involved with immune response regulation (Figure 6.2A). Pathways involved in cell division were also found to be enriched in ER vs PTC at week 48, which might correlate with enhanced viral transcription. Of note, immune regulation pathways were not enriched at Week 0 in PTC, as they were at Week 48. However, in Week 0, there was enrichment in PTC of pathways associated with the regulation of cell-replication (Figure 6.2B), which may be disrupted by viral accessory proteins (D. Zhou et al., 2020; Zimmerman et al., 2006), and with evidence for an association with increased production of pro-inflammatory cytokines (Ragu et al., 2020).

6. ***Expression of type I interferon-associated genes at antiretroviral therapy interruption predicts HIV virological rebound***

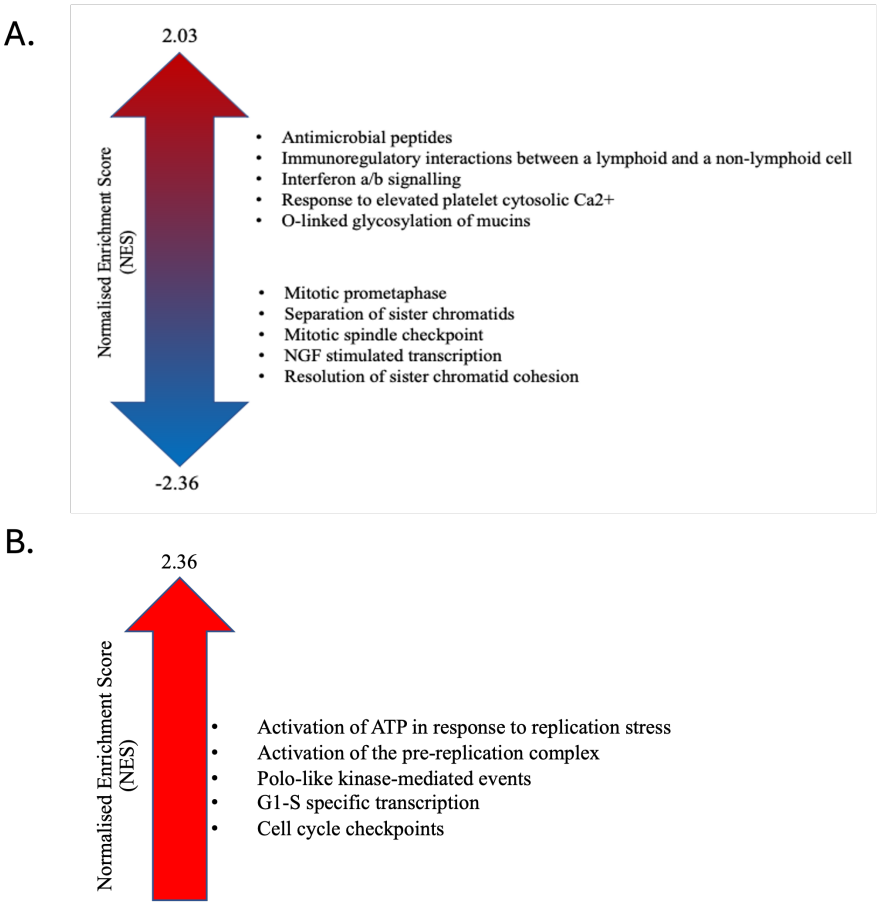

Figure 6.2: GSEA enrichment. A. The top ten enriched pathways (FDR<0.25) for Week 48 PTC vs ER by GSEA. Ranking is by Normalised Enrichment Score (NES), B. Week 0 pathway enrichment in PTC vs ER according to clinical phenotype using GSEA and the Reactome pathway database.

6.3.4 Weighted Gene Co-expression Network Analysis (WGCNA) identifies module enriched in IFN-I as associated with days to rebound

For interrogation of the transcriptomics data based purely on days to rebound, Weighted Gene Co-expression Network Analysis (WGCNA) was employed to identify clusters of co-expressed genes (modules) and to inform on pathway enrichment at the point of TI in an unsupervised manner. Time to Rebound was used as a clinical trait of interest, as it offered the opportunity to explore the genetic correlations without having to make an *a priori* decision on sample grouping. WGCNA constructs a weighted network that represents the interaction patterns among genes, by emphasising the strong gene–gene correlations at the expense

of the weak ones in order to reduce noise. Here, the co-expression network was built using the expression data of a total of 6006 genes, that were retained after filtering for low variability and low read counts. A scale-free topology network was calculated by raising the correlation values to a power of beta=20, for which the scale-free topology fit index was above 0.8 (Figure 6.3A). WGCNA then clustered all genes with similar co-expression patterns into modules, conventionally denoted by colour names. A mean expression value (module eigenvalue), based on the expression of all genes within every module, was then associated with "Days to Rebound" as a continuous variable.

The 'salmon module', named Module 1 here, had the strongest positive correlation with time to rebound (cor=0.7, p-value=0.006) (Figure 6.3B) The module consists of 36 genes, the majority of which - for example, *IFI44, XAF1, ISG15, USP18, TRIM25, IFIT1, RSAD2* - are interferon stimulated genes (ISG). A significantly high correlation between Module Membership (MM) and Gene Trait Significance (GS) is reported for Module 1 (cor=0.51; p-value=0.0015), demonstrating that the genes driving the expression of the module eigenvalue, are the ones that correlate with days to rebound (Figure 6.3C).

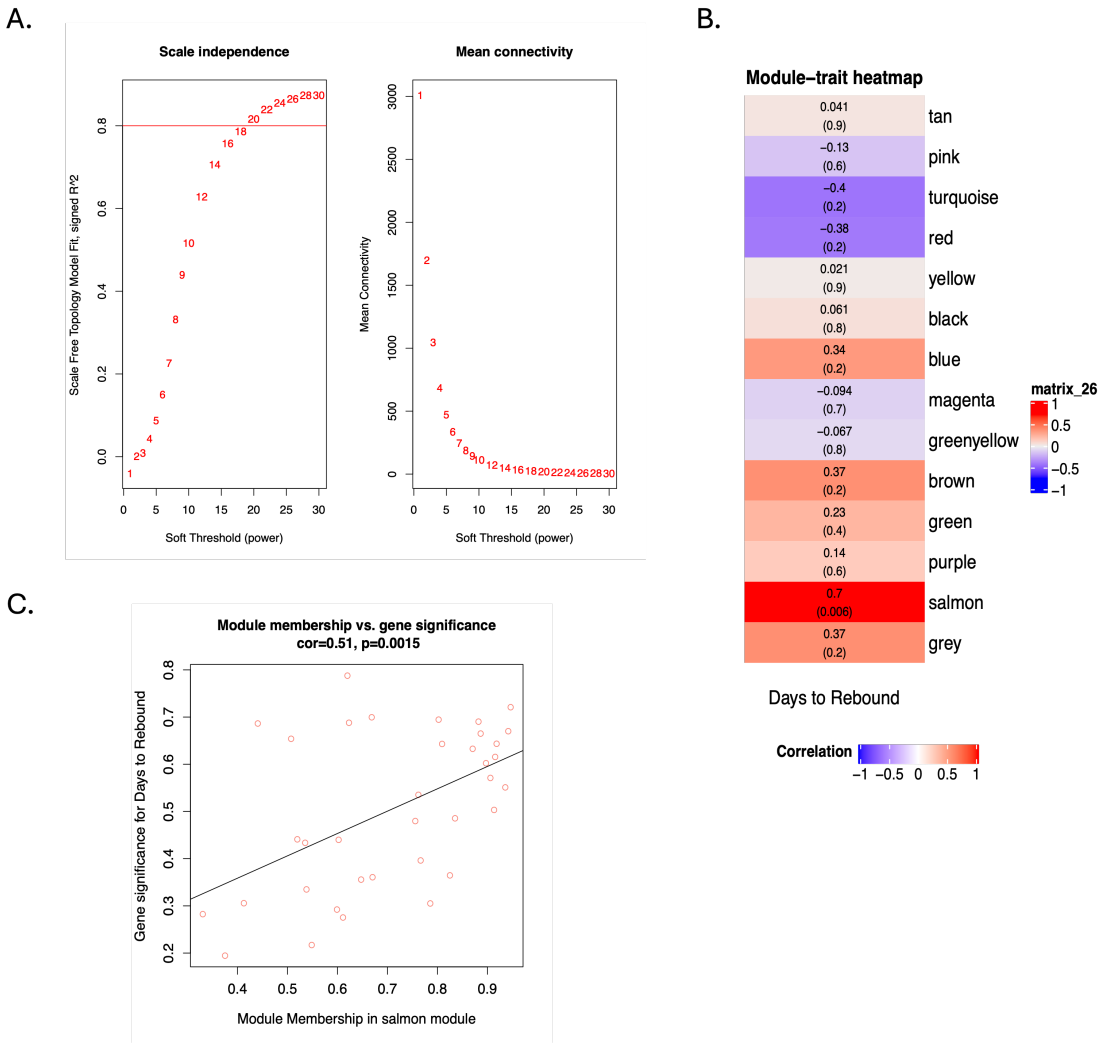

Figure 6.3: WGCNA module identification. A. A power of 20 was selected to achieve scale-free topology of R2 $>$ 0.8 and Mean Connectivity close to 0. B. Heatmap plot of WGCNA gene modules on TI associated with 'days to rebound'. Trait correlations and statistical significance (in parenthesis) are shown for each module. Modules are colour-coded based on direction and intensity of correlation. The salmon module which was identified for further analysis is marked with a box and labelled as 'Module 1'. The heatmap was made with WGCNA (package version 1.70.3). C.Scatterplot of gene significance (GS) for trait of interest versus module membership (MM) for Module 1.

6.3.5 Functional enrichment of WGCNA modules associated with PTC phenotype and Days to Rebound indicates Interferon Type I pathway involvement

Protein–protein interaction (PPI) and high correlation with both module membership and days to rebound (MM and GS scores, respectively) were used as criteria to identify the hub genes, in a two-step validation process. MM and GS

6. ***Expression of type I interferon-associated genes at antiretroviral therapy interruption predicts HIV virological rebound***

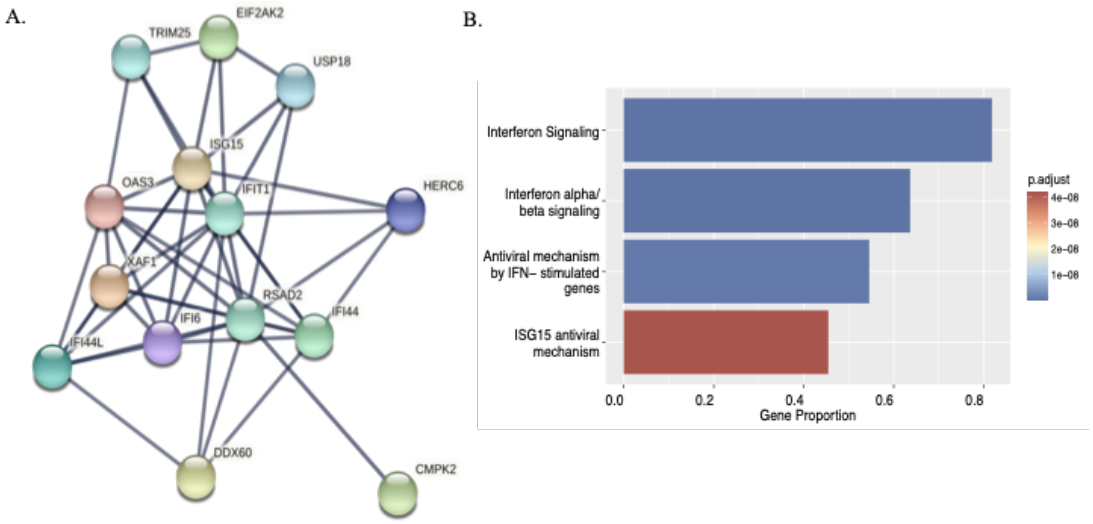

Figure 6.4: Protein Interactions and Pathways Enrichment for genes protective for viral rebound. A. Visualisation of the Protein-Protein Interaction network of key genes within Module 1 using STRING for cross-validation of hub genes identified through GS and MM scoring. B. Pathways enrichment bar plot identified using STRING and the Reactome database. The proportion of hub genes to pathway genes is shown on x-axis.

scores were measured by Pearson's correlation and PPI was visualised on STRING. Figure 6.4A shows only the interacting module genes, after selecting for a high interaction score (>0.9). Thirteen interacting genes, which also satisfied the GS (>0.2) and MM criteria (>0.8), were regarded as hub genes and were taken forward to Gene Set Enrichment Analysis. To be consistent with the GSEA, the Reactome pathway database was used to report the enrichment. Module 1 hub genes showed significant enrichment (p-value <0.05) in pathways associated with response to IFN-I (Figure 6.4B).

6.3.6 Risk score calculation based on the expression of two genes can potentially predict time to rebound

As a next step, we looked to see if any of the individual hub genes identified in the WGCNA results were more closely linked to progression, potentially leading to a signature that might predict longer post-TI viral suppression. Univariable analysis showed that the expression of 7 out of 13 hub genes contained in Module 1 (*ISG15, IFI6, IFI44, RSAD2, XAF1, USP18* and *TRIM25)* were significantly associated

Table 6.1: Univariable Cox regression for individual hub genes.

Gene	HR (95% CI for HR)	P value
ISG15	**0.29 (0.11-0.81)**	**0.0091**
IFI6	**0.18 (0.037-0.86)**	**0.0140**
IFI44L	0.55 (0.27-1.1)	0.0830
IFI44	**0.23 (0.047-1.2)**	**0.0450**
IFIT1	0.37 (0.12-1.1)	0.0540
OAS3	0.52 (0.22-1.3)	0.1500
XAF1	**0.3 (0.1-0.92)**	**0.0270**
TRIM25	**0.074 (0.0068-0.8)**	**0.0230**
CMPK2	0.23 (0.037-1.5)	0.0740
RSAD2	**0.2 (0.041-0.99)**	**0.0320**
EIF2AK2	0.54 (0.12-2.4)	0.4200
USP18	**0.23 (0.062-0.84)**	**0.0220**
HERC6	0.16 (0.019-1.3)	0.0570

with a protective Hazard Ratio (HR) for viral rebound (Table 6.1). A multivariable Cox Regression analysis was performed including these seven genes. Least Absolute Shrinkage and Selection Operator (LASSO) was used to eliminate genes with zero coefficients (*IFI6, IFI44* and *RSAD2*) and only four genes (*ISG15*; cor=-0.41, *TRIM25*; cor=-0.32, *XAF1*; cor=-0.06 and *USP18*; cor=-0.14) were retained.

A Risk Score (RS) was calculated for the fourteen female participants using the expression of these four genes, and their LASSO coefficients were classified as either low or high relative to the mean RS (Table 6.2).

Kaplan Meier analysis showed that a lower RS with higher expression of *ISG15, USP18, XAF1* and *TRIM25* was significantly associated with longer suppression post-TI, compared to participants with a high RS (p=value<0.01) (Figure 6.5A). Boxplots showing the risk score for each participant in the PTC and ER groups based on expression of the Cox-LASSO derived genes (Figure 6.5B) and the ROC curve (Figure 6.5C) shows the effectiveness of the signature (AUC=0.909) in distinguishing rebounders from non-rebounders.

6.4 Discussion

The aim of the study was to gain further understanding of how host gene expression might affect the duration of post-TI viral control. The SPARTAC trial offered a

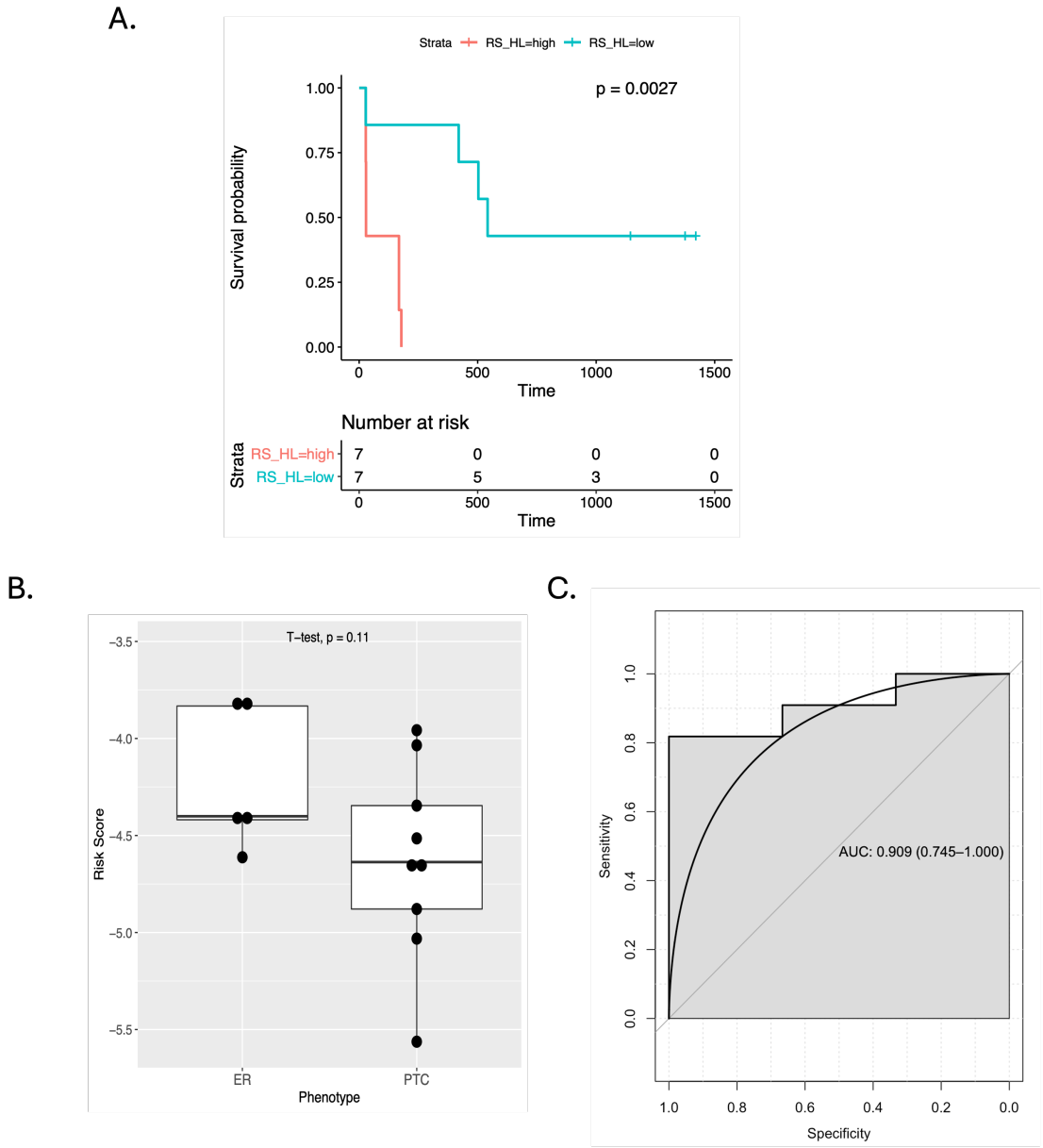

Figure 6.5: Survival analysis and gene signature validation. A. Kaplan-Meier survival analysis of gene expression-based Risk Score (RS) comprising genes ISG15, XAF1, USP18 and TRIM25, predicting the likelihood of early and late post-TI rebound. Blue and red lines represent low and high-risk score, respectively, divided by the mean cohort score. + represents censored samples. B. Expression of the risk score genes for each participant plotted for different phenotypes. ER Early Rebounder PTC Post-Treatment Controller. C. ROC curve demonstrating efficiency of applying the Risk Score to identify participants that reported rebound versus those that did not. AUC = Area Under the Curve; Confidence Interval in brackets.

Table 6.2: Individual Risk Score per participant, based on the expression of gene signature

Participant	Days to Rebound	Incidence	Risk Score (RS)
SJV026005	1421	0	-5.56
SJC030002	542	1	-5.01
SJE030001	1376	0	-4.88
SJH027017	420	1	-4.67
SJE021010	1145	0	-4.64
SUN036016	28	1	-4.61
SJL026018	503	1	-4.51
SJS025009	29	1	-4.42
SJZ026003	28	1	-4.40
SJV101017	168	1	-4.34
SJJ027008	178	1	-4.03
SJK023006	168	1	-3.96
SJR026007	28	1	-3.83
SJA023044	29	1	-3.81

unique opportunity to study samples from participants with PHI that had been followed-up for an average of four years post-TI (Fidler et al., 2013). To minimise the noise caused by averaging the expression of different cell types, I studied CD4 T cells as they are key to virological control (Frater et al., 2014) and comprise the majority of the HIV reservoir. Therefore, any variability in transcriptional activity might impact the likelihood of proviral expression. In addition, we restricted our analyses to women to exclude potential confounding factors from sex.

Due to the small sample size and the major variance between the phenotypes, DGE analysis identified only two genes differentially expressed between PTC and ER. *IFITM3*, which was upregulated in PTC, plays a critical role in actively preventing infection by inhibiting viral-cell fusion (Spence et al., 2019). In turn, *POMC*, a precursor of melanocortins ACTH and MSH, was downregulated in PTC. Evidence to associate melanocortins with anti-inflammatory action has been reported *in vivo* and *in vitro* (W. Wang et al., 2019). Downregulation of POMC in PTC may denote inflammation suppression, which may be protective against viral rebound at the early stage of TI.

The results of GSEA - which is less impacted by sample size - revealed that

the PTC phenotype (i.e. rebound > 100 days after TI) showed enrichment for the Type I Interferon (IFN-I) signaling pathway as well as O-glycosylation and platelet activation pathways. Response to IFN-I was also found to be associated with days to rebound in the WGCNA approach, which made no prior assumptions about definitions of post-treatment control. IFN-I pathways comprise a family of cytokines playing a critical role in the regulation of the innate immune response in infection (McNab et al., 2015). Studies in SIV models illustrate the benefit of IFN-I administration at the early stage of infection in inhibiting viral replication (Deeks et al., 2017; Sandler et al., 2014; Van der Sluis et al., 2020). Similarly, HIV develops strategies to evade IFN-I and to inhibit the functionality of the proteins regulated by IFN-I (Fenton-May et al., 2013), suggestive of a fundamental role of this pathway in viraemic control. Previous studies have highlighted the importance of IFN-I in controlling HIV infection, by showing that founder viruses that are able to establish infection are usually IFN-resistant but may be less fit (Adland et al., 2020; Cohn et al., 2018; Iyer et al., 2017). Recent findings from Gondim et al. (P. et al., 2021), showed that viral resistance to IFN-I fluctuates throughout infection and, notably, post-TI plasma viruses are the most IFN-I resistant. This suggests that the induction of IFN-I immediately after infection or treatment interruption can clear IFN-I sensitive viruses and only allow IFN-I resistant viruses to replicate. Although there is no reported association between T-cell immune escape and changes in IFN-I sensitivity, CTL escape (Roberts et al., 2015; Zimbwa et al., 2007) has been well-described during primary infection and the possibility of this affecting IFN-I sensitivity should be investigated. O-linked glycosylation may also contribute to the regulation of the immune system and T-cell development (Pereira et al., 2018), with recent evidence of a link between type I interferons and modulation of the host glycome in HIV infection (Giron et al., 2020). The association of the PTC phenotype with platelet activation is intriguing and possibly consistent with reports that release of chemokines by activated platelets can function as an extra barrier at the early stages of HIV infection (Solomon

Tsegaye et al., 2013). However, further investigation is required to determine the role of platelets in the defense against HIV.

WGCNA was performed to determine how gene modules associate with specific clinical traits. For an unbiased analysis, 'time to rebound' was used as a trait to examine whether WGCNA findings corresponded with the GSEA analysis. The analysis identified one dominant module that was associated with 'Time to Rebound'. The gene ontology and pathway analysis for this Module showed a clear enrichment for IFN-I associated genes, supporting the previous results for the phenotype traits. The majority of genes reported as hub genes were ISG, again consistent with the argument that the response to type I interferons is impacting rebound. None of the hub genes in the Module were found among the DE genes. This is not surprising, given that WGCNA associates gene co-expression modules with the trait of interest, rather than individual genes. Besides, DGE analysis was based on arbitrary clustering of participant phenotypes, which may have made singling out genes less robust and accurate. To this end, only genes identified with WGCNA were used to build a gene signature in the subsequent steps.

A univariable Cox analysis identified seven genes, mostly ISGs, associated with remission in the participants. Based on a multivariable Cox regression with LASSO screening of these seven genes, a risk score based on the expression of four (*ISG15, XAF1,TRIM25* and *USP18*) was derived to predict the likelihood of viral rebound. Higher expression of these four genes was strongly protective for post-TI rebound. *XAF1* is a pro-apoptotic tumor suppressor protein, which is induced by IFN-I and tumor necrosis factor alpha (TNFa) (Jeong et al., 2018). *ISG15* is an interferon stimulated ubiquitin-like protein and a critical component of protein modification and cell cycle regulation (Dzimianski et al., 2019; Perng & Lenschow, 2018). *TRIM25* is an E3 ligase that positively regulates *ISG15* conjugation to pathogen proteins, in a process with reported antiviral effects called ISGylation (Martín-Vicente et al., 2017). *USP18* is a negative regulator of IFN-I signalling that dampens its detrimental effects (Dzimianski et al., 2019; Honke et al., 2016; X. Zhang et al., 2015). Although more work is underway to characterise the role

of these pathways in HIV infection, this independent identification of these genes would be consistent with a role in maintaining virological remission.

This study has several limitations, including the small sample size on which the analysis was performed, as well as the lack of diversity in terms of sex and the viral clade of the participants. In this subcohort, we analyzed only samples from females due to an enrichment of African female participants in the SPARTAC PTCs (Gossez et al., 2019). This resulted in a greater availability of PTC samples from women compared to men. Additionally, given the significant differences in gene expression between men and women in this study, where sex could not be excluded as a confounding factor, we opted not to include samples from both sexes. In addition, our analysis was limited to bulk CD4+ T cells, with no enrichment for those cells that were HIV-specific or contained proviral DNA. In the era of single-cell RNA sequencing, a more exploratory study of how each cell type proportion or gene expression change contributes to the phenotype may be more informative. A further limitation is that due to a lack of remaining samples we have been unable to carry out any subsequent confirmatory experiments to test the significance of the genes identified. The other factor to consider is whether our choice of clinical phenotypes accurately discriminated between 'post-treatment controllers' and 'elite controllers'. The latter have been well characterised (Martin et al., 2017), and more generally associated with effective HLA Class I-restricted T cell responses (Kiepiela et al., 2007), whereas it is still unclear as to which mechanisms are driving PTC. Our analysis of HLA types does reveal a number of protective alleles, but not enough to explain our data. Larger studies in more diverse populations will be needed to tease out these differences. However, that two independent analyses conferred the same statistically significant results of pathway enrichment should be taken into consideration. The finding of a strong type I interferon signal associating with delayed rebound in this small study needs to be confirmed in larger clinical trials incorporating TI. If these data are reproducible, they could help with the identification of a valuable biomarkers of remission and pathways to drug discovery for the HIV cure field.

7

An exploratory study of the impact of bnAbs on the host immune response

Contents

7.1 Context

bnAbs have shown remarkable efficacy in neutralising a wide range of HIV-1 strains, offering hope for a functional cure. However, understanding the full impact of bnAb therapy on the host immune response remains an ongoing area of investigation. Previous studies have described the mechanism of HIV neutralisation by bnAbs

7. ***An exploratory study of the impact of bnAbs on the host immune response***

in collaboration with other elements of the host immune response (Bournazos et al., 2014; Caskey et al., 2019; Junker et al., 2020). Additionally, findings suggest that passive administration of 10-1074 and 3BNC117 may enhance T-cell responses, mainly CD8+, facilitating long-term viral clearance in primates and humans (Niessl et al., 2020; Nishimura et al., 2017; Rosás-Umbert et al., 2022). However, at the time of writing this thesis, no study to characterise the effect of bnAbs on the transcriptome of host immune cells had been conducted.

Transcriptomic analysis provides a powerful tool for investigating the molecular mechanisms underlying the effects of bnAb therapy. By studying gene expression patterns, we can gain insights into the cellular and molecular pathways activated or suppressed in response to bnAb treatment. Due to the exploratory nature of this study, high-resolution analysis and a detailed investigation of the impact of bnAbs on specific cell types were deemed essential. To comprehensively assess the broad immune response to 10-1074 and 3BNC117 treatment at the transcriptomic level, we employed single-cell RNA sequencing (scRNA-seq) to profile PBMCs from selected RIO participants before and after bnAb treatment, without pre-selecting for HIV-specific responses.

The findings of this study could provide valuable insights into the mechanisms of bnAb therapy and inform the development of strategies for more effective bnAb treatment.

7.2 Aims

I hypothesised that people who receive bnAb treatment would have distinct gene expression profiles associated with immune activation, viral control, and potential long-term effects on the host immune system. Furthermore, if a bnAb-induced vaccinal effect exists, altered cell proportions and differential gene expression before and after treatment are likely to be observed in CD8+ T cells, NK cells, and/or antigen-presenting cells (Naranjo-Gomez & Pelegrin, 2019; Tipoe et al., 2022).

7. ***An exploratory study of the impact of bnAbs on the host immune response***

1. Determine if there are any differences in cell composition in PBMCs before and after bnAb treatment
2. Identify gene signatures of the effect of bnAb treatment in PBMCs.
3. Explore transcriptomic signatures of the vaccinal effect in PBMCs.

7.3 Results

7.3.1 Cohort

In total, PBMCs from 8 RIO participant sampled at UJ (baseline, on ART) and UT (12 weeks post-bnAb administration and TI) were profiled using scRNA-seq for this study. All but two participants were enrolled in Arm A, to reduce complexity, and were undetectable at UT (Figure 7.1).

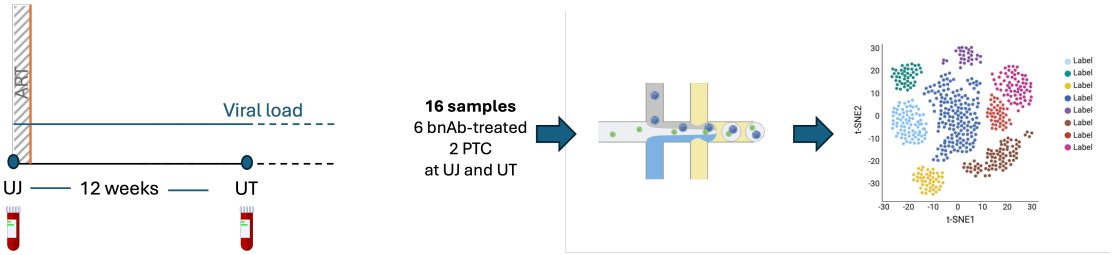

Figure 7.1: Single cell RNA seq study design.

The two Arm B participants were classified as PTCs, as no bnAb titers were found in samples taken from them at any point during the trial (Table A.6). Participants were selected based on the absence of viral rebound until the UT timepoint (12 weeks post the first bnAb dose) and ideally for at least 40 weeks after the first bnAb dose, which was the estimated time frame of bnAb falling below 10 ug/ml. Participants did not have any evidence of bnAb resistance at screening or at rebound at the time of selection and no protective HLAs were found. Unfortunately, a clog on the 10x chip caused the encapsulation of PBMCs from the UJ samples from participants 001-018 and 007-002 to fail. Therefore, the UT samples from these participants were only used for annotation and not for downstream analysis in this thesis.

7. An exploratory study of the impact of bnAbs on the host immune response

The clinical data shown in Table A.6 suggest that different mechanisms may be responsible for viral control post-ART interruption for different groups of participants included in this study who received bnAb treatment. For instance, participant 003-003 had not experienced viral rebound 53 weeks after the concentration of bnAbs fell below 10 ug/ml in the blood. The sustained viral suppression in this individual could potentially be attributed to a durable immune response triggered by a vaccinal effect, or alternatively, to post-ART control. In contrast, participant 001-012 remained undetectable for 42 weeks post bnAb-dose and experienced viral rebound while the concentration of bnAbs was still detectable in the blood. This raises the possibility that this participant developed resistance to bnAbs. Notably, no sequences were amplified for this participant at neither baseline nor at the post-bnAb rebound timepoint. The viral rebound of participant 003-006 coincided with the decline of bnAb concentrations below the 10 ţg/mL mark, which could suggest that bnAbs worked direct antiviral agent, with control being lost once the therapeutic threshold was no longer maintained. Lastly, participants 008-001 (who experienced low viral blips throughout follow-up) and 005-001 rebounded 39 and 16 weeks respectively, after bnAbs were washed out (Figure 7.2).The prolonged maintenance of viral suppression in both individuals, despite the absence of ART and detectable levels of bnAbs, implies a possible role for the vaccinal effect in sustaining immune control. In the case of 008-001, it is possible that the continuous exposure to low level viral antigen may have contributed to a continued stimulation of the immune system, potentially modulating the vaccinal effect (Naranjo-Gomez & Pelegrin, 2019).

7. *An exploratory study of the impact of bnAbs on the host immune response*

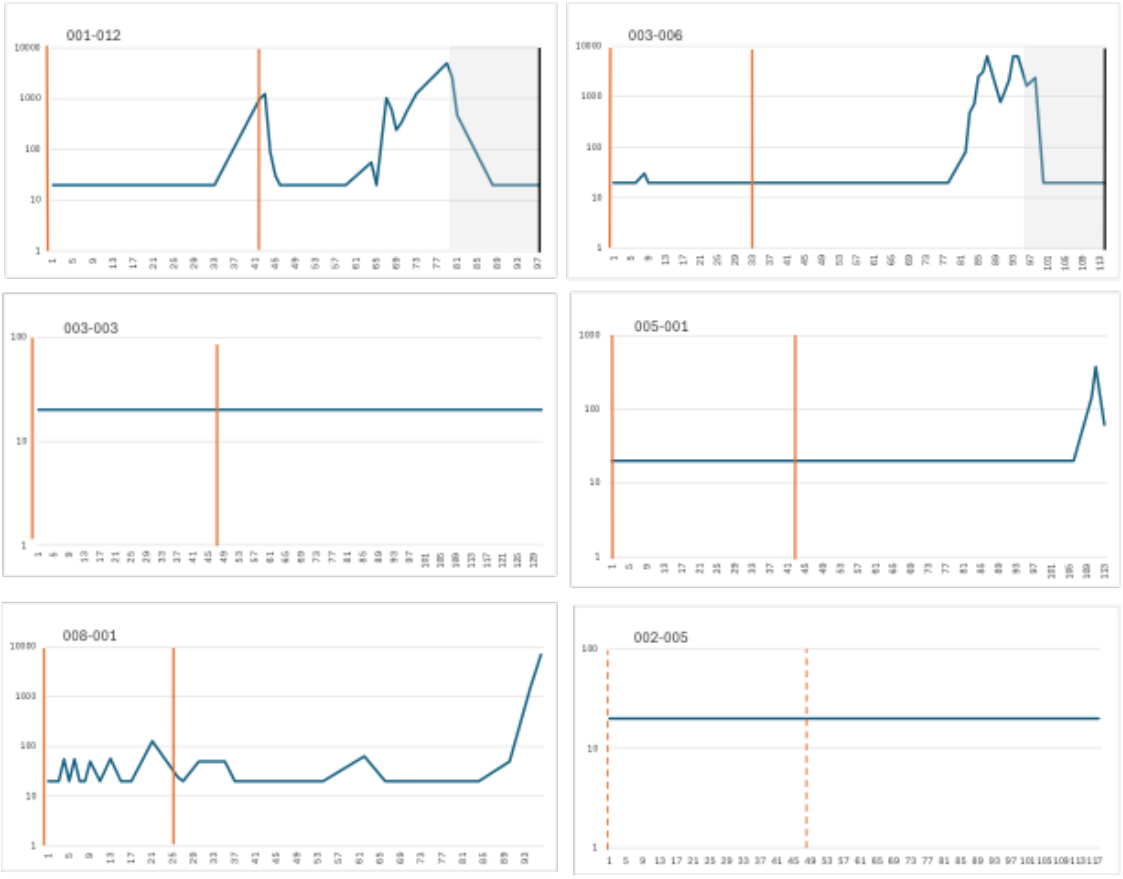

Figure 7.2: Viral Load plots for participants in the sc-RNA seq study. Blue line shows the viral load trajectory for each participant. The vertical orange lines show the timepoint where bnAbs were administrated. For participant 002-005, the saline dose is shown with a dashed line. The shaded box represents periods of ART and the black line marks the end of study timepoint.

Gene expression profiles of 77216 cells, an average of 5140 cells per participant per timepoint, were acquired following the experimental procedures detailed in Chapter Materials and Methods, Section 2.5. Post-annotation, downstream analysis was performed using 66764 cells from 6 participants. Following data quality filtering (which included regression of mitochondrial and ribosomal genes, doublet removal, count normalisation, and batch-effect correction), principal-component analysis (PCA) and clustering on the informative PCA space (n=18, resolution=1.5) were performed.

A total of 33 clusters were identified by Uniform Manifold Approximation and Projection (UMAP) analysis and broad cell types were manually annotated based

on established cell type markers (Figure 7.3). After collapsing due to high similarity, the final number of clusters came to 28. Clusters 13/18 and 8 lacked canonical markers to differentiate them from other major cell types. Both clusters lacked the typical markers associated with major cell types. Interestingly, cluster 13/18 was characterised by the expression of SERINC5, a host restriction factor that reduces HIV infectivity when it is incorporated in the viral envelope, and BACH2, a known target for HIV integration and regulator of T cell differentiation (Richer et al., 2016). Cluster 8 presented a transcriptomic profile similar to neighboring CD8+ and NK cells, as well as dendritic cells, but lacked all the canonical markers associated with these clusters. Several genes highly expressed in cluster 8, such as *STAT4, PRKCH, SYNE1, ZEB2* and *FYN* are directly associated with immune responses, T-cell differentiation and T-cell receptor signalling. Cluster 7 was characterised by CD4+ naive T cell markers, as was Cluster 2. The two clusters differed at the expression of BACH2, TSHZ2, and PDE3B, which were moderately upregulated in Cluster 7 and are associated with T cell naivety (Newton et al., 2016; Richer et al., 2016). Therefore Cluster 2 was considered to be a CD4+ naive cluster with differentiation potential and was annotated as such (CD4 naive diff). Cluster 20, which was mainly present in the UJ samples from participant 008-001 expressed CD14 and CXCL8, to differentiate it from the other CD14+ monocyte clusters. Cluster 22, a cluster expressing cytotoxic T-cell markers, was found uniquely in the samples from participant 008-001. Lastly, a subset of cells in cluster 5 distinctly expressed conventional DC markers and therefore it was annotated as "CD14+monocyte/cDC1".

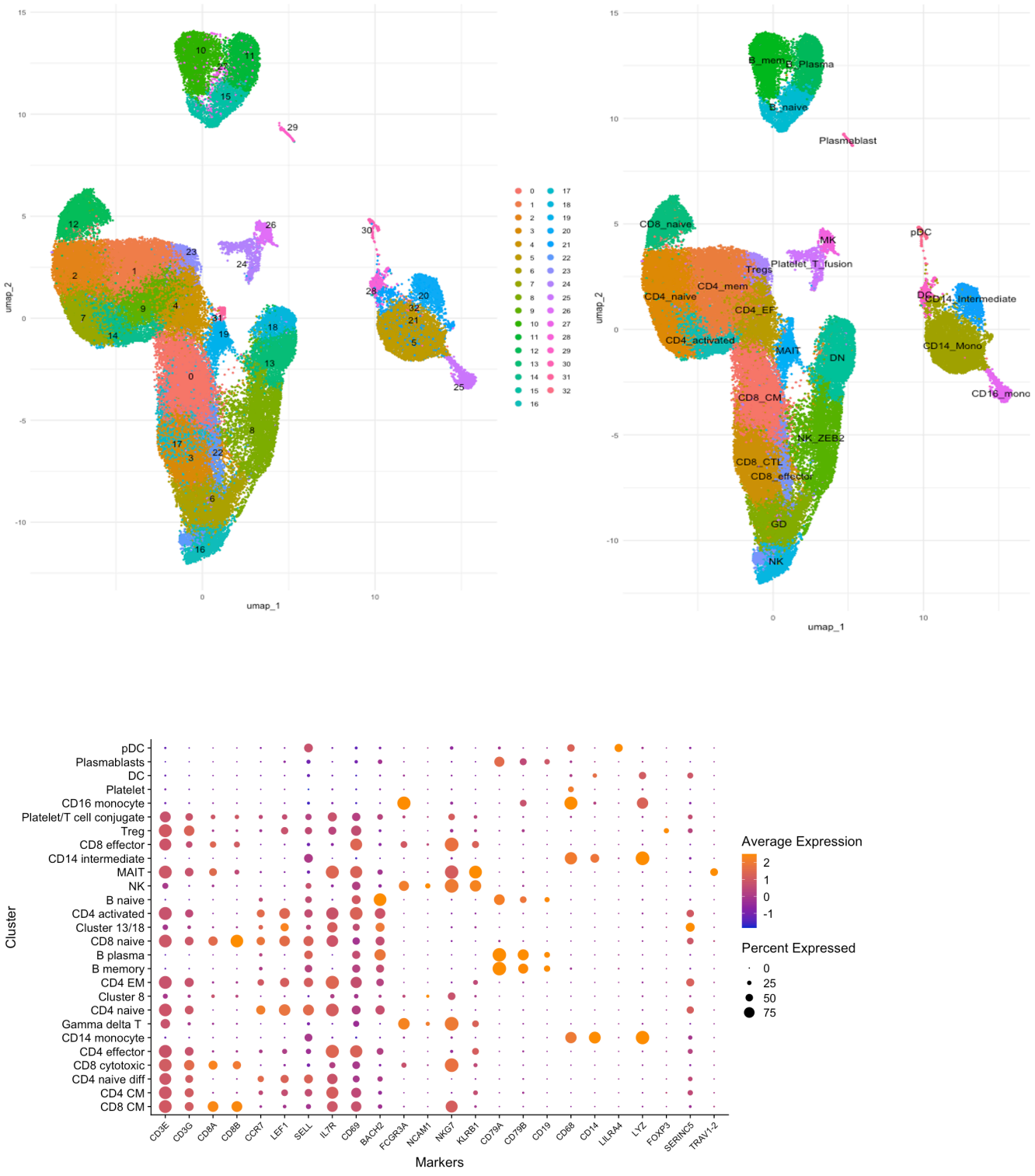

Figure 7.3: UMAPs clustering analysis of PBMC. On the left UMAP each cluster is coloured by cluster identity.On the right, UMAP analysis with clusters annotated by canoninal cell markers. Dotplot on the bottom shows the canonical marker expression per cluster. Gene expression is color coded based on range and size represents the cell proportion expressing the gene within the cluster.

7.3.2 Differentiation is increased post-ART interruption and bnAb treatment

As the first step in exploring the effect of bnAbs in the immune landscape in individuals with HIV, I calculated the frequency of different cell types before and after treatment with bnAbs. Paired samples from 5 participants who received bnAbs were included in this analysis as well as the one PTC, who underwent TI without having bnAbs.

Compared to baseline, an increase in the frequency of CD8+ cytotoxic, CD8+ EM, CD4+ EM, CD4+ naïve differentiating, CD4+ activated, B memory, B plasma, CD8+ naïve, and CD16+ monocytes was marked at UT. Conversely, the frequency of CD14+ monocytes, CD4+ CM, CD4+ activated, CD4+ naïve, CD8+ effector cells, and macrophages decreased at UT (Figure 7.4A). In other words, we observed an increase in the frequency of cells with a more activated phenotype at UT, suggesting that more naïve cells at UJ may have differentiated into activated cells post-bnAb treatment (Figure 7.4A).

The RIO trial is unusual as these participants stop ART but do not experience viral rebound. There is a question as to whether the removal of the potential toxicities associated with ART may impact gene expression, but this would be contemporaneous with any impact of the bnAbs. In certain cell types, such as in CD8+ EM, CD8+ cytotoxic, NKT cells, CD16+ monocytes, plasmablast and pDCs, the changes observed in bnAb-treated participants were in the opposite direction compared to those in PTCs. Notably, the changes in most CD4+ T cells (except for CD4+ activated), all B cells, CD8+ effector cells, platelets, and Cluster 13/18 were similar in direction to those in PTCs but exhibited a greater magnitude. This may suggest that bnAb treatment amplifies the changes in cell type frequency that would happen post-ART interruption (Figure 7.4B).

7. *An exploratory study of the impact of bnAbs on the host immune response*

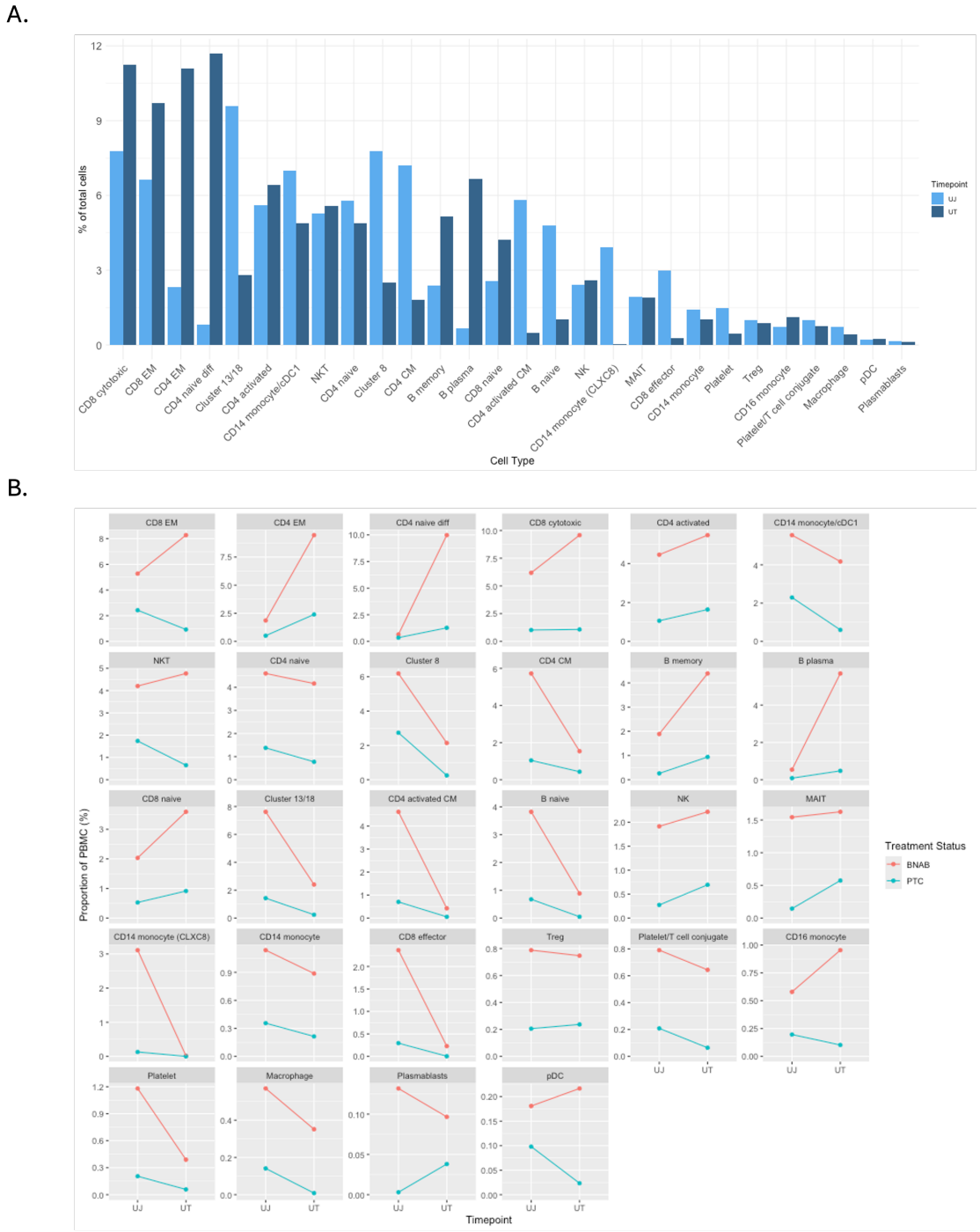

Figure 7.4: Impact of bnAbs on the cell clusters. Panel A shows the proportion of each cell type at baseline, before bnAb treatment and 12 weeks after bnAb dose. Different shades are used for the two timepoints. Panel B shows the difference in average cell count per cell type, before and after bnAb treatment. The cell counts of the PTC per cell type is shown for comparison. Different groups are coloured in blue (participants who received bnAbs) and red (bnAb-naive PTC).

7.3.3 Metabolic shift towards increased energy production and utilisation following bnAb treatment

To gain a more granular understanding of cell type-specific effects, I conducted differential gene expression analysis on individual clusters before and after bnAb treatment. A total of 1173 unique genes were identified as differentially expressed (up- or downregulated) between UT and UJ, across all cell types, with a false discovery rate < 0.05 and an absolute log2 fold change (log2FC) > 1. In bnAb-untreated participant samples, the most frequently upregulated genes across multiple clusters were associated with cellular energy requirements, such as *ATP5ME*, *NDUFB1*, and *NDUFA3*. However, genes with the largest log2FC values were *DYNLL1*, *C1orf162*, *SERTAD1*, *SNHG9*, and *STMN1*. Conversely, frequently downregulated genes included *TALAM1*, *MYH9*, *TXNIP*, *PDE3A*, *FOS*, *AHNAK*, *KLF10*, and *PRRC2A*. Notably, *PDR3A*, along with *IGFBP2*, *ARRDC4*, and *EGR1*, were among the top downregulated genes by log2FC. While most of these genes are not directly associated with HIV, their roles in cellular processes such as AMP signaling, cell adhesion, and growth may indirectly influence immune responses.

To elucidate the biological processes implicated by these differentially expressed genes, I performed GSEA on each cluster separately. A total of 40 pathways were enriched with an FDR < 0.25. Oxidative phosphorylation, reactive oxygen species (ROS) and fatty acid metabolism pathways were enriched in most cell clusters at UT compared to UJ. Notably, inflammation pathways, such as response to interferon alpha and gamma, TNFa signaling via NFkB, TGFb signaling and hypoxia pathways were enriched at the UJ clusters (Figure 7.5).

*7. **An exploratory study of the impact of bnAbs on the host immune response***

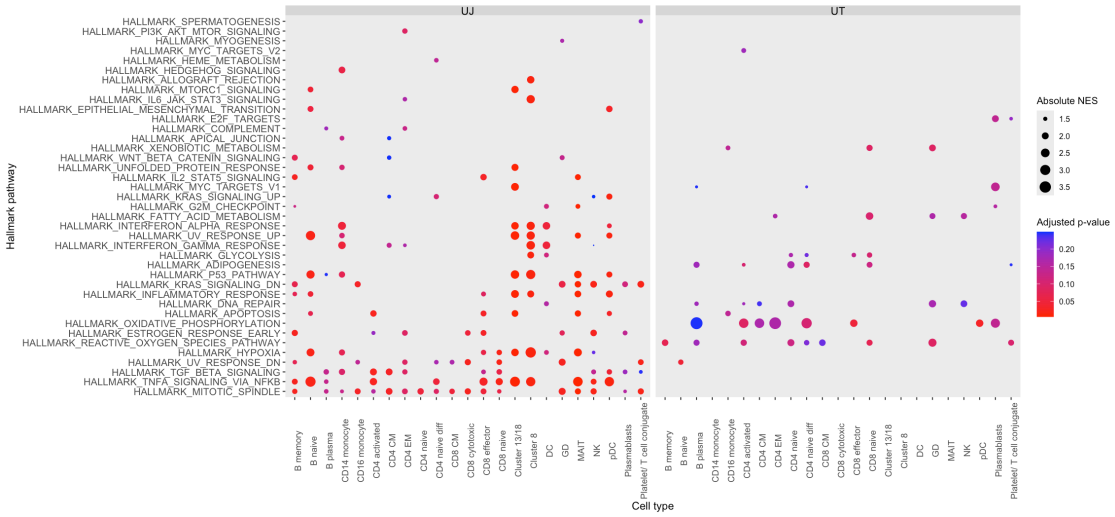

Figure 7.5: Pathway enrichment in paired bnAb-naive and bnAb-treated RIO participants per cluster.The two panels show which pathawys are enriched in which cluster at each timepoint. The dot size and colour represents the NES and adjp, respectively

7.3.4 Heterogeneity of bnAb effects in individual participants

Building upon the initial analysis of all participants, in this section I set out to investigate what are the immunological factors that may influence specific clinical outcomes in individuals who receive bnAb therapy. To start with, I explored the changes in cell proportions between UJ and UT. As previously stated, the clinical data suggest that these individuals may control HIV using bnAbs in different ways and therefore classification into "clinical response" groups was not meaningful.

The cell proportion trend was universal across all participant in specific cell clusters; a increase was observed in CD4+ CM, CD4+ naive diff and B plasma cells in all participants who interrupted ART, from UJ to UT. A general decrease was seen in platelets and CD14+ intermediate monocytes. Notably, in the CD14+ monocyte/cDC1, CD4+ naive, and EM clusters, the cell proportion changes for 008-001 were the opposite direction compared to all the rest. Additionally, the CD8+ effector and CD14+ monocytes expressing CXCL8 clusters were particularly prevalent at the UJ sample from 008-001 compared to other participants. These

findings may indicate that changes in cell proportions between UJ and UT in these cell types is associated with the presence of viral antigen.

Participant 003-003, who may be controlling through vaccinal effect, showed an increase of CD8+ EM and pDC proportions from UJ to UT but a decrease in NK and, uniquely, in CD8+ naive cells. The opposite trend was seen in the PTC, 002-005, who has a decrease in CD8+ EM, in all APCs, including pDCs, and in NKT cells. However, an increase was observed in the NK, CD4+ effector and MAIT cells. Participants 005-001 and 003-006 show a similar clinical response to bnAbs, as both rebound within 0-6 weeks of bnAb concentrations falling below 10 ug/ml. However, the cell proportions changes differ in direction and magnitude in several clusters, such as CD4+ activated, B naive, NK, MAIT, Treg cells, CD16+ monocytes and pDCs. Participant 001-012, who maintained viral control for the shortest period after bnAb treatment, was shown to have very moderate cell proportion changes across different clusters, in comparison to other participants. The steepest decrease was observed in Tregs and it was unique for 001-012 as well as in macrophages and CD14+ monocytes, which was in line with the changes seen in 002-005 (Figure 7.6A). Single-cell T cell receptor profiling data, which was performed in parallel with gene expression analysis, showed HIV specific-TCR clone expansion in 005-001 and 003-003, whereas this was not confirmed for the other 4 participants (Figure 7.6B). This TCR clone expansion is an indicator of a functional adaptive immune response and could suggest a vaccinal effect. I hypothesised that these two participants may be examples of long-term viral control mediated through the vaccinal effect and to investigate potential signatures, I conducted differential gene expression analysis on samples from these two individuals, before and after bnAb treatment. I focused this analysis at cell types known to play a pivotal role in the generation of the vaccinal effect.

7. *An exploratory study of the impact of bnAbs on the host immune response*

A.

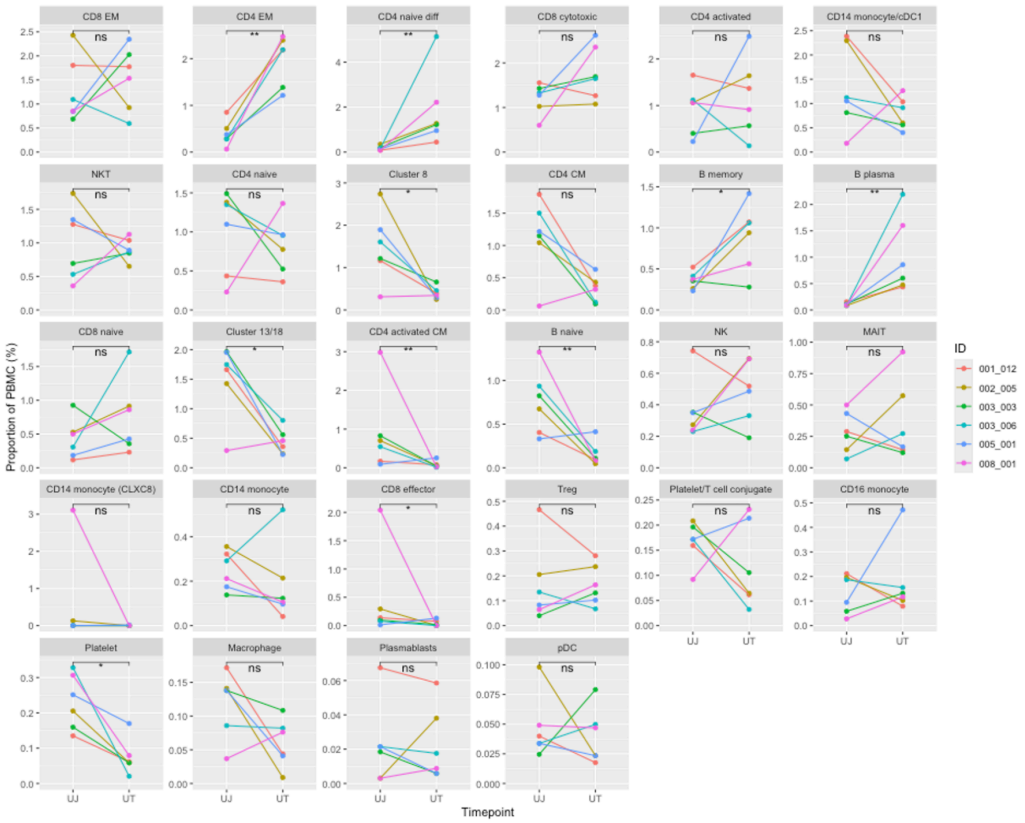

B.

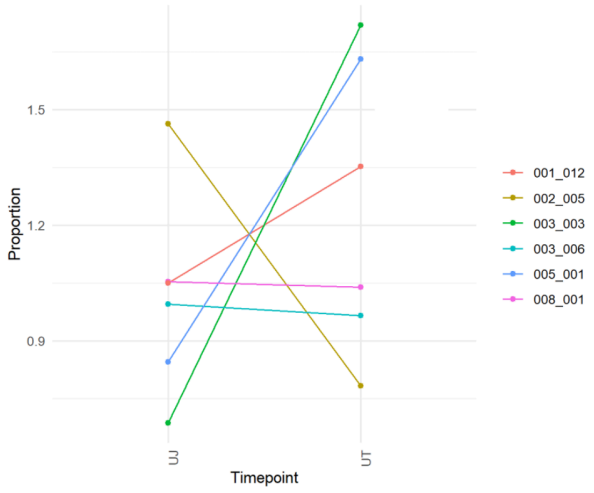

Figure 7.6: Individual participant analysis. A. Cell frequencies at each timepoint for every individual participant, marked in different colours. Statistical significance of the changes in each panel is noted as ns: non significant, *: <0.05, **<0.01. B. Proportion of HIV-specfic TCRs in all TCRs at UJ and UT. TCRs selected here were those for which a 90% identity match was found in the VDJ DB database.

7. ***An exploratory study of the impact of bnAbs on the host immune response***

The analysis revealed a greater number of differentially expressed genes in participant 005-001 compared to 003-003, suggesting distinct immune responses to bnAbs despite the shared trend of HIV-specific TCR clone expansion. In participant 005-001, HLA-C and CXCR4 were consistently upregulated across multiple clusters (Figure A.1A). HLA-C is a class I MHC molecule that presents antigens to cytotoxic T cells and has been associated with NK cell regulation (Vollmers et al., 2021). Its upregulation could suggest increased immune activation and a potential attempt to control the virus at UT compared to UJ. CXCR4 is one of the two co-receptors that allow HIV to latch and enter a host cell. This was trend was not observed on 003-003, or any other participant in this subset of the RIO cohort. Conversely, HLA-B and CXCR4 were downregulated at UT in several clusters in participant 003-003. DGE on CD14+ monocytes from participant 003-003 showed upregulation of CD52, a marker which has been associated with T-cell activation suppression (Rashidi et al., 2018) (Figure A.1A). Additionally, TNFRSF18, a T cell activation marker, was downregulated in CD8+ cytotoxic and B memory cells from participant 003-003 at UT compared to UJ.

GSEA analysis identified distinct pathway enrichments between the two participants (Figure A.1B). Specifically, TNFa signaling was enriched in UT clusters for 005-001, while in 003-001, it was more prevalent in baseline clusters. Although response to interferon pathways were enriched in both participants at UJ, more clusters showed enrichment in 005-001 compared to 003-003. Lastly, the apoptosis pathway was enriched in CD14+ monocytes and macrophages sampled from participant 005-001 at UT vs UJ while the pathway was not among the top10 pathways for participant 003-001.

7.4 Discussion

The aim of this study was to identify the effect of bnAbs on the immune landscape of individuals who receive bnAb treatment, if any. To map the alterations in perturbations and transcriptomic signatures at a high resolution, single-cell RNA

seq PBMC data was used, and no prior selection was performed. The selection of participants to be included in this study was made on the basis of time of viral control >12 weeks post-bnAb dose and the availability of clinical data. Seven participants were undetectable at baseline (UJ timepoint), as they were still on ART and at UT timepoint, 12 weeks after ART interruption and bnAb dose. One participant experienced low viral blips since ART interruption and throughout the duration of follow-up until viral rebound and therefore a viral load of 57 copies/ml was measured at UT. Out of 8 participants initially planned to be included, sequencing data were only available for 6. Samples from two timepoints were used to compare the transcriptomic signatures before and after treatment but also to be used as a control for intra-participant heterogeneity.

The annotation of the single-cell gene expression dataset cluster was based on canonical markers but some clusters, such as Cluster 8 and Cluster 13/18 were not annotated, due to lack of distinguishing canonical markers. Notably, the expression of SERINC5, an anti-HIV host factor, as well as BACH2, a preferred target for HIV integration, in cluster 8 may suggest that these are dysfunctional HIV infected cells. This may suggest that this cluster is A proportion of cluster 8 cells expressed CD56 and CD16 and therefore its is likely that they are a subset of NK cells. Lastly, a cluster which expressed both platelet and T cell markers was annotated as "Platelet/ T cell conjugates". In the context of HIV infection, these may be a cause of inflammation (Dai et al., 2021).

A comprehensive analysis of cell proportions and gene expression revealed notable changes in the composition of cells in bnAb-treated participants between UJ and UT. A general increase in the frequency of activated and differentiated immune cells in parallel with the decrease of naive and uncharacterised clusters (such as Cluster 8 and Cluster 13/18) was observed at UT vs UJ. Differential gene expression and pathway analysis using both a cluster-agnostic and cluster-specific approach showed enrichment of genes and pathways associated with cellular metabolism requirements and cellular stress at UT compared to UJ. This may be due to antigen-induced stress on immune cells following ART interruption, although

viremia is controlled by bnAbs and viral load remains clinically undetectable. On the other end, inflammation pathways were enriched at UJ vs UT. This confirms that immune activation and inflammation may persist in PWH despite ART (Zicari et al., 2019) and may suggest that bnAbs induce less inflammation responses compared to ART. Contrary to the findings presented in Chapter 5 (Section 6.3.5), response to interferon type I was enriched at UJ compared to UT. This indicates that the mechanism of bnAb-mediated control is different to that of PTC. However, contrary to the SPARTAC cohort, participants analysed here were all male and non-C subtype.

Despite the individual variability in clinical responses and cell type alterations between the bnAb-naive and bnAb-treated groups at UJ and UT respectively, the detection of HIV-specific TCR clones in participants 005-001 and 003-003 suggests a potential vaccinal effect. The DGE and pathway analysis however did not reveal any shared signatures. Interestingly, participant 005-001 exhibited a unique pattern of gene expression, with upregulation of CXCR4 and HLA-C across multiple clusters in the UT sample. This was not observed in any other participant.Contrary to the general trend observed in the UT versus UJ samples, 005-001 showed enrichment of inflammatory response and TNFa signaling pathways at UT compared to UJ. This might indicate increased inflammation and immune activation at UT, contrasting with the findings in 003-001 and the overall group analysis. Against our expectations based on the mechanism of bnAb-induced viral control (Naranjo-Gomez & Pelegrin, 2019; Tipoe et al., 2022), the DGE and pathway analysis did not reveal significant evidence of enhanced immune activation at UT compared to UJ. This could be attributed to a loss of signal due to pooling PBMCs and a focus on non-HIV-specific immune cells as well as that 12 weeks post-bnAb dosing might be too early for responses of high magnitude to be detectable. The heterogeneity of participant responses and immune cell profiles limited the statistical power of the analysis. Additionally, the lack of healthy control samples hindered our ability to draw more definitive conclusions.

7. ***An exploratory study of the impact of bnAbs on the host immune response***

Further investigations are warranted to delve deeper into the data. Techniques such as weighted gene co-expression network analysis (WGCNA) and RNA trajectory analysis could provide valuable insights into the underlying biological processes and dynamic changes occurring in these samples. By incorporating these additional analyses, we can potentially uncover more subtle and complex patterns within the data, leading to a more comprehensive understanding of the immune responses and vaccinal effect in HIV infection.

8
Discussion

The aim of this thesis was to explore the complex interplay between HIV and the host immune response, focusing on the genomic and transcriptomic factors associated with viral control following anti-HIV treatment in PHI. A large part of my research was focused on bnAb treatment, in particular with 10-1074-LS and 3BNC117-LS, which were used in the RIO trial. In this context, I presented findings on the prevalence and evolution of bnAb resistance-associated mutations in key populations of PLH, the impact of predicted sensitivity on bnAb treatment efficacy, the transcriptomic signatures of post-ART control and the effect of bnAb treatment on immune cell transcriptomes.

bnAbs offer a promising alternative to traditional ART for HIV infection. Unlike ART, which targets viral replication, bnAbs directly neutralise virions, augment immunity and may target infected cells. Nevertheless, there are concerns about the potential for clinical bnAb resistance to develop over time, particularly when resistant viral variants are present before treatment. To mitigate this risk, models predicting bnAb resistance prior to treatment with bnAbs have been developed in the past few years, utilising bnAb neutralisation data from experimental assays and paired Env sequences. However, due to limited training datasets, especially for bnAbs with high neutralisation breadth, the accuracy of these predictions

has not been extensively validated on a large scale. In this thesis, the Rockefeller model was used to predict bnAb sensitivity by examining the envelope sequence for specificndefined mutations associated with bnAb resistance. Although the outcome of this model is binary (either resistant or sensitive), which does not fully capture the spectrum of viral sensitivity to bnAbs, it is easily interpreted. Moreover, for 10-1074, the critical residues identified by the model to confer bnAb resistance have been validated in the laboratory.

The analysis of clade B HIV Env sequences samples longitudinally throughout the pandemic showed an increase in the prevalence of mutations associated with bnAb resistance, which may be a result of the virus adapting to humoral responses targeting similar epitopes on a population level. This trend has important implications for the efficacy of bnAbs as treatment or prevention in specific populations and underscores the need for screening bnAb sensitivity prior to administration. Like in HIV, similar surveillance is needed for viruses, such as hepatitis C and B, for which bnAbs are considered as treatments or for novel vaccine designs (Colbert et al., 2019; Hehle et al., 2020; Skinner & Bailey, 2020; Q. Wang et al., 2020), to assess whether selective pressures from immune responses, treatment, or passive immunotherapy drive viral escape at a population level. Insights from other viruses reinforce the need for such monitoring; in SARS-CoV-2, variants such as Omicron have accumulated mutations that significantly reduce nAb effectiveness, requiring updates to monoclonal antibody treatments and vaccines (Cameroni et al., 2022). Likewise, influenza undergoes continuous antigenic drift, leading to decreased neutralisation by existing antibodies and necessitating yearly vaccine reformulations (Petrova & Russell, 2018).

bnAb sensitivity analysis showed that approximately 28% of people who started ART at PHI in the HEATHER cohort had pre-existing 10-1074 resistance-associated mutations whereas approximately 15% of people in the same cohort had 3BNC117 resistance-associated mutations. The highest resistance-associated mutation rate was found in individuals with CRF01-AE for 10-1074 and in those with F1 clade for 3BNC117. Among individuals with clade B HIV, who were the majority in

this cohort, 74.3% were predicted as fully sensitive to 10-1074 and 84.4% were predicted as fully sensitive to 3BNC117. Notably, individuals with ART adherence issues and non-B clade HIV in the BONDY cohort exhibited higher rates of 10-1074 resistance (62.2% of all participants in the cohort). Although there are doubts about the efficiency of bnAb sensitivity prediction algorithms, the increasing bnAb resistance in the population level and the prevalence of resistance in the UK key populations living with HIV reinforce the arguments for bnAb sensitivity screening prior to bnAb treatment, especially in those with non-B clade HIV or those who struggle with ART adherence.

Tracking the origin of bnAb resistance-associated mutations in bnAb-naive PLH is crucial for informing effective treatment strategies. Our findings suggest that these mutations often arise in the later stages of infection and can persist over time, aligning with the timeline of neutralising antibody development. This implies that individuals with chronic HIV may have a higher prevalence of pre-existing resistance, underscoring the importance of bnAb sensitivity screening before treatment. To confirm these findings and to identify genetic signatures predicting the emergence of bnAb resistance-associated mutations, it is essential to study longitudinal samples from a larger, untreated cohort, including transmission pairs. Furthermore, the findings in this thesis suggest that proviral Env sequences are valuable for assessing bnAb sensitivity, particularly in early-stage infection.

RIO is currently the largest clinical trial testing the efficacy of 10-1074 and 3BNC117 in participants with PHI and bnAb sensitive reservoirs. Individual proviral Env sequences obtained using SGA from candidates with PHI were screened for 10-1074 sensitivity, using the Rockefeller sensitivity prediction model. Only those with screening samples classified as 10-1074 sensitive, ranging from fully sensitive to low frequency resistance-associated mutations or non-amplifiable sequences, were recruited in the trial. While 3BNC117 resistance was also predicted at baseline, it was not factored into bnAb sensitivity eligibility criteria for trial recruitment, due to low reliability. Participants were randomised in two trial arms, where they would be offered either bnAbs (Arm A) or placebo (Arm B) as they stopped ART.

Arm B participants who rebounded were offered to proceed to stage 2, where they were given bnAbs with 6 months of ART, in order to investigate the potential for post-bnAb control beyond therapeutic levels, and following dosing during viremia. Although RIO was not designed to assess the impact of bnAb resistance on the clinical outcome, we had the unique opportunity to assess how participants with reservoirs predicted as sensitive did after bnAb treatment. We found that these participants had a median time of viral suppression of 26 weeks post TI compared to the control group who rebounded a median of 4 weeks post TI, without any intervention. Furthermore, I reported that out of all Arm A participants who were predicted as fully sensitive at baseline, 91% rebounded more than 8 weeks after TI and 69% rebounded after the concentration of bnAbs fell in the blood below 50 ug/ml, a threshold that we set to define resistance based on clinical outcome. Conversely, one participant with baseline resistance to 10-1074 and two to 3BNC117 rebounded in a similar time frame as individuals who underwent TI at Arm B stage 1 and received no other intervention. Additionally, two in three rebounded before 8 weeks post-TI and all rebounded before they reached the 50 ug/ml bnAb concentration threshold. While these results indicate the prediction model effectively identified resistant individuals, more data (full-length HIV sequences and neutralisation assay data) are needed to improve model accuracy and better predict *in vivo* outcomes. Furthermore, analyzing proviral sequences in longitudinal samples from RIO participants who remain undetectable in the absence of ART, could reveal changes, particularly in bnAb epitopes, indicative of residual viral replication and selection pressure. This approach may help define the therapeutic concentration threshold of bnAbs.

To determine the role of the host immune response in maintaining viral control following treatment, I studied the gene expression patterns of host immune cells of participants who received ART and participants who received bnAbs, as part of two separate projects. First, I used bulk RNA sequencing to profile CD4+ cells from a subset of female participants in SPARTAC, who received ART for 48 weeks at PHI and subsequently underwent ATI. I compared the gene expression profiles

of participants who rebounded early vs PTC, as defined by their clinical data. Both supervised (GSEA on DGE) and unsupervised (WGCNA) analyses showed that Interferon Type I pathways were enriched in the PTC samples at the time of TI, compared to individuals who rebounded early. Additionally, a gene signature consisting of four genes (ISG15, XAF1, TRIM25, and USP18) was identified as predictive of viral rebound. While these findings provide valuable insights into the mechanisms underlying post-TI viral control, further work is needed to validate them in larger, more inclusive cohorts, to investigate the transcriptomic profile of other immune cells, and to confirm their biological relevance in the laboratory, using functional assays.

Sex-based differences in immune responses, both generally and in HIV infection, are well documented and may influence the development and function of antibodies, and consequently, the intra-host evolution of the virus (S. L. Klein & Flanagan, 2016; Scully, 2018). Although so far there exist no robust evidence that escape mutation patterns differ by sex, the potential impact of sex hormones and immunological profiles on bnAb responses requires further investigation, particularly in the context of bnAb immunotherapy. A key limitation in examining the prevalence and evolution of bnAb resistance-associated mutations in this thesis was the limited availability of samples from female participants. This reflects a broader issue in the field, as most HIV research cohorts include predominantly male participants, especially in high-income countries (Curno et al., 2016; Johnston et al., 2023). Addressing this issue requires the implementation of more inclusive study designs and improved support infrastructure, such as access to contraceptive options, flexible visit scheduling, and tailored educational materials. Moreover, mandating and funding research that includes participants of all sexes and genders should be a priority to ensure equal representation and more widely applicable findings.

Given the novelty of bnAb treatment, the precise mechanisms through which the host immune response is modulated following administration are not yet clear. To gain a deeper understanding of the cellular and molecular changes induced within the host by bnAbs, I conducted an exploratory study using single-cell

RNA sequencing to profile the entire repertoire of immune cells in the blood following bnAb treatment. I used samples from selected participants in Arm A, taken at baseline and 12 weeks after bnAb dosing. Indeed, bnAbs induce changes in the composition of immune cells, such as an increase in activated and differentiated immune cells and a decrease in naive cell populations. Additionally, pathways associated with cellular stress and metabolism were enriched at the post-bnAb treatment timepoint, indicating the metabolic demands of immune activation. However, the study was limited by the small sample size and the heterogeneity of responses among participants. Moving forward, we plan to include more samples from RIO participants as well as from healthy donors in the existing datasets in order to enhance the robustness and accuracy of our findings and better capture the variability in immune responses post-bnAb treatment. In addition I will perform unsupervised analysis, such as WGCNA, to correlate immune responses with clinical outcomes without having to group them using arbitrary criteria.

In summary, this thesis contributes to a body of knowledge on bnAb resistance, the predictive value of proviral Env sequences, and the host immune factors associated with post-treatment viral control. By integrating genomic, transcriptomic, and clinical data, this work highlights the importance of bnAb sensitivity screening, the need for improved predictive models, and the role of immune activation in maintaining viral suppression. While bnAbs hold great promise as a cure for HIV, further research is essential to optimise strategies on their use, mitigate resistance, and better understand the interplay between host and virus, which shapes the long-term control of HIV.

Appendices

A Appendix

A.1 Chapter 4

Table A.1: Demographics of the MACS participants. Resistance to bnAbs and mutations are presented as proportion of sequences in each time point

						HXB2 sites of bnAb resistance associated mutations										
ID	Months post-Sero-conversion	No Sequences	Resistance to 10-1074	Resistance to 3BN117	Viral Load (log)	334	456	332	279	330	325, 332	330, 334	279, 334	279, 332	332, 334	456, 457
2	5	11	0.00	0.00	4.84	0.00	0.00	0.00	0.00	0.00	0.00	0.0	0.00	0.0	0.00	0.00
	20	12	0.00	0.00	4.65	0.00	0.00	0.00	0.00	0.00	0.00	0.0	0.00	0.0	0.00	0.00
	30	9	0.11	0.00	3.78	0.11	0.00	0.00	0.00	0.00	0.00	0.0	0.00	0.0	0.00	0.00
	51	12	0.00	0.00	5.34	0.00	0.00	0.00	0.00	0.00	0.00	0.0	0.00	0.0	0.00	0.00
	61	11	0.00	0.00	4.67	0.00	0.00	0.00	0.00	0.00	0.00	0.0	0.00	0.0	0.00	0.00
	73	10	0.00	0.00	4.69	0.00	0.00	0.00	0.00	0.00	0.00	0.0	0.00	0.0	0.00	0.00
	85	12	0.00	0.67	5.54	0.00	0.58	0.00	0.00	0.00	0.00	0.0	0.00	0.0	0.00	0.08
	103	11	0.00	1.00	4.92	0.00	1.00	0.00	0.00	0.00	0.00	0.0	0.00	0.0	0.00	0.00
	126	11	0.00	1.00	5.21	0.00	1.00	0.00	0.00	0.00	0.00	0.0	0.00	0.0	0.00	0.00
	4	20	0.00	0.00	5.06	0.00	0.00	0.00	0.00	0.00	0.00	0.0	0.00	0.0	0.00	0.00
	9	16	0.00	0.00	4.76	0.00	0.00	0.00	0.00	0.00	0.00	0.0	0.00	0.0	0.00	0.00
	15	13	0.00	0.00	4.77	0.00	0.00	0.00	0.00	0.00	0.00	0.0	0.00	0.0	0.00	0.00
	21	21	0.00	0.00	4.57	0.00	0.00	0.00	0.00	0.00	0.00	0.0	0.00	0.0	0.00	0.00
	27	15	0.00	0.00	4.21	0.00	0.00	0.00	0.00	0.00	0.00	0.0	0.00	0.0	0.00	0.00
	33	16	0.12	0.00	3.57	0.00	0.00	0.12	0.00	0.00	0.00	0.0	0.00	0.0	0.00	0.00
	38	15	0.40	0.00	4.86	0.00	0.00	0.40	0.00	0.00	0.00	0.0	0.00	0.0	0.00	0.00
	42	24	0.08	0.00	2.00	0.04	0.00	0.04	0.00	0.00	0.00	0.0	0.00	0.0	0.00	0.00
	48	17	0.47	0.00	4.96	0.06	0.00	0.35	0.00	0.06	0.00	0.0	0.00	0.0	0.00	0.00
	53	13	0.85	0.00	4.79	0.00	0.00	0.85	0.00	0.00	0.00	0.0	0.00	0.0	0.00	0.00

4	59	19	0.68	0.00	3.67	0.00	0.00	0.53	0.00	0.00	0.16	0.0	0.00	0.0	0.00	0.00
	65	13	0.00	0.00	5.32	0.00	0.00	0.00	0.00	0.00	0.00	0.0	0.00	0.0	0.00	0.00
	71	16	0.31	0.00	5.40	0.00	0.00	0.12	0.00	0.06	0.12	0.0	0.00	0.0	0.00	0.00
	76	14	0.07	0.00	5.11	0.00	0.00	0.07	0.00	0.00	0.00	0.0	0.00	0.0	0.00	0.00
	89	18	0.00	0.00	5.37	0.00	0.00	0.00	0.00	0.00	0.00	0.0	0.00	0.0	0.00	0.00
7	2	9	0.00	0.00	3.80	0.00	0.00	0.00	0.00	0.00	0.00	0.0	0.00	0.0	0.00	0.00
	44	12	0.17	0.00	4.34	0.17	0.00	0.00	0.00	0.00	0.00	0.0	0.00	0.0	0.00	0.00
	80	10	0.10	0.00	4.88	0.10	0.00	0.00	0.00	0.00	0.00	0.0	0.00	0.0	0.00	0.00
8	17	10	0.00	0.00	4.18	0.00	0.00	0.00	0.00	0.00	0.00	0.0	0.00	0.0	0.00	0.00
	41	11	0.18	0.00	4.54	0.09	0.00	0.09	0.00	0.00	0.00	0.0	0.00	0.0	0.00	0.00
	65	10	0.00	0.00	5.06	0.00	0.00	0.00	0.00	0.00	0.00	0.0	0.00	0.0	0.00	0.00
	14	2	0.00	0.00	2.09	0.00	0.00	0.00	0.00	0.00	0.00	0.0	0.00	0.0	0.00	0.00
	20	4	0.00	0.00	2.48	0.00	0.00	0.00	0.00	0.00	0.00	0.0	0.00	0.0	0.00	0.00
	26	11	0.00	0.00	2.90	0.00	0.00	0.00	0.00	0.00	0.00	0.0	0.00	0.0	0.00	0.00
	32	10	0.00	0.00	2.76	0.00	0.00	0.00	0.00	0.00	0.00	0.0	0.00	0.0	0.00	0.00
	38	5	0.00	0.00	3.00	0.00	0.00	0.00	0.00	0.00	0.00	0.0	0.00	0.0	0.00	0.00
	44	7	0.00	0.00	3.50	0.00	0.00	0.00	0.00	0.00	0.00	0.0	0.00	0.0	0.00	0.00
	50	9	0.00	0.00	3.60	0.00	0.00	0.00	0.00	0.00	0.00	0.0	0.00	0.0	0.00	0.00
	54	5	0.00	0.00	3.70	0.00	0.00	0.00	0.00	0.00	0.00	0.0	0.00	0.0	0.00	0.00
	62	12	0.00	0.00	3.80	0.00	0.00	0.00	0.00	0.00	0.00	0.0	0.00	0.0	0.00	0.00
	67	10	0.50	0.00	3.90	0.40	0.00	0.00	0.00	0.00	0.00	0.1	0.00	0.0	0.00	0.00
	74	17	0.65	0.00	4.00	0.59	0.00	0.06	0.00	0.00	0.00	0.0	0.00	0.0	0.00	0.00
	80	15	0.73	0.00	4.10	0.73	0.00	0.00	0.00	0.00	0.00	0.0	0.00	0.0	0.00	0.00
	86	5	0.80	0.20	4.04	0.60	0.00	0.00	0.00	0.00	0.00	0.0	0.00	0.2	0.00	0.00
	92	14	1.00	0.07	3.80	0.64	0.00	0.29	0.00	0.00	0.00	0.0	0.07	0.0	0.00	0.00
	98	10	0.60	0.00	3.60	0.60	0.00	0.00	0.00	0.00	0.00	0.0	0.00	0.0	0.00	0.00

10	105	4	0.50	0.00	3.50	0.50	0.00	0.00	0.00	0.00	0.00	0.0	0.00	0.0	0.00	0.00
	110	6	0.33	0.00	3.40	0.00	0.00	0.00	0.00	0.00	0.00	0.0	0.00	0.0	0.33	0.00
	117	14	0.21	0.00	3.20	0.14	0.00	0.00	0.00	0.00	0.00	0.0	0.00	0.0	0.07	0.00
	134	12	0.00	0.00	3.00	0.00	0.00	0.00	0.00	0.00	0.00	0.0	0.00	0.0	0.00	0.00
	140	6	0.00	0.00	2.90	0.00	0.00	0.00	0.00	0.00	0.00	0.0	0.00	0.0	0.00	0.00
	147	8	0.00	0.00	2.88	0.00	0.00	0.00	0.00	0.00	0.00	0.0	0.00	0.0	0.00	0.00
	154	9	0.00	0.00	2.64	0.00	0.00	0.00	0.00	0.00	0.00	0.0	0.00	0.0	0.00	0.00
	158	7	0.00	0.00	2.75	0.00	0.00	0.00	0.00	0.00	0.00	0.0	0.00	0.0	0.00	0.00
	-3	6	0.00	0.00	5.31	0.00	0.00	0.00	0.00	0.00	0.00	0.0	0.00	0.0	0.00	0.00
	3	8	0.00	0.00	4.73	0.00	0.00	0.00	0.00	0.00	0.00	0.0	0.00	0.0	0.00	0.00
	29	8	0.00	0.00	2.87	0.00	0.00	0.00	0.00	0.00	0.00	0.0	0.00	0.0	0.00	0.00
	42	6	0.00	0.17	2.69	0.00	0.00	0.00	0.17	0.00	0.00	0.0	0.00	0.0	0.00	0.00
11	58	10	0.00	0.00	2.67	0.00	0.00	0.00	0.00	0.00	0.00	0.0	0.00	0.0	0.00	0.00
	70	7	0.14	0.00	3.25	0.14	0.00	0.00	0.00	0.00	0.00	0.0	0.00	0.0	0.00	0.00
	100	7	0.71	0.00	2.00	0.43	0.00	0.00	0.00	0.00	0.00	0.0	0.00	0.0	0.29	0.00

A.2 Chapter 5

Table A.2: RIO Arm B Demographics.

		Sensitivity			Time to Rebound (weeks)		bnAb concentration at rebound		bnAb concentration at 2nd TI		
ID	VL at dosing	Baseline	Rebound	No of Doses	Stage 1	Stage 2	10-1074	3BNC117	10-1074.	3BNC117.	Elispot Gag response (2nd TI)
005-004	20	Sensitive	NA	2	2	4	28.8	31.1	33.8	37.0	265.0
001-009	162	10-1074	10-1074	2	2	3	36.0	35.0	36.3	39.7	660.0
001-002	497	Sensitive	10-1074	1	2	5	29.0	35.4	33.7	45.7	40.0
001-019	663	Sensitive	10-1074	2	2	7	29.3	28.7	42.2	43.5	35.0
006-010	20500	Sensitive	Sensitive	1	2	4	41.1	38.4	49.8	51.2	1190.0
001-017	58	Minor 10-1074	10-1074	2	3	3	36.6	37.5	42.2	43.5	200.0
003-018	86	Sensitive	Not rebounded	2	3	5	NA	NA	41.7	53.0	NA
005-006	126	Sensitive	NA	2	3	8	26.9	20.3	64.0	67.7	380.0
001-013	2070	Sensitive	on ART	2	3	NA	NA	NA	42.0	39.7	367.5
001-020	32800	Minor 3BNC117	NA	2	3	4	49.3	41.4	58.7	54.3	1800.0
003-001	31	Minor 10-1074	10-1074	1	4	119	NA	NA	55.2	63.3	180.0
003-004	40	Sensitive	10-1074	2	4	26	16.8	11.6	56.6	65.1	52.5
002-001	168	Sensitive	Sensitive	1	4	9	27.6	43.2	39.7	62.5	345.5
001-003	196	Sensitive	10-1074	1	4	28	10.8	9.9	28.0	35.4	435.0
007-007	515	Sensitive	Sensitive	2	4	4	25.7	33.3	29.3	28.1	1002.5
002-004	225	Sensitive	NA	2	5	5	12.9	6.9	12.5	9.0	207.5
008-004	20	Sensitive	on ART	1	6	NA	NA	NA	36.2	38.7	NA
007-012	41	3BNC117	Not rebounded	2	6	13	34.1	30.8	36.2	38.7	NA
008-012	46	Sensitive	Not rebounded	2	6	17	NA	NA	79.7	91.1	NA
003-016	87	Sensitive	on ART	2	6	NA	NA	NA	39.5	45.5	0.0
001-027	126	Minor 3BNC117	Not rebounded	2	6	8	NA	NA	58.2	70.7	95.0
008-014	233	Sensitive	Not rebounded	2	6	8	NA	NA	20.5	22.2	120.0
007-003	30	Sensitive	Sensitive	2	8	27	10.1	10.1	48.8	71.1	177.5
008-010	30	Sensitive	Not rebounded	2	8	31	NA	NA	29.6	31.1	NA

Table A.3: Arm A Participants predicted as sensitive at baseline and resistant based on outcome.

	Sensitivity (Rockefeller Algorithm)			bnAb concentration=50 ug/ml (Week post last dose)				bnAb-ReP Neutralisation prediction at baseline (range)		Median IC80 at baseline (ug/ml)	
ID	Baseline	Rebound	Time to Rebound	10-1074 (ug/ml)	3BNC117 (ug/ml)	Resistance (TTR)	Resistance(PK)	10-1074	3BNC117	10-1078 concentar-tion	3BNC117 concentration
001-021	Sensitive	Minor 3BNC117	7	21	20	Yes	Yes	0.9 (0.88-0.93)	0.98 (0.53-0.98)	27.6	0.57
001-032	NA	NA	12	19	19	No	Yes	NA	NA	NA	NA
003-009	Sensitive	Sensitive	11	20	20	No	Yes	0.86 (0.86)	0.84 (0.84)	NA	NA
004-003	Sensitive	NA	12	17	19	No	Yes	0.82 (0.82)	0.46 (0.46)	NA	NA
006-003	Sensitive	10-1074	17	24	24	No	Yes	0.96 (0.96)	0.94 (0.94)	NA	NA
007-001	Sensitive	10-1074	18	22	24	No	Yes	0.93 (0.93)	0.97 (0.97)	NA	NA
007-014	Minor 3BNC117	NA	14	21	22	No	Yes	0.94 (0.91-0.94)	0.83 (0.37-0.97)	NA	NA
007-016	Sensitive	NA	7	NA	NA	Yes	NA	0.93 (0.92-0.94)	0.5 (0.42-0.94)	NA	NA

Table A.4: Average variable and hypervariable loop 1-5 length and number of PNGs in the same Env regions.

ID	Timepoint	Mutations	V1	HV1	V2	HV2	V1V2	HV1V2	V3	V4	HV4	V5	HV5	V1_PNG	HV1_PNG	V2_PNG	HV2_PNG	V1V2_PNG	HV1V2_PNG	V3_PNG	V4_PNG	HV4_PNG	V5_PNG	HV5_PNG
001-002	Baseline	Sensitive	25.0	17.0	42	7.0	65.0	24.0	37	38.7	18.7	11	5	5.0	3.0	2	1	7.0	4.0	2	5.7	2.8	1.0	1.0
NA	Post-Treatment	S/T334G	25.0	17.0	42	7.0	65.0	24.0	37	38.7	18.7	11	5	5.0	3.0	2	1	7.0	4.0	2	5.7	2.8	1.0	1.0
001-003	Baseline	Sensitive	32.0	24.0	41	6.0	71.0	30.0	37	37.0	21.0	14	8	5.0	3.0	2	1	7.0	4.0	1	3.0	6.0	3.0	2.0
NA	Post-Treatment	S/T334N (+H/Y330L)	30.2	22.2	41	6.1	69.2	28.2	37	33.3	15.6	14	8	4.1	2.1	2	1	6.1	3.1	1	5.2	2.8	2.0	2.0
001-010	Baseline	Sensitive	29.0	21.0	41	6.0	68.0	27.0	37	32.0	15.7	12	6	4.0	2.0	2	1	6.0	3.0	2	3.2	4.8	2.9	1.9
NA	Post-Treatment	S/T334N	29.0	21.0	41	6.0	68.0	27.0	37	31.7	12.4	12	6	4.0	2.0	2	1	6.0	3.0	2	5.0	2.0	2.0	1.0
007-001	Baseline	Sensitive	34.0	26.0	44	9.0	76.0	35.0	37	27.0	9.9	13	7	4.0	3.0	2	1	6.0	4.0	1	2.1	2.9	2.1	2.9
NA	Post-Treatment	N332K or S/T334N	34.0	26.0	44	9.0	76.0	35.0	37	27.0	8.0	13	7	4.0	3.0	2	1	6.0	4.0	1	3.0	1.0	3.0	2.0
001-018	Baseline	Sensitive	33.4	25.4	39	4.0	70.4	29.4	37	35.0	17.9	15	9	4.7	2.7	2	1	6.7	3.7	1	5.0	2.0	2.0	1.0
NA	Post-Treatment	S/T334R	35.0	27.0	39	4.0	72.0	31.0	37	35.0	18.0	15	9	5.0	3.0	2	1	7.0	4.0	1	5.0	2.0	2.0	1.0
006-003	Baseline	Sensitive	30.0	22.0	41	6.0	69.0	28.0	37	29.0	8.0	13	7	3.9	2.0	2	1	5.9	3.0	2	4.0	1.0	2.0	2.0
NA	Post-Treatment	N332D/S	30.0	22.0	41	6.0	69.0	28.0	37	29.0	8.0	13	7	4.0	2.0	2	1	6.0	3.0	2	4.0	1.0	2.0	2.0

A.3 Chapter 6

A.4 Chapter 7

Table A.5: Participant demographics. Number of participants stratified by clinical rebound timing. Numbers of participants analysed by age, country of origin, viral clade, Time to Rebound (Days), Rebound Phenotype, pre-ART viral load, HLA B Types and Sample Availablity per timpoint.

Characteristic	**Overall** N = 18	**Female** N = 14	**Male** N = 4
Age	27 (23, 35)	25 (22, 31)	35 (31, 41)
Country			
South Africa	12 (67%)	12 (86%)	0 (0%)
UK	4 (22%)	1 (7.1%)	3 (75%)
Italy	1 (5.6%)	0 (0%)	1 (25%)
Uganda	1 (5.6%)	1 (7.1%)	0 (0%)
Viral Clade			
C	14 (78%)	14 (100%)	0 (0%)
A/ B	1 (5.6%)	0 (0%)	1 (25%)
AG/B	1 (5.6%)	0 (0%)	1 (25%)
B	1 (5.6%)	0 (0%)	1 (25%)
D	1 (5.6%)	0 (0%)	1 (25%)
Days to Rebound	173 (28, 503)	173 (29, 542)	103 (26, 240)
Rebound Phenotype			
PTC	11 (61%)	9 (64%)	2 (50%)
ER	7 (39%)	5 (36%)	2 (50%)
Pre-ART Viral Load (log)	4.38 (3.11, 4.82)	4.16 (2.83, 4.78)	4.92 (3.97, 5.35)
HLA B Types			
-	3 (17%)	2 (14%)	1 (25%)
B*15:10, B*58:02	2 (11%)	2 (14%)	0 (0%)
B*15:03, B*42:01	1 (5.6%)	1 (7.1%)	0 (0%)
B*35:01, B*57:03	1 (5.6%)	1 (7.1%)	0 (0%)
B*35:01, B*81:01	1 (5.6%)	1 (7.1%)	0 (0%)
B*41:01, B*42:01	1 (5.6%)	1 (7.1%)	0 (0%)
B*42:02, B*51:01	1 (5.6%)	1 (7.1%)	0 (0%)
B*44:02, B*44:02	1 (5.6%)	0 (0%)	1 (25%)
B*44:02, B*81:01	1 (5.6%)	1 (7.1%)	0 (0%)
B*44:03, B*58:02	1 (5.6%)	1 (7.1%)	0 (0%)
B*45:01, B*51:01	1 (5.6%)	0 (0%)	1 (25%)
B*7:02, B*39:10	1 (5.6%)	1 (7.1%)	0 (0%)
B*8:01, B*13:02	1 (5.6%)	1 (7.1%)	0 (0%)
B*8:01, B*15:03	1 (5.6%)	1 (7.1%)	0 (0%)
B*8:01, B*35:01	1 (5.6%)	0 (0%)	1 (25%)
Samples Available			
Both	11 (61%)	11 (79%)	0 (0%)
Week 48 only	7 (39%)	3 (21%)	4 (100%)

[1] Median (Q1, Q3); n (%)

Table A.6: Participant demographics

			bnAb concentration at rebound (ug/ml)		Sensitivity (Rockefeller)				HLA					
ID	VL at UT (copies/ml)	Time to rebound (weeks after 10 ug/ml)	10-1074	3BNC117	Baseline	Rebound	Time on ART (Years)	Clade	HLAA1	HLAA2	HLAB1	HLAB2	HLAC1	HLAC2
001-012	0	NA	42.46	50.92	NA	NA	6	CRF02-AG	03:01	30:01	08:01	13:02	06:02	07:02
001-018	0	NA	54.61	84.85	Sensitive	10-1074	6	B	02:01	03:01	14:01	39:06	07:02	08:02
002-005	0	PTC	PTC	PTC	PTC	PTC	11	B	02:01	03:01	15:16	18:01	05:01/03	14:02
003-003	0	53	Not rebounded	Not rebounded	Sensitive	Not rebounded	7	B	02:01	32:01	15:01	44:02	03:04	05:01/03
003-006	0	0	11.11	8.38	Sensitive	NA	8	B	02:01	68:01	35:02	51:08	04:01	15:02
005-001	0	6	NA	NA	Sensitive	NA	6	B	02:01	03:01	14:02	37:01	06:02	08:02
007-002	0	PTC	PTC	PTC	PTC	PTC	7	B	24:02	26:01	27:05	35:01	02:02	04:01
008-001	57	14	5.05	2.48	Sensitive	NA	8	B	02:01	02:01	07:02	44:03	07:02	16:01

A.

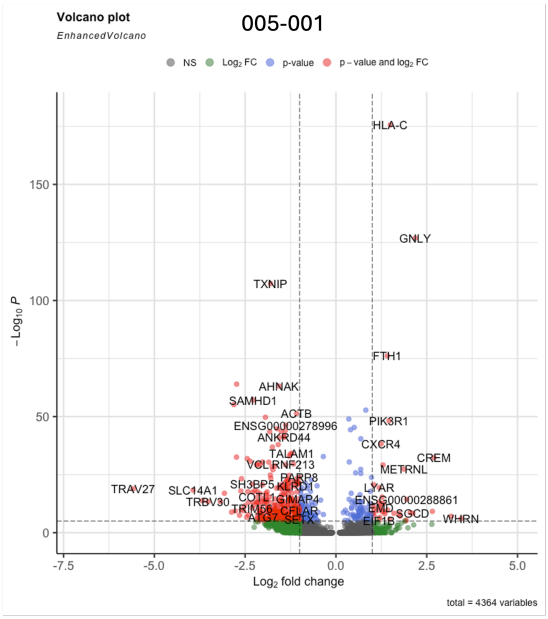

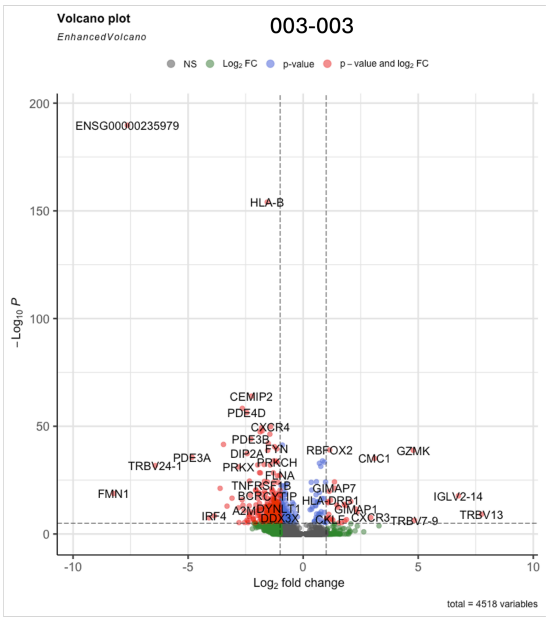

CD8+ EM

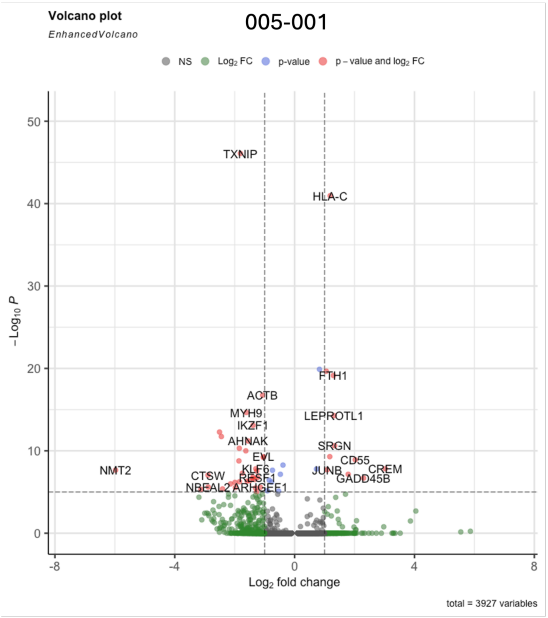

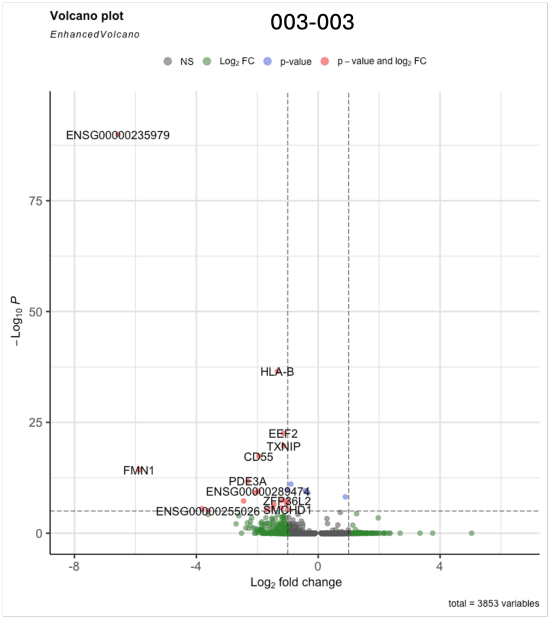

CD4+ EM

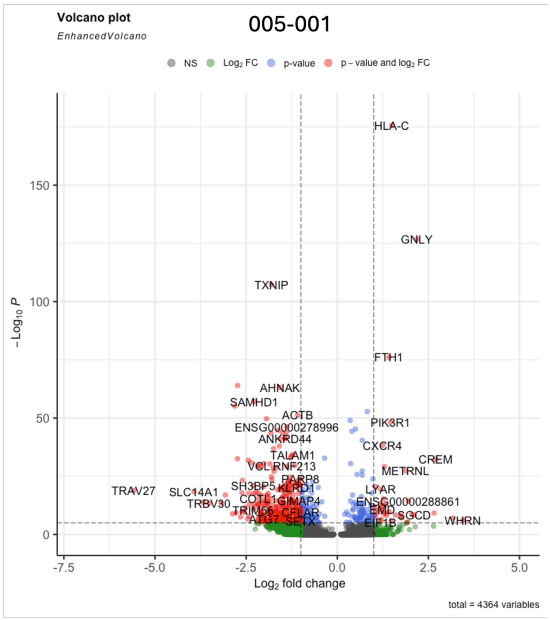

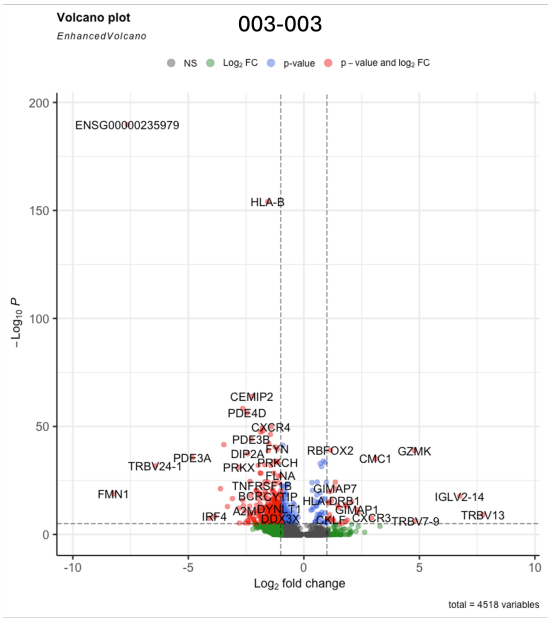

CD8+ cytotoxic

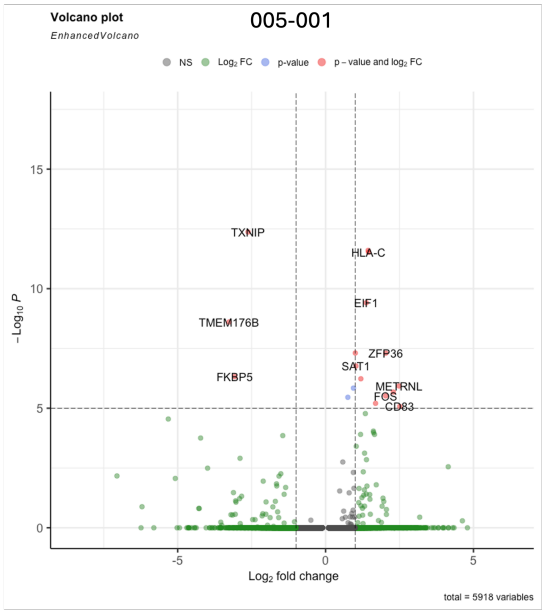

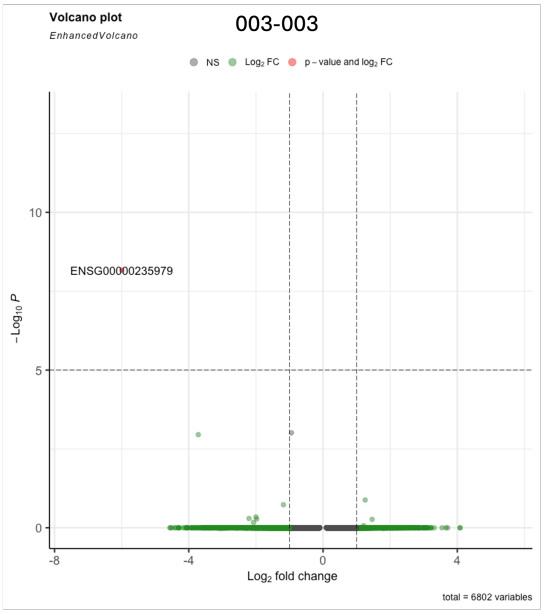

CD16+ monocytes

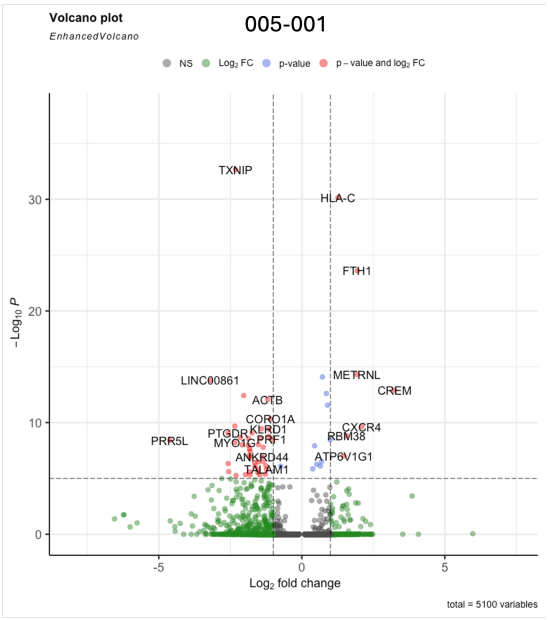

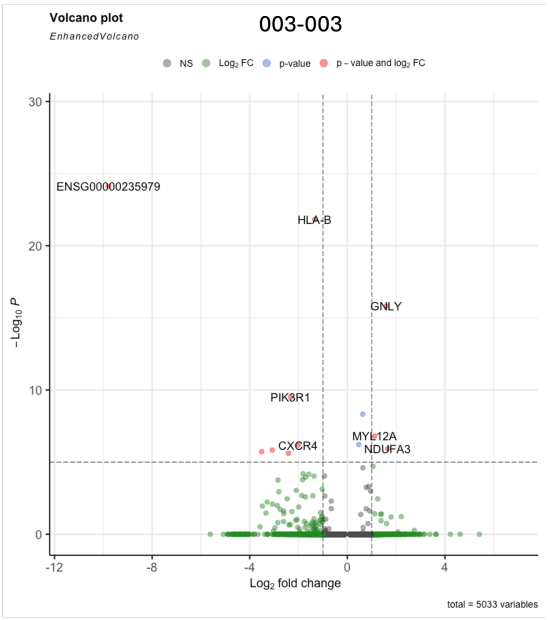

NK cells

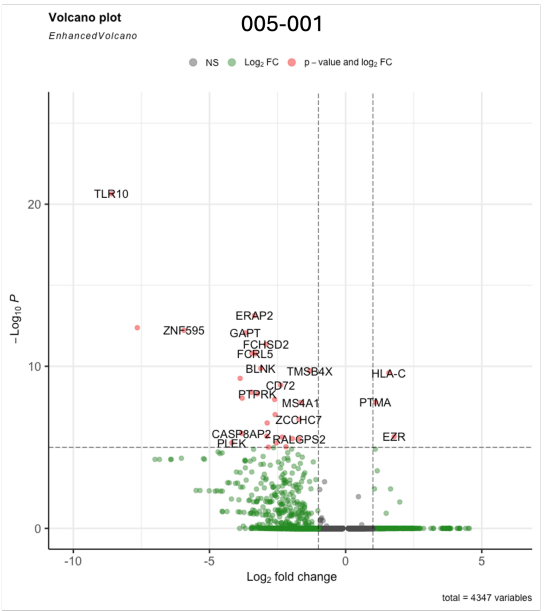

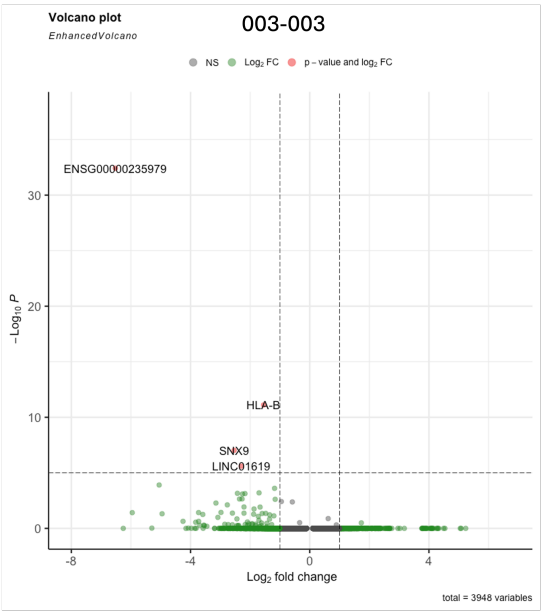

Plasma B cells

A. Appendix

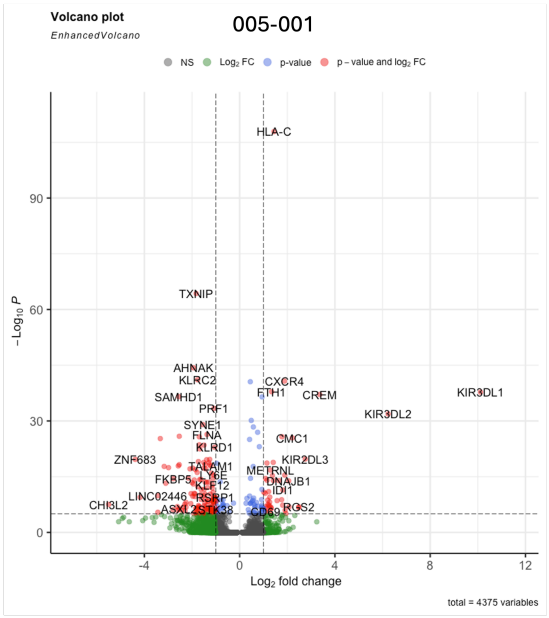

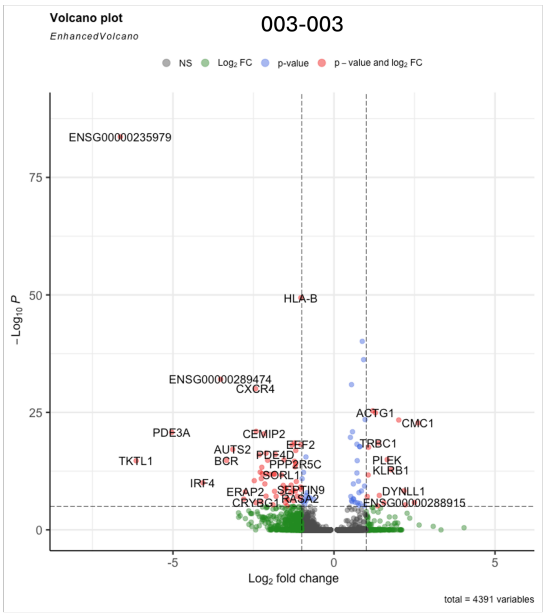

NKT

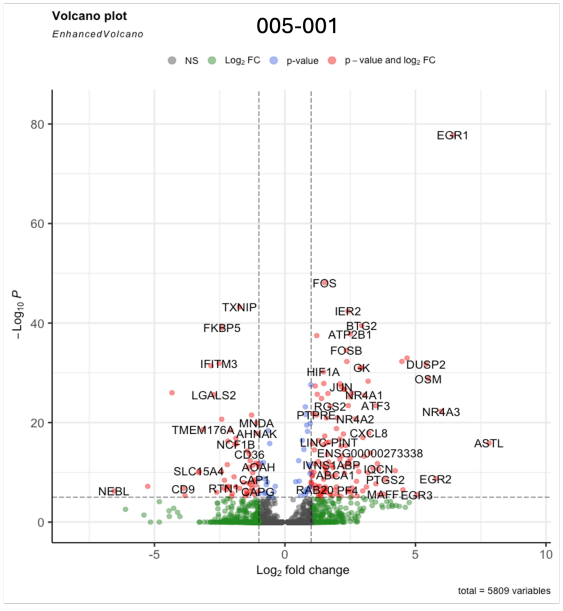

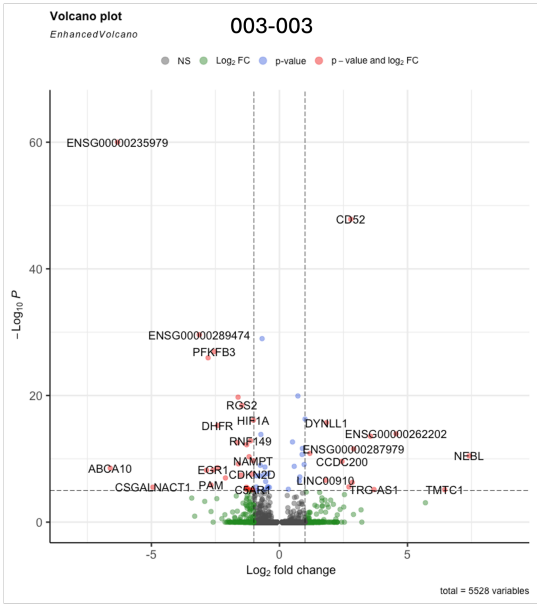

CD14+ monocytes/ cDC1

B.

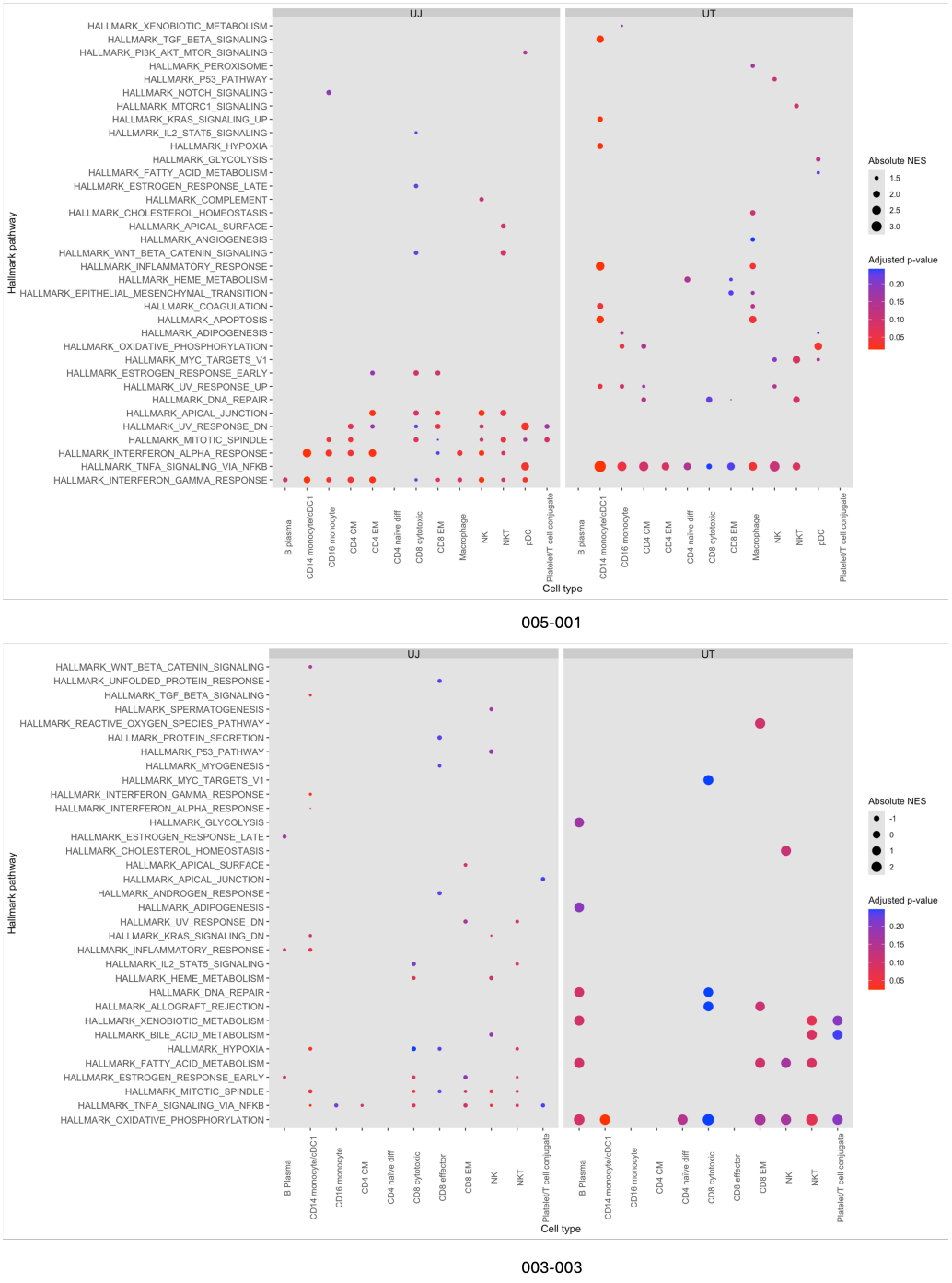

005-001

003-003

Figure A.1: Differential gene expression and pathway enrichment analysis for different cell type clusters, in 005-001 and 003-003. Panel A shows volcano plots with differentially expressed genes in UT vs UJ. DE genes are defined by |log2FC|>1 and padj<0.05. Panel B shows pathways enriched at UJ and UT in different cell type clusters, based on DGE identified in specific cell types.

References

Abrahams, M.-R., Joseph, S. B., Garrett, N., Tyers, L., Moeser, M., Archin, N., Council, O. D., Matten, D., Zhou, S., Doolabh, D., et al. (2019). The replication-competent HIV-1 latent reservoir is primarily established near the time of therapy initiation. *Science Translational Medicine*, *11*(513), eaaw5589.

Adland, E., Millar, J., Bengu, N., Muenchhoff, M., Fillis, R., Sprenger, K., Ntlantsana, V., Roider, J., Vieira, V., Govender, K., Adamson, J., Nxele, N., Ochsenbauer, C., Kappes, J., Mori, L., Lobenstein, J. van, Graza, Y., Chinniah, K., Kapongo, C., ... Goulder, P. (2020). Sex-specific innate immune selection of HIV-1 in utero is associated with increased female susceptibility to infection. *Nature Communications*, *11*(1), 1767. https://doi.org/10.1038/s41467-020-15632-y

Aghaizu, A., Murphy, G., Tosswill, J., DeAngelis, D., Charlett, A., Gill, O., Ward, H., Lattimore, S., Simmons, R., & Delpech, V. (2014). Recent infection testing algorithm (RITA) applied to new HIV diagnoses in england, wales and northern ireland, 2009 to 2011. *Eurosurveillance*, *19*(2), 20673.

Anne, P., Dana, P., A., B. C., M., B. J., Walter, J., Scott, M. R., & Julie, O. (2009). Breadth of Neutralizing Antibody Response to Human Immunodeficiency Virus Type 1 Is Affected by Factors Early in Infection but Does Not Influence Disease Progression. *Journal of Virology*, *83*(19), 10269–10274. https://doi.org/10.1128/jvi.01149-09

Anthony, C., York, T., Bekker, V., Matten, D., Selhorst, P., Ferreria, R.-C., Garrett, N. J., Karim, S. S. A., Morris, L., Wood, N. T., Moore, P. L., & Williamson, C. (2017). Cooperation between Strain-Specific and Broadly Neutralizing Responses Limited Viral Escape and Prolonged the Exposure of the

Broadly Neutralizing Epitope. *Journal of Virology*, *91*(18). https://doi.org/10.1128/JVI.00828-17

Apetrei C, Hahn B, Rambaut A, Wolinsky S, Brister JR, Keele B, F. C. (2021). *HIV Sequence Compendium 2021*. Los Alamos National Laboratory. https://www.hiv.lanl.gov/content/sequence/HIV/COMPENDIUM/2021/sequence2021.pdf

Bai, H., Lewitus, E., Li, Y., Thomas, P. V., Zemil, M., Merbah, M., Peterson, C. E., Thuraisamy, T., Rees, P. A., Hajduczki, A., Dussupt, V., Slike, B., Mendez-Rivera, L., Schmid, A., Kavusak, E., Rao, M., Smith, G., Frey, J., Sims, A., ... Rolland, M. (2024). Contemporary HIV-1 consensus Env with AI-assisted redesigned hypervariable loops promote antibody binding. *Nature Communications*, *15*(1), 3924. https://doi.org/10.1038/s41467-024-48139-x

Bailón, L., Llano, A., Cedeño, S., Escribà, T., Rosás-Umbert, M., Parera, M., Casadellà, M., Lopez, M., Pérez, F., Oriol-Tordera, B., Ruiz-Riol, M., Coll, J., Perez, F., Rivero, À., Leselbaum, A. R., McGowan, I., Sengupta, D., Wee, E. G., Hanke, T., ... Group, the A. S. (2022). Safety, immunogenicity and effect on viral rebound of HTI vaccines in early treated HIV-1 infection: a randomized, placebo-controlled phase 1 trial. *Nature Medicine*, *28*(12), 2611–2621. https://doi.org/10.1038/s41591-022-02060-2

Banach, B. B., Pletnev, S., Olia, A. S., Xu, K., Zhang, B., Rawi, R., Bylund, T., Doria-Rose, N. A., Nguyen, T. D., Fahad, A. S., Lee, M., Lin, B. C., Liu, T., Louder, M. K., Madan, B., McKee, K., O'Dell, S., Sastry, M., Schön, A., ... DeKosky, B. J. (2023). Antibody-directed evolution reveals a mechanism for enhanced neutralization at the HIV-1 fusion peptide site. *Nature Communications*, *14*(1), 7593. https://doi.org/10.1038/s41467-023-42098-5

Bar, K. J., Sneller, M. C., Harrison, L. J., Justement, J. S., Overton, E. T., Petrone, M. E., Salantes, D. B., Seamon, C. A., Scheinfeld, B., Kwan, R. W., Learn, G. H., Proschan, M. A., Kreider, E. F., Blazkova, J., Bardsley, M., Refsland, E. W., Messer, M., Clarridge, K. E., Tustin, N. B., ... Chun, T.-W. (2016). Effect

of HIV Antibody VRC01 on Viral Rebound after Treatment Interruption. *New England Journal of Medicine*, *375*(21), 2037–2050. https://doi.org/10.1056/NEJMoa1608243

Barnes, C. O., Gristick, H. B., Freund, N. T., Escolano, A., Lyubimov, A. Y., Hartweger, H., West Jr, A. P., Cohen, A. E., Nussenzweig, M. C., & Bjorkman, P. J. (2018). Structural characterization of a highly-potent V3-glycan broadly neutralizing antibody bound to natively-glycosylated HIV-1 envelope. *Nature Communications*, *9*(1), 1251. https://doi.org/10.1038/s41467-018-03632-y

Bar-On, Y., Gruell, H., Schoofs, T., Pai, J. A., Nogueira, L., Butler, A. L., Millard, K., Lehmann, C., Suárez, I., Oliveira, T. Y., Karagounis, T., Cohen, Y. Z., Wyen, C., Scholten, S., Handl, L., Belblidia, S., Dizon, J. P., Vehreschild, J. J., Witmer-Pack, M., ... Nussenzweig, M. C. (2018). Safety and antiviral activity of combination HIV-1 broadly neutralizing antibodies in viremic individuals. *Nature Medicine*, *24*(11), 1701–1707. https://doi.org/10.1038/s41591-018-0186-4

Barouch, D. H. (2008). Challenges in the development of an HIV-1 vaccine. *Nature*, *455*(7213), 613–619. https://doi.org/10.1038/nature07352

Bbosa, N., Kaleebu, P., & Ssemwanga, D. (2019). HIV subtype diversity worldwide. *Current Opinion in HIV and AIDS*, *14*(3). https://journals.lww.com/co-hivandaids/fulltext/2019/05000/hiv_subtype_diversity_worldwide.3.aspx

Bekker, L.-G., Beyrer, C., Mgodi, N., Lewin, S. R., Delany-Moretlwe, S., Taiwo, B., Masters, M. C., & Lazarus, J. V. (2023). HIV infection. *Nature Reviews Disease Primers*, *9*(1), 42. https://doi.org/10.1038/s41572-023-00452-3

Bertagnolli, L. N., Varriale, J., Sweet, S., Brockhurst, J., Simonetti, F. R., White, J., Beg, S., Lynn, K., Mounzer, K., Frank, I., Tebas, P., Bar, K. J., Montaner, L. J., Siliciano, R. F., & Siliciano, J. D. (2020). Autologous IgG antibodies block outgrowth of a substantial but variable fraction of viruses in the latent reservoir for HIV-1. *Proceedings of the National Academy of Sciences of the*

United States of America, *117*(50), 32066–32077. https://doi.org/10.1073/pnas.2020617117

Blassel, L., Zhukova, A., Villabona-Arenas, C. J., Atkins, K. E., Hué, S., & Gascuel, O. (2021). Drug resistance mutations in HIV: new bioinformatics approaches and challenges. *Current Opinion in Virology*, *51*, 56–64. https://doi.org/https://doi.org/10.1016/j.coviro.2021.09.009

Blattner, W., Gallo, R. C., & Temin, H. M. (1988). HIV Causes AIDS. *Science*, *241*(4865), 515. https://doi.org/10.1126/science.3399881

Bournazos, S., Klein, F., Pietzsch, J., Seaman, M. S., Nussenzweig, M. C., & Ravetch, J. V. (2014). Broadly neutralizing anti-HIV-1 antibodies require fc effector functions for in vivo activity. *Cell*, *158*(6), 1243–1253.

Bouvin-Pley, M., Morgand, M., Meyer, L., Goujard, C., Moreau, A., Mouquet, H., Nussenzweig, M., Pace, C., Ho, D., Bjorkman, P., et al. (2014). Drift of the HIV-1 envelope glycoprotein gp120 toward increased neutralization resistance over the course of the epidemic: A comprehensive study using the most potent and broadly neutralizing monoclonal antibodies. *Journal of Virology*, *88*(23), 13910–13917.

Bouvin-Pley, M., Morgand, M., Moreau, A., Jestin, P., Simonnet, C., Tran, L., Goujard, C., Meyer, L., Barin, F., & Braibant, M. (2013). Evidence for a continuous drift of the HIV-1 species towards higher resistance to neutralizing antibodies over the course of the epidemic. *PLoS Pathogens*, *9*(7), e1003477.

Brenner, B. G., Routy, J.-P., Petrella, M., Moisi, D., Oliveira, M., Detorio, M., Spira, B., Essabag, V., Conway, B., Lalonde, R., Sekaly, R.-P., & Wainberg, M. A. (2002). Persistence and Fitness of Multidrug-Resistant Human Immunodeficiency Virus Type 1 Acquired in Primary Infection. *Journal of Virology*, *76*(4), 1753–1761. https://doi.org/10.1128/jvi.76.4.1753-1761.2002

Bricault, C. A., Yusim, K., Seaman, M. S., Yoon, H., Theiler, J., Giorgi, E. E., Wagh, K., Theiler, M., Hraber, P., Macke, J. P., Kreider, E. F., Learn, G. H., Hahn, B. H., Scheid, J. F., Kovacs, J. M., Shields, J. L., Lavine, C. L., Ghantous, F., Rist, M., ... Korber, B. (2019). HIV-1 Neutralizing Antibody

Signatures and Application to Epitope-Targeted Vaccine Design. *Cell Host & Microbe*, *25*(1), 59–72.e8. https://doi.org/https://doi.org/10.1016/j.chom.2018.12.001

Bruner, K. M., Murray, A. J., Pollack, R. A., Soliman, M. G., Laskey, S. B., Capoferri, A. A., Lai, J., Strain, M. C., Lada, S. M., Hoh, R., et al. (2016). Defective proviruses rapidly accumulate during acute HIV-1 infection. *Nature Medicine*, *22*(9), 1043–1049.

Bruner, K. M., Wang, Z., Simonetti, F. R., Bender, A. M., Kwon, K. J., Sengupta, S., Fray, E. J., Beg, S. A., Antar, A. A., Jenike, K. M., et al. (2019). A quantitative approach for measuring the reservoir of latent HIV-1 proviruses. *Nature*, *566*(7742), 120–125.

Buell, K. G., Chung, C., Chaudhry, Z., Puri, A., Nawab, K., & Ravindran, R. P. (2016). Lifelong antiretroviral therapy or HIV cure: The benefits for the individual patient. *AIDS Care*, *28*(2), 242–246.

Bunnik, E. M., Euler, Z., Welkers, M. R., Boeser-Nunnink, B. D., Grijsen, M. L., Prins, J. M., & Schuitemaker, H. (2010). Adaptation of HIV-1 envelope gp120 to humoral immunity at a population level. *Nature Medicine*, *16*(9), 995–997.

Burton, D. R., & Hangartner, L. (2016). Broadly Neutralizing Antibodies to HIV and Their Role in Vaccine Design. *Annual Review of Immunology*, *34*, 635–659. https://doi.org/10.1146/annurev-immunol-041015-055515

Buzon MJ, P. F., Martin-Gayo E. (2014). Long-Term Antiretroviral Treatment Initiated at Primary HIV-1 Infection Affects the Size, Composition, and Decay Kinetics of the Reservoir of HIV-1-Infected CD4 T Cells. *Journal of Virology*, *88*(17), 10056–10065. https://doi.org/10.1128/jvi.01046-14

Cai, H., Zhang, R.-S., Orwenyo, J., Giddens, J., Yang, Q., LaBranche, C. C., Montefiori, D. C., & Wang, L.-X. (2018). Synthetic HIV V3 Glycopeptide Immunogen Carrying a N334 N-Glycan Induces Glycan-Dependent Antibodies with Promiscuous Site Recognition. *Journal of Medicinal Chemistry*, *61*(22), 10116–10125. https://doi.org/10.1021/acs.jmedchem.8b01290

Caillat, C., Guilligay, D., Sulbaran, G., & Weissenhorn, W. (2020). Neutralizing Antibodies Targeting HIV-1 gp41. *Viruses*, *12*(11). https://doi.org/10.3390/v12111210

Cameroni, E., Bowen, J. E., Rosen, L. E., Saliba, C., Zepeda, S. K., Culap, K., Pinto, D., VanBlargan, L. A., De Marco, A., Iulio, J. di, et al. (2022). Broadly neutralizing antibodies overcome SARS-CoV-2 omicron antigenic shift. *Nature*, *602*(7898), 664–670.

Cao, Y., Qin, L., Zhang, L., Safrit, J., & Ho, D. D. (1995). Virologic and immunologic characterization of long-term survivors of human immunodeficiency virus type 1 infection. *New England Journal of Medicine*, *332*(4), 201–208. https://doi.org/10.1056/NEJM199501263320401

Caskey, M., Klein, F., Lorenzi, J. C. C., Seaman, M. S., West, A. P., Buckley, N., Kremer, G., Nogueira, L., Braunschweig, M., Scheid, J. F., Horwitz, J. A., Shimeliovich, I., Ben-Avraham, S., Witmer-Pack, M., Platten, M., Lehmann, C., Burke, L. A., Hawthorne, T., Gorelick, R. J., ... Nussenzweig, M. C. (2015). Viraemia suppressed in HIV-1-infected humans by broadly neutralizing antibody 3BNC117. *Nature*, *522*(7557), 487–491. https://doi.org/10.1038/nature14411

Caskey, M., Klein, F., & Nussenzweig, M. C. (2019). Broadly neutralizing anti-HIV-1 monoclonal antibodies in the clinic. *Nature Medicine*, *25*(4), 547–553. https://doi.org/10.1038/s41591-019-0412-8

Caskey, M., & Kuritzkes, D. R. (2022). Monoclonal Antibodies as Long-Acting Products: What Are We Learning From Human Immunodeficiency Virus (HIV) and Coronavirus Disease 2019 (COVID-19)? *Clinical Infectious Diseases : An Official Publication of the Infectious Diseases Society of America*, *75*(Suppl 4), S530–S540. https://doi.org/10.1093/cid/ciac751

Caskey, M., Schoofs, T., Gruell, H., Settler, A., Karagounis, T., Kreider, E. F., Murrell, B., Pfeifer, N., Nogueira, L., Oliveira, T. Y., Learn, G. H., Cohen, Y. Z., Lehmann, C., Gillor, D., Shimeliovich, I., Unson-O'Brien, C., Weiland, D., Robles, A., Kümmerle, T., ... Klein, F. (2017). Antibody 10-1074 suppresses

viremia in HIV-1-infected individuals. *Nature Medicine*, *23*(2), 185–191. https://doi.org/10.1038/nm.4268

Chandrasekar, A. P., Cummins, N. W., Natesampillai, S., Misra, A., Alto, A., Laird, G., & Badley, A. D. (2022). The BCL-2 Inhibitor Venetoclax Augments Immune Effector Function Mediated by Fas Ligand, TRAIL, and Perforin/Granzyme B, Resulting in Reduced Plasma Viremia and Decreased HIV Reservoir Size during Acute HIV Infection in a Humanized Mouse Model. *Journal of Virology*, *96*(24), e0173022. https://doi.org/10.1128/jvi.01730-22

Chang, J. J., & Altfeld, M. (2010). Innate immune activation in primary HIV-1 infection. *The Journal of Infectious Diseases*, *202 Suppl 2*(Suppl 2), S297–301. https://doi.org/10.1086/655657

Chen, J., Zhou, T., Zhang, Y., Luo, S., Chen, H., Chen, D., Li, C., & Li, W. (2022). The reservoir of latent HIV. *Frontiers in Cellular and Infection Microbiology*, *12*, 945956. https://doi.org/10.3389/fcimb.2022.945956

Chomont, N., El-Far, M., Ancuta, P., Trautmann, L., Procopio, F. A., Yassine-Diab, B., Boucher, G., Boulassel, M.-R., Ghattas, G., Brenchley, J. M., Schacker, T. W., Hill, B. J., Douek, D. C., Routy, J.-P., Haddad, E. K., & Sékaly, R.-P. (2009). HIV reservoir size and persistence are driven by T cell survival and homeostatic proliferation. *Nature Medicine*, *15*(8), 893–900. https://doi.org/10.1038/nm.1972

Chu, C., Armenia, D., Walworth, C., Santoro, M. M., & Shafer, R. W. (2022). Genotypic Resistance Testing of HIV-1 DNA in Peripheral Blood Mononuclear Cells. *Clinical Microbiology Reviews*, *35*(4), e0005222. https://doi.org/10.1128/cmr.00052-22

Chun, T.-W., Carruth, L., Finzi, D., Shen, X., DiGiuseppe, J. A., Taylor, H., Hermankova, M., Chadwick, K., Margolick, J., Quinn, T. C., Kuo, Y.-H., Brookmeyer, R., Zeiger, M. A., Barditch-Crovo, P., & Siliciano, R. F. (1997). Quantification of latent tissue reservoirs and total body viral load in HIV-1 infection. *Nature*, *387*(6629), 183–188. https://doi.org/10.1038/387183a0

Chun, T.-W., Engel, D., Berrey, M. M., Shea, T., Corey, L., & Fauci, A. S. (1998). Early establishment of a pool of latently infected, resting CD4+ t cells during primary HIV-1 infection. *Proceedings of the National Academy of Sciences*, *95*(15), 8869–8873.

Chun, T.-W., Finzi, D., Margolick, J., Chadwick, K., Schwartz, D., & Siliciano, R. F. (1995). In vivo fate of HIV-1-infected t cells: Quantitative analysis of the transition to stable latency. *Nature Medicine*, *1*(12), 1284–1290.

Clavel, F., & Hance, A. J. (2004). HIV Drug Resistance. *New England Journal of Medicine*, *350*(10), 1023–1035. https://doi.org/10.1056/NEJMra025195

Clutter, D. S., Jordan, M. R., Bertagnolio, S., & Shafer, R. W. (2016). HIV-1 drug resistance and resistance testing. *Infection, Genetics and Evolution*, *46*, 292–307. https://doi.org/https://doi.org/10.1016/j.meegid.2016.08.031

Cohen, Y. Z., Lorenzi, J. C. C., Krassnig, L., Barton, J. P., Burke, L., Pai, J., Lu, C.-L., Mendoza, P., Oliveira, T. Y., Sleckman, C., Millard, K., Butler, A. L., Dizon, J. P., Belblidia, S. A., Witmer-Pack, M., Shimeliovich, I., Gulick, R. M., Seaman, M. S., Jankovic, M., … Nussenzweig, M. C. (2018). Relationship between latent and rebound viruses in a clinical trial of anti-HIV-1 antibody 3BNC117. *The Journal of Experimental Medicine*, *215*(9), 2311–2324. https://doi.org/10.1084/jem.20180936

Cohn, L. B., Chomont, N., & Deeks, S. G. (2020). The Biology of the HIV-1 Latent Reservoir and Implications for Cure Strategies. *Cell Host & Microbe*, *27*(4), 519–530. https://doi.org/https://doi.org/10.1016/j.chom.2020.03.014

Cohn, L. B., Silva, I. T. da, Valieris, R., Huang, A. S., Lorenzi, J. C. C., Cohen, Y. Z., Pai, J. A., Butler, A. L., Caskey, M., Jankovic, M., & Nussenzweig, M. C. (2018). Clonal CD4+ T cells in the HIV-1 latent reservoir display a distinct gene profile upon reactivation. *Nature Medicine*, *24*(5), 604–609. https://doi.org/10.1038/s41591-018-0017-7

Colbert, M. D., Flyak, A. I., Ogega, C. O., Kinchen, V. J., Massaccesi, G., Hernandez, M., Davidson, E., Doranz, B. J., Cox, A. L., Crowe Jr, J. E., et al. (2019).

Broadly neutralizing antibodies targeting new sites of vulnerability in hepatitis c virus E1E2. *Journal of Virology*, *93*(14), 10–1128.

Colby, D. J., Sarnecki, M., Barouch, D. H., Tipsuk, S., Stieh, D. J., Kroon, E., Schuetz, A., Intasan, J., Sacdalan, C., Pinyakorn, S., Grandin, P., Song, H., Tovanabutra, S., Shubin, Z., Kim, D., Paquin-Proulx, D., Eller, M. A., Thomas, R., Souza, M. de, … Ananworanich, J. (2020). Safety and immunogenicity of Ad26 and MVA vaccines in acutely treated HIV and effect on viral rebound after antiretroviral therapy interruption. *Nature Medicine*, *26*(4), 498–501. https://doi.org/10.1038/s41591-020-0774-y

Colby, D. J., Trautmann, L., Pinyakorn, S., Leyre, L., Pagliuzza, A., Kroon, E., Rolland, M., Takata, H., Buranapraditkun, S., Intasan, J., Chomchey, N., Muir, R., Haddad, E. K., Tovanabutra, S., Ubolyam, S., Bolton, D. L., Fullmer, B. A., Gorelick, R. J., Fox, L., … Group, T. R. study. (2018). Rapid HIV RNA rebound after antiretroviral treatment interruption in persons durably suppressed in Fiebig I acute HIV infection. *Nature Medicine*, *24*(7), 923–926. https://doi.org/10.1038/s41591-018-0026-6

Collins, K. L., Chen, B. K., Kalams, S. A., Walker, B. D., & Baltimore, D. (1998). HIV-1 nef protein protects infected primary cells against killing by cytotoxic t lymphocytes. *Nature*, *391*(6665), 397–401.

Conway, J. M., Perelson, A. S., & Li, J. Z. (2019). Predictions of time to HIV viral rebound following ART suspension that incorporate personal biomarkers. *PLoS Computational Biology*, *15*(7), e1007229. https://doi.org/10.1371/journal.pcbi.1007229

Curno, M. J., Rossi, S., Hodges-Mameletzis, I., Johnston, R., Price, M. A., & Heidari, S. (2016). A systematic review of the inclusion (or exclusion) of women in HIV research: From clinical studies of antiretrovirals and vaccines to cure strategies. *JAIDS Journal of Acquired Immune Deficiency Syndromes*, *71*(2), 181–188.

Dai, X.-P., Wu, F.-Y., Cui, C., Liao, X.-J., Jiao, Y.-M., Zhang, C., Song, J.-W., Fan, X., Zhang, J.-Y., He, Q., & Wang, F.-S. (2021). Increased Platelet-CD4(+)

T Cell Aggregates Are Correlated With HIV-1 Permissiveness and CD4(+) T Cell Loss. *Frontiers in Immunology*, *12*, 799124. https://doi.org/10.3389/fimmu.2021.799124

Daniels, C. N., & Saunders, K. O. (2019). *Chapter Two - Antibody responses to the HIV-1 envelope high mannose patch* (F. B. T.-. A. in I. Alt, Ed.; Vol. 143, pp. 11–73). Academic Press. https://doi.org/https://doi.org/10.1016/bs.ai.2019.08.002

Darcis, G., Van Driessche, B., & Van Lint, C. (2017). HIV Latency: Should We Shock or Lock? *Trends in Immunology*, *38*(3), 217–228. https://doi.org/10.1016/j.it.2016.12.003

Deeks, S. G. (2012). Shock and kill. *Nature*, *487*(7408), 439–440. https://doi.org/10.1038/487439a

Deeks, S. G., Archin, N., Cannon, P., Collins, S., Jones, R. B., Jong, M. A. W. P. de, Lambotte, O., Lamplough, R., Ndung'u, T., Sugarman, J., Tiemessen, C. T., Vandekerckhove, L., Lewin, S. R., Deeks, S., Lewin, S., Jong, M. de, Ndhlovu, Z., Chomont, N., Brumme, Z., … Working Group 8: (Social, ethical aspects of cure). (2021). Research priorities for an HIV cure: International AIDS Society Global Scientific Strategy 2021. *Nature Medicine*, *27*(12), 2085–2098. https://doi.org/10.1038/s41591-021-01590-5

Deeks, S. G., Odorizzi, P. M., & Sekaly, R.-P. (2017). The interferon paradox: can inhibiting an antiviral mechanism advance an HIV cure? *The Journal of Clinical Investigation*, *127*(1), 103–105. https://doi.org/10.1172/JCI91916

Deeks, S. G., & Walker, B. D. (2007). Human Immunodeficiency Virus Controllers: Mechanisms of Durable Virus Control in the Absence of Antiretroviral Therapy. *Immunity*, *27*(3), 406–416. https://doi.org/10.1016/j.immuni.2007.08.010

Delporte, M., Lambrechts, L., Blomme, E. E., Snippenberg, W. van, Rutsaert, S., Verschoore, M., De Smet, E., Noppe, Y., De Langhe, N., De Scheerder, M.-A., et al. (2025). Integrative assessment of total and intact HIV-1 reservoir by

a 5-region multiplexed rainbow DNA digital PCR assay. *Clinical Chemistry*, *71*(1), 203–214.

Derache, A., Iwuji, C. C., Baisley, K., Danaviah, S., Marcelin, A.-G., Calvez, V., Oliveira, T. de, Dabis, F., Porter, K., & Pillay, D. (2019). Impact of next-generation sequencing defined human immunodeficiency virus pretreatment drug resistance on virological outcomes in the ANRS 12249 treatment-as-prevention trial. *Clinical Infectious Diseases*, *69*(2), 207–214.

Derdeyn, C. A., Decker, J. M., Bibollet-Ruche, F., Mokili, J. L., Muldoon, M., Denham, S. A., Heil, M. L., Kasolo, F., Musonda, R., Hahn, B. H., et al. (2004). Envelope-constrained neutralization-sensitive HIV-1 after heterosexual transmission. *Science*, *303*(5666), 2019–2022.

Ding, C., Patel, D., Ma, Y., Mann, J. F. S., Wu, J., & Gao, Y. (2021). Employing Broadly Neutralizing Antibodies as a Human Immunodeficiency Virus Prophylactic & Therapeutic Application. *Frontiers in Immunology*, *12*. https://doi.org/10.3389/fimmu.2021.697683

Dingens, A. S., Arenz, D., Weight, H., Overbaugh, J., & Bloom, J. D. (2019). An Antigenic Atlas of HIV-1 Escape from Broadly Neutralizing Antibodies Distinguishes Functional and Structural Epitopes. *Immunity*, *50*(2), 520–532.e3. https://doi.org/10.1016/j.immuni.2018.12.017

Duchemin, M., Tudor, D., Cottignies-Calamarte, A., & Bomsel, M. (2020). Antibody-Dependent Cellular Phagocytosis of HIV-1-Infected Cells Is Efficiently Triggered by IgA Targeting HIV-1 Envelope Subunit gp41. *Frontiers in Immunology*, *11*, 1141. https://doi.org/10.3389/fimmu.2020.01141

Dzimianski, J. V., Scholte, F. E. M., Bergeron, É., & Pegan, S. D. (2019). ISG15: It's Complicated. *Journal of Molecular Biology*, *431*(21), 4203–4216. https://doi.org/https://doi.org/10.1016/j.jmb.2019.03.013

Einkauf, K. B., Lee, G. Q., Gao, C., Sharaf, R., Sun, X., Hua, S., Chen, S. M., Jiang, C., Lian, X., Chowdhury, F. Z., et al. (2019). Intact HIV-1 proviruses accumulate at distinct chromosomal positions during prolonged antiretroviral therapy. *The Journal of Clinical Investigation*, *129*(3), 988–998.

El-Sadr, W., Lundgren, J., Neaton, J., Gordin, F., Abrams, D., Arduino, R., et al. (2006). Strategies for management of antiretroviral therapy therapy (smart) study group.(smart) study group. Cd4+ count-guided interruption of antiretroviral treatment. *N Engl J Med*, *355*, 2283–2296.

English, S., Katzourakis, A., Bonsall, D., Flanagan, P., Duda, A., Fidler, S., Weber, J., McClure, M., Investigators, S. T., Phillips, R., & Frater, J. (2011). Phylogenetic analysis consistent with a clinical history of sexual transmission of HIV-1 from a single donor reveals transmission of highly distinct variants. *Retrovirology*, *8*, 54. https://doi.org/10.1186/1742-4690-8-54

Etemad, B., Esmaeilzadeh, E., & Li, J. Z. (2019). *Learning From the Exceptions: HIV Remission in Post-treatment Controllers* (Vol. 10, p. 1749). https://www.frontiersin.org/article/10.3389/fimmu.2019.01749

Etemad, B., Sun, X., Li, Y., Melberg, M., Moisi, D., Gottlieb, R., Ahmed, H., Aga, E., Bosch, R. J., Acosta, E. P., Yuki, Y., Martin, M. P., Carrington, M., Gandhi, R. T., Jacobson, J. M., Volberding, P., Connick, E., Mitsuyasu, R., Frank, I., … Li, J. Z. (2023). HIV post-treatment controllers have distinct immunological and virological features. *Proceedings of the National Academy of Sciences of the United States of America*, *120*(11), e2218960120. https://doi.org/10.1073/pnas.2218960120

Fagard, C., Oxenius, A., Günthard, H., Garcia, F., Le Braz, M., Mestre, G., Battegay, M., Furrer, H., Vernazza, P., Bernasconi, E., Telenti, A., Weber, R., Leduc, D., Yerly, S., Price, D., Dawson, S. J., Klimkait, T., Perneger, T. V., McLean, A., … for the Swiss HIV Cohort Study. (2003). A Prospective Trial of Structured Treatment Interruptions in Human Immunodeficiency Virus Infection. *Archives of Internal Medicine*, *163*(10), 1220–1226.

Fenton-May, A. E., Dibben, O., Emmerich, T., Ding, H., Pfafferott, K., Aasa-Chapman, M. M., Pellegrino, P., Williams, I., Cohen, M. S., Gao, F., Shaw, G. M., Hahn, B. H., Ochsenbauer, C., Kappes, J. C., & Borrow, P. (2013). Relative resistance of HIV-1 founder viruses to control by interferon-alpha. *Retrovirology*, *10*(1), 146. https://doi.org/10.1186/1742-4690-10-146

Fidler, S., & Fox, J. (2016). Primary HIV infection: A medical and public health emergency requiring rapid specialist management. *Clinical Medicine*, *16*(2), 180–183.

Fidler, S., Porter, K., Ewings, F., Frater, J., Ramjee, G., Cooper, D., Rees, H., Fisher, M., Schechter, M., Kaleebu, P., Tambussi, G., Kinloch, S., Miro, J. M., Kelleher, A., McClure, M., Kaye, S., Gabriel, M., Phillips, R., Weber, J., & Babiker, A. (2013). Short-course antiretroviral therapy in primary HIV infection. *The New England Journal of Medicine*, *368*(3), 207–217. https://doi.org/10.1056/NEJMoa1110039

Fiebig, E. W., Wright, D. J., Rawal, B. D., Garrett, P. E., Schumacher, R. T., Peddada, L., Heldebrant, C., Smith, R., Conrad, A., Kleinman, S. H., et al. (2003). Dynamics of HIV viremia and antibody seroconversion in plasma donors: Implications for diagnosis and staging of primary HIV infection. *Aids*, *17*(13), 1871–1879.

Finzi, D., Hermankova, M., Pierson, T., Carruth, L. M., Buck, C., Chaisson, R. E., Quinn, T. C., Chadwick, K., Margolick, J., Brookmeyer, R., et al. (1997). Identification of a reservoir for HIV-1 in patients on highly active antiretroviral therapy. *Science*, *278*(5341), 1295–1300.

Frater, J., Ewings, F., Hurst, J., Brown, H., Robinson, N., Fidler, S., Babiker, A., Weber, J., Porter, K., & Phillips, R. E. (2014). HIV-1-specific CD4+ responses in primary HIV-1 infection predict disease progression. *AIDS*, *28*(5). https://journals.lww.com/aidsonline/Fulltext/2014/03130/HIV_1_specific_CD4__responses_in_primary_HIV_1.7.aspx

Frattari, G. S., Caskey, M., & Søgaard, O. S. (2023). Broadly neutralizing antibodies for HIV treatment and cure approaches. *Current Opinion in HIV and AIDS*, *18*(4). https://journals.lww.com/co-hivandaids/fulltext/2023/07000/broadly%7B/_%7Dneutralizing%7B/_%7Dantibodies%7B/_%7Dfor%7B/_%7Dhiv%7B/_%7Dtreatment.2.aspx

Freed, E. O. (2015). HIV-1 assembly, release and maturation. *Nature Reviews Microbiology*, *13*(8), 484–496. https://doi.org/10.1038/nrmicro3490

Freund, N. T., Horwitz, J. A., Nogueira, L., Sievers, S. A., Scharf, L., Scheid, J. F., Gazumyan, A., Liu, C., Velinzon, K., Goldenthal, A., Sanders, R. W., Moore, J. P., Bjorkman, P. J., Seaman, M. S., Walker, B. D., Klein, F., & Nussenzweig, M. C. (2015). A New Glycan-Dependent CD4-Binding Site Neutralizing Antibody Exerts Pressure on HIV-1 In Vivo. *PLOS Pathogens*, *11*(10), 1–19. https://doi.org/10.1371/journal.ppat.1005238

Friedrich, N., Stiegeler, E., Glögl, M., Lemmin, T., Hansen, S., Kadelka, C., Wu, Y., Ernst, P., Maliqi, L., Foulkes, C., Morin, M., Eroglu, M., Liechti, T., Ivan, B., Reinberg, T., Schaefer, J. V., Karakus, U., Ursprung, S., Mann, A., … Trkola, A. (2021). Distinct conformations of the HIV-1 V3 loop crown are targetable for broad neutralization. *Nature Communications*, *12*(1), 6705. https://doi.org/10.1038/s41467-021-27075-0

Fromentin, R., Bakeman, W., Lawani, M. B., Khoury, G., Hartogensis, W., DaFonseca, S., Killian, M., Epling, L., Hoh, R., Sinclair, E., et al. (2016). CD4+ t cells expressing PD-1, TIGIT and LAG-3 contribute to HIV persistence during ART. *PLoS Pathogens*, *12*(7), e1005761.

Frost, S. D. W., Magalis, B. R., & Kosakovsky Pond, S. L. (2018). Neutral Theory and Rapidly Evolving Viral Pathogens. *Molecular Biology and Evolution*, *35*(6), 1348–1354. https://doi.org/10.1093/molbev/msy088

Gaebler, C., Falcinelli, S. D., Stoffel, E., Read, J., Murtagh, R., Oliveira, T. Y., Ramos, V., Lorenzi, J. C. C., Kirchherr, J., James, K. S., Allard, B., Baker, C., Kuruc, J. D., Caskey, M., Archin, N. M., Siliciano, R. F., Margolis, D. M., & Nussenzweig, M. C. (2021). Sequence Evaluation and Comparative Analysis of Novel Assays for Intact Proviral HIV-1 DNA. *Journal of Virology*, *95*(6), e01986–20. https://doi.org/10.1128/JVI.01986-20

Gaebler, C., Lorenzi, J. C. C., Oliveira, T. Y., Nogueira, L., Ramos, V., Lu, C.-L., Pai, J. A., Mendoza, P., Jankovic, M., Caskey, M., & Nussenzweig, M. C. (2019). Combination of quadruplex qPCR and next-generation sequencing for qualitative and quantitative analysis of the HIV-1 latent reservoir. *The Journal*

of Experimental Medicine, *216*(10), 2253–2264. https://doi.org/10.1084/jem.20190896

Gaebler, C., Nogueira, L., Stoffel, E., Oliveira, T. Y., Breton, G., Millard, K. G., Turroja, M., Butler, A., Ramos, V., Seaman, M. S., Reeves, J. D., Petroupoulos, C. J., Shimeliovich, I., Gazumyan, A., Jiang, C. S., Jilg, N., Scheid, J. F., Gandhi, R., Walker, B. D., ... Nussenzweig, M. C. (2022). Prolonged viral suppression with anti-HIV-1 antibody therapy. *Nature*. https://doi.org/10.1038/s41586-022-04597-1

Ganser-Pornillos, B. K., & Pornillos, O. (2019). Restriction of HIV-1 and other retroviruses by TRIM5. *Nature Reviews. Microbiology*, *17*(9), 546–556. https://doi.org/10.1038/s41579-019-0225-2

Gao, F., Bailes, E., Robertson, D. L., Chen, Y., Rodenburg, C. M., Michael, S. F., Cummins, L. B., Arthur, L. O., Peeters, M., Shaw, G. M., et al. (1999). Origin of HIV-1 in the chimpanzee pan troglodytes troglodytes. *Nature*, *397*(6718), 436–441.

García, F., Plana, M., Climent, N., León, A., Gatell, J. M., & Gallart, T. (2013). Dendritic cell based vaccines for HIV infection: the way ahead. *Human Vaccines & Immunotherapeutics*, *9*(11), 2445–2452. https://doi.org/10.4161/hv.25876

Gero, H., Daniel, N., Maximilian, M., Susanne, G., Arne, M., Kristina, A., Thomas, S., Jörg, H., Claudia, K., Olga, B., W., B. I., K., H. W., & Eckhard, T. (2024). Long-Term Control of HIV by CCR5 Delta32/Delta32 Stem-Cell Transplantation. *New England Journal of Medicine*, *360*(7), 692–698. https://doi.org/10.1056/NEJMoa0802905

Giron, L. B., Colomb, F., Papasavvas, E., Azzoni, L., Yin, X., Fair, M., Anzurez, A., Damra, M., Mounzer, K., Kostman, J. R., Tebas, P., O'Doherty, U., Tateno, H., Liu, Q., Betts, M. R., Montaner, L. J., & Abdel-Mohsen, M. (2020). Interferon-α alters host glycosylation machinery during treated HIV infection. *EBioMedicine*, *59*, 102945. https://doi.org/https://doi.org/10.1016/j.ebiom.2020.102945

Gnanakaran, S., Bhattacharya, T., Daniels, M., Keele, B. F., Hraber, P. T., Lapedes, A. S., Shen, T., Gaschen, B., Krishnamoorthy, M., Li, H., et al. (2011). Recurrent signature patterns in HIV-1 b clade envelope glycoproteins associated with either early or chronic infections. *PLoS Pathogens*, *7*(9), e1002209.

Gossez, M., Martin, G. E., Pace, M., Ramjee, G., Premraj, A., Kaleebu, P., Rees, H., Inshaw, J., Stöhr, W., Meyerowitz, J., et al. (2019). Virological remission after antiretroviral therapy interruption in female african HIV seroconverters. *Aids*, *33*(2), 185–197.

Goulder, P. J. R., & Watkins, D. I. (2008). Impact of MHC class I diversity on immune control of immunodeficiency virus replication. *Nature Reviews Immunology*, *8*(8), 619–630. https://doi.org/10.1038/nri2357

Granger, L. A., Huettner, I., Debeljak, F., Kaleebu, P., Schechter, M., Tambussi, G., Weber, J., Miro, J. M., Phillips, R., Babiker, A., Cooper, D. A., Fisher, M., Ramjee, G., Fidler, S., Frater, J., Fox, J., & Doores, K. J. (2021). Broadly neutralizing antibody responses in the longitudinal primary HIV-1 infection Short Pulse Anti-Retroviral Therapy at Seroconversion cohort. *AIDS (London, England)*, *35*(13), 2073–2084. https://doi.org/10.1097/QAD.0000000000002988

Gray, E. S., Madiga, M. C., Hermanus, T., Moore, P. L., Wibmer, C. K., Tumba, N. L., Werner, L., Mlisana, K., Sibeko, S., Williamson, C., Abdool Karim, S. S., Morris, L., & Team, C. S. (2011). The neutralization breadth of HIV-1 develops incrementally over four years and is associated with CD4+ T cell decline and high viral load during acute infection. *Journal of Virology*, *85*(10), 4828–4840. https://doi.org/10.1128/JVI.00198-11

Griffith, S. A., & McCoy, L. E. (2021). To bnAb or Not to bnAb: Defining Broadly Neutralising Antibodies Against HIV-1. *Frontiers in Immunology*, *12*, 708227. https://doi.org/10.3389/fimmu.2021.708227

Grossman, Z., Singh, N. J., Simonetti, F. R., Lederman, M. M., Douek, D. C., Deeks, S. G., Kawabe, T., Bocharov, G., Meier-Schellersheim, M., Alon, H., Chomont, N., Grossman, Z., Sousa, A. E., Margolis, L., & Maldarelli, F. (2020).

‘Rinse and Replace’: Boosting T Cell Turnover To Reduce HIV-1 Reservoirs. *Trends in Immunology*, *41*(6), 466–480. https://doi.org/10.1016/j.it.2020.04.003

Gruell, H., Gunst, J. D., Cohen, Y. Z., Pahus, M. H., Malin, J. J., Platten, M., Millard, K. G., Tolstrup, M., Jones, R. B., Conce Alberto, W. D., Lorenzi, J. C. C., Oliveira, T. Y., Kümmerle, T., Suárez, I., Unson-O'Brien, C., Nogueira, L., Olesen, R., Østergaard, L., Nielsen, H., … Søgaard, O. S. (2022). Effect of 3BNC117 and romidepsin on the HIV-1 reservoir in people taking suppressive antiretroviral therapy (ROADMAP): a randomised, open-label, phase 2A trial. *The Lancet. Microbe*, *3*(3), e203–e214. https://doi.org/10.1016/S2666-5247(21)00239-1

Gunst, J. D., Pahus, M. H., Rosás-Umbert, M., Lu, I.-N., Benfield, T., Nielsen, H., Johansen, I. S., Mohey, R., Østergaard, L., Klastrup, V., Khan, M., Schleimann, M. H., Olesen, R., Støvring, H., Denton, P. W., Kinloch, N. N., Copertino, D. C., Ward, A. R., Alberto, W. D. C., … Søgaard, O. S. (2022). Early intervention with 3BNC117 and romidepsin at antiretroviral treatment initiation in people with HIV-1: a phase 1b/2a, randomized trial. *Nature Medicine*, *28*(11), 2424–2435. https://doi.org/10.1038/s41591-022-02023-7

Günthard, H. F., Calvez, V., Paredes, R., Pillay, D., Shafer, R. W., Wensing, A. M., Jacobsen, D. M., & Richman, D. D. (2019). Human Immunodeficiency Virus Drug Resistance: 2018 Recommendations of the International Antiviral Society–USA Panel. *Clinical Infectious Diseases*, *68*(2), 177–187. https://doi.org/10.1093/cid/ciy463

Gupta, R. K., Peppa, D., Hill, A. L., Gálvez, C., Salgado, M., Pace, M., McCoy, L. E., Griffith, S. A., Thornhill, J., Alrubayyi, A., Huyveneers, L. E. P., Nastouli, E., Grant, P., Edwards, S. G., Innes, A. J., Frater, J., Nijhuis, M., Wensing, A. M. J., Martinez-Picado, J., & Olavarria, E. (2020). Evidence for HIV-1 cure after CCR5Δ32/Δ32 allogeneic haemopoietic stem-cell transplantation 30 months post analytical treatment interruption: a

case report. *The Lancet HIV*, *7*(5), e340–e347. https://doi.org/10.1016/S2352-3018(20)30069-2

Hahn, B. H., Shaw, G. M., De, K. M., Cock, & Sharp, P. M. (2000). AIDS as a zoonosis: Scientific and public health implications. *Science*, *287*(5453), 607–614.

Hake, A., & Pfeifer, N. (2017). Prediction of HIV-1 sensitivity to broadly neutralizing antibodies shows a trend towards resistance over time. *PLoS Computational Biology*, *13*(10), e1005789. https://doi.org/10.1371/journal.pcbi.1005789

Hao, Y., Stuart, T., Kowalski, M. H., Choudhary, S., Hoffman, P., Hartman, A., Srivastava, A., Molla, G., Madad, S., Fernandez-Granda, C., & Satija, R. (2023). Dictionary learning for integrative, multimodal and scalable single-cell analysis. *Nature Biotechnology*. https://doi.org/10.1038/s41587-023-01767-y

Harris, J. E. (2022). The repeated setbacks of HIV vaccine development laid the groundwork for SARS-CoV-2 vaccines. *Health Policy and Technology*, *11*(2), 100619. https://doi.org/10.1016/j.hlpt.2022.100619

Haynes, B. F. (2015). New approaches to HIV vaccine development. *Current Opinion in Immunology*, *35*, 39–47. https://doi.org/https://doi.org/10.1016/j.coi.2015.05.007

Haynes, B. F., Saunders, K. O., Kelsoe, G., Mascola, J. R., & Nabel, G. J. (2015). *Chapter 24 - The Cellular and Molecular Biology of HIV-1 Broadly Neutralizing Antibodies* (F. W. Alt, T. Honjo, A. Radbruch, & M. B. T.-. M. B. of B. C. (Second. E. Reth, Eds.; pp. 441–461). Academic Press. https://doi.org/https://doi.org/10.1016/B978-0-12-397933-9.00024-2

Haynes, B. F., Wiehe, K., Borrow, P., Saunders, K. O., Korber, B., Wagh, K., McMichael, A. J., Kelsoe, G., Hahn, B. H., Alt, F., & Shaw, G. M. (2023). Strategies for HIV-1 vaccines that induce broadly neutralizing antibodies. *Nature Reviews. Immunology*, *23*(3), 142–158. https://doi.org/10.1038/s41577-022-00753-w

Hehle, V., Beretta, M., Bourgine, M., Ait-Goughoulte, M., Planchais, C., Morisse, S., Vesin, B., Lorin, V., Hieu, T., Stauffer, A., et al. (2020). Potent human broadly neutralizing antibodies to hepatitis b virus from natural controllers. *Journal of Experimental Medicine*, *217*(10), e20200840.

Hemelaar, J., Elangovan, R., Yun, J., Dickson-Tetteh, L., Fleminger, I., Kirtley, S., Williams, B., Gouws-Williams, E., Ghys, P. D., Abimiku, A. G., Agwale, S., Archibald, C., Avidor, B., Barbás, M. G., Barre-Sinoussi, F., Barugahare, B., Belabbes, E. H., Bertagnolio, S., Birx, D., ... Zhang, R. (2019). Global and regional molecular epidemiology of HIV-1, 1990–2015: a systematic review, global survey, and trend analysis. *The Lancet Infectious Diseases*, *19*(2), 143–155. https://doi.org/10.1016/S1473-3099(18)30647-9

Henderson M.S.C., Fidler S., Cheung M., F. C. (2023). The BONDY Study: Bone Density in Youth Living with Perinatally-Acquired HIV. *CROI*.

Henrich, T. J., Hatano, H., Bacon, O., Hogan, L. E., Rutishauser, R., Hill, A., Kearney, M. F., Anderson, E. M., Buchbinder, S. P., Cohen, S. E., et al. (2017). HIV-1 persistence following extremely early initiation of antiretroviral therapy (ART) during acute HIV-1 infection: An observational study. *PLoS Medicine*, *14*(11), e1002417.

Hepler, N. L., Scheffler, K., Weaver, S., Murrell, B., Richman, D. D., Burton, D. R., Poignard, P., Smith, D. M., & Kosakovsky Pond, S. L. (2014). IDEPI: Rapid Prediction of HIV-1 Antibody Epitopes and Other Phenotypic Features from Sequence Data Using a Flexible Machine Learning Platform. *PLOS Computational Biology*, *10*(9), e1003842. https://doi.org/10.1371/journal.pcbi.1003842

Hessell, A. J., Hangartner, L., Hunter, M., Havenith, C. E. G., Beurskens, F. J., Bakker, J. M., Lanigan, C. M. S., Landucci, G., Forthal, D. N., Parren, P. W. H. I., Marx, P. A., & Burton, D. R. (2007). Fc receptor but not complement binding is important in antibody protection against HIV. *Nature*, *449*(7158), 101–104. https://doi.org/10.1038/nature06106

Hiener, B., Horsburgh, B. A., Eden, J.-S., Barton, K., Schlub, T. E., Lee, E., Stockenstrom, S. von, Odevall, L., Milush, J. M., Liegler, T., et al. (2017). Identification of genetically intact HIV-1 proviruses in specific CD4+ t cells from effectively treated participants. *Cell Reports*, *21*(3), 813–822.

Ho, Y.-C., Shan, L., Hosmane, N. N., Wang, J., Laskey, S. B., Rosenbloom, D. I. S., Lai, J., Blankson, J. N., Siliciano, J. D., & Siliciano, R. F. (2013). Replication-Competent Noninduced Proviruses in the Latent Reservoir Increase Barrier to HIV-1 Cure. *Cell*, *155*(3), 540–551. https://doi.org/https://doi.org/10.1016/j.cell.2013.09.020

Hocqueloux, L., Prazuck, T., Avettand-Fenoel, V., Lafeuillade, A., Cardon, B., Viard, J.-P., & Rouzioux, C. (2010). Long-term immunovirologic control following antiretroviral therapy interruption in patients treated at the time of primary HIV-1 infection. *Aids*, *24*(10), 1598–1601.

Hogan, L. E., Vasquez, J., Hobbs, K. S., Hanhauser, E., Aguilar-Rodriguez, B., Hussien, R., Thanh, C., Gibson, E. A., Carvidi, A. B., Smith, L. C., et al. (2018). Increased HIV-1 transcriptional activity and infectious burden in peripheral blood and gut-associated CD4+ t cells expressing CD30. *PLoS Pathogens*, *14*(2), e1006856.

Honke, N., Shaabani, N., Zhang, D.-E., Hardt, C., & Lang, K. S. (2016). Multiple functions of USP18. *Cell Death & Disease*, *7*(11), e2444–e2444. https://doi.org/10.1038/cddis.2016.326

Hsu, D. C., Mellors, J. W., & Vasan, S. (2021). Can Broadly Neutralizing HIV-1 Antibodies Help Achieve an ART-Free Remission? *Frontiers in Immunology*, *12*, 710044. https://doi.org/10.3389/fimmu.2021.710044

Hurst, J., Hoffmann, M., Pace, M., Williams, J. P., Thornhill, J., Hamlyn, E., Meyerowitz, J., Willberg, C., Koelsch, K. K., Robinson, N., Brown, H., Fisher, M., Kinloch, S., Cooper, D. A., Schechter, M., Tambussi, G., Fidler, S., Babiker, A., Weber, J., … Frater, J. (2015). Immunological biomarkers predict HIV-1 viral rebound after treatment interruption. *Nature Communications*, *6*, 8495. https://doi.org/10.1038/ncomms9495

Hussein, M., Molina, M. A., Berkhout, B., & Herrera-Carrillo, E. (2023). A CRISPR-Cas Cure for HIV/AIDS. *International Journal of Molecular Sciences*, *24*(2). https://doi.org/10.3390/ijms24021563

Hütter, G., Nowak, D., Mossner, M., Ganepola, S., MüSSig, A., Allers, K., Schneider, T., Hofmann, J., Kücherer, C., Blau, O., et al. (2009). Long-term control of HIV by CCR5 Delta32/Delta32 stem-cell transplantation. *New England Journal of Medicine*, *360*(7), 692–698.

Hyrcza, M. D., Kovacs, C., Loutfy, M., Halpenny, R., Heisler, L., Yang, S., Wilkins, O., Ostrowski, M., & Der, S. D. (2007). Distinct Transcriptional Profiles in Ex Vivo CD4+ and CD8+ T Cells Are Established Early in Human Immunodeficiency Virus Type 1 Infection and Are Characterized by a Chronic Interferon Response as Well as Extensive Transcriptional Changes in CD8+ T Cells. *Journal of Virology*, *81*(7), 3477–3486. https://doi.org/10.1128/JVI.01552-06

Iyer, S. S., Bibollet-Ruche, F., Sherrill-Mix, S., Learn, G. H., Plenderleith, L., Smith, A. G., Barbian, H. J., Russell, R. M., Gondim, M. V. P., Bahari, C. Y., Shaw, C. M., Li, Y., Decker, T., Haynes, B. F., Shaw, G. M., Sharp, P. M., Borrow, P., & Hahn, B. H. (2017). Resistance to type 1 interferons is a major determinant of HIV-1 transmission fitness. *Proceedings of the National Academy of Sciences*, *114*(4), E590 LP–E599. https://doi.org/10.1073/pnas.1620144114

J., van G. M., M., B. E., D., B.-N. B., A., B. J., Marijke, T.-K., Naomi, V., & Hanneke, S. (2011). Longer V1V2 Region with Increased Number of Potential N-Linked Glycosylation Sites in the HIV-1 Envelope Glycoprotein Protects against HIV-Specific Neutralizing Antibodies . *Journal of Virology*, *85*(14), 6986–6995. https://doi.org/10.1128/JVI.00268-11

Jain, A., Canepa, G. E., Liou, M.-L., Fledderman, E. L., Chapoval, A. I., Xiao, L., Mukherjee, I., Balogun, B. M., Huaman-Vergara, H., Galvin, J. A., Kumar, P. N., Bordon, J., Conant, M. A., & Boyle, J. S. (2024). *Multiple treatment interruptions and protecting HIV-specific CD4 T cells enable durable CD8 T*

cell response and viral control (Vol. 11). https://www.frontiersin.org/articles/10.3389/fmed.2024.1342476

Jain, V., Hartogensis, W., Bacchetti, P., Hunt, P. W., Hatano, H., Sinclair, E., Epling, L., Lee, T.-H., Busch, M. P., McCune, J. M., Pilcher, C. D., Hecht, F. M., & Deeks, S. G. (2013). Antiretroviral therapy initiated within 6 months of HIV infection is associated with lower T-cell activation and smaller HIV reservoir size. *The Journal of Infectious Diseases*, *208*(8), 1202–1211. https://doi.org/10.1093/infdis/jit311

Jassal, B., Matthews, L., Viteri, G., Gong, C., Lorente, P., Fabregat, A., Sidiropoulos, K., Cook, J., Gillespie, M., Haw, R., Loney, F., May, B., Milacic, M., Rothfels, K., Sevilla, C., Shamovsky, V., Shorser, S., Varusai, T., Weiser, J., ... D'Eustachio, P. (2020). The reactome pathway knowledgebase. *Nucleic Acids Research*, *48*(D1), D498–D503. https://doi.org/10.1093/nar/gkz1031

Jensen, B.-E. O., Knops, E., Cords, L., Lübke, N., Salgado, M., Busman-Sahay, K., Estes, J. D., Huyveneers, L. E. P., Perdomo-Celis, F., Wittner, M., Gálvez, C., Mummert, C., Passaes, C., Eberhard, J. M., Münk, C., Hauber, I., Hauber, J., Heger, E., De Clercq, J., ... Kobbe, G. (2023). In-depth virological and immunological characterization of HIV-1 cure after CCR5Δ32/Δ32 allogeneic hematopoietic stem cell transplantation. *Nature Medicine*, *29*(3), 583–587. https://doi.org/10.1038/s41591-023-02213-x

Jeong, S.-I., Kim, J.-W., Ko, K.-P., Ryu, B.-K., Lee, M.-G., Kim, H.-J., & Chi, S.-G. (2018). XAF1 forms a positive feedback loop with IRF-1 to drive apoptotic stress response and suppress tumorigenesis. *Cell Death & Disease*, *9*(8), 806. https://doi.org/10.1038/s41419-018-0867-4

Jiang, C., Lian, X., Gao, C., Sun, X., Einkauf, K. B., Chevalier, J. M., Chen, S. M. Y., Hua, S., Rhee, B., Chang, K., Blackmer, J. E., Osborn, M., Peluso, M. J., Hoh, R., Somsouk, M., Milush, J., Bertagnolli, L. N., Sweet, S. E., Varriale, J. A., ... Yu, X. G. (2020). Distinct viral reservoirs in individuals with spontaneous control of HIV-1. *Nature*, *585*(7824), 261–267. https://doi.org/10.1038/s41586-020-2651-8

Johnston, C. D., O'Brien, R., & Côté, H. C. (2023). Inclusion of women in HIV research and clinical trials. *Aids*, *37*(6), 995–997.

Jordan, M. R., Kearney, M., Palmer, S., Shao, W., Maldarelli, F., Coakley, E. P., Chappey, C., Wanke, C., & Coffin, J. M. (2010). Comparison of standard PCR/cloning to single genome sequencing for analysis of HIV-1 populations. *Journal of Virological Methods*, *168*(1-2), 114–120.

Joseph, S. B., Swanstrom, R., Kashuba, A. D. M., & Cohen, M. S. (2015). Bottlenecks in HIV-1 transmission: insights from the study of founder viruses. *Nature Reviews Microbiology*, *13*(7), 414–425. https://doi.org/10.1038/nrmicro3471

Julg, B., Dee, L., Ananworanich, J., Barouch, D. H., Bar, K., Caskey, M., Colby, D. J., Dawson, L., Dong, K. L., Dubé, K., Eron, J., Frater, J., Gandhi, R. T., Geleziunas, R., Goulder, P., Hanna, G. J., Jefferys, R., Johnston, R., Kuritzkes, D., ... Walker, B. D. (2019). Recommendations for analytical antiretroviral treatment interruptions in HIV research trials-report of a consensus meeting. *The Lancet. HIV*, *6*(4), e259–e268. https://doi.org/10.1016/S2352-3018(19)30052-9

Junker, F., Gordon, J., & Qureshi, O. (2020). Fc gamma receptors and their role in antigen uptake, presentation, and t cell activation. *Frontiers in Immunology*, *11*, 1393.

Karuna, S. T., & Corey, L. (2020). Broadly Neutralizing Antibodies for HIV Prevention [Journal Article]. *Annual Review of Medicine*, *71*(Volume 71, 2020), 329–346. https://doi.org/https://doi.org/10.1146/annurev-med-110118-045506

Kaslow, R. A., Ostrow, D. G., Detels, R., Phair, J. P., Polk, B. F., Rinaldo Jr., C. R., & Study, for the M. A. C. (1987). The Multicenter AIDS Cohort Study: rationale, organization, and selected characteristics of the participants. *American Journal of Epidemiology*, *126*(2), 310–318. https://doi.org/10.1093/aje/126.2.310

Kazer, S. W., Walker, B. D., & Shalek, A. K. (2020). Evolution and Diversity of Immune Responses during Acute HIV Infection. *Immunity*, *53*(5), 908–924. https://doi.org/https://doi.org/10.1016/j.immuni.2020.10.015

Kearney, M. F., Spindler, J., Shao, W., Yu, S., Anderson, E. M., O'Shea, A., Rehm, C., Poethke, C., Kovacs, N., Mellors, J. W., Coffin, J. M., & Maldarelli, F. (2014). Lack of Detectable HIV-1 Molecular Evolution during Suppressive Antiretroviral Therapy. *PLOS Pathogens*, *10*(3), 1–14. https://doi.org/10.1371/journal.ppat.1004010

Keele, B. F., Giorgi, E. E., Salazar-Gonzalez, J. F., Decker, J. M., Pham, K. T., Salazar, M. G., Sun, C., Grayson, T., Wang, S., Li, H., Wei, X., Jiang, C., Kirchherr, J. L., Gao, F., Anderson, J. A., Ping, L.-H., Swanstrom, R., Tomaras, G. D., Blattner, W. A., ... Shaw, G. M. (2008). Identification and characterization of transmitted and early founder virus envelopes in primary HIV-1 infection. *Proceedings of the National Academy of Sciences*, *105*(21), 7552 LP–7557. https://doi.org/10.1073/pnas.0802203105

Kiepiela, P., Ngumbela, K., Thobakgale, C., Ramduth, D., Honeyborne, I., Moodley, E., Reddy, S., Pierres, C. de, Mncube, Z., Mkhwanazi, N., Bishop, K., Stok, M. van der, Nair, K., Khan, N., Crawford, H., Payne, R., Leslie, A., Prado, J., Prendergast, A., ... Goulder, P. (2007). CD8+ T-cell responses to different HIV proteins have discordant associations with viral load. *Nature Medicine*, *13*(1), 46–53. https://doi.org/10.1038/nm1520

Kijak, G. H., & McCutchan, F. E. (2005). HIV diversity, molecular epidemiology, and the role of recombination. *Current Infectious Disease Reports*, *7*(6), 480–488. https://doi.org/10.1007/s11908-005-0051-8

Kinloch, N. N., Ren, Y., Conce Alberto, W. D., Dong, W., Khadka, P., Huang, S. H., Mota, T. M., Wilson, A., Shahid, A., Kirkby, D., et al. (2021). HIV-1 diversity considerations in the application of the intact proviral DNA assay (IPDA). *Nature Communications*, *12*(1), 165.

Kirchhoff, F. (2021). HIV Life Cycle: Overview. In T. J. Hope, M. Stevenson, & D. Richman (Eds.), *Encyclopedia of AIDS* (pp. 1–9). Springer New York. https://doi.org/10.1007/978-1-4614-9610-6_60-1

Kirchner, J. T. (2023). 21C3Origin, Evolution, and Spread of HIV1 & HIV2. In *Fundamentals of HIV medicine 2023*. Oxford University Press. https://doi.org/10.1093/med/9780197679098.003.0003

Klein, F., Mouquet, H., Dosenovic, P., Scheid, J. F., Scharf, L., & Nussenzweig, M. C. (2013). Antibodies in HIV-1 vaccine development and therapy. *Science (New York, N.Y.)*, *341*(6151), 1199–1204. https://doi.org/10.1126/science.1241144

Klein, S. L., & Flanagan, K. L. (2016). Sex differences in immune responses. *Nature Reviews Immunology*, *16*(10), 626–638.

Krebs, S. J., & Ananworanich, J. (2016). Immune activation during acute HIV infection and the impact of early antiretroviral therapy. *Current Opinion in HIV and AIDS*, *11*(2). https://journals.lww.com/co-hivandaids/Fulltext/2016/03000/Immune_activation_during_acute_HIV_infection_and.7.aspx

Kühnert, D., Kouyos, R., Shirreff, G., Peerska, J., Scherrer, A. U., Böni, J., Yerly, S., Klimkait, T., Aubert, V., Günthard, H. F., et al. (2018). Quantifying the fitness cost of HIV-1 drug resistance mutations through phylodynamics. *PLoS Pathogens*, *14*(2), e1006895.

Kuniholm, J., Coote, C., & Henderson, A. J. (2022). Defective HIV-1 genomes and their potential impact on HIV pathogenesis. *Retrovirology*, *19*(1), 13. https://doi.org/10.1186/s12977-022-00601-8

Kwong, P. D., & Mascola, J. R. (2012). Human antibodies that neutralize HIV-1: identification, structures, and B cell ontogenies. *Immunity*, *37*(3), 412–425. https://doi.org/10.1016/j.immuni.2012.08.012

Laird, G. M., Eisele, E. E., Rabi, S. A., Lai, J., Chioma, S., Blankson, J. N., Siliciano, J. D., & Siliciano, R. F. (2013). Rapid quantification of the latent

reservoir for HIV-1 using a viral outgrowth assay. *PLoS Pathogens*, *9*(5), e1003398.

Landais, E., & Moore, P. L. (2018). Development of broadly neutralizing antibodies in HIV-1 infected elite neutralizers. *Retrovirology*, *15*(1), 61. https://doi.org/10.1186/s12977-018-0443-0

Langfelder, P., & Horvath, S. (2008). WGCNA: an R package for weighted correlation network analysis. *BMC Bioinformatics*, *9*(1), 559. https://doi.org/10.1186/1471-2105-9-559

Lau, J. S., Smith, M. Z., Lewin, S. R., & McMahon, J. H. (2019). Clinical trials of antiretroviral treatment interruption in HIV-infected individuals. *Aids*, *33*(5), 773–791.

Lee, M. J., Collins, S., Babalis, D., Johnson, N., Falaschetti, E., Prevost, A. T., Ashraf, A., Cole, T., Hurley, L., Pace, M., Ogbe, A., Khan, M., Zacharopoulou, P., Brown, H., Box, H., Fox, J., Deeks, S., Horowitz, J., Nussenzweig, M. C., ... Fidler, S. (2021). The RIO Trial: Rationale, Design, And The Role of Community Involvement In A Randomised Placebo-Controlled Trial of Antiretroviral Therapy Plus Dual Long-Acting HIV-Specific Broadly Neutralising Antibodies (bNAbs) In Participants Diagnosed With Recent HIV. *Trials*. https://doi.org/10.21203/rs.3.rs-617615/v1

Lee, M. J., Fidler, S., & Frater, J. (2022). Immunotherapeutic approaches to HIV cure and remission. *Current Opinion in Infectious Diseases*, *35*(1). https://journals.lww.com/co-infectiousdiseases/fulltext/2022/02000/immunotherapeutic_approaches_to_hiv_cure_and.6.aspx

Leitner, T., & Albert, J. (1999). The molecular clock of HIV-1 unveiled through analysis of a known transmission history. *Proceedings of the National Academy of Sciences of the United States of America*, *96*(19), 10752–10757. https://doi.org/10.1073/pnas.96.19.10752

Lemey, P., Rambaut, A., & Pybus, O. G. (2006). HIV evolutionary dynamics within and among hosts. *Aids Rev*, *8*(3), 125–140.

Lepelley, A., Louis, S., Sourisseau, M., Law, H. K. W., Pothlichet, J., Schilte, C., Chaperot, L., Plumas, J., Randall, R. E., Si-Tahar, M., Mammano, F., Albert, M. L., & Schwartz, O. (2011). Innate Sensing of HIV-Infected Cells. *PLOS Pathogens*, *7*(2), 1–15. https://doi.org/10.1371/journal.ppat.1001284

Levy, C. N., Hughes, S. M., Roychoudhury, P., Reeves, D. B., Amstuz, C., Zhu, H., Huang, M.-L., Wei, Y., Bull, M. E., Cassidy, N. A. J., McClure, J., Frenkel, L. M., Stone, M., Bakkour, S., Wonderlich, E. R., Busch, M. P., Deeks, S. G., Schiffer, J. T., Coombs, R. W., ... Hladik, F. (2021). A highly multiplexed droplet digital PCR assay to measure the intact HIV-1 proviral reservoir. *Cell Reports. Medicine*, *2*(4), 100243. https://doi.org/10.1016/j.xcrm.2021.100243

Leyre, L., Kroon, E., Vandergeeten, C., Sacdalan, C., Colby, D. J., Buranapraditkun, S., Schuetz, A., Chomchey, N., Souza, M. de, Bakeman, W., Fromentin, R., Pinyakorn, S., Akapirat, S., Trichavaroj, R., Chottanapund, S., Manasnayakorn, S., Rerknimitr, R., Wattanaboonyoungcharoen, P., Kim, J. H., ... Chomont, N. (2020). Abundant HIV-infected cells in blood and tissues are rapidly cleared upon ART initiation during acute HIV infection. *Science Translational Medicine*, *12*(533). https://doi.org/10.1126/scitranslmed.aav3491

Li, J. Z., Etemad, B., Ahmed, H., Aga, E., Bosch, R. J., Mellors, J. W., Kuritzkes, D. R., Lederman, M. M., Para, M., & Gandhi, R. T. (2016). The size of the expressed HIV reservoir predicts timing of viral rebound after treatment interruption. *AIDS (London, England)*, *30*(3), 343–353. https://doi.org/10.1097/QAD.0000000000000953

Li, W.-H., Tanimura, M., & Sharp, P. M. (1988). Rates and dates of divergence between AIDS virus nucleotide sequences. *Molecular Biology and Evolution*, *5*(4), 313–330.

Lorenzi, J. C., Cohen, Y. Z., Cohn, L. B., Kreider, E. F., Barton, J. P., Learn, G. H., Oliveira, T., Lavine, C. L., Horwitz, J. A., Settler, A., et al. (2016). Paired quantitative and qualitative assessment of the replication-competent

HIV-1 reservoir and comparison with integrated proviral DNA. *Proceedings of the National Academy of Sciences*, *113*(49), E7908–E7916.

Love, M. I., Huber, W., & Anders, S. (2014). Moderated estimation of fold change and dispersion for RNA-seq data with DESeq2. *Genome Biology*, *15*(12), 550. https://doi.org/10.1186/s13059-014-0550-8

Lynch, R. M., Shen, T., Gnanakaran, S., & Derdeyn, C. A. (2009). Appreciating HIV type 1 diversity: subtype differences in Env. *AIDS Research and Human Retroviruses*, *25*(3), 237–248. https://doi.org/10.1089/aid.2008.0219

Lynch, R. M., Wong, P., Tran, L., O'Dell, S., Nason, M. C., Li, Y., Wu, X., & Mascola, J. R. (2015). HIV-1 fitness cost associated with escape from the VRC01 class of CD4 binding site neutralizing antibodies. *Journal of Virology*, *89*(8), 4201–4213. https://doi.org/10.1128/JVI.03608-14

Lythgoe, K. A., & Fraser, C. (2012). New insights into the evolutionary rate of HIV-1 at the within-host and epidemiological levels. *Proceedings of the Royal Society B: Biological Sciences*, *279*(1741), 3367–3375. https://doi.org/10.1098/rspb.2012.0595

Macharia, G. N., Yue, L., Staller, E., Dilernia, D., Wilkins, D., Song, H., McGowan, E., King, D., Fast, P., Imami, N., Price, M. A., Sanders, E. J., Hunter, E., & Gilmour, J. (2020). Infection with multiple HIV-1 founder variants is associated with lower viral replicative capacity, faster CD4+ T cell decline and increased immune activation during acute infection. *PLOS Pathogens*, *16*(9), e1008853. https://doi.org/10.1371/journal.ppat.1008853

Margolis, D. M., Archin, N. M., Cohen, M. S., Eron, J. J., Ferrari, G., Garcia, J. V., Gay, C. L., Goonetilleke, N., Joseph, S. B., Swanstrom, R., Turner, A.-M. W., & Wahl, A. (2020). Curing HIV: Seeking to Target and Clear Persistent Infection. *Cell*, *181*(1), 189–206. https://doi.org/10.1016/j.cell.2020.03.005

Martin, G. E., & Frater, J. (2018). Post-treatment and spontaneous HIV control. *Current Opinion in HIV and AIDS*, *13*(5). https://journals.lww.com/co-hivandaids/fulltext/2018/09000/post_treatment_and_spontaneous_hiv_control.6.aspx

Martin, G. E., Gossez, M., Williams, J. P., Stöhr, W., Meyerowitz, J., Leitman, E. M., Goulder, P., Porter, K., Fidler, S., Frater, J., & Investigators, the S. T. (2017). Post-treatment control or treated controllers? Viral remission in treated and untreated primary HIV infection. *AIDS (London, England)*, *31*(4), 477–484. https://doi.org/10.1097/QAD.0000000000001382

Martin, G. E., Pace, M., Thornhill, J. P., Phetsouphanh, C., Meyerowitz, J., Gossez, M., Brown, H., Olejniczak, N., Lwanga, J., Ramjee, G., et al. (2018). CD32-expressing CD4 t cells are phenotypically diverse and can contain proviral HIV DNA. *Frontiers in Immunology*, *9*, 928.

Martinsen, J. T., Gunst, J. D., Højen, J. F., Tolstrup, M., & Søgaard, O. S. (2020). The Use of Toll-Like Receptor Agonists in HIV-1 Cure Strategies. *Frontiers in Immunology*, *11*, 1112. https://doi.org/10.3389/fimmu.2020.01112

Martín-Vicente, M., Medrano, L. M., Resino, S., García-Sastre, A., & Martínez, I. (2017). TRIM25 in the Regulation of the Antiviral Innate Immunity. *Frontiers in Immunology*, *8*, 1187. https://doi.org/10.3389/fimmu.2017.01187

Mayer, K. H., Hanna, G. J., & D'Aquila, R. T. (2001). Clinical Use of Genotypic and Phenotypic Drug Resistance Testing to Monitor Antiretroviral Chemotherapy. *Clinical Infectious Diseases*, *32*(5), 774–782. https://doi.org/10.1086/319231

McCoy, L. E. (2018). The expanding array of HIV broadly neutralizing antibodies. *Retrovirology*, *15*(1), 70. https://doi.org/10.1186/s12977-018-0453-y

McCoy, L. E., & McKnight, Á. (2017). Lessons learned from humoral responses of HIV patients. *Current Opinion in HIV and AIDS*, *12*(3). https://journals.lww.com/co-hivandaids/Fulltext/2017/05000/Lessons_learned_from_humoral_responses_of_HIV.3.aspx

McMichael, A. J., Borrow, P., Tomaras, G. D., Goonetilleke, N., & Haynes, B. F. (2010). The immune response during acute HIV-1 infection: clues for vaccine development. *Nature Reviews. Immunology*, *10*(1), 11–23. https://doi.org/10.1038/nri2674

McNab, F., Mayer-Barber, K., Sher, A., Wack, A., & O'Garra, A. (2015). Type I interferons in infectious disease. *Nature Reviews Immunology*, *15*(2), 87–103. https://doi.org/10.1038/nri3787

Meijers, M., Vanshylla, K., Gruell, H., Klein, F., & Lässig, M. (2021). Predicting in vivo escape dynamics of HIV-1 from a broadly neutralizing antibody. *Proceedings of the National Academy of Sciences*, *118*(30), e2104651118. https://doi.org/10.1073/pnas.2104651118

Mendoza, P., Gruell, H., Nogueira, L., Pai, J. A., Butler, A. L., Millard, K., Lehmann, C., Suárez, I., Oliveira, T. Y., Lorenzi, J. C. C., Cohen, Y. Z., Wyen, C., Kümmerle, T., Karagounis, T., Lu, C.-L., Handl, L., Unson-O'Brien, C., Patel, R., Ruping, C., ... Nussenzweig, M. C. (2018). Combination therapy with anti-HIV-1 antibodies maintains viral suppression. *Nature*, *561*(7724), 479–484. https://doi.org/10.1038/s41586-018-0531-2

Mendoza, P., Jackson, J. R., Oliveira, T. Y., Gaebler, C., Ramos, V., Caskey, M., Jankovic, M., Nussenzweig, M. C., & Cohn, L. B. (2020). Antigen-responsive CD4+ T cell clones contribute to the HIV-1 latent reservoir. *The Journal of Experimental Medicine*, *217*(7). https://doi.org/10.1084/jem.20200051

Metzner, K. J. (2022). Technologies for HIV-1 drug resistance testing: inventory and needs. *Current Opinion in HIV and AIDS*, *17*(4). https://journals.lww.com/co-hivandaids/Fulltext/2022/07000/Technologies_for_HIV_1_drug_resistance_testing_.9.aspx

Michaud, H.-A., Gomard, T., Gros, L., Thiolon, K., Nasser, R., Jacquet, C., Hernandez, J., Piechaczyk, M., & Pelegrin, M. (2010). A Crucial Role for Infected-Cell/Antibody Immune Complexes in the Enhancement of Endogenous Antiviral Immunity by Short Passive Immunotherapy. *PLOS Pathogens*, *6*(6), e1000948. https://doi.org/10.1371/journal.ppat.1000948

Moore, P. L., Ranchobe, N., Lambson, B. E., Gray, E. S., Cave, E., Abrahams, M.-R., Bandawe, G., Mlisana, K., Abdool Karim, S. S., Williamson, C., & Morris, L. (2009). Limited neutralizing antibody specificities drive neutralization escape

in early HIV-1 subtype C infection. *PLoS Pathogens*, *5*(9), e1000598. https://doi.org/10.1371/journal.ppat.1000598

Mootha, V. K., Lindgren, C. M., Eriksson, K.-F., Subramanian, A., Sihag, S., Lehar, J., Puigserver, P., Carlsson, E., Ridderstråle, M., Laurila, E., Houstis, N., Daly, M. J., Patterson, N., Mesirov, J. P., Golub, T. R., Tamayo, P., Spiegelman, B., Lander, E. S., Hirschhorn, J. N., ... Groop, L. C. (2003). PGC-1α-responsive genes involved in oxidative phosphorylation are coordinately downregulated in human diabetes. *Nature Genetics*, *34*(3), 267–273. https://doi.org/10.1038/ng1180

Moraka, N. O., Choga, W. T., Pema, M. N., Chawawa, M. K., Gobe, I., Mokomane, M., Bareng, O. T., Bhebhe, L., Kelentse, N., Mulenga, G., et al. (2023). Predicted resistance to broadly neutralizing antibodies (bnAbs) and associated HIV-1 envelope characteristics among seroconverting adults in botswana. *Scientific Reports*, *13*(1), 18134.

Mouquet, H., Scharf, L., Euler, Z., Liu, Y., Eden, C., Scheid, J. F., Halper-Stromberg, A., Gnanapragasam, P. N. P., Spencer, D. I. R., Seaman, M. S., Schuitemaker, H., Feizi, T., Nussenzweig, M. C., & Bjorkman, P. J. (2012). Complex-type N-glycan recognition by potent broadly neutralizing HIV antibodies. *Proceedings of the National Academy of Sciences of the United States of America*, *109*(47), E3268–E3277. https://doi.org/10.1073/pnas.1217207109

Mu, Z., Haynes, B. F., & Cain, D. W. (2021). *HIV mRNA Vaccines—Progress and Future Paths* (No. 2; Vol. 9). https://doi.org/10.3390/vaccines9020134

Naif, H. M. (2013). Pathogenesis of HIV infection. *Infectious Disease Reports*, *5*(Suppl 1), e6.

Namazi, G., Fajnzylber, J. M., Aga, E., Bosch, R. J., Acosta, E. P., Sharaf, R., Hartogensis, W., Jacobson, J. M., Connick, E., Volberding, P., Skiest, D., Margolis, D., Sneller, M. C., Little, S. J., Gianella, S., Smith, D. M., Kuritzkes, D. R., Gulick, R. M., Mellors, J. W., ... Li, J. Z. (2018). The Control of HIV After Antiretroviral Medication Pause (CHAMP) Study: Posttreatment

Controllers Identified From 14 Clinical Studies. *The Journal of Infectious Diseases*, *218*(12), 1954–1963. https://doi.org/10.1093/infdis/jiy479

Naranjo-Gomez, M., Cahen, M., Lambour, J., Boyer-Clavel, M., & Pelegrin, M. (2021). Immunomodulatory Role of NK Cells during Antiviral Antibody Therapy. *Vaccines*, *9*(2). https://doi.org/10.3390/vaccines9020137

Naranjo-Gomez, M., & Pelegrin, M. (2019). Vaccinal effect of HIV-1 antibody therapy. *Current Opinion in HIV and AIDS*, *14*(4), 325–333. https://doi.org/10.1097/COH.0000000000000555

Nassal, M. (2015). HBV cccDNA: Viral persistence reservoir and key obstacle for a cure of chronic hepatitis b. *Gut*, *64*(12), 1972–1984.

Ndjoyi-Mbiguino, A., Zoa-Assoumou, S., Mourembou, G., & Ennaji, M. M. (2020). Chapter 10 - human immunodeficiency virus: A brief review. In M. M. Ennaji (Ed.), *Emerging and reemerging viral pathogens* (pp. 183–200). Academic Press. https://doi.org/https://doi.org/10.1016/B978-0-12-819400-3.00010-7

Newton, R., Priyadharshini, B., & Turka, L. A. (2016). Immunometabolism of regulatory T cells. *Nature Immunology*, *17*(6), 618–625. https://doi.org/10.1038/ni.3466

Niessl, J., Baxter, A. E., Mendoza, P., Jankovic, M., Cohen, Y. Z., Butler, A. L., Lu, C.-L., Dubé, M., Shimeliovich, I., Gruell, H., Klein, F., Caskey, M., Nussenzweig, M. C., & Kaufmann, D. E. (2020). Combination anti-HIV-1 antibody therapy is associated with increased virus-specific T cell immunity. *Nature Medicine*, *26*(2), 222–227. https://doi.org/10.1038/s41591-019-0747-1

Nijhuis, M., Deeks, S., & Boucher, C. (2001). Implications of antiretroviral resistance on viral fitness. *Current Opinion in Infectious Diseases*, *14*(1). https://journals.lww.com/co-infectiousdiseases/fulltext/2001/02000/implications%7B/_%7Dof%7B/_%7Dantiretroviral%7B/_%7Dresistance%7B/_%7Don%7B/_%7Dviral.5.aspx

Nishimura, Y., Gautam, R., Chun, T.-W., Sadjadpour, R., Foulds, K. E., Shingai, M., Klein, F., Gazumyan, A., Golijanin, J., Donaldson, M., Donau, O. K., Plishka, R. J., Buckler-White, A., Seaman, M. S., Lifson, J. D., Koup, R. A.,

Fauci, A. S., Nussenzweig, M. C., & Martin, M. A. (2017). Early antibody therapy can induce long-lasting immunity to SHIV. *Nature*, *543*(7646), 559–563. https://doi.org/10.1038/nature21435

Nuvor, S. V. (2018). *Natural Killer Cells Function and Innate Immunity in HIV-2 Infection BT - Encyclopedia of AIDS* (T. J. Hope, D. D. Richman, & M. Stevenson, Eds.; pp. 1442–1451). Springer New York. https://doi.org/10.1007/978-1-4939-7101-5_40

Okulicz, J. F., & Lambotte, O. (2011). Epidemiology and clinical characteristics of elite controllers. *Current Opinion in HIV and AIDS*, *6*(3), 163–168.

Oxenius, A., Price, D. A., Günthard, H. F., Dawson, S. J., Fagard, C., Perrin, L., Fischer, M., Weber, R., Plana, M., Garca, F., et al. (2002). Stimulation of HIV-specific cellular immunity by structured treatment interruption fails to enhance viral control in chronic HIV infection. *Proceedings of the National Academy of Sciences*, *99*(21), 13747–13752.

P., G. M. V., Scott, S.-M., Frederic, B.-R., M., R. R., Stephanie, T., G., S. A., Yingying, L., Weimin, L., N., A. A., C., D. J., Jesse, C., E., F.-M. A., Pierre, P., Ian, W., Emmanouil, P., C., L. J. C., Brenda, S. D., Felicity, M., Alexandra, M. M., … H., H. B. (2021). Heightened resistance to host type 1 interferons characterizes HIV-1 at transmission and after antiretroviral therapy interruption. *Science Translational Medicine*, *13*(576), eabd8179. https://doi.org/10.1126/scitranslmed.abd8179

Pahus, M. H., Zheng, Y., Olefsky, M., Gunst, J. D., Tebas, P., Taiwo, B., Søgaard, O. S., Peluso, M. J., Lie, Y., Reeves, J. D., et al. (2024). Evaluation and real-world experience of a neutralization susceptibility screening assay for broadly neutralizing anti–HIV-1 antibodies. *The Journal of Infectious Diseases*, jiae486.

Palmer, S., Kearney, M., Maldarelli, F., Halvas, E. K., Bixby, C. J., Bazmi, H., Rock, D., Falloon, J., Davey Jr, R. T., Dewar, R. L., et al. (2005). Multiple, linked human immunodeficiency virus type 1 drug resistance mutations in treatment-experienced patients are missed by standard genotype analysis. *Journal of Clinical Microbiology*, *43*(1), 406–413.

Panel on Antiretroviral Guidelines for Adults, N.-. (2022). Guidelines for the Use of Antiretroviral Agents in Adults and Adolescents with HIV How to Cite the Adult and Adolescent Guidelines: Panel on Antiretroviral Guidelines for Adults and Adolescents. Guidelines for the Use of Antiretroviral Agents in Adults an. *October*, *13*(1), 1–334. https://clinicalinfo.hiv.gov/

Paradis, E., & Schliep, K. (2019). ape 5.0: an environment for modern phylogenetics and evolutionary analyses in R. *Bioinformatics*, *35*(3), 526–528. https://doi.org/10.1093/bioinformatics/bty633

Parren, P. W. H. I., Burton, D. R., & Sattentau, Q. J. (1997). HIV-1 antibody — debris or virion? *Nature Medicine*, *3*(4), 366–367. https://doi.org/10.1038/nm0497-366d

Parthasarathy, D., Pothula, K. R., Ratnapriya, S., Cervera Benet, H., Parsons, R., Huang, X., Sammour, S., Janowska, K., Harris, M., Sodroski, J., et al. (2024). Conformational flexibility of HIV-1 envelope glycoproteins modulates transmitted/founder sensitivity to broadly neutralizing antibodies. *Nature Communications*, *15*(1), 7334.

Patel, H., & Dubé, K. (2023). To pre-screen or not to pre-screen for broadly neutralizing antibody sensitivity in HIV cure-related trials. *Journal of Virus Eradication*, 100339. https://doi.org/https://doi.org/10.1016/j.jve.2023.100339

Pelegrin, M., Marsile-Medun, S., Abba-Moussa, D., Souchard, M., & Naranjo-Gomez, M. (2022). Fc-Dependent Immunomodulation Induced by Antiviral Therapeutic Antibodies: New Perspectives for Eliciting Protective Immune Responses. *Antibodies (Basel, Switzerland)*, *11*(3). https://doi.org/10.3390/antib11030050

Pereira, M. S., Alves, I., Vicente, M., Campar, A., Silva, M. C., Padrão, N. A., Pinto, V., Fernandes, Â., Dias, A. M., & Pinho, S. S. (2018). *Glycans as Key Checkpoints of T Cell Activity and Function* (Vol. 9, p. 2754). https://www.frontiersin.org/article/10.3389/fimmu.2018.02754

Perng, Y.-C., & Lenschow, D. J. (2018). ISG15 in antiviral immunity and beyond. *Nature Reviews Microbiology*, *16*(7), 423–439. https://doi.org/10.1038/s41579-018-0020-5

Petrova, V. N., & Russell, C. A. (2018). The evolution of seasonal influenza viruses. *Nature Reviews Microbiology*, *16*(1), 47–60.

Phelps, M., & Balazs, A. B. (2021). Contribution to HIV Prevention and Treatment by Antibody-Mediated Effector Function and Advances in Broadly Neutralizing Antibody Delivery by Vectored Immunoprophylaxis. *Frontiers in Immunology*, *12*, 734304. https://doi.org/10.3389/fimmu.2021.734304

Pinto, D., Fenwick, C., Caillat, C., Silacci, C., Guseva, S., Dehez, F., Chipot, C., Barbieri, S., Minola, A., Jarrossay, D., Tomaras, G. D., Shen, X., Riva, A., Tarkowski, M., Schwartz, O., Bruel, T., Dufloo, J., Seaman, M. S., Montefiori, D. C., … Weissenhorn, W. (2019). Structural Basis for Broad HIV-1 Neutralization by the MPER-Specific Human Broadly Neutralizing Antibody LN01. *Cell Host & Microbe*, *26*(5), 623–637.e8. https://doi.org/10.1016/j.chom.2019.09.016

Porichis, F., & Kaufmann, D. E. (2018). HIV and SIV, CD4 T-Cell Responses to. In T. J. Hope, D. D. Richman, & M. Stevenson (Eds.), *Encyclopedia of AIDS* (pp. 661–669). Springer New York. https://doi.org/10.1007/978-1-4939-7101-5_184

Ragu, S., Matos-Rodrigues, G., & Lopez, B. S. (2020). Replication Stress, DNA Damage, Inflammatory Cytokines and Innate Immune Response. *Genes*, *11*(4), 409. https://doi.org/10.3390/genes11040409

Rambaut, A., Posada, D., Crandall, K. A., & Holmes, E. C. (2004). The causes and consequences of HIV evolution. *Nature Reviews Genetics*, *5*(1), 52–61. https://doi.org/10.1038/nrg1246

Ranasinghe, S., & Walker, B. (2018). *HIV and SIV, CD8 T Cell Responses to BT - Encyclopedia of AIDS* (T. J. Hope, D. D. Richman, & M. Stevenson, Eds.; pp. 669–677). Springer New York. https://doi.org/10.1007/978-1-4939-7101-5_185

Rashidi, M., Bandala-Sanchez, E., Lawlor, K. E., Zhang, Y., Neale, A. M., Vijayaraj, S. L., O'Donoghue, R., Wentworth, J. M., Adams, T. E., Vince, J. E., & Harrison, L. C. (2018). CD52 inhibits Toll-like receptor activation of NF-κB and triggers apoptosis to suppress inflammation. *Cell Death & Differentiation*, *25*(2), 392–405. https://doi.org/10.1038/cdd.2017.173

Rawi, R., Mall, R., Shen, C.-H., Farney, S. K., Shiakolas, A., Zhou, J., Bensmail, H., Chun, T.-W., Doria-Rose, N. A., Lynch, R. M., Mascola, J. R., Kwong, P. D., & Chuang, G.-Y. (2019). Accurate Prediction for Antibody Resistance of Clinical HIV-1 Isolates. *Scientific Reports*, *9*(1), 14696. https://doi.org/10.1038/s41598-019-50635-w

Richer, M. J., Lang, M. L., & Butler, N. S. (2016). T Cell Fates Zipped Up: How the Bach2 Basic Leucine Zipper Transcriptional Repressor Directs T Cell Differentiation and Function. *The Journal of Immunology*, *197*(4), 1009–1015. https://doi.org/10.4049/jimmunol.1600847

Roberts, H. E., Hurst, J., Robinson, N., Brown, H., Flanagan, P., Vass, L., Fidler, S., Weber, J., Babiker, A., Phillips, R. E., McLean, A. R., Frater, J., & Investigators, S. trial. (2015). Structured Observations Reveal Slow HIV-1 CTL Escape. *PLOS Genetics*, *11*(2), e1004914. https://doi.org/10.1371/journal.pgen.1004914

Robertson, D. L., Anderson, J. P., Bradac, J. A., Carr, J. K., Foley, B., Funkhouser, R. K., Gao, F., Hahn, B. H., Kalish, M. L., Kuiken, C., Learn, G. H., Leitner, T., McCutchan, F., Osmanov, S., Peeters, M., Pieniazek, D., Salminen, M., Sharp, P. M., Wolinsky, S., & Korber, B. (2000). HIV-1 nomenclature proposal. *Science*, *288*(5463), 55–55. https://doi.org/10.1126/science.288.5463.55d

Rock, K. L., & Goldberg, A. L. (1999). Degradation of cell proteins and the generation of MHC class I-presented peptides. *Annual Review of Immunology*, *17*, 739–779. https://doi.org/10.1146/annurev.immunol.17.1.739

Rosás-Umbert, M., Gunst, J. D., Pahus, M. H., Olesen, R., Schleimann, M., Denton, P. W., Ramos, V., Ward, A., Kinloch, N. N., Copertino, D. C., Escribà, T.,

Llano, A., Brumme, Z. L., Brad Jones, R., Mothe, B., Brander, C., Fox, J., Nussenzweig, M. C., Fidler, S., ... Søgaard, O. S. (2022). Administration of broadly neutralizing anti-HIV-1 antibodies at ART initiation maintains long-term CD8(+) T cell immunity. *Nature Communications*, *13*(1), 6473. https://doi.org/10.1038/s41467-022-34171-2

Rosenberg, E. S., Altfeld, M., Poon, S. H., Phillips, M. N., Wilkes, B. M., Eldridge, R. L., Robbins, G. K., D'Aquila, R. T., Goulder, P. J. R., & Walker, B. D. (2000). Immune control of HIV-1 after early treatment of acute infection. *Nature*, *407*(6803), 523–526. https://doi.org/10.1038/35035103

Roux, H., & Chomont, N. (2023). Measuring Human Immunodeficiency Virus Reservoirs: Do We Need to Choose Between Quantity and Quality? *The Journal of Infectious Diseases*, *229*(3), 635–643. https://doi.org/10.1093/infdis/jiad381

Rudensky, A., Preston-Hurlburt, P., Hong, S. C., Barlow, A., & Janeway, C. A. J. (1991). Sequence analysis of peptides bound to MHC class II molecules. *Nature*, *353*(6345), 622–627. https://doi.org/10.1038/353622a0

Rusert, P., Kouyos, R. D., Kadelka, C., Ebner, H., Schanz, M., Huber, M., Braun, D. L., Hozé, N., Scherrer, A., Magnus, C., Weber, J., Uhr, T., Cippa, V., Thorball, C. W., Kuster, H., Cavassini, M., Bernasconi, E., Hoffmann, M., Calmy, A., ... Study, T. S. H. I. V. C. (2016). Determinants of HIV-1 broadly neutralizing antibody induction. *Nature Medicine*, *22*(11), 1260–1267. https://doi.org/10.1038/nm.4187

Rusert, P., Krarup, A., Magnus, C., Brandenberg, O. F., Weber, J., Ehlert, A.-K., Regoes, R. R., Günthard, H. F., & Trkola, A. (2011). Interaction of the gp120 V1V2 loop with a neighboring gp120 unit shields the HIV envelope trimer against cross-neutralizing antibodies. *The Journal of Experimental Medicine*, *208*(7), 1419–1433. https://doi.org/10.1084/jem.20110196

Sáez-Cirión, A. (2019). Post-treatment control. *International AIDS Society Meeting*.

Sáez-Cirión, A., Bacchus, C., Hocqueloux, L., Avettand-Fenoel, V., Girault, I., Lecuroux, C., Potard, V., Versmisse, P., Melard, A., Prazuck, T., Descours, B., Guergnon, J., Viard, J.-P., Boufassa, F., Lambotte, O., Goujard, C., Meyer, L., Costagliola, D., Venet, A., ... Group, A. V. S. (2013). Post-treatment HIV-1 controllers with a long-term virological remission after the interruption of early initiated antiretroviral therapy ANRS VISCONTI Study. *PLoS Pathogens*, *9*(3), e1003211–e1003211. https://doi.org/10.1371/journal.ppat.1003211

Salantes, D. B., Zheng, Y., Mampe, F., Srivastava, T., Beg, S., Lai, J., Li, J. Z., Tressler, R. L., Koup, R. A., Hoxie, J., Abdel-Mohsen, M., Sherrill-Mix, S., McCormick, K., Overton, E. T., Bushman, F. D., Learn, G. H., Siliciano, R. F., Siliciano, J. M., Tebas, P., & Bar, K. J. (2018). HIV-1 latent reservoir size and diversity are stable following brief treatment interruption. *The Journal of Clinical Investigation*, *128*(7), 3102–3115. https://doi.org/10.1172/JCI120194

Salazar-Gonzalez, J. F., Bailes, E., Pham, K. T., Salazar, M. G., Guffey, M. B., Keele, B. F., Derdeyn, C. A., Farmer, P., Hunter, E., Allen, S., Manigart, O., Mulenga, J., Anderson, J. A., Swanstrom, R., Haynes, B. F., Athreya, G. S., Korber, B. T. M., Sharp, P. M., Shaw, G. M., & Hahn, B. H. (2008). Deciphering human immunodeficiency virus type 1 transmission and early envelope diversification by single-genome amplification and sequencing. *Journal of Virology*, *82*(8), 3952–3970. https://doi.org/10.1128/JVI.02660-07

Saleh, S., Solomon, A., Wightman, F., Xhilaga, M., Cameron, P. U., & Lewin, S. R. (2007). CCR7 ligands CCL19 and CCL21 increase permissiveness of resting memory CD4+ t cells to HIV-1 infection: A novel model of HIV-1 latency. *Blood, The Journal of the American Society of Hematology*, *110*(13), 4161–4164.

Sanders, R. W., Derking, R., Cupo, A., Julien, J.-P., Yasmeen, A., Val, N. de, Kim, H. J., Blattner, C., Peña, A. T. de la, Korzun, J., et al. (2013). A next-generation cleaved, soluble HIV-1 env trimer, BG505 SOSIP. 664 gp140,

expresses multiple epitopes for broadly neutralizing but not non-neutralizing antibodies. *PLoS Pathogens*, *9*(9), e1003618.

Sandler, N. G., Bosinger, S. E., Estes, J. D., Zhu, R. T. R., Tharp, G. K., Boritz, E., Levin, D., Wijeyesinghe, S., Makamdop, K. N., Prete, G. Q. del, Hill, B. J., Timmer, J. K., Reiss, E., Yarden, G., Darko, S., Contijoch, E., Todd, J. P., Silvestri, G., Nason, M., ... Douek, D. C. (2014). Type I interferon responses in rhesus macaques prevent SIV infection and slow disease progression. *Nature*, *511*(7511), 601–605. https://doi.org/10.1038/nature13554

Scheid, J. F., Horwitz, J. A., Bar-On, Y., Kreider, E. F., Lu, C.-L., Lorenzi, J. C. C., Feldmann, A., Braunschweig, M., Nogueira, L., Oliveira, T., Shimeliovich, I., Patel, R., Burke, L., Cohen, Y. Z., Hadrigan, S., Settler, A., Witmer-Pack, M., West Anthony P., Jr., Juelg, B., ... Caskey, M. (2016). HIV-1 antibody 3BNC117 suppresses viral rebound in humans during treatment interruption. *Nature*, *535*(7613), 556–560. https://doi.org/10.1038/nature18929

Schommers, P., Gruell, H., Abernathy, M. E., Tran, M.-K., Dingens, A. S., Gristick, H. B., Barnes, C. O., Schoofs, T., Schlotz, M., Vanshylla, K., et al. (2020). Restriction of HIV-1 escape by a highly broad and potent neutralizing antibody. *Cell*, *180*(3), 471–489.

Schoofs, T., Barnes, C. O., Suh-Toma, N., Golijanin, J., Schommers, P., Gruell, H., West, A. P., Bach, F., Lee, Y. E., Nogueira, L., Georgiev, I. S., Bailer, R. T., Czartoski, J., Mascola, J. R., Seaman, M. S., McElrath, M. J., Doria-Rose, N. A., Klein, F., Nussenzweig, M. C., & Bjorkman, P. J. (2019). Broad and Potent Neutralizing Antibodies Recognize the Silent Face of the HIV Envelope. *Immunity*, *50*(6), 1513–1529.e9. https://doi.org/https://doi.org/10.1016/j.immuni.2019.04.014

Schoofs, T., Klein, F., Braunschweig, M., Kreider, E. F., Feldmann, A., Nogueira, L., Oliveira, T., Lorenzi, J. C. C., Parrish, E. H., Learn, G. H., West Jr, A. P., Bjorkman, P. J., Schlesinger, S. J., Seaman, M. S., Czartoski, J., McElrath, M. J., Pfeifer, N., Hahn, B. H., Caskey, M., & Nussenzweig, M. C. (2016). HIV-1 therapy with monoclonal antibody 3BNC117 elicits host immune responses

against HIV-1. *Science (New York, N.Y.)*, *352*(6288), 997–1001. https://doi.org/10.1126/science.aaf0972

Schriek, A. I., Aldon, Y. L. T., Gils, M. J. van, & Taeye, S. W. de. (2024). Next-generation bNAbs for HIV-1 cure strategies. *Antiviral Research*, *222*, 105788. https://doi.org/https://doi.org/10.1016/j.antiviral.2023.105788

Schwetz, T. A., & Fauci, A. S. (2019). The extended impact of human immunodeficiency virus/AIDS research. *The Journal of Infectious Diseases*, *219*(1), 6–9.

Scully, E. P. (2018). Sex differences in HIV infection. *Current HIV/AIDS Reports*, *15*, 136–146.

Shaik, M. M., Peng, H., Lu, J., Rits-Volloch, S., Xu, C., Liao, M., & Chen, B. (2019). Structural basis of coreceptor recognition by HIV-1 envelope spike. *Nature*, *565*(7739), 318–323. https://doi.org/10.1038/s41586-018-0804-9

Shankarappa, R., Margolick, J. B., Gange, S. J., Rodrigo, A. G., Upchurch, D., Farzadegan, H., Gupta, P., Rinaldo, C. R., Learn, G. H., He, X., Huang, X. L., & Mullins, J. I. (1999). Consistent viral evolutionary changes associated with the progression of human immunodeficiency virus type 1 infection. *Journal of Virology*, *73*(12), 10489–10502. https://doi.org/10.1128/JVI.73.12.10489-10502.1999

Sharaf, R., Lee, G. Q., Sun, X., Etemad, B., Aboukhater, L. M., Hu, Z., Brumme, Z. L., Aga, E., Bosch, R. J., Wen, Y., Namazi, G., Gao, C., Acosta, E. P., Gandhi, R. T., Jacobson, J. M., Skiest, D., Margolis, D. M., Mitsuyasu, R., Volberding, P., … Li, J. Z. (2018). HIV-1 proviral landscapes distinguish posttreatment controllers from noncontrollers. *The Journal of Clinical Investigation*, *128*(9), 4074–4085. https://doi.org/10.1172/JCI120549

Sharp, P. M., & Hahn, B. H. (2011). Origins of HIV and the AIDS pandemic. *Cold Spring Harbor Perspectives in Medicine:*, *1*(1).

Shaw, G. M., & Hunter, E. (2012). HIV transmission. *Cold Spring Harbor Perspectives in Medicine*, *2*(11). https://doi.org/10.1101/cshperspect.a006965

Shelton, E. M., Reeves, D. B., & Bender Ignacio, R. A. (2020). Initiation of Antiretroviral Therapy during Primary HIV Infection: Effects on the Latent HIV Reservoir, Including on Analytic Treatment Interruptions. *AIDS Reviews*, *23*(1), 28–39. https://doi.org/10.24875/AIDSRev.20000001

Siliciano, J. D., & Siliciano, R. F. (2021). Low inducibility of latent human immunodeficiency virus type 1 proviruses as a major barrier to cure. *The Journal of Infectious Diseases*, *223*(Supplement_1), S13–S21.

Siliciano, J. D., & Siliciano, R. F. (2022). In Vivo Dynamics of the Latent Reservoir for HIV-1: New Insights and Implications for Cure. *Annual Review of Pathology*, *17*, 271–294. https://doi.org/10.1146/annurev-pathol-050520-112001

Simmonds, P., Zhang, L. Q., McOmish, F., Balfe, P., Ludlam, C. A., & Brown, A. J. (1991). Discontinuous sequence change of human immunodeficiency virus (HIV) type 1 env sequences in plasma viral and lymphocyte-associated proviral populations in vivo: implications for models of HIV pathogenesis. *Journal of Virology*, *65*(11), 6266–6276. https://doi.org/10.1128/JVI.65.11.6266-6276.1991

Skinner, N. E., & Bailey, J. R. (2020). Broadly neutralizing antibodies against hepatitis c virus: Location, location, location. *Journal of Hepatology*, *72*(4), 604–606.

Sneller, M. C., Blazkova, J., Justement, J. S., Shi, V., Kennedy, B. D., Gittens, K., Tolstenko, J., McCormack, G., Whitehead, E. J., Schneck, R. F., Proschan, M. A., Benko, E., Kovacs, C., Oguz, C., Seaman, M. S., Caskey, M., Nussenzweig, M. C., Fauci, A. S., Moir, S., & Chun, T.-W. (2022). Combination anti-HIV antibodies provide sustained virological suppression. *Nature*, *606*(7913), 375–381. https://doi.org/10.1038/s41586-022-04797-9

Snippenberg, W. van, Gleerup, D., Rutsaert, S., Vandekerckhove, L., De Spiegelaere, W., & Trypsteen, W. (2022). Triplex digital PCR assays for the quantification of intact proviral HIV-1 DNA. *Methods*, *201*, 41–48.

Sok, D., & Burton, D. R. (2018). Recent progress in broadly neutralizing antibodies to HIV. *Nature Immunology*, *19*(11), 1179–1188. https://doi.org/10.1038/s41590-018-0235-7

Sok, D., Pauthner, M., Briney, B., Lee, J. H., Saye-Francisco, K. L., Hsueh, J., Ramos, A., Le, K. M., Jones, M., Jardine, J. G., Bastidas, R., Sarkar, A., Liang, C.-H., Shivatare, S. S., Wu, C.-Y., Schief, W. R., Wong, C.-H., Wilson, I. A., Ward, A. B., ... Burton, D. R. (2016). A Prominent Site of Antibody Vulnerability on HIV Envelope Incorporates a Motif Associated with CCR5 Binding and Its Camouflaging Glycans. *Immunity*, *45*(1), 31–45. https://doi.org/https://doi.org/10.1016/j.immuni.2016.06.026

Solomon Tsegaye, T., GnirSS, K., Rahe-Meyer, N., Kiene, M., Krämer-Kühl, A., Behrens, G., Münch, J., & Pöhlmann, S. (2013). Platelet activation suppresses HIV-1 infection of T cells. *Retrovirology*, *10*(1), 48. https://doi.org/10.1186/1742-4690-10-48

Spence, J. S., He, R., Hoffmann, H.-H., Das, T., Thinon, E., Rice, C. M., Peng, T., Chandran, K., & Hang, H. C. (2019). IFITM3 directly engages and shuttles incoming virus particles to lysosomes. *Nature Chemical Biology*, *15*(3), 259–268. https://doi.org/10.1038/s41589-018-0213-2

Stefic, K., Bouvin-Pley, M., Braibant, M., & Barin, F. (2019). *Impact of HIV-1 Diversity on Its Sensitivity to Neutralization* (No. 3; Vol. 7). https://doi.org/10.3390/vaccines7030074

Stefic, K., Bouvin-Pley, M., Essat, A., Visdeloup, C., Moreau, A., Goujard, C., Chaix, M.-L., Braibant, M., Meyer, L., & Barin, F. (2019). Sensitivity to broadly neutralizing antibodies of recently transmitted HIV-1 clade CRF02_AG viruses with a focus on evolution over time. *Journal of Virology*, *93*(2), 10–1128.

Stöhr, W., Fidler, S., McClure, M., Weber, J., Cooper, D., Ramjee, G., Kaleebu, P., Tambussi, G., Schechter, M., Babiker, A., Phillips, R. E., Porter, K., & Frater, J. (2013). Duration of HIV-1 viral suppression on cessation of antiretroviral therapy in primary infection correlates with time on therapy. *PloS One*, *8*(10), e78287–e78287. https://doi.org/10.1371/journal.pone.0078287

Su, B., Dispinseri, S., Iannone, V., Zhang, T., Wu, H., Carapito, R., Bahram, S., Scarlatti, G., & Moog, C. (2019). Update on Fc-Mediated Antibody Functions Against HIV-1 Beyond Neutralization. *Frontiers in Immunology*, *10*, 2968. https://doi.org/10.3389/fimmu.2019.02968

Subramanian, A., Tamayo, P., Mootha, V. K., Mukherjee, S., Ebert, B. L., Gillette, M. A., Paulovich, A., Pomeroy, S. L., Golub, T. R., Lander, E. S., & Mesirov, J. P. (2005). Gene set enrichment analysis: A knowledge-based approach for interpreting genome-wide expression profiles. *Proceedings of the National Academy of Sciences*, *102*(43), 15545 LP–15550. https://doi.org/10.1073/pnas.0506580102

Sutar, J., Deshpande, S., Mullick, R., Hingankar, N., Patel, V., & Bhattacharya, J. (2021). Geospatial HIV-1 subtype C gp120 sequence diversity and its predicted impact on broadly neutralizing antibody sensitivity. *PloS One*, *16*(5), e0251969. https://doi.org/10.1371/journal.pone.0251969

Szklarczyk, D., Gable, A. L., Lyon, D., Junge, A., Wyder, S., Huerta-Cepas, J., Simonovic, M., Doncheva, N. T., Morris, J. H., Bork, P., Jensen, L. J., & Mering, C. von. (2019). STRING v11: protein-protein association networks with increased coverage, supporting functional discovery in genome-wide experimental datasets. *Nucleic Acids Research*, *47*(D1), D607–D613. https://doi.org/10.1093/nar/gky1131

Tee, K. K., Thomson, M. M., & Hemelaar, J. (2022). Editorial: HIV-1 genetic diversity, volume II. *Frontiers in Microbiology*, *13*. https://doi.org/10.3389/fmicb.2022.1007037

Terry, T. (2020). A package for Survival Analysis in R. *CRAN*. https://cran.r-project.org/package=survival

The SPARTAC Trial Investigators. (2013). Short-Course Antiretroviral Therapy in Primary HIV Infection. *New England Journal of Medicine*, *368*(3), 207–217. https://doi.org/10.1056/NEJMoa1110039

Tipoe, T., Fidler, S., & Frater, J. (2022). An exploration of how broadly neutralizing antibodies might induce HIV remission: the 'vaccinal' effect. *Current*

Opinion in HIV and AIDS, *17*(3), 162–170. https://doi.org/10.1097/COH.0000000000000731

Travers, K. J., Chin, C.-S., Rank, D. R., Eid, J. S., & Turner, S. W. (2010). A flexible and efficient template format for circular consensus sequencing and SNP detection. *Nucleic Acids Research*, *38*(15), e159–e159. https://doi.org/10.1093/nar/gkq543

UNAIDS. (2023). *UNAIDS Global HIV & AIDS statistics—2023 fact sheet*.

Van der Sluis, R. M., Zerbato, J. M., Rhodes, J. W., Pascoe, R. D., Solomon, A., Kumar, N. A., Dantanarayana, A. I., Tennakoon, S., Dufloo, J., McMahon, J., Chang, J. J., Evans, V. A., Hertzog, P. J., Jakobsen, M. R., Harman, A. N., Lewin, S. R., & Cameron, P. U. (2020). Diverse effects of interferon alpha on the establishment and reversal of HIV latency. *PLoS Pathogens*, *16*(2), e1008151–e1008151. https://doi.org/10.1371/journal.ppat.1008151

Van Lint, C., Bouchat, S., & Marcello, A. (2013). HIV-1 transcription and latency: an update. *Retrovirology*, *10*(1), 67. https://doi.org/10.1186/1742-4690-10-67

van Zyl, G. U., Dorfman, J. R., & Kearney, M. F. (2022). HIV drug resistance in various body compartments. *Current Opinion in HIV and AIDS*, *17*(4). https://journals.lww.com/co-hivandaids/fulltext/2022/07000/hiv%7B/_%7Ddrug%7B/_%7Dresistance%7B/_%7Din%7B/_%7Dvarious%7B/_%7Dbody%7B/_%7Dcompartments.7.aspx

van Zyl, G., Bale, M. J., & Kearney, M. F. (2018). HIV evolution and diversity in ART-treated patients. *Retrovirology*, *15*(1), 14. https://doi.org/10.1186/s12977-018-0395-4

Vargas, B., & Sluis-Cremer, N. (2022). *Toward a Functional Cure for HIV-1 Infection: The Block and Lock Therapeutic Approach* (Vol. 2). https://www.frontiersin.org/articles/10.3389/fviro.2022.917941

Victora, G. D., & Nussenzweig, M. C. (2012). Germinal centers. *Annual Review of Immunology*, *30*, 429–457.

Vollmers, S., Lobermeyer, A., & Körner, C. (2021). The New Kid on the Block: HLA-C, a Key Regulator of Natural Killer Cells in Viral Immunity. *Cells*, *10*(11). https://doi.org/10.3390/cells10113108

Wagh, K., Hahn, B. H., & Korber, B. (2020). Hitting the sweet spot: exploiting HIV-1 glycan shield for induction of broadly neutralizing antibodies. *Current Opinion in HIV and AIDS*, *15*(5). https://journals.lww.com/co-hivandaids/Fulltext/2020/09000/Hitting_the_sweet_spot__exploiting_HIV_1_glycan.2.aspx

Wagner, T. A., McLaughlin, S., Garg, K., Cheung, C. Y. K., Larsen, B. B., Styrchak, S., Huang, H. C., Edlefsen, P. T., Mullins, J. I., & Frenkel, L. M. (2014). HIV latency. Proliferation of cells with HIV integrated into cancer genes contributes to persistent infection. *Science (New York, N.Y.)*, *345*(6196), 570–573. https://doi.org/10.1126/science.1256304

Walker, B. D., & Yu, X. G. (2013). Unravelling the mechanisms of durable control of HIV-1. *Nature Reviews Immunology*, *13*(7), 487–498. https://doi.org/10.1038/nri3478

Walker, B., & McMichael, A. (2012). The t-cell response to HIV. *Cold Spring Harbor Perspectives in Medicine*, a007054.

Walker, L. M., Phogat, S. K., Chan-Hui, P.-Y., Wagner, D., Phung, P., Goss, J. L., Wrin, T., Simek, M. D., Fling, S., Mitcham, J. L., Lehrman, J. K., Priddy, F. H., Olsen, O. A., Frey, S. M., Hammond, P. W., Kaminsky, S., Zamb, T., Moyle, M., Koff, W. C., … Burton, D. R. (2009). Broad and potent neutralizing antibodies from an African donor reveal a new HIV-1 vaccine target. *Science (New York, N.Y.)*, *326*(5950), 285–289. https://doi.org/10.1126/science.1178746

Wang, Q., Michailidis, E., Yu, Y., Wang, Z., Hurley, A. M., Oren, D. A., Mayer, C. T., Gazumyan, A., Liu, Z., Zhou, Y., et al. (2020). A combination of human broadly neutralizing antibodies against hepatitis b virus HBsAg with distinct epitopes suppresses escape mutations. *Cell Host & Microbe*, *28*(2), 335–349.

Wang, W., Guo, D.-Y., Lin, Y.-J., & Tao, Y.-X. (2019). Melanocortin Regulation of Inflammation. *Frontiers in Endocrinology*, *10*, 683. https://doi.org/10.3389/fendo.2019.00683

Wang, Z., Simonetti, F. R., Siliciano, R. F., & Laird, G. M. (2018). Measuring replication competent HIV-1: advances and challenges in defining the latent reservoir. *Retrovirology*, *15*(1), 21. https://doi.org/10.1186/s12977-018-0404-7

Wedrychowski, A., Martin, H. A., Li, Y., Telwatte, S., Kadiyala, G. N., Melberg, M., Etemad, B., Connick, E., Jacobson, J. M., Margolis, D. M., Skiest, D., Volberding, P., Hecht, F., Deeks, S., Wong, J. K., Li, J. Z., & Yukl, S. A. (2023). Transcriptomic Signatures of Human Immunodeficiency Virus Post-Treatment Control. *Journal of Virology*, *97*(1), e0125422. https://doi.org/10.1128/jvi.01254-22

Wei, X., Decker, J. M., Wang, S., Hui, H., Kappes, J. C., Wu, X., Salazar-Gonzalez, J. F., Salazar, M. G., Kilby, J. M., Saag, M. S., Komarova, N. L., Nowak, M. A., Hahn, B. H., Kwong, P. D., & Shaw, G. M. (2003). Antibody neutralization and escape by HIV-1. *Nature*, *422*(6929), 307–312. https://doi.org/10.1038/nature01470

Wei, Y., Davenport, T. C., Collora, J. A., Ma, H. K., Pinto-Santini, D., Lama, J., Alfaro, R., Duerr, A., & Ho, Y.-C. (2023). Single-cell epigenetic, transcriptional, and protein profiling of latent and active HIV-1 reservoir revealed that IKZF3 promotes HIV-1 persistence. *Immunity*, *56*(11), 2584–2601.e7. https://doi.org/https://doi.org/10.1016/j.immuni.2023.10.002

West Jr, A. P., Scharf, L., Horwitz, J., Klein, F., Nussenzweig, M. C., & Bjorkman, P. J. (2013). Computational analysis of anti-HIV-1 antibody neutralization panel data to identify potential functional epitope residues. *Proceedings of the National Academy of Sciences of the United States of America*, *110*(26), 10598–10603. https://doi.org/10.1073/pnas.1309215110

Wibmer, C. K., Gorman, J., Ozorowski, G., Bhiman, J. N., Sheward, D. J., Elliott, D. H., Rouelle, J., Smira, A., Joyce, M. G., Ndabambi, N., Druz, A.,

Asokan, M., Burton, D. R., Connors, M., Abdool Karim, S. S., Mascola, J. R., Robinson, J. E., Ward, A. B., Williamson, C., ... Moore, P. L. (2017). Structure and Recognition of a Novel HIV-1 gp120-gp41 Interface Antibody that Caused MPER Exposure through Viral Escape. *PLoS Pathogens*, *13*(1), e1006074. https://doi.org/10.1371/journal.ppat.1006074

Wickam, H. (2016). *ggplot2: Elegant Graphics for Data Analysis*. Springer-Verlang New York. https://ggplot2.tidyverse.org

Wieczorek, L., Sanders-Buell, E., Zemil, M., Lewitus, E., Kavusak, E., Heller, J., Molnar, S., Rao, M., Smith, G., Bose, M., et al. (2023). Evolution of HIV-1 envelope towards reduced neutralization sensitivity, as demonstrated by contemporary HIV-1 subtype b from the united states. *PLoS Pathogens*, *19*(12), e1011780.

Williams, A., Menon, S., Crowe, M., Agarwal, N., Biccler, J., Bbosa, N., Ssemwanga, D., Adungo, F., Moecklinghoff, C., Macartney, M., & Oriol-Mathieu, V. (2023). Geographic and Population Distributions of Human Immunodeficiency Virus (HIV)–1 and HIV-2 Circulating Subtypes: A Systematic Literature Review and Meta-analysis (2010–2021). *The Journal of Infectious Diseases*, jiad327. https://doi.org/10.1093/infdis/jiad327

Williams, J. P., Hurst, J., Stöhr, W., Robinson, N., Brown, H., Fisher, M., Kinloch, S., Cooper, D., Schechter, M., Tambussi, G., Fidler, S., Carrington, M., Babiker, A., Weber, J., Koelsch, K. K., Kelleher, A. D., Phillips, R. E., & Frater, J. (2014). HIV-1 DNA predicts disease progression and post-treatment virological control. *eLife*, *3*, e03821. https://doi.org/10.7554/eLife.03821

Williamson, B. D., Magaret, C. A., Gilbert, P. B., Nizam, S., Simmons, C., & Benkeser, D. (2021). Super LeArner Prediction of NAb Panels (SLAPNAP): a containerized tool for predicting combination monoclonal broadly neutralizing antibody sensitivity. *Bioinformatics*, *37*(22), 4187–4192. https://doi.org/10.1093/bioinformatics/btab398

Wyatt, R., Kwong, P. D., Desjardins, E., Sweet, R. W., Robinson, J., Hendrickson, W. A., & Sodroski, J. G. (1998). The antigenic structure of the HIV gp120

envelope glycoprotein. *Nature*, *393*(6686), 705–711. https://doi.org/10.1038/31514

Xu, W., Li, H., Wang, Q., Hua, C., Zhang, H., Li, W., Jiang, S., & Lu, L. (2017). Advancements in Developing Strategies for Sterilizing and Functional HIV Cures. *BioMed Research International*, *2017*, 6096134. https://doi.org/10.1155/2017/6096134

Yeh, Y.-H. J., Yang, K., Razmi, A., & Ho, Y.-C. (2021). The Clonal Expansion Dynamics of the HIV-1 Reservoir: Mechanisms of Integration Site-Dependent Proliferation and HIV-1 Persistence. *Viruses*, *13*(9). https://doi.org/10.3390/v13091858

Yoon, H., Macke, J., West Jr, A. P., Foley, B., Bjorkman, P. J., Korber, B., & Yusim, K. (2015). CATNAP: a tool to compile, analyze and tally neutralizing antibody panels. *Nucleic Acids Research*, *43*(W1), W213–W219. https://doi.org/10.1093/nar/gkv404

Yu, W.-H., Su, D., Torabi, J., Fennessey, C. M., Shiakolas, A., Lynch, R., Chun, T.-W., Doria-Rose, N., Alter, G., Seaman, M. S., Keele, B. F., Lauffenburger, D. A., & Julg, B. (2019). Predicting the broadly neutralizing antibody susceptibility of the HIV reservoir. *JCI Insight*, *4*(17), e130153. https://doi.org/10.1172/jci.insight.130153

Yuan, M., Cottrell, C. A., Ozorowski, G., Gils, M. J. van, Kumar, S., Wu, N. C., Sarkar, A., Torres, J. L., Val, N. de, Copps, J., Moore, J. P., Sanders, R. W., Ward, A. B., & Wilson, I. A. (2019). Conformational Plasticity in the HIV-1 Fusion Peptide Facilitates Recognition by Broadly Neutralizing Antibodies. *Cell Host & Microbe*, *25*(6), 873–883.e5. https://doi.org/10.1016/j.chom.2019.04.011

Yucha, R., Litchford, M. L., Fish, C. S., Yaffe, Z. A., Richardson, B. A., Maleche-Obimbo, E., John-Stewart, G., Wamalwa, D., Overbaugh, J., & Lehman, D. A. (2023). Higher HIV-1 Env gp120-Specific Antibody-Dependent Cellular Cytotoxicity (ADCC) Activity Is Associated with Lower Levels of Defective HIV-1 Provirus. *Viruses*, *15*(10). https://doi.org/10.3390/v15102055

Zacharopoulou, P., Ansari, M. A., & Frater, J. (2022). A calculated risk: Evaluating HIV resistance to the broadly neutralising antibodies10-1074 and 3BNC117. *Current Opinion in HIV and AIDS*, *17*(6). https://journals.lww.com/co-hivandaids/Fulltext/2022/11000/A_calculated_risk__Evaluating_HIV_resistance_to.5.aspx

Zalevsky, J., Chamberlain, A. K., Horton, H. M., Karki, S., Leung, I. W., Sproule, T. J., Lazar, G. A., Roopenian, D. C., & Desjarlais, J. R. (2010). Enhanced antibody half-life improves in vivo activity. *Nature Biotechnology*, *28*(2), 157–159.

Zanini, F., Brodin, J., Thebo, L., Lanz, C., Bratt, G., Albert, J., & Neher, R. A. (2015). Population genomics of intrapatient HIV-1 evolution. *eLife*, *4*, e11282. https://doi.org/10.7554/eLife.11282

Zhang, B., & Horvath, S. (2005). A general framework for weighted gene co-expression network analysis. *Statistical Applications in Genetics and Molecular Biology*, *4*, Article17. https://doi.org/10.2202/1544-6115.1128

Zhang, X., Bogunovic, D., Payelle-Brogard, B., Francois-Newton, V., Speer, S. D., Yuan, C., Volpi, S., Li, Z., Sanal, O., Mansouri, D., Tezcan, I., Rice, G. I., Chen, C., Mansouri, N., Mahdaviani, S. A., Itan, Y., Boisson, B., Okada, S., Zeng, L., ... Pellegrini, S. (2015). Human intracellular ISG15 prevents interferon-α/β over-amplification and auto-inflammation. *Nature*, *517*(7532), 89–93. https://doi.org/10.1038/nature13801

Zhou, D., Hayashi, T., Jean, M., Kong, W., Fiches, G., Biswas, A., Liu, S., Yosief, H. O., Zhang, X., Bradner, J., Qi, J., Zhang, W., Santoso, N., & Zhu, J. (2020). Inhibition of Polo-like kinase 1 (PLK1) facilitates the elimination of HIV-1 viral reservoirs in CD4(+) T cells ex vivo. *Science Advances*, *6*(29), eaba1941–eaba1941. https://doi.org/10.1126/sciadv.aba1941

Zhou, P., Wang, H., Fang, M., Li, Y., Wang, H., Shi, S., Li, Z., Wu, J., Han, X., Shi, X., Shang, H., Zhou, T., & Zhang, L. (2019). Broadly resistant HIV-1 against CD4-binding site neutralizing antibodies. *PLoS Pathogens*, *15*(6), e1007819. https://doi.org/10.1371/journal.ppat.1007819

Zhou, T., Georgiev, I., Wu, X., Yang, Z.-Y., Dai, K., Finzi, A., Kwon, Y. D., Scheid, J. F., Shi, W., Xu, L., Yang, Y., Zhu, J., Nussenzweig, M. C., Sodroski, J., Shapiro, L., Nabel, G. J., Mascola, J. R., & Kwong, P. D. (2010). Structural basis for broad and potent neutralization of HIV-1 by antibody VRC01. *Science (New York, N.Y.)*, *329*(5993), 811–817. https://doi.org/10.1126/science.1192819

Zhou, T., Zhu, J., Wu, X., Moquin, S., Zhang, B., Acharya, P., Georgiev, I. S., Altae-Tran, H. R., Chuang, G.-Y., Joyce, M. G., et al. (2013). Multidonor analysis reveals structural elements, genetic determinants, and maturation pathway for HIV-1 neutralization by VRC01-class antibodies. *Immunity*, *39*(2), 245–258.

Zhu, X., Borchers, C., Bienstock, R. J., & Tomer, K. B. (2000). Mass spectrometric characterization of the glycosylation pattern of HIV-gp120 expressed in CHO cells. *Biochemistry*, *39*(37), 11194–11204.

Zicari, S., Sessa, L., Cotugno, N., Ruggiero, A., Morrocchi, E., Concato, C., Rocca, S., Zangari, P., Manno, E. C., & Palma, P. (2019). *Immune Activation, Inflammation, and Non-AIDS Co-Morbidities in HIV-Infected Patients under Long-Term ART* (No. 3; Vol. 11). https://doi.org/10.3390/v11030200

Zimbwa, P., Milicic, A., Frater, J., Scriba, T. J., Willis, A., Goulder, P. J. R., Pillay, T., Gunthard, H., Weber, J. N., Zhang, H.-T., & Phillips, R. E. (2007). Precise Identification of a Human Immunodeficiency Virus Type 1 Antigen Processing Mutant. *Journal of Virology*, *81*(4), 2031 LP–2038. https://doi.org/10.1128/JVI.00968-06

Zimmerman, E. S., Sherman, M. P., Blackett, J. L., Neidleman, J. A., Kreis, C., Mundt, P., Williams, S. A., Warmerdam, M., Kahn, J., Hecht, F. M., Grant, R. M., Noronha, C. M. C. de, Weyrich, A. S., Greene, W. C., & Planelles, V. (2006). Human Immunodeficiency Virus Type 1 Vpr Induces DNA Replication Stress InVitro and In Vivo. *Journal of Virology*, *80*(21), 10407 LP–10418. https://doi.org/10.1128/JVI.01212-06